AVERTISSEMENT

Ce document est le fruit d'un long travail approuvé par le jury de soutenance et mis à disposition de l'ensemble de la communauté universitaire élargie.

Il est soumis à la propriété intellectuelle de l'auteur. Ceci implique une obligation de citation et de référencement lors de l'utilisation de ce document.

D'autre part, toute contrefaçon, plagiat, reproduction illicite encourt une poursuite pénale.

Contact : ddoc-theses-contact@univ-lorraine.fr

LIENS

Code de la Propriété Intellectuelle. articles L 122. 4
Code de la Propriété Intellectuelle. articles L 335.2- L 335.10
http://www.cfcopies.com/V2/leg/leg_droi.php
http://www.culture.gouv.fr/culture/infos-pratiques/droits/protection.htm

UNIVERSITE DE LORRAINE
Ecole Nationale Supérieure des Mines de Nancy
Laboratoire GeoRessources
Ecole Doctorale SIReNa

§

UNIVERSITE LIBANAISE
Ecole Doctorale des Sciences et de Technologie

THESE EN COTUTELLE
Présentée en vue du grade de docteur
En Mécanique Génie Civil
Par

EL KAHI Elio

Comportement des ouvrages soumis à des tassements différentiels – Prise en compte des incertitudes

Soutenue publiquement le 23 Janvier 2020
Devant le jury composé de

Anne Pantet, *Professeur*	Université du Havre	Rapporteur
Sidi-Mohammed Elachachi, *Professeur*	Université de Bordeaux	Rapporteur
Fabrice Emeriault, *Professeur*	Grenoble INP	Examinateur
Christelle Salameh, *Chef de projet*	Tractebel-Engie, Paris	Examinateur
Olivier Deck, *Professeur*	Université de Lorraine	Directeur
Pierre Rahme, *Professeur*	Université Libanaise	Directeur
Rasool Mehdizadeh, *Maître de conférences*	Université de Lorraine	Co-directeur
Michel Khouri, *Maître de conférences*	Université Libanaise	Co-directeur

Dedication

I dedicate my thesis to my family: A special feeling of gratitude to my parents, Gen. Gaby EL KAHI & Pr. Hala El KAHI who always believe in my abilities to excel. Their words of encouragement ring in my ears. I will always appreciate all what they have done.
I also dedicate this study to my brothers and sister (Antonio, Georgio & Rita-Theresa) who always consider me as a role model, which had always given me a huge support but also a massive responsibility to be always at the level of their expectation.

Appreciation

First, I want to appreciate my supervisors for their help, their support, their assistance and their solicitude all over this research study and thesis period. They provided an exceptional opportunity of achieving this degree in the respective universities, Lorraine and Lebanese universities, which I am proud of being a member of their families. Second, I want to thank all those who had contributed for the success of this PhD.

Contents

Dedication 2
Appreciation 2
Contents 3
List of Tables 6
List of Figures 7
Résumé 12
I. Introduction 17
II. State of Art 22
II.1 Transmission of ground movements to structures 22
1. Free-field movement 22
2. Behavior of structures submitted to ground movements 30
II.2 Soil-structure interaction / Transmission of the ground movement 35
1. Analytical modeling 37
2. Numerical modeling 44
3. Experimental modeling 48
4. Comparison of various SSI field data, analytical, numerical and experimental studies . 51
II.3 Uncertainties affecting the transmission of ground movements 53
1. Uncertainties Categories 53
2. Uncertainties Modeling 54
3. Confidence Intervals 54
4. Sensitivity Analyses 55
II.4 Conclusion 58
II.5 References 59
III. Thesis overview 63
III.1 Thesis plan 63
III.2 Presentation of Chapter IV. Simplified probabilistic evaluation of the variability of soil-structure interaction parameters on the elastic transmission of ground movements 64
III.3 Presentation of Chapter V. Influence of uncertainties on the evaluation of building deflections induced by ground movements 66
III.4 Presentation of Chapter VI. A new simplified meta-model to evaluate the transmission of ground movements to structures integrating the elastoplastic soil behavior 68
III.5 Presentation of Chapter VII. Influence of Spatial Variability of Soil Properties on Structures Response 70
III.6 Presentation of Chapter VIII. Experimental evaluation of the stiffness variability of masonry structures affecting the transmission of ground movements 71
III.7 Presentation of Annex 1-4 71
IV. Simplified probabilistic evaluation of the variability of soil-structure interaction parameters on the elastic transmission of ground movements 73
IV.1 Abstract 74
IV.2 Keywords 74
IV.3 Introduction 75
1. Background 75

2. Literature review 76
3. Presence of uncertainties 80
4. Simplified probabilistic approach 81
IV.4 Procedure and modeling 82
1. Analytical modeling 83
2. Development of the meta-model 84
3. Sensitivity analysis methods 85
IV.5 Results and discussion 87
1. Sensitivity analysis results 87
2. Confidence intervals of $\Delta/\Delta\mathbf{0}$ versus ρ* 93
3. Comparison with Finite Element Models 94
IV.6 Conclusions 95
IV.7 Acknowledgement 96
IV.8 References 96
V. Influence of uncertainties on the evaluation of building deflections induced by ground movements 99
V.1 Abstract 100
V.2 Keywords: 100
V.3 Introduction 100
1. Background 100
2. Literature review 101
3. Presence of uncertainties 105
4. Choice of an analytical approach 106
V.4 Procedure and modeling 106
V.5 Results & Discussion 107
1. Free-field shape 108
2. Building position to the settlement curvature 112
3. Homogeneity of building stiffness 114
4. A new coefficient to evaluate the influence of uncertainties on the transmission ratio 116
V.6 Conclusions & Perspectives 119
V.7 Acknowledgement 120
V.8 References 120
VI. A new simplified meta-model to evaluate the transmission of ground movements to structures integrating the elastoplastic soil behavior 122
VI.1 Abstract 123
VI.2 Keywords 123
VI.3 Introduction 123
VI.4 Procedure & Modeling 126
1. Elastic Deck & Singh SSI analytical model 127
2. Elastic Basmaji et al. SSI analytical model 128
3. Validation of elastic analytical models 130
VI.5 Results & Discussion 133
1. $(\Delta/\Delta_0)_{Elastic}$ 133
2. Integrate the elastoplastic soil behavior 133

3. Validation with finite-element models 136
4. Reduction coefficient 137
VI.6 Conclusions 141
VI.7 Acknowledgment 142
VI.8 References 142
VII. Influence of Spatial Variability of Soil Properties on Structures Response 144
VII.1 Geostatistics background 145
VII.2 Abstract 147
VII.3 Keywords: 147
VII.4 Introduction 148
VII.5 Spatial Variability (SV) and Geostatistics 148
Sequential Gaussian Simulation 149
VII.6 Analytical Approach 151
1. Soil & Structure Modeling 151
2. Transmission Ratio & Relative Stiffness 152
VII.7 Results & Discussion 153
VII.8 Conclusions & Perspectives 159
VII.9 Acknowledgement 160
VII.10 References 160
VIII. Experimental evaluation of the stiffness variability of masonry structures affecting the transmission of ground movements 161
VIII.1 Abstract 162
VIII.2 Keywords: 162
VIII.3 Introduction 163
VIII.4 Procedure and Modelling 166
1. Masonry Structures 166
2. Characterization of constituent materials 166
VIII.5 Results and Discussion 169
1. Experimental Setup 169
2. Characterization of the wooden beam 171
3. Bending test on the whole system (wall and beam) 173
VIII.6 Conclusion and perspectives 174
VIII.7 Acknowledgement 175
VIII.8 References 175
IX. Conclusions 177
X. Annex 1. Comparison Winkler / Continuum 181
XI. Annex 2. Artificial Neural Network to evaluate the influence of Plasticity and Gap Formation for Sagging Mines 184
XII. Annex 3. Sinkhole case with different gap volume & variation of position 187
XIII. Annex 4. Influence of equivalent stiffness on the behavior of buildings subjected to soil settlements 190
Abstract 196
Résumé 197

List of Tables

Table I-1: Advantages & disadvantages of the numerical/experimental/analytical models to study the influence of uncertainties....18
Table II-1 Mathematical formulas for estimating the minimum value of the radius of curvature of a subsidence (Deck (2002) [15])....29
Table II-2. Advantages and disadvantages of the 3 considered materials by Ngheim (2015) [52]....50
Table II-3 Comparison between local and global methods....55
Table II-4. Sensitivity analysis results....57
Table III-1. Presentation of chapters....64
Table IV-1. Model parameters....84
Table IV-2. Comparison between local and global methods....86
Table IV-3. Model parameters Effect of the SSI parameters on Δ/Δ0 (First approach with a uniform distribution for all SSI parameters)....88
Table IV-4. Effect of the SSI parameters on Δ/Δ_0 (Second approach with a normal distribution having COV = 10% for each parameter) – Combination of EI/B=250 GN.m^2/m, L=20 m and k=250 MPa/m....89
Table IV-5. Various combinations considered for the calculation of the variability of k....91
Table IV-6. Effect of the SSI parameters on Δ/Δ_0 (Third approach with a normal distribution for all SSI parameters and COV = 40% for EI/B and k; COV = 5% for L) – Combination of EI/B=250 GN.m^2/m, L=20 m and k=250 MPa/m....91
Table V-1: Regular geometrical free-field movement shapes functions....108
Table V-2: Model parameters....109
Table V-3: Different possible homogeneous stiffness definitions for the building....115
Table V-4: Proposed values of the coefficient A, considering the free-field shape uncertainty....117
Table V-5: Maximum relative difference and proposed values of the coefficient A considering the heterogeneity of building stiffness....119
Table VI-1: Model Parameters....138
Table VI-2: Effect of every increasing factor on a....139
Table VII-1. The basic idea of the sequential Gaussian simulation....150
Table VII-2. Model Parameters....154
Table VIII-1. Mechanical tests for 3 concrete mix designs: mean values, coefficient of variation and number of specimens tested for Young's modulus (E)....164
Table VIII-2. Comparison of 3 existing experimental tests in the literature to evaluate the masonry structures variability....164
Table VIII-3. Composition of the manufactured mortar formula....168
Table VIII-4. Results of three-point compression and bending tests....168
Table X-1. Model parameters for Case 1....182
Table XIII-1. Soil properties used in numerical simulations....191

List of Figures

Fig. I.1 Diagram representing the ground movement transmission to the structures due to Soil-Structure Interaction (SSI). 18
Fig. II.1 Illustration of the mining subsidence phenomenon (Modified from Deck (2002) [15]). 24
Fig. II.2 Movement induced by tunneling (Modified from Serratrice and Magnan 2002 [48]) 26
Fig. II.3 Illustration of the Sinkhole phenomenon (Modified from Vachat 1982 [50]) 27
Fig. II.4 Vertical displacement, curvature, and slope of grounds. 28
Fig. II.5 Example of an analytical profile describing soil movement on free-field ground following tunneling work in London. 29
Fig. II.6 Comparison between measured and calculated displacements for tunneling work in London (Farrell et al. (2014) [58]). 30
Fig. II.7 Representative illustrations of the behavior of structures versus the ground curvature according to various authors (a to g) – Deck (2002) [15]. 33
Fig. II.8 Experiments highlighting the behavior of a masonry structure and the orientation of cracking - Deck (2002) 34
Fig. II.9 Redistribution of stresses due to the slope of the soil. 34
Fig. II.10. Building deflection caused by ground movements: (a) Case of tunneling. (b) Case of underground mine. 35
Fig. II.11. Free-field deflection Δ_0. 36
Fig. II.12. Behavior of structures subjected to ground movement. (a) High-stiffness structure on soft ground. (b) Intermediate ground and structure stiffness. (c) Flexible structure on stiff ground. 36
Fig. II.13 Representation of Winkler model. 39
Fig. II.14 Deformation of the Filonenko-Borodich model, (a) ground without load, (b) point load, (c) point load on a stiff foundation and (d) distributed load Filonenko-Borodich (1940). 39
Fig. II.15 Pasternak Model 40
Fig. II.16 Kerr foundation. 41
Fig. II.17 Interactive/coupled springs. 41
Fig. II.18: Building modeled by an elastic Euler-Bernoulli beam. 42
Fig. II.19: Sign conventions adopted for the soil-structure interaction model. 42
Fig. II.20: Multi-stage frame superstructure model. 43
Fig. II.21: Studied configurations and used notations 43
Fig. II.22 Geometry of the problem of the numerical analysis of Potts and Addenbrooke (1997)[6]. 45
Fig. II.23 $MsagDR$deflection transmission rate (equivalent to Δ / Δ_0) versus the relative stiffness ρ* (Potts and Addenbrooke (1997))[6]. 45
Fig. II.24 Results of Franzius et al. (2004)[41], showing the influence of building weight and building stiffness in comparison with the Potts and Addenbrooke curve (1997)[6]. 46
Fig. II.25 Deflection transmission rate in relation to the relative stiffness defined by Franzius et al. (2006)[40]. 46
Fig. II.26 Numerical and experimental results showing the transmission rate of deflection in relation to relative stiffness according to Mair (2013) [44]. 47
Fig. II.27 Empirical results showing the transmission rate of deflection in relation to relative stiffness according to Goh (2010)[43] and Goh and Mair (2011)[9]. 48
Fig. II.28 The model polycarbonate tray type with overloading of lead balls placed in small bags to ensure good load distribution during testing. 49
Fig. II.29 Model combining silicone foundation and sugar block structural element. 49
Fig. II.30 Ngheim (2015) model. 50
Fig. II.31 Building representation by the physical model (Farrell et al. (2014)[58]). 51

Fig. II.32 Comparison between various SSI models. 53
Fig. II.33: Uncertainties affecting the transmission of ground movements due to SSI. 59
Fig. III.1: Graphical abstract of Chapter IV. 65
Fig. III.2: Main hypotheses considered in the Deck & Singh methodology (2010). 66
Fig. III.3: Graphical abstract of Chapter V. 67
Fig. III.4: Graphical abstract of Chapter VI. 69
Fig. III.5: Graphical abstract of Chapter VII. 70
Fig. III.6: Graphical abstract of Chapter VII. 71
Fig. IV.1. Building deflection caused by ground movements: (a) Case of tunneling. (b) case of underground mine. 75
Fig. IV.2 Free-field deflection Δ_0. 76
Fig. IV.3. Behavior of structures subjected to ground movement. (a) High-stiffness structure on soft ground. (b) Intermediate ground and structure stiffness. (c) Flexible structure on stiff ground. 76
Fig. IV.4. Comparison between Mair (2013); Deck & Singh (2010); Pasternak-Basmaji *et al*. (2017); Winkler-Basmaji *et al*. (2017), Franza *et al*. (2019) results and numerical (Plaxis 2D) results. 77
Fig. IV.5. Description of the finite element model used to compare analytical results of the deflection transmission ratio with numerical results. 79
Fig. IV.6. Deflection transmission ratio Δ/Δ_0 versus the relative stiffness ρ^* for different forms of free-field ground movements. 82
Fig. IV.7. Presentation of the SSI parameters. 83
Fig. IV.8. Development of an analytical meta-model for the deflection transmission ratio $\Delta/\Delta 0$ versus the relative stiffness ratio ρ^*. 85
Fig. IV.9. Three approaches to evaluate the influence of the variability of SSI parameters on $\Delta/\Delta 0$ 87
Fig. IV.10. Relative influence $ASi(McKay)$ of each parameter on Δ/Δ_0 for various relative stiffness values. 92
Fig. IV.11. Confidence intervals of the transmission ratio Δ/Δ_0 versus the relative stiffness ρ^*. 94
Fig. IV.12. Comparison between the analytical confidence intervals and the numerical confidence intervals evaluated for the 3 particular cases, 1,000 numerical simulations for each case. 95
Fig. V.1: Building deflection caused by ground movements. 101
Fig. V.2: Free-field deflection Δ_0. 101
Fig. V.3: Behavior of structures subjected to ground movement. (a) High-stiffness structure on soft ground. (b) Intermediate ground and structure stiffness. (c) Flexible structure on stiff ground. 101
Fig. V.4: Comparison between Mair (2013); Deck & Singh (2010); Pasternak-Basmaji *et al*. (2017); Winkler-Basmaji *et al*. (2017), Franza *et al*. (2019) results and numerical (Plaxis 2D) results. 103
Fig. V.5: Description of the finite element model used to compare analytical results of the deflection transmission ratio with numerical results. 104
Fig. V.6: Winkler model. 107
Fig. V.7: Building modeled by an elastic Euler-Bernoulli beam. 107
Fig. V.8: Displacements of the ground and the building under conditions of static equilibrium 107
Fig. V.9: Main hypotheses considered in the Deck & Singh methodology (2010). 107
Fig. V.10: Deflection transmission ratio Δ/Δ_0 versus the relative stiffness ρ^* for different continuous regular geometrical shapes of free-field ground movements. 109
Fig. V.11: Δ/Δ_0 versus ρ^* for the discontinuous shape in comparison with the polynomial shape. 110
Fig. V.12: Δ/Δ_0 versus ρ^* for the Gaussian shape, for various configurations of the Gaussian shape in comparison with the polynomial shape. 111
Fig. V.13: Results of the numerical comparison between concave and convex soil curvatures for the deflection transmission ratio. 113
Fig. V.14: Influence of building position – Continuous shape. 114

Fig. V.15: Influence of building position – Discontinuous shape. 114
Fig. V.16: Transmission ratio Δ/Δ0 versus the building position: (a)-Continuous approach, (b) Discontinuous Approach. 114
Fig. V.17: Beam divided into 2, 3 or 4 parts. 114
Fig. V.18: Comparison of the deflection transmission ratio versus the relative stiffness for different possible homogeneous stiffness definitions for a beam divided into two parts for a=40%. 116
Fig. V.19: Numerical evaluation of Δ/Δ_0 versus ρ* for different for a beam divided into two, three and four parts for a=40%. 116
Fig. V.20: Abacus of the coefficient A to evaluate the relative influence of the building position for continuous and discontinuous approaches. 118
Fig. VI.1. Building deflection caused by ground movements: (a) Case of tunneling. (b) Case of underground mine. 124
Fig. VI.2. Free-field deflection Δ_0. 124
Fig. VI.3. Behavior of structures subjected to ground movement. (a) High-stiffness structure on soft ground. (b) Intermediate ground and structure stiffness. (c) Flexible structure on stiff ground. 125
Fig. VI.4. Structure on a soil modelled analytically with the one parameter Winkler's elastic model or the two parameters Pasternak's elastic model [6]. 126
Fig. VI.5. Diagram representing the study plan. 126
Fig. VI.6. Deck & Singh (2010) analytical model for the SSI and the building deflection induced by ground movements. 127
Fig. VI.7. Results of the deflection transmission ratio Δ/Δ_0 versus the relative stiffness ratio ρ*(Deck & Singh) obtained for K values and for Es values coupled with Vesic formula. 128
Fig. VI.8. Definition of parameters used to model the beam deflection according to Pasternak model [6]. 130
Fig. VI.9. Description of the finite element model used to compare analytical results of the deflection transmission ratio with numerical results. 131
Fig. VI.10. Comparison between Mair (2013); Deck & Singh (2010); Pasternak-Basmaji *et al*. (2017); Winkler-Basmaji *et al*. (2017) and numerical results. 132
Fig. VI.11. Presentation of the applied procedure. 134
Fig. VI.12. Vertical displacements at the soil-structure interface according to the elastic and elastoplastic behavior of the ground. 135
Fig. VI.13. Vertical pressure along the half beam (a) without plasticity; (b) with plasticity. 136
Fig. VI.14. Results of the comparison between analytical and numerical results of the deflection transmission ratio. 137
Fig. VI.15. Deflection transmission ratio Δ/Δ_0 versus the relative stiffness ρ* for elastic/elastoplastic behavior of soil for various soil bearing capacities. 139
Fig. VI.16. Graph of observed values versus expected values. 140
Fig. VI.17. Methodology of evaluation of the new simplified meta-model to calculate the transmission of ground movements to structures integrating the elastoplastic soil behavior. 141
Fig. VII.1. Winkler Model. 151
Fig. VII.2. Displacements of the ground and the building under conditions of static equilibrium. 152
Fig. VII.3. Presentation of the free-field deflection. 152
Fig. VII.4. Results of the deflection transmission ratio Δ/Δ_0 versus the relative stiffness ρ* ratio for the El Kahi *el al.* model (2018). 153
Fig. VII.5. Variogram model fitting a curve to the results. 154
Fig. VII.6. First simulation of k distribution for μ_k = 20 MPa/m for four considered correlation lengths for L=10 m. 155

Fig. VII.7. Results of the deflection transmission ratio Δ/Δ_0 versus the relative stiffness ρ^* ratio for L1=2L. 156
Fig. VII.8. Results of the deflection transmission ratio Δ/Δ_0 for different L1 values for L=10m, μ_k=500MPa/m and EI=20GN.m^2. 157
Fig. VII.9. Relationship between α and the beam stiffness. 157
Fig. VII.10. Relationship between α and the beam length. 158
Fig. VII.11. Relationship between α and the soil modulus mean value. 158
Fig. VIII.1. Diagram representing the ground movement transmission to the structures due to Soil-Structure Interaction (SSI). 163
Fig. VIII.2. Presentation of the free field deflection Δo and the structure deflection Δ [14]. 165
Fig. VIII.3. Confidence intervals to the curve of the transmission ratio Δ/Δ_0 versus the relative stiffness ρ^* [14]....165
Fig. VIII.4. Wall built horizontally. 166
Fig. VIII.5. Prismatic mortar test (4*4*16) manufactured to test the characteristics of the considered formulation of manufactured mortar. 167
Fig. VIII.6. Bending and compression tests of mortar specimen. 169
Fig. VIII.7. Cutting of cellular concrete blocks. 170
Fig. VIII.8. Geometry of masonry walls tested in the bending test and illustration of the wall. 170
Fig. VIII.9. Joints filled with mortar from the other side. 170
Fig. VIII.10. Geometry of masonry walls tested in the bending test and illustration of the wall. 171
Fig. VIII.11. System installation. 171
Fig. VIII.12. Bending test for the wooden beam. 172
Fig. VIII.13. Vertical load versus the deflection of the beam. 173
Fig. VIII.14. Cracks appearing in the wall. 174
Fig. VIII.15. Comparison between the four tested walls. 175
Fig. X.1. Continuum model used by Franza et al. 181
Fig. X.2. Case 1 - (a) Greenfield & subsidence induced beam deflections. (b) Subsidence induced reactions. (c) Post ground movement reactions. EP: Elastoplastic – EL: Elastic – GF: Free-field (greenfield) deflection. 182
Fig. X.3. Case 2 - (a) Greenfield & subsidence induced beam deflections. (b) Subsidence induced reactions. (c) Post ground movement reactions. 182
Fig. X.4. Case 3 - (a) Greenfield & subsidence induced beam deflections. (b) Subsidence induced reactions. (c) Post ground movement reactions. 183
Fig. XI.1. Comparison between the predicted values (PV) based on the meta-model and the calculated results (CR) based on the continuum SSI model of Franza *et al.* (2019) for different values of B/L for the elastic evaluation of the transmission ratio. 185
Fig. XII.1. Presentation of the sinkhole case with a variable gap position. 187
Fig. XII.2. Deflection transmission ratio Δ/Δ_0 versus the relative stiffness ρ^* for the sinkhole case. 187
Fig. XII.3. Assumed rectangular free-field ground movement. 188
Fig. XII.4. Assumed trapezoidal free-field ground movement. 188
Fig. XII.5. Influence of the gap position on maximum beam deflection Δ for the trapezoidal and rectangular approaches. 188
Fig. XIII.1. Meshing and interface in model. 190
Fig. XIII.2. Various beam typologies (EI represents the value of EI_{ref}). 191
Fig. XIII.3. Beam and soil displacements. 192
Fig. XIII.4. Comparison of the stiffness ratio EI_{eq}/EI_{ref} for different values of L and a% for the 4 considered beam partitions (EI_{ref} = 30 GN.m^2/m). 192

Fig. XIII.5. Comparison of the stiffness ratio EI_{eq}/EI_{ref} for different values of L and a% for the 4 considered beam partitions (EI_{ref}= 50 GN.m^2/m). 192
Fig. XIII.6. Comparison of the stiffness ratio EI_{eq}/EI_{ref} for different values of L and a% for the 4 considered beam partitions (EI_{ref} = 100 GN.m^2/m). 193
Fig. XIII.7. Relationship between the equivalent stiffness and beam partition type. 193
Fig. XIII.8. Relationship between the equivalent stiffness and the variant coefficient. 193
Fig. XIII.9. Relationship between the equivalent stiffness and reference beam stiffness value. 194
Fig. XIII.10. Relationship between the equivalent stiffness and beam length. 194

Résumé

De nombreux bâtiments peuvent être endommagés par des mouvements de terrain associés à des excavations souterraines, des tunnels, des mines ou des excavations en milieu urbain. L'évaluation du mouvement du terrain transmis au bâti est alors l'une des préoccupations majeures et la présence des incertitudes peut avoir une influence significative sur le comportement de la structure dû à l'Interaction Sol-Structure (ISS). Le but de cette étude est d'étudier le comportement d'une structure existante assise sur un sol soumis à un mouvement de terrain en tenant compte des nombreuses sources des incertitudes. Une triple approche (analytique, numérique et expérimentale) est appliquée. Les résultats révèlent l'influence de la prise en compte de ces incertitudes sur l'évaluation de la transmission des mouvements du terrain. Ils montrent l'effet des incertitudes sur la réponse de la structure ce qui affecte directement la prévision des dommages structurels.

Les mouvements de terrain désignent une large gamme de déplacements du sol, d'origine naturelle ou anthropique, tels que le phénomène de retrait-gonflement des sols argileux, l'influence d'excavations du sous-sol à proximité d'ouvrages (tunnels, parking, etc.) et les mouvements associés à l'instabilité de vides souterrains tels que les affaissements miniers et les fontis.

Ces mouvements de terrain peuvent se produire en l'absence de toute structure à proximité. Ce cas représente le mouvement de terrain en champ libre. En cas de présence d'une structure, tout ou partie de ce mouvement peut être transmis au bâtiment (El Kahi *et al*., 2018) et peut causer des dommages structurels (Ricceri et Soranzo, 1985). Il n'est pas approprié de considérer que les mouvements en champ libre sont systématiquement entièrement transmis au bâtiment (Mair, 2013 ; Potts et Addenbrooke, 1997 ; Boscardin et Cording, 1989) en raison d'une interaction entre le sol et la structure (ISS). On appelle Δ_0 la déflexion maximale qu'aurait subi un bâtiment si les mouvements en champ libre étaient intégralement transmis.

En supposant que le mouvement du sol en champ libre est à peu près circulaire sous le bâtiment, on peut le caractériser par son rayon de courbure R. Une relation géométrique, l'équation [1], peut être déterminée pour calculer Δ_0 en combinant R avec L (longueur du bâtiment), comme illustré à la Figure 1. On appelle alors Δ la déflexion maximale du bâtiment compte tenu de la prise en compte des phénomènes d'ISS et Δ/Δ_0 désigne alors le taux de transmission des mouvements en champ libre (Figure 2).

$$\Delta_0 = L^2/8R \qquad [1]$$

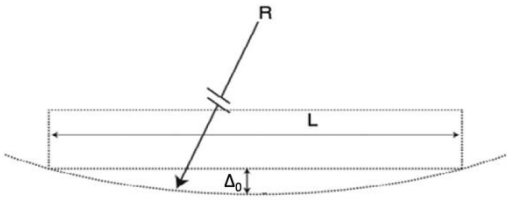


Fig. 0.1. Présentation du déplacement en champ libre Δ_0.

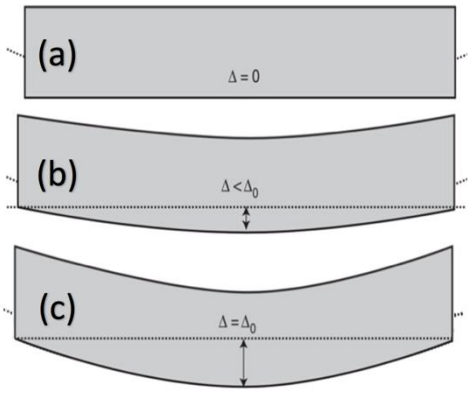


Fig. 0.2. Comportement des structures soumises au mouvement du terrain. (a) Structure de haute rigidité sur sol souple. (b) Structure de rigidité intermédiaire sur sol intermédiaire. (c) Structure flexible sur sol dur.

Différentes approches ont été développées pour étudier le comportement de structures soumises à un tassement différentiel pour prédire le taux de transmission des mouvements du sol : numériques (Haji *et al*., 2018 ; Potts et Addenbrooke, 1997), analytiques (El Kahi *et al*., 2018 ; Deck et Singh, 2010), expérimentales (Nghiem, 2015) et observationnelles (Goh, 2010).

Mis à part les méthodes observationnelles qui s'appuient sur des observations réelles d'ouvrages existants, toutes ces méthodes sont aujourd'hui appliquées à des modèles simplifiés, de type poutre, dans un soucis d'évaluation de la tendance globale des phénomènes et non d'étude spécifique d'un cas particulier.

Toutes ces approches convergent pour suggérer que le taux de transmission peut être estimé en fonction d'un paramètre de rigidité relative ρ* entre le bâti et le terrain (Figure 3). Cette rigidité dépend principalement de trois facteurs, EI/B la rigidité équivalente du bâti (E le module de Young équivalent du bâti, B sa largeur et I son inertie équivalente), Es le module de Young du terrain (qui peut être remplacé par k (module de Winkler)) et L la longueur du bâti.

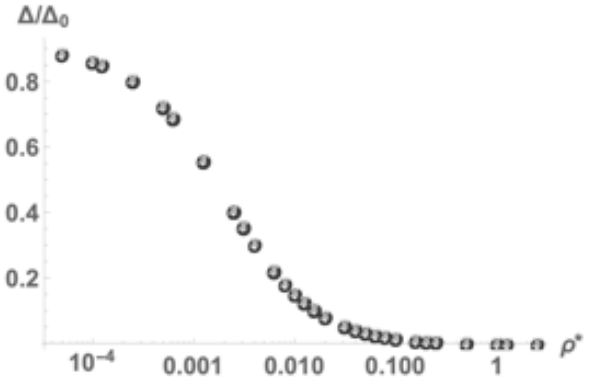


Fig. 0.3. Résultats de la variation du taux de transmission Δ Δ_0 par rapport à rigidité relative ρ* selon le modèle de El Kahi *el al*. (2018).

Ainsi, bien que les différentes approches développées fournissent une bonne prévision des mouvements des terrains en champs libre transmis aux ouvrages, compte tenu des phénomènes d'interaction sol-structure, ces développements soulèvent néanmoins des questions relatives à

l'influence des incertitudes liées au comportement du bâti et du terrain pour la prévision de ces mouvements transmis. Une problématique importante sera ainsi la prise en compte des incertitudes dans la prévision de la réponse de la structure soumise à des mouvements des terrains.

L'objectif de la thèse est donc d'approfondir la question des incertitudes relative aux trois éléments de l'interaction sol-structure (sol, bâti, mouvement transmis). Les résultats de cette étude révèlent l'influence de la prise en compte des incertitudes sur l'évaluation de la transmission des mouvements du terrain. Ils montrent la différence de la réponse de la structure entre une approche déterministe et une approche probabiliste, ce qui affecte directement la prévision des dommages structurels.

Ainsi, les résultats sont principalement basés sur la modélisation analytique et se concentrent sur les quatre incertitudes suivantes:

- Incertitudes sur la valeur des principaux paramètres géo-mécaniques: longueur du bâtiment, rigidité du bâtiment et rigidité du sol
- Incertitudes sur le déplacement du sol en champ libre et la position du bâtiment
- Incertitudes sur le sol ou variabilité de la rigidité du bâtiment
- Incertitudes sur le comportement élastoplastique du sol

Pour évaluer l'impact de ces incertitudes et présenter un moyen pratique de prédire les déformations du bâtiment induites par les mouvements du sol, différentes techniques peuvent être utilisées. Par exemple, en se basant sur les résultats déterministes du taux de transmission, un facteur de modification A, a ou α (selon le chapitre correspondant) peut être proposé pour que $(\Delta/\Delta_0)_{\text{avec incertitudes}} = A\ (\Delta/\Delta_0)_{\text{sans incertitudes}}$; ce coefficient est évalué en calculant un nombre significatif d'itérations. Il peut être présenté à l'aide d'un graphique ou d'une équation évaluée par des procédures statistiques comme les réseaux de neurones artificiels. Une autre technique pour prendre en compte les incertitudes consiste à tracer des intervalles de confiance afin de permettre une évaluation probabiliste du taux de transmission au lieu d'une évaluation déterministe.

Dans un premier temps, cette thèse étudie les incertitudes affectant la prédiction de la réponse de la structure aux mouvements du sol en tenant compte de la variabilité des paramètres ISS. Les résultats révèlent que Δ/Δ_0 dépend significativement de la variabilité des paramètres ISS, de leur loi de distribution probabiliste et de leur coefficient de variation (COV). Pour une distribution uniforme et une distribution normale avec le même COV pour les 3 paramètres ISS, L a la plus forte influence.

En étudiant la variabilité de EI/B, L et k selon une distribution normale avec le COV correspondant défini dans la littérature, on constate que l'effet de chaque paramètre varie en fonction de la valeur ρ^* considérée. Globalement, l'effet de EI/B augmente avec l'augmentation des valeurs de la rigidité relative; cependant, l'effet de k diminue lorsque ρ^* augmente.

Si la variabilité de L est limitée (COV = 5%) par rapport à celle de EI/B et k (COV = 40%), pour les faibles valeurs ρ^*, k a la plus grande influence. Cependant, pour les grandes valeurs ρ^*, EI/B a la plus grande influence. Pour les valeurs intermédiaires de ρ^*, EI/B et k ont presque le même effet. En revanche, en réduisant la variabilité des paramètres, COV (EI/B) = COV (k) = 20%, les résultats révèlent que l'influence des variabilités des paramètres ISS est comparable.

Les intervalles de confiance sont ensuite développés analytiquement et validés numériquement en variant les paramètres ISS. Une gamme de résultats de $(\Delta / \Delta_0)_{\text{avec incertitudes}}$ est associée à chaque valeur de la rigidité relative en considérant un niveau de confiance qui se situe entre 70 et 95%. Ces intervalles de confiance fournissent une évaluation probabiliste simplifiée qui peut être directement adoptée par les ingénieurs lors de la conception pour évaluer une valeur de Δ/Δ_0 en considérant l'effet de ces incertitudes.

Deuxièmement, en se basant sur le modèle de Winkler couplé à une poutre élastique d'Euler-Bernoulli, une approche analytique est appliquée pour évaluer l'influence de sources importantes d'incertitudes liées aux conditions et propriétés ISS, comme le profil de mouvement du sol en champ libre et la position du bâtiment par rapport à la courbure de tassement. L'approche analytique est ensuite validée par des modèles numériques d'éléments finis qui sont appliqués à l'aide de Plaxis 2D.

L'effet du profil de mouvement du sol en champ libre a été étudié en considérant plusieurs formes continues (polynomiale, trapézoïdale, sinusoïdale, triangulaire et semi-triangulaire), une forme discontinue (rectangulaire) et une forme gaussienne. Pour les cas continus, les résultats du taux de transmission maximal sont légèrement différents. Pour la forme discontinue, le taux de transmission ne suit pas une courbe alignée comme pour les formes continues même s'il respecte la courbure globale; une différence significative est obtenue. Pour la forme gaussienne, la distance horizontale entre le point d'inflexion de tassement et la ligne centrale du bâtiment a une influence significative sur les résultats. Deux cas gaussiens sont considérés et les résultats montrent que pour une structure ayant une longueur comparable à la longueur de courbure, Δ/Δ_0 ont des valeurs globalement similaires aux modèles ISS précédents.

La position du bâtiment par rapport à la courbure du tassement a été étudiée en considérant deux cas. Le premier cas est celui d'un bâtiment éloigné du point d'inflexion où la déflexion de la structure présente une courbure entièrement concave / convexe. Cependant, les formes concave et convexe donnent exactement les mêmes résultats du taux de transmission Δ/Δ_0. Le deuxième cas est lorsque le point d'inflexion du mouvement en champ libre est proche ou sous la structure, alors la structure peut être partiellement concave et convexe, et sa position affecte fortement la prédiction de Δ/Δ_0. Des approches continues et discontinues sont considérées et les résultats révèlent que le cas le plus défavorable correspond au cas où le centre de courbure coïncide avec la ligne centrale du bâtiment ce qui surestime la réponse de la structure. Pour une utilisation opérationnelle, un coefficient A est proposé; ce coefficient peut être utilisé par les ingénieurs et les concepteurs pour évaluer les dommages aux bâtiments induits par la transmission des mouvements du sol aux structures en tenant compte de ces incertitudes.

Troisièmement, des approches analytiques et numériques sont également appliquées pour étudier la réponse d'une structure existante assise sur un sol soumis à un mouvement du sol en intégrant l'élastoplasticité du sol à travers le paramètre de capacité portante du sol. Un nouveau méta-modèle simplifié est proposé pour évaluer la différence dans le taux de transmission entre la considération d'un comportement élastique ou élastoplastique du sol. Ce méta-modèle est évalué en utilisant la technique du réseau neuronal artificiel basée sur un nombre significatif d'itérations pour diverses combinaisons de paramètres ISS.

Quatrièmement, une étude est menée pour étudier l'influence de la variabilité naturelle des propriétés du sol et de la variabilité de la rigidité de la structure, causée par l'hétérogénéité des matériaux de construction et des ouvertures (portes, fenêtres, etc.), sur l'évaluation de la transmission de mouvements du sol.

La variabilité du sol est considérée en utilisant un champ aléatoire pour évaluer le module de Young. Les résultats révèlent l'effet de la prise en compte de la variabilité spatiale du sol sur le taux de transmission; pour un sol hétérogène, les propriétés se compensent de sorte que l'effet final devient similaire au cas où il n'y a pas de variabilité spatiale. Cependant, lorsque la longueur de corrélation augmente, le sol devient homogène, mais l'influence de la variabilité spatiale est plus importante. Pour une utilisation opérationnelle, un coefficient α est proposé; ce coefficient peut être utilisé par les ingénieurs et les concepteurs pour évaluer les dommages aux bâtiments induits par la transmission des mouvements du sol aux structures en tenant compte de ces incertitudes.

Les incertitudes liées à la rigidité du bâtiment sont étudiées à l'aide de deux procédures. Tout d'abord, la variation de la rigidité de la structure est étudiée en considérant différentes partitions de rigidité de la poutre. Les résultats indiquent que l'évaluation de la transmission du mouvement dépend de la variation de rigidité et une différence est observée entre le cas homogène et le cas hétérogène où le cas homogène sous-estime généralement la prédiction du taux de transmission. Deuxièmement, la variabilité de la rigidité du bâtiment est étudiée en réalisant des tests expérimentaux sur les murs de maçonnerie afin d'étudier l'évolution de la variabilité de la rigidité de ces murs soumis à un tassement du sol. Les résultats ont montré un COV comparable aux valeurs considérées de la variation de rigidité utilisées dans l'évaluation de l'effet de la variabilité des paramètres ISS sur le taux de transmission.

I. Introduction

Managing the risks associated with the impact of ground movements on the nearby existing structures constitutes a global challenge. This has been significantly studied and developed in urban areas that are located near to mines and underground quarries. On one hand, in urban areas, to satisfy the needs for further underground transportation and services, new tunnels are often excavated near existing structures such as the Grand Paris Express project where more than 200 km of underground works take place in urbanized areas. As part of the tunneling design project, engineers need to assess displacements and deformations of existing surface structures resulting from soil-structure interaction (SSI). On the other hand, ground movements may have their origin in the existence of mines and underground quarries because of the exploitation of raw materials. These movements can produce disturbances on nearby structures. In particular, a large number of old underground operations containing voids abandoned at different depths exist in Lorraine. Moreover, five subsidence cases have occurred in the Lorraine iron basin in the last 25 years, and these have damaged more than 500 buildings. Up to now, these voids constitute a serious risk because the overlying soil is eligible to serious deformation due to any mine collapse that can occur. Thus, the behavior of structures subjected to ground movements has been, since several years, a global topic of research that was developed at the GeoRessources laboratory and the Ecole des Mines de Nancy.

The objective of this thesis is to consider the impact of uncertainties affecting the evaluation of the structures behavior submitted to differential settlement in order to assess their vulnerability. The innovation of this thesis is to apply a triple approaches methodology (analytical, numerical and experimental) in order to consider the uncertainties, their origin, their impact, and their influence on the transmission of the ground movements from the soil to the structure. The main expected results are confidence intervals to evaluate the transmission of ground movements to structures considering the uncertainties related to the most influential and significant parameters that have to be taken in the analysis of soil-structure interaction problems, and also the development of a methodology to evaluate the overall uncertainties of the estimation of the differential settlements that affect the structure.

As shown in Fig. I.1, ground movements may have different "sources" (origins) such as the shrink-swell phenomenon of clay soils (Jahangir *et al.* (2013)), the influence of nearby excavations (tunnels) (Potts & Addenbrooke (1997)) and the presence of underground voids such as mining subsidence, sinkhole, etc. (Aissaoui (1999)). These sources will cause soil settlement. Thus, the displacement which a ground would have in the absence of a structure, represents the "free-field ground movement" or “greenfield movement”. However, in the presence of an existing structure, this movement may be considerably affected. Since it is not possible to consider that these movements in the free-field are transmitted entirely to the building (Mair (2013)), it is necessary to take into account the soil-structure interaction phenomenon. Consequently, the soil settlement produced by the free-field ground movements affects the structure and can cause structural damage (Basmaji *et al.* (2017)). Although these phenomena of structures subjected to ground movements are now widely studied (Basmaji *et al.* (2017); Saeidi (2010); Son & Cording (2007)), each study is based on a set of hypotheses that does not allow the generalization of the results obtained. The question of uncertainties, their identification and their influence are therefore the essential matters of this study.

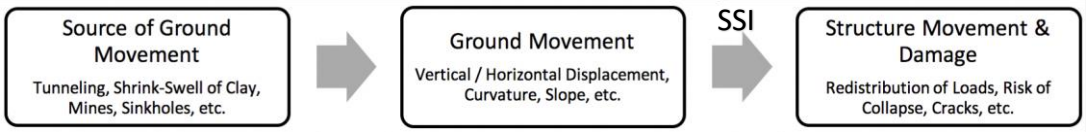


Fig. I.1 Diagram representing the ground movement transmission to the structures due to Soil- Structure Interaction (SSI).

Different methods (analytical, numerical, experimental, empirical field data results) have been developed to predict the building deflection in response to the ground movements (Franza *et al*. (2019); Hassoun *et al*. (2018); Haji *et al*. (2018); Basmaji *et al*. (2017); Farrell & Mair (2011); Goh & Mair (2011); Deck & Singh (2010); Aissaoui (1999); Potts & Addenbrooke (1997)). In particular, the question of uncertainties affecting the building deflection has been seldom studied before, although the comparison of the overall results demonstrates the existence of significant uncertainties. These uncertainties can be differently studied, based on the implemented approach: analytical, numerical and experimental approaches. As shown in Table I-1, each approach presents its own disadvantages and advantages to study the influence of uncertainties.

Table I-1: Advantages & disadvantages of the numerical/experimental/analytical models to study the influence of uncertainties

	Numerical model	**Experimental model**	**Analytical model**
Disadvantages	The more complex and realistic is the model, the greater is the number of variables that are all source of uncertainties. Lack of generality and possible extensive computation time.	Cost and time. Limited results. Scale effects when based on reduced scale models.	Based on very simple models of both the ground and the structure. It can't be used to get precise results and not all uncertainties may be studied.
Advantages	Many sources of uncertainties can be studied (even those which cannot be easily studied by analytical models): - building "real" geometry (2D or 3D) and materials. - Presence of openings in the structure (windows). - Ground geological profile.	The unique real physical result.	An easy method to study some major uncertainties: (Soil deformation profile, Soil representative model (Winkler, Pasternak, elastic/elastoplastic etc.), Building stiffness variability, Building position to the center of the basin, etc.). Rapid evaluation avoiding computation difficulties.

Except empirical methods based on observations of real existing structures, all of these methods do not consider a specific study of a particular case but they are applied to simplified structures, such as beams, in order to assess the global trend of ground movements induced phenomena.

Among the approaches developed to study the SSI phenomenon, only numerical methods offer great flexibility for taking into account the complexity of the SSI conditions (Potts & Addenbrooke (1997)).

Although it is relatively simple to consider complex soil and structures behaviors in numerical models, their use may be criticized by the justification of the numerical values of all parameters and conditions. In addition, numerical models present difficulties to generalize results, because of the need to reproduce the same scenario numerous times, by varying a particular SSI parameter in each repetition to cover the extent of the variation range of all parameters. Thus, they can be considered as time-consuming processes (Deck & Singh (2010)).

To avoid these difficulties, it is possible to obtain results through analytical methods that develop simple equations that represent the structural deflection. Analytical methods may be considered as a complementary tool to the numerical ones, allowing quick calculations for a wide range of variation of parameters, without considering complex configurations (Basmaji *et al.* (2017)). In these analytical models, the soil is modelled with simple elastic stiffness elements as elastic springs and the building by simplified structures such as beams.
On one hand, the scope of numerical methods is incomparably wider than that of analytical methods and its use may be necessary to model complex conditions with a high degree of realism, including nonlinear stress–strain behavior, non-homogeneous material conditions, and changes in geometry and so on. However, care must be taken about the required time to develop such numerical models to investigate influence of uncertainties.
On the other hand, though its importance to physically reproduce the real case, the experimental approach presents even more disadvantages from the point of view of the required time to study the influence of uncertainties. The choice of the analogical model respecting the scale and the building properties constitutes by itself a major source of uncertainty that dominates all the other sources, and that needs to be studied alone.
Consequently, the analytical approach appears to be a suitable method to study the majority of uncertainties in this thesis. However, the numerical and experimental approaches can be significantly important to validate some of the results obtained in the analytical approach.

At first, a bibliographical study will be devoted to the presentation of the phenomena of ground movements, their sources and their influence on constructions, and the different approaches used to estimate the movements of buildings following these movements. Then, the different methods used to quantify and represent the impact of the various sources of uncertainties, which can affect the evaluation of the transmission of ground movements to structures, are presented.

At second, a chapter that summarizes the sequence of targets set in this thesis and the main results obtained in each paper is presented. Since the objective of every paper is unique, the target of this chapter is to present a global vision that links these papers issued separately in order to reach the final target of the thesis.

At third, a paper titled “Simplified probabilistic evaluation of the variability of soil-structure interaction parameters on the transmission of ground movements” is presented to consider the uncertainty related to the evaluation of the transmission of ground movements to structures considering the influence of the variability of the soil-structure interaction (SSI) parameters. This probabilistic approach aims to quantify the relative importance of the variability of the main SSI parameters on the structure response via a sensitivity analysis (SA). The structure response is evaluated using analytical

and numerical models. The objective is to evaluate the impact of the parameters variability which are assumed to be of a random nature. To avoid time and computation difficulties, a simplified analytical meta-model that reflects the structure response is proposed. Based on this meta-model, the SA is performed using three selected procedures, one local and two global, namely, one-way analysis, Sobol and McKay respectively. Results reveal the contribution of each input parameter on the variability of the response using various sampling techniques, such as random Monte-Carlo Simulations (MCS) and the Latin Hypercube Sampling (LHS). Results also reveal the influence of the variability of the main SSI parameters on the rate of the ground movement that is transmitted to structures; confidence intervals are set and can be used by engineers and designers when evaluating the induced building damage in response to the transmission of ground movements taking into consideration these uncertainties.

At forth, a paper titled “Influence of uncertainties on the evaluation of building deflections induced by ground movements” is presented. An evaluation of the influence of important sources of uncertainties related to the Soil-Structure Interaction (SSI) conditions and properties is applied, namely, the free-field ground movement profile, the building position to the settlement curvature and the variability of the structure stiffness caused by the heterogeneity of structural materials and openings (doors, windows, etc.). Results reveal the discrepancy in the response of a structure by considering these uncertainties in the entire domain of variation of the SSI parameters. For an operational use, a coefficient A is proposed; this coefficient can be used by engineers and designers when evaluating the building damage induced by the transmission of ground movements to structures taking into consideration these uncertainties.

At fifth, a paper titled “A new simplified meta-model to evaluate the transmission of ground movements to structures integrating the elastoplastic soil behavior” is presented. The purpose of this paper is to compare various approaches to evaluate the structure response and to propose a new simplified meta-model that integrates the soil elastoplasticity to evaluate the transmission of ground movements to structures using the technique of neural networks.

At sixth, a paper titled “Influence of spatial variability of soil properties on structures response” is presented. The target of this paper is to investigate the influence of natural variability of soil properties on the evaluation of the transmission of ground movements. A probabilistic study is done using an analytical approach coupled with a numerical model. In order to propagate geostatistical conditions to represent the soil, a modified soil elastic representative model is developed where the soil is assimilated to a juxtaposition of elastic springs characterized by a particular stiffness value for every spring according to the SGS (Sequential Gaussian Simulation) method.

At seventh, the stiffness variability is investigated experimentally. The objective of this experimental approach is to carry out tests on masonry walls in order to study the evolution of the stiffness variability of these walls subjected to a ground settlement. To reproduce the settlement conditions, the experimental study is carried out on masonry structures undergoing bending tests through a progressively increasing vertical load. Four bending tests are carried out on identical masonry walls simply supported at their ends, bending under the effect of vertical loads, in order to follow the evolution of their displacement and consequently the stiffness variation. The results are compared to

the considered values of the stiffness variation in the evaluation of the effect of the variability of SSI parameters on the transmission ratio.

Finally, 4 annexes present some additional work done in this thesis. The results shown in these annexes are the subject of other papers which are not presented in this manuscript, or papers that are under preparation.

1- Annex 1 presents a complementary part of the simplified meta-model that integrates the elastoplastic soil behavior. This annex summarizes a part of the scientific collaboration realized with the Polytechnic University of Madrid. In fact, a mobility grant has been associated to this thesis from Lorraine University of Excellence to realize an exchange program for three months (September-November, 2019). During this period spent in Madrid, a comparison has been done between the SSI analytical models developed in the literature by: (a) Deck & Singh (2010) that is based on Winkler model and Franza *et al.* (2019) that is based on Continuum model. Comparison results reveal that Winkler model provides moderate results even if its use may be criticized for some restrictions.
2- Annex 2 presents another part of the work realized with the Polytechnic University of Madrid, considering a continuum model. In this chapter, the artificial neural network was used to evaluate the influence of plasticity and gap formation for sagging and hogging mines, in addition to the influence of eccentricity for the tunneling induced movements based on Franza *et al.* (2019) continuum model.
3- Annex 3 presents an extension to the model and geometric uncertainties paper (free-field shape, building position and stiffness variability) that shows the results that were presented in the JFMS-2018 (10èmes journées Fiabilité des Matériaux et des Structures - Bordeaux, 27-28 Mars 2018), to investigate the influence of some relevant parameters on the same free-field ground form; for example, the influence of the gap position generated by the variation of the gap form due to the ground displacement.
4- Annex 4 presents the results of the numerical study of the influence of equivalent stiffness on the behavior of buildings subjected to soil settlements. A synthesis of this work was presented in ESREL-2019 conference (Proceedings of the 29th European Safety and Reliability Conference).

II. State of Art

Ground movements produced by subsurface cavities, tunnels or shrink-swell of clay soils may be transmitted to buildings to cause damage. Managing the risks associated with these movements requires an establishment of relationships between ground movements and their consequences on the surface, particularly on buildings.

There are many bibliographical references addressing the question of the transmission of ground movements to buildings due to SSI, and the question of structures response, in addition to the evaluation of their damage (threshold values of movements, analytical methods, numerical, etc.) [1-12]. However, the uncertainties related to the evaluation of the transmission of ground movements are scarcely assessed since most of the SSI studies are based on particular conditions for particular cases, so the results obtained cannot be generalized.

So, this chapter is divided into two parts: (a) the transmission of ground movements to structures and (b) the uncertainties affecting the transmission phenomenon. The first part presents a review of the sources of ground movements and their effect on the free-field, their transmission and the structures response. The second part presents a discussion about the uncertainties affecting the estimation of the transmission of ground movements, their impact and their evaluation.

II.1 Transmission of ground movements to structures

1. Free-field movement

a) Sources of ground movement

Ground movements include a series of displacements of the soil or subsoil, of natural or anthropogenic origin [8, 13-14]. This study focuses more specifically on movements induced by tunnels and underground cavities (mines, quarries, etc.). It is with respect to these movements that the phenomena of soil-structure interaction will be studied.

(1) Mining subsidence

For the mining subsidence, nowadays, the exploitation of raw materials (iron, salt, gypsum, etc.) through underground mines and quarries leaves underground voids abandoned at different depths and under different environmental and climatic conditions.
As shown in Figure II.1, after the termination of operations, subsidence may occur as a result of breakage of pillars or covering issues. The problem of mining subsidence and its impact on buildings and above-ground structures, can be essential to manage the risks associated with these operations. There are two main types of subsidence: the progressive subsidence and the brutal subsidence.
The mining subsidence causes the appearance of a curvature on the surface. The curvature has a three-dimensional geometry that depends on many factors related to the geometry of the mine, the method of exploitation, the geology of the subsoil, the mechanical properties of the land, etc. The surface undergoes differential displacements. The vertical displacements are at the origin of a slope and a

curvature of the ground which varies in the subsidence zone. The horizontal displacements are at the origin of a horizontal deformation of the field that is of extension type towards the outside of the subsidence and of compressive type towards the interior. In order to describe these movements, it is necessary to define and investigate various “mining” parameters and to assess the methods of describing and predicting the subsidence phenomenon: vertical displacement, curvature and horizontal deformation [10, 15-16].

The methods of predicting the mining subsidence are many:

- Empirical methods [13, 17] that are based on the observed results of mining subsidence. They take the form of mathematical formulas or charts.
- Semi-empirical methods [16-18] that are mainly functions of profile and influence. They are based on the superposition principle which is applied to infinitesimal parts of the exploited area. The final subsidence is obtained by considering all the infinitesimal elements of the exploited surface of the mine.
- Analytical methods [10, 15] that are based on the simplifying hypotheses that do not make it possible to study a discontinuous zone but they make it possible to characterize the movement of the grounds and also to study the behavior of the roof by analogy with the theory of the beams.
- Physical methods [19, 20] that use reduced models made of artificial materials such as solidified gelatin, stratified sand, gypsum which have mechanical behaviors similar to those of the field materials. The actual subsidence parameters are then deduced by similarity laws.
- Numerical methods [21, 22] such as finite elements, finite differences and discrete elements can also be used for the prediction of mine subsidence. They make it possible to predict subsidence and horizontal deformations from constitutive laws such as elasticity, plasticity, viscoplasticity or considering a discontinuous mass.

The order of magnitude of the movements induced by mining subsidence is highly variable, with radii of curvature varying from a few hundred meters to a few kilometers. For a building of 20m in length, these curves are then associated with structural deflections that have the order of millimeters to centimeters [23].

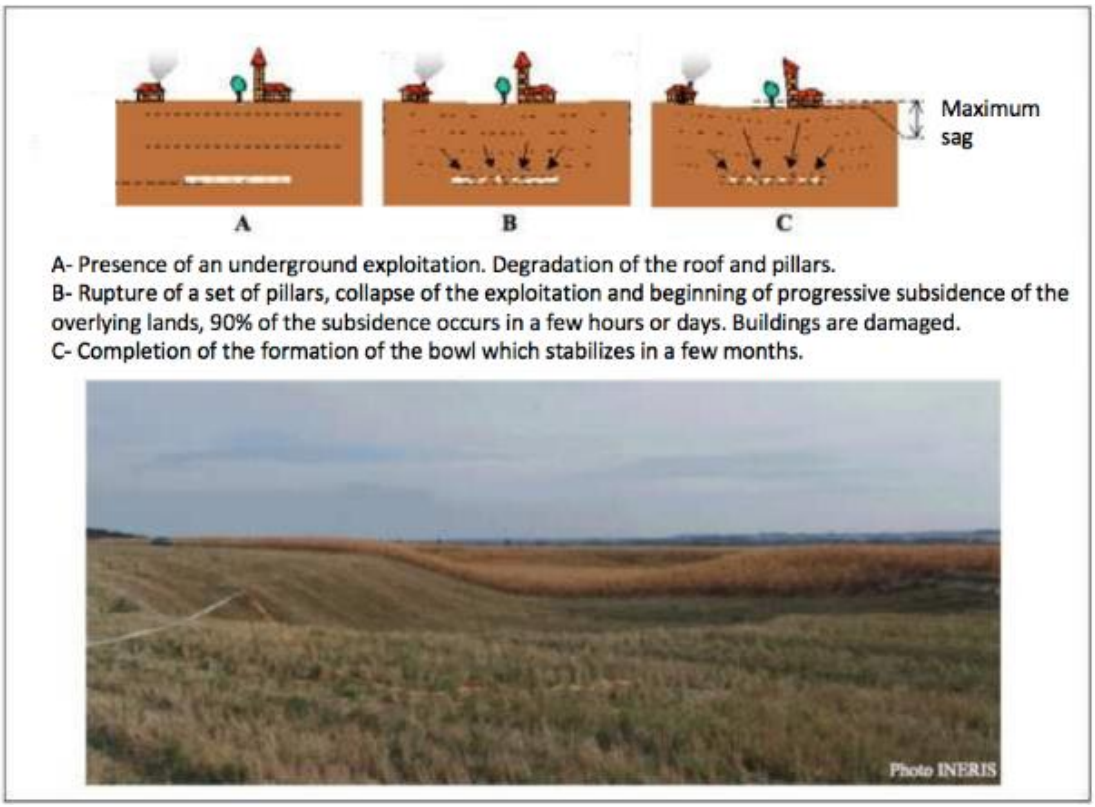


Fig. II.1 Illustration of the mining subsidence phenomenon (Modified from Deck (2002) [15]).

(2) Tunneling

On the other hand, tunneling can induce ground movements (Fig. II.2). These movements are not uniform but are concentrated in line with the underground structure in the form of a curvature. In fact, the response to the perturbation generated by the tunneling depends essentially on the nature of the soil and the tunneling technique. For example, the problem of tunnel stability is relevant to the tunnel heading where a portion of the soil may be unsupported, if the linings (temporary/permanent) have not yet been placed, or partially supported. To evaluate tunnel stability in undrained conditions, Broms and Bennermark (1967) [24] introduced the tunnel stability factor, defined as the sum of the surface surcharge pressure, the unit weight of the overburden material by the depth to the tunnel axis and the pressurized slurry over the undrained shear strength. The higher the stability ratio the more unstable is the tunnel heading. On the basis of laboratory tests and field observations, a failure is associated with the critical stability ratio of 6 [25]. According to a comprehensive review of latest findings performed by Leca *et al*. (2007) [26], care is recommended in the evaluation of settlement risk when this factor is between 3 and 6, with particular attention to possible ground loss if it is higher than 5. Centrifuge model tests performed by Mair (1979) [27] and Kimura and Mair (1981) [28] displayed that the critical value increases with cover to diameter ratio and decreases with the unsupported length of the tunnel head. Theoretical solutions supporting these findings were developed by Davis *et al*. (1980) [29].
Ground movements caused by tunneling are mainly caused by the soil moving towards the drilling machine due to the stress-relief, which results in a ground loss. In general, depending on the tunnel construction method, it is possible to identify the main sources of the ground loss, listed by Mair and Taylor (1999) [30].

The implementation of a proper tunnel deformation shape assumes a fundamental role in the analytical analysis where the volume loss area has been attributed to a cavity contraction, i.e. by a uniform tunnel convergence. Nevertheless, this straightforward assumption may not describe the actual field displacement adequately: centrifuge modelling confirmed that little ground displacement occurs at the tunnel invert [27, 31]. The actual tunnel ground loss is distributed according to a roughly elliptical shape in clays [32, 33], whereas the ground loss should be concentrated at the tunnel crown in sands [34, 35].

The problem is particularly existent in cities, where these movements affect all components of the urban structures, either buildings, roads or networks. The estimation of ground movements is the first step to perform a reliable risk-assessment of the potential effects on building and buried infrastructure, which is essential for the design of tunneling in urban areas. Although a certain understanding of the free-field tunnel-induced settlements has been reached in the literature, there has been a limited discussion about its validation [25].

The study of movements associated with tunneling and their consequences have been the subject of several studies worldwide [6, 9, 11, 36,-44].

Numerical methods have been extensively applied to tunneling and to the induced soil deformation patterns because of the possibility to implement various geometries, details of the construction procedures and complex soil constitutive models. However, there are many cases, especially in the preliminary stages of the design, in which the soil data are not adequate to characterize complex constitutive models and the excavation method is not fully defined. Therefore, if closed-form solution is not possible, the empirical methods present an effective instrument to carry out low computational cost, approximate and sensible evaluation of practical study cases [9, 11, 43].

Tunneling-induced settlement troughs are generally described by tunnel engineers using simple empirical methods. As proposed by Peck (1969) [45], in undrained conditions, the shape of transverse settlement troughs agrees with a standard Gaussian curve.

The vertical displacement decreases with the increase in the tunnel depth (H) because the tunnel tends to behave as in an infinite space. According to the results shown by Pinto and Whittle (2006) [46], the ratio $\Delta uz/\varepsilon$ (uz is the vertical settlement and ε the tunnel contraction parameter) is approximately within the range of 0.2-0.4 for $R/H = 0.2-0.4$ (where R is the tunnel radius). Neaupane and Adhikari (2006) [47] presented ranges between 0.92 cm and 10.5 cm for the vertical displacements of soils in areas overlying tunnels (Mexico City 10.5 cm, USA 0.92 cm).

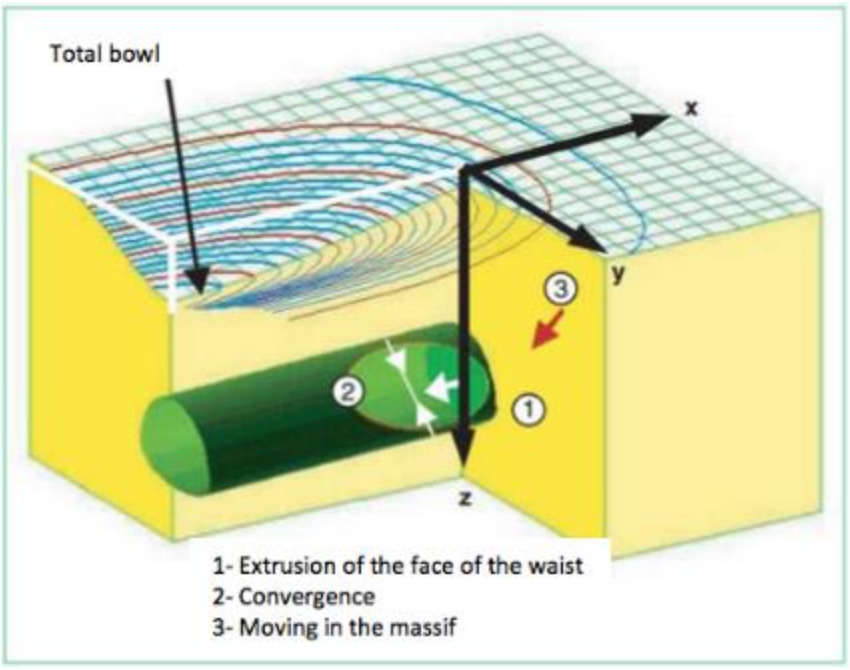
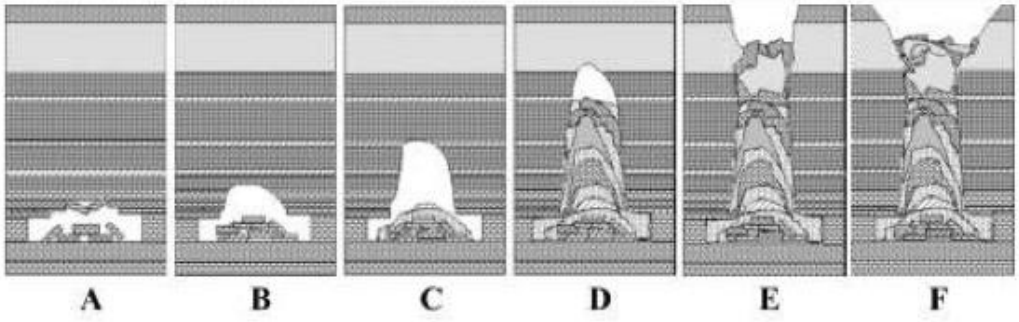


Fig. II.2 Movement induced by tunneling (Modified from Serratrice and Magnan 2002 [48])

(3) Sinkholes

Sinkholes can also be considered as sources of ground movements. A sinkhole is a depression or hole at the ground surface caused by some local collapse of the surface layer due to the presence of a cavity. Horizontal extension of sinkholes is limited to few meters. This subsidence can have a high amplitude which causes discontinuities on the surface. Fayad (2004) [49] studied the stability of the roof of the underground quarries. Also, Vachat (1982) [50] studied a sinkhole that appeared on the top of a former granular limestone quarry at Malakoff in the Paris basin. This resulted in a depression on the surface of the ground of 2.5m diameter and 2m deep. At the bottom, an opening having a bell shape at the surface of 8m height with an angle of 80 ° appeared at the base.

Also, the sinkholes were the subject of study of various experimental models that have been developed to better understand the phenomenon and its influence on buildings [51-53].



A- Rupture of roof with falls of blocks in an old exploitation.
B- Climb of vault by successive falls of blocks of the rooftop.
C- Beginning of formation of a sinkhole bell. A cone of scree begins to form.
D- The sinkhole bell continues to grow towards the surface. The cone of soil filled the underground cavity.
E- The sinkhole opens until causing the collapse of the surface grounds.
F- Following the alteration of superficial soils, the sinkhole takes the form of a stable funnel.

Fig. II.3 Illustration of the Sinkhole phenomenon (Modified from Vachat 1982 [50])

(4) Shrink-swell phenomenon of clay soils

The shrink-swell phenomenon of clay soils belongs to the category of climate risks that is presented here for information. Clay soils behavior depends on their water content; they can also undergo significant volume variations that tend to induce settlements or swellings. Thus, when the water content increases in a clay soil, there is an increase in the soil volume which is referred as swelling. A water deficit will cause a reverse phenomenon called shrinkage. These shrinkage and swelling effects can therefore cause several damages at the surface. These effects have been studied by various authors. For example, Driscoll (1983) cited by Quoc Viet (2010) [54] noted that vertical settlements between 4.1 cm and 5.8 cm may occur for clay soils in southwestern England.
Tunneling induced movements can also be associated with the shrink-swell phenomenon of clay soils. Mair and Taylor (1999) [30] concluded, based on a review of several research projects, that volume losses in stiff clays, such as London Clay, are generally between 1% and 2% when the open-face tunneling technique is adopted. Sprayed concrete linings (NATM) in London Clay could provide a control of ground movements with volume losses between 0.5% and 1.5%.

b) Description of the free-field ground movement

Ground surface movements can be described according to various parameters such as vertical displacement, horizontal displacement, slope, curvature and horizontal deformation of the ground.
In the following, the free field ground movement at the surface in the absence of any interaction with a structure is presented in details in addition to the problematic of the soil-structure interaction and the prediction of the rate of transmission of these movements to the building. This transmission of the movement of the ground towards the building depends on the phenomena of soil-structure interaction making it possible to identify the transmission rate. Thus, the behavior of buildings may vary according to the nature of the movement transmitted and to the nature of the ground as well as that of the structural properties (soil-structure interaction).

Fig. II.4 represents the vertical displacement as well as the slope of ground and its curvature. The free-field shape presented in this figure typically corresponds to the movements induced by mining subsidence and tunneling.

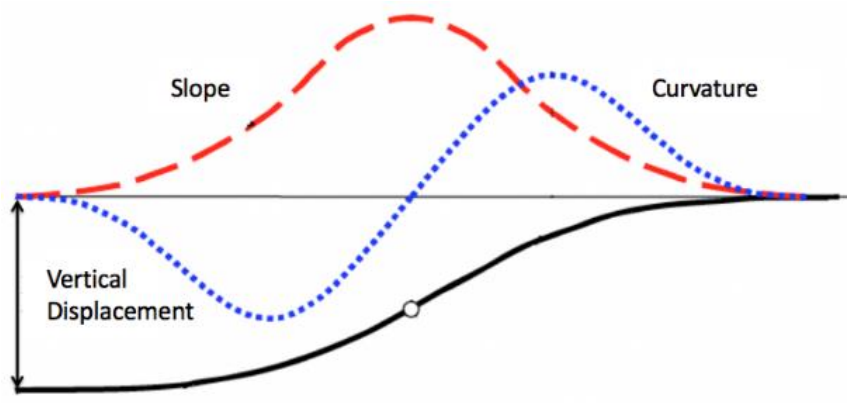


Fig. II.4 Vertical displacement, curvature, and slope of grounds.

(1) The movements associated with mining subsidence and its components

Several methods have been developed to estimate the mining subsidence and its components. Aissaoui (1999) [10] classified these methods into 5 groups: empirical, semi empirical, analytical, physical and numerical methods. Empirical and semi-empirical methods rely on theoretical and empirical considerations. Numerical methods as well as experimental and empirical approaches are always used to estimate these movements [49, 53, 55, 56].

Deck (2002) grouped the mathematical formulas for describing surface subsidence; two large families of functions appear. The first is based on the inverse of the exponential function and the second on the hyperbolic tangent function.

The ground curvature can be calculated from the theoretical functions of the vertical subsidence profile. Eq. II-1 is the exact formula of the curvature of the ground; it can be simplified as in Eq. II-2 if the slope of the curvature is small, as per Saeidi (2010).

$$\frac{1}{R} = \frac{\frac{d^2V(x)}{dx^2}}{\sqrt{[1 + (\frac{dV(x)}{dx})^2]^3}} \qquad \textit{Eq. II-1}$$

$$If\ \frac{dV(x)}{dx} << 1 \rightarrow \frac{1}{R} = \frac{d^2V(x)}{dx^2} \qquad \textit{Eq. II-2}$$

Where V(x) represents the function of the vertical subsidence profile and R the radius of curvature.

Table II-1 presents several mathematical formulas by various researchers to estimate the minimum value of the radius of curvature of a subsidence basin. Authors agree on expressing the radius of the

minimum curvature as a function of the H^2/Am ratio (H: depth of the mine, Am: maximum subsidence).

Table II-1 Mathematical formulas for estimating the minimum value of the radius of curvature of a subsidence (Deck (2002) [15]).

Prediction of the maximum subsidence	
Author	Formula
Kratzsch (1983) [19]	$R_{min} = K.H^2/A_m$ $K = 0.05\ to\ 0.3$
Yokel, Salmone and Gray (1982)	$R_{min} = 0.172\ H^2/A_m$ (ex-URSS) $R_{min} = 0.077\ H^2/A_m$ (National Coal Board)
Proust (1964) [57]	$R_{min} = 0.1\ H^2/A_m$
R_{min} : Minimum radius (m) A_m : Maximum subsidence at the curvature center H : Mine depth	

(2) The movements associated with tunneling

The estimation and the prediction of the displacements induced by the digging of tunnels have been treated by several publications. Peck (1969) suggested the well-known relationship in this domain (Fig. II.5). In this figure, $S'_{v,\,max}$ is the maximum settlement while $S_{v,\,max}$ is the settlement at the inflection point. $S_v(x)$ is the displacement of soil in the compression zone and $S'_v(x)$ is the displacement of the soil outside the compression zone.

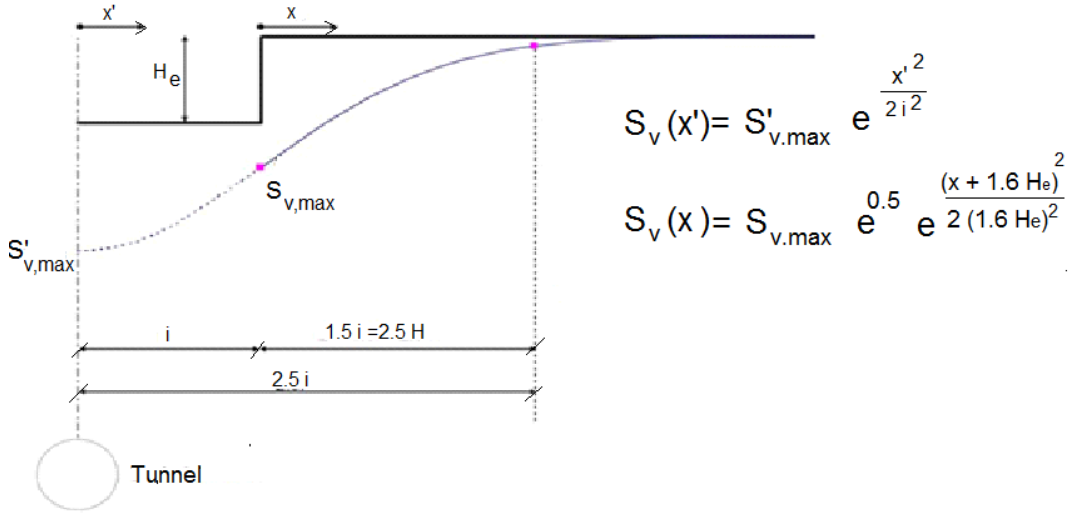


Fig. II.5 Example of an analytical profile describing soil movement on free-field ground following tunneling work in London.

Farrell *et al*. (2014) [58] measured the movement of soil in London during the excavation of the tunnel. The displacements they measured were very close to displacements calculated from an exponential function (Fig. II.6).

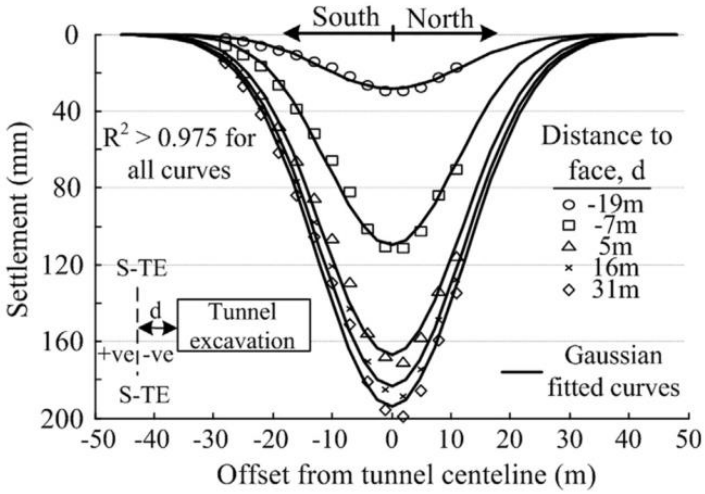


Fig. II.6 Comparison between measured and calculated displacements for tunneling work in London (Farrell et al. (2014) [58]).

This figure shows that typical analytical relationships of Peck (1969) are sufficient to estimate the surface settlement induced by tunneling.

2. Behavior of structures submitted to ground movements

Ground movements are transmitted to structures; deformed structures follow ground movements either partially or totally, leading to structural or functional damage. Different approaches have been used to estimate the damage level of a structure by taking into account the various soil and structure parameters. For example, NCB (1975) [13] and Wagner and Schumman (1991) [17] have proposed charts to estimate the damage of buildings according to their length and the horizontal deformation of the ground. Wagner and Schumman (1991) [17] also proposed an abacus to estimate the degradation as a function of the horizontal deformation and the slope of the ground. There is also the Polish method of Kwiatek (1998) [59] which uses seven criteria to estimate the degradation of a building (3 to describe the geometry of the structure, 3 for its technical characteristics and a parameter to describe the subsurface).

For a subsidence, for example, it is necessary to take into account mainly the effect of the horizontal deformation and the curvature of the ground. For movements associated with tunneling or shrink-swell, it is essentially curvature that matters.

Giardina *et al.* (2013) [60] conducted numerical and experimental studies to analyze the level of damage to a masonry facade following tunneling work. They showed the important role that the initiation of damage to a building can play on SSI phenomena and the level of final damage that the structure may suffer. Serhal *et al*. (2017) [61] proposed various equations to estimate the post-damage stiffness evolution for masonry structures using a numerical and an experimental approach. These equations were then considered by Basmaji *et al*. (2017) [8] to evaluate the transmission of ground movements to structures and showed that the impact of ground movements on damaged structures is higher.

The various possible behaviors of a building subjected to movements of the ground have been described and synthesized by Deck (2002) [15] and Fayad (2004) [49].

a) Behavior of buildings versus the horizontal deformation

Several studies have been done to understand the behavior of structures located in a zone of horizontal deformation: Shahin *et al.* (2004) [62], Deck (2002) [15], Arcamone (1980) [64], Geddes (1984) [66], Burland *et al.* (1977) [65] and Soots (1969) [63].

Ground horizontal deformation has an effect on the structure according to two main modes of transmission: an earth pressure (compression case) and a friction of the ground along the structure. The rate of transmission of horizontal deformation depends on the relative stiffness of a structure relative to that of the soil. Boscardin and Cording (1989) [67], Potts and Addenbrooke (1997) [6] tried to quantify the transmission rate for stiff structures or for flexible structures. According to the study conducted by Boscardin and Cording (1989) [67], the order of magnitude of this parameter is 10 to 30% for stiff buildings and 30 to 100% for flexible buildings.

Because horizontal strains may be induced in the structures by ground movements, Mair *et al*. (1996) [68] suggested to account for the horizontal building strain by using an average value computed along the building portion undergoing hogging or sagging. As reported by Mair *et al*. (1996) [68], the combination of shear, bending and horizontal deformations leads to a correlation with the total maximum bending strain and diagonal strain.

To identify the start of serviceability loss, Burland *et al.* (1977) [65] used the concept of "limiting tensile strain", which allows engineers to identify with elastic beam analysis (considering the structure properties) the state corresponding to the onset of visible cracks. To measure the degree of damage, Burland *et al.* (1977) [65], and at a later stage Boscardin and Cording (1989) [67], adopted a classification based on "ease of repair" of the visible damage. This classification provides five categories, ranging from negligible to severe damage, with an associated description of the cracks. These categories were correlated to a range of limiting tensile strains by Boscardin and Cording (1989) [67].

b) Behavior of buildings versus the Ground Curvature

The ground curvature is divided into two categories: concave or convex. The concave zone (sagging) is located towards center of the curvature and the convex zone (hogging) towards its edges. A procedure for preliminary risk assessment of surface structures to ground movements induced movements was proposed by Mair *et al.* (1996) [68] based on the assumptions of plane-strain conditions where the building-foundation was represented by an equivalent linear elastic beam, and that the building is divided into two independent structures in the hogging and sagging zones.

The Mair *et al*. (1996) [68] procedure consists of the following steps.

1. Free-field surface movements are calculated; only if the settlement trough affecting the building exceeds 10mm magnitude, it is necessary to proceed to step 2. The authors assumed the empirical method based on Gaussian curves to predict horizontal and vertical movements; however, a generic approach may be implemented.

2. The beam is constrained to displace as the free-field movements and the resulting maximum tensile strains in the hogging and sagging zones are calculated. Subsequently, the damage

assessment in hogging and/or sagging is performed by comparing maximum building tensile strain with the limiting tensile strain and relating it to the expected damage level.

3. Step 2 leads to a conservative assessment because it neglects the structural stiffness (i.e. the building exhibits a fully-flexible behavior). However, a detailed evaluation of the building deformations (accounting for the soil-structure interaction, 3D geometries of structure and tunnels) should be carried out, which may result in a decrease of the damage category.

On the other hand, Attewell and Yeates (1984) [67], Boscardin and Cording (1989) [69], Kratzch (1983) [19], Arcamone (1980) [64], Soots (1969) [63], Burland *et al*. (1977) [65], Burland and Worth (1974) [70], Neuhaus (1965) [71], Geddes (1984) [66], Potts and Addenbrooke (1997) [6], Franzius *et al.* (2006) [40], Deck and Singh (2010) [7] and Nghiem (2015) [52] have studied the behavior of structures in the curvature zone of the field. As shown in Fig. II.7, the overall effect of a concave curvature is to increase the transfer of vertical stresses due to the weight of the structure towards its edges. For large curvatures, the load effect can even be completely null at the center. The structure thus undergoes concave flexure and tensile stresses appear in the lower fiber.

The overall effect of a convex curvature is to increase the vertical stresses due to the weight of the structure towards its center. For large curvatures, the structure can even be completely unloaded at its ends. The structure takes a convex curvature and tensile stresses appear in higher fiber.

The objective is to evaluate the final curvature of the building and whether or not this curvature has the same shape as that of the free-field ground. This evaluation depends upon the interaction between the soil and the structure. Fig. II.7 provides a schematic description of the behavior of the structure in a concave or convex zone.

In the concave zone, the increase in vertical stresses under the ends of the structure is remarkable, whereas the increase in vertical stresses in the convex zone is under the center of the structure. For large curvatures, the structure can be detached at its ends (in the convex zone) or at its center (in the concave zone), depending on the stiffness of the ground and the structure.

Fig. II.7-g shows that the curvature of the ground can be the cause of a stress on the structure due to bending and shear.

In general, a concave curvature of the ground generates inclined cracks, concentrated at the bottom of the structure and oriented from the lower ends of the structure towards its center. A convex curvature leads to a contrary effect, with cracks concentrated in the upper part of the structure and oriented from the center of the structure towards its upper extremities. This result is substantially consistent with Fig. II.7-d.

When the structure is damaged, the orientation of the cracks depends on the direction of the curvature. Fig. II.8 shows the cracks in masonry walls according to the direction of curvature. The experience of Cox (1980) also shows the influence of the openings in the walls on their distribution. Burland and Wroth (1974) [70] illustrate the orientation and location of cracks according to the curvature and the mode of stress (bending or shear).

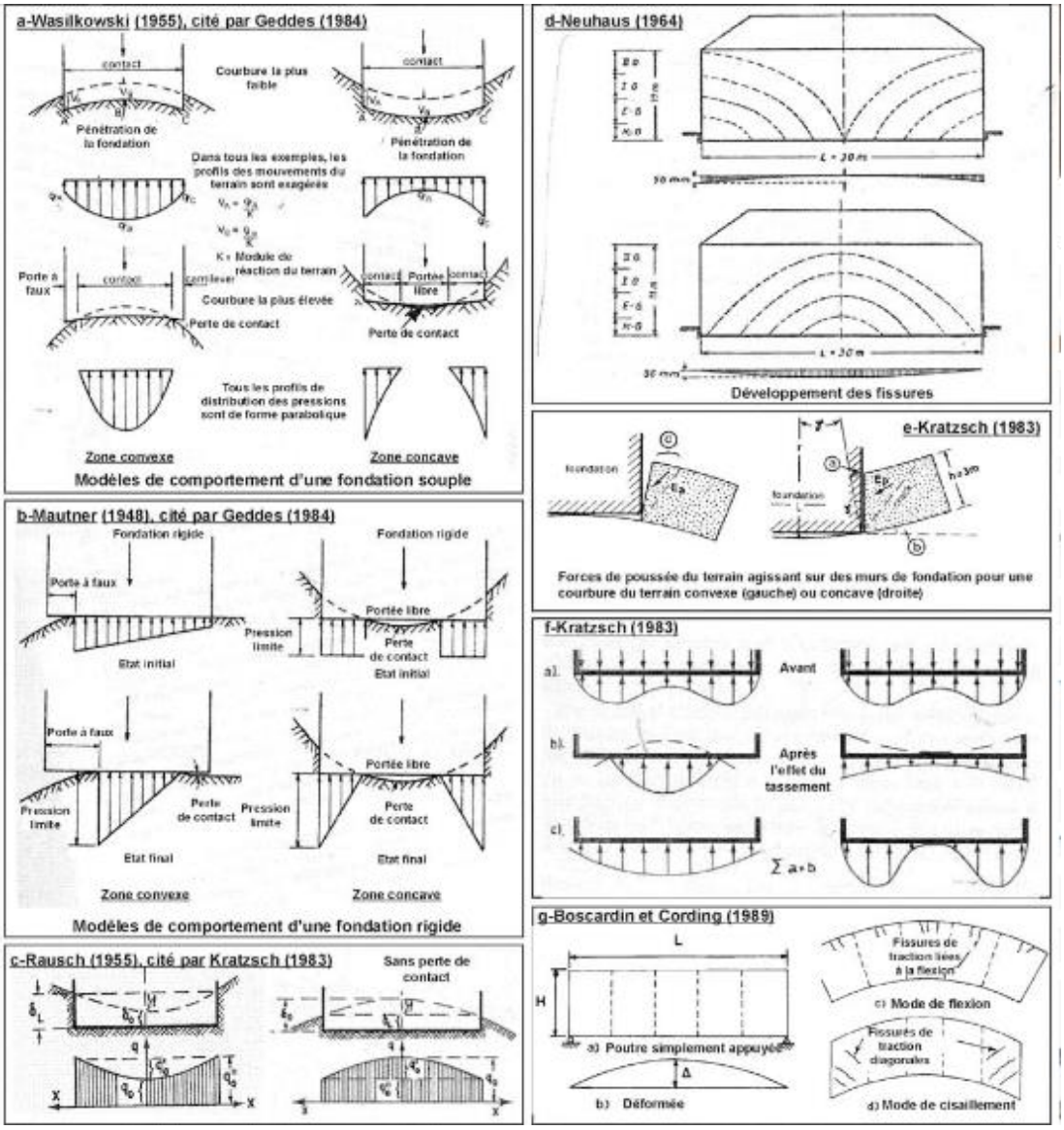


Fig. II.7 Representative illustrations of the behavior of structures versus the ground curvature according to various authors (a to g) – Deck (2002) [15].

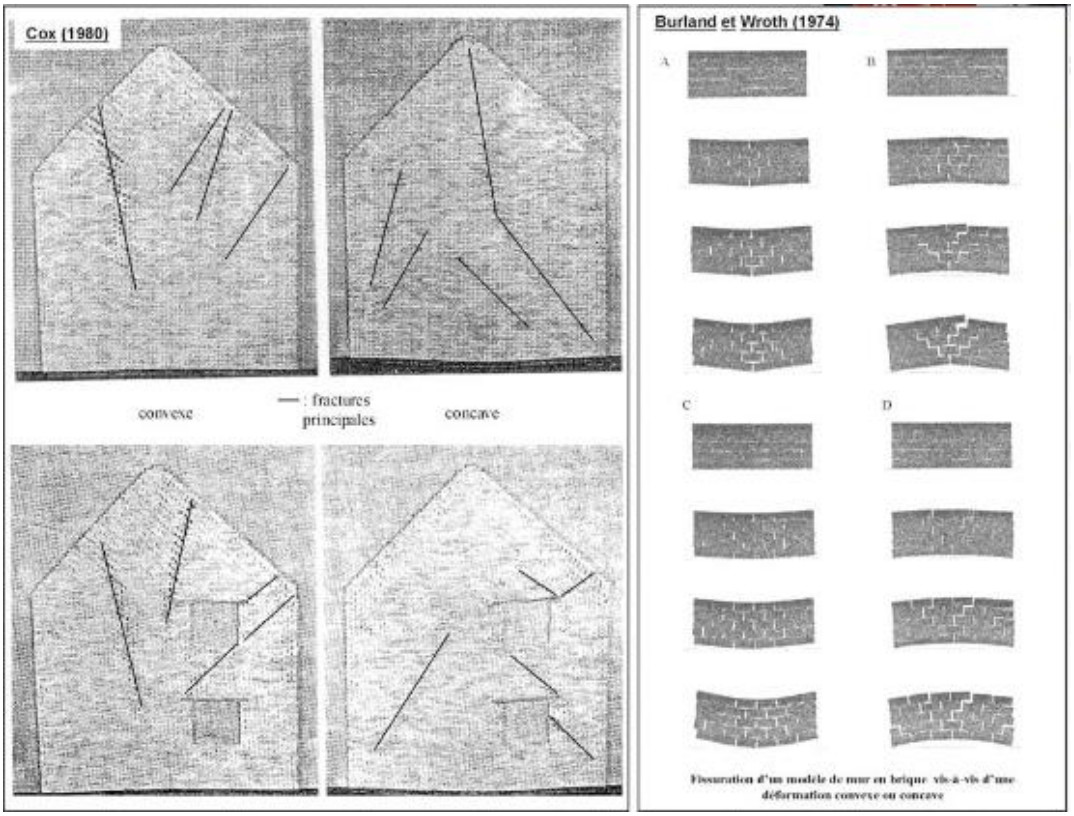


Fig. II.8 Experiments highlighting the behavior of a masonry structure and the orientation of cracking - Deck (2002)

c) Behavior of buildings versus the ground slope

A slope causes a redistribution of stresses in the soil (Fig. II.9), which become higher downstream and lower upstream below a structure.

The slope also causes a change of load path in the structure. The load-bearing elements on the side of the inclination are more compressed; it puts in tension some of these elements if the inclination is quite strong (Fig. II.9). On the side, the facades are not designed to support tension that can be the origin of a risk of collapse of the structure.

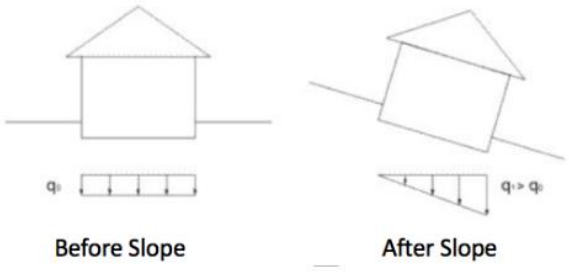


Fig. II.9 Redistribution of stresses due to the slope of the soil.

d) Global behavior of buildings

The global behavior of a building versus the accumulation of the curvature, the deformation of the ground, and the different displacements of the ground is quite delicate to explain. Some observations can be made!

- The tension zone (convex) is more likely to cause damage in the structure, because the tensile strength of the structure is generally less than the compressive strength.
- The movements that cause the main redistribution of vertical stresses in the soil are the slope and curvature of the ground.
- Most of the cracks that appear in the walls are inclined or vertical. Only compressive deformation can cause horizontal cracks.
- The influence of the typology of the building plays an important role. A flexible building has the tendency to follow the displacements of the ground, which limits the losses of supports at the level of foundations, but will cause important internal deformations which can block its use. On the other hand, if the building is stiff, it will have accumulations of stresses at the level of hard points, which can be the origin of its damage.

II.2 Soil-structure interaction / Transmission of the ground movement

A soil that is subjected to ground movements influences the above structures differently due to the interdependence of the mechanical behavior between the soil under the foundations and the structure sitting on these foundations. This interdependence is called the "Soil-Structure Interaction (SSI)"; it is strongly dependent on the stiffness of the structure as well as that of the soil (Mair (2013) [44]).

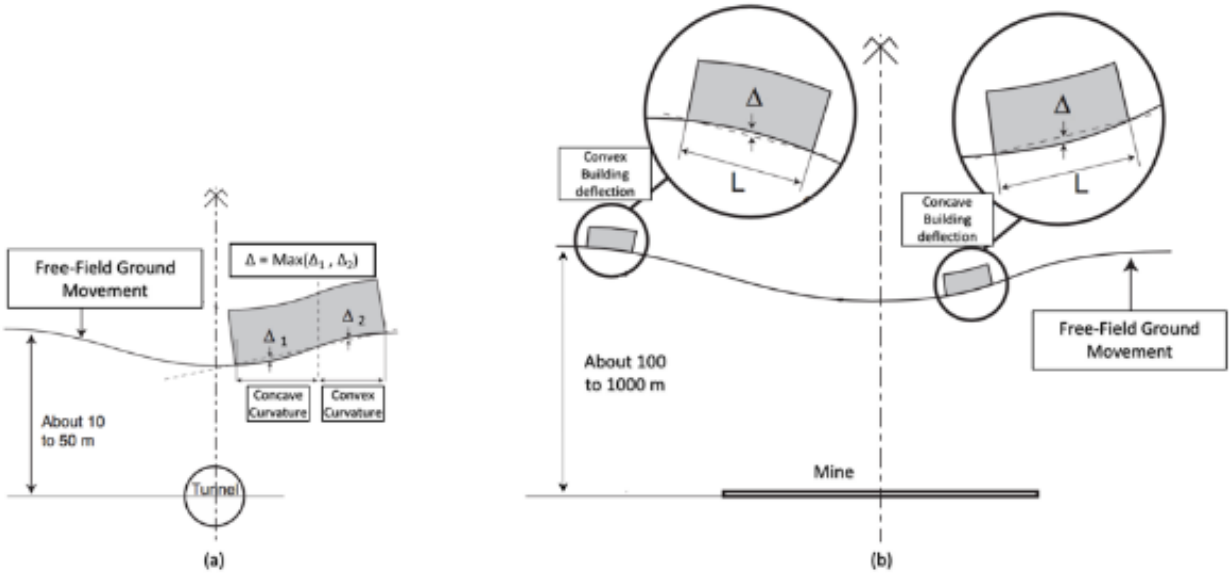


Fig. II.10. Building deflection caused by ground movements: (a) Case of tunneling. (b) Case of underground mine.

As discussed previously and shown in Fig. II.10, the free-field ground movement represents the soil displacement produced by the source (tunnel, mine, etc.), without taking into account the influence of possible constructions on the surface. In the presence of an existing structure, the free-field ground

movement is partially or totally transmitted to the building which may result in a structural or functional damage.

By neglecting the impact of the interaction between the soil and the structure (SSI), the free-field ground movements are integrally transmitted to the building. Under this assumption, Δ_0 represents the maximum deflection of the building. Assuming that free-field ground motion is symmetrical and roughly circular under the building, Δ_0 represents the maximum free-field deflection under the building (for an integrally transmitted movement); it depends upon the ground radius of curvature R and the building length L (Fig. II.11).

By considering the impact of the SSI, the ground movement may be partially transmitted to the structure which results in a building deflection characterized by its maximum value Δ with $\Delta \leq \Delta_0$. Consequently, as shown in Fig. II.12, if the structure is stiff, it can resist the ground movement and the induced deformation is limited ($\Delta < \Delta_0$); if it is flexible, then it perfectly follows the settlement of the soil ($\Delta = \Delta_0$).

For a symmetrical free-field movement with respect to the structure, the deflection Δ corresponds to the maximum differential settlement under the building. For a non-symmetrical free-field movement case, Δ represents the maximum deflection of the building whether the structure has a concave or a convex deformation (Fig. II.10-a). The Δ / L ratio, called the deflection rate, is frequently used to assess the behavior of structures subject to differential settlement and to evaluate their damage [7, 8].

The objective of this thesis is to evaluate the structure response to the ground movement through the deflection transmission ratio, defined as Δ/Δ_0, that is used to quantify the rate of movement transmitted to the building.

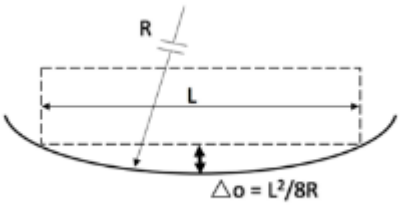


Fig. II.11. Free-field deflection Δ_0.

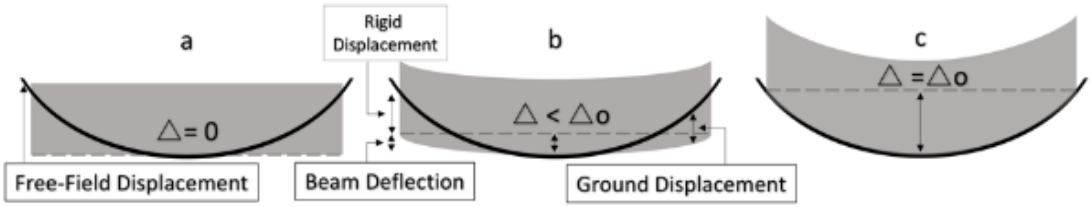


Fig. II.12. Behavior of structures subjected to ground movement. (a) High-stiffness structure on soft ground. (b) Intermediate ground and structure stiffness. (c) Flexible structure on stiff ground.

Different methods (analytical, numerical, experimental, etc.) have been developed to predict the building deflection in response to ground movements. Except empirical methods based on observations of real existing structures, all of these methods do not consider a specific study of a particular case but they are applied to simplified structures, such as beams, in order to assess the global trend of ground movements induced phenomena.

Among the approaches developed to study the SSI phenomenon, only numerical methods offer great flexibility for taking into account the complexity of the SSI conditions [6]. Although it is relatively simple to consider complex soil and structures behaviors in numerical models, their use may be criticized by the justification of the numerical values of all parameters and conditions. In addition, numerical models present difficulties to generalize results, because of the need to reproduce the same scenario numerous times, by varying a particular SSI parameter in each repetition to cover the extent of the variation range of all parameters. Thus, they can be considered as time-consuming processes [7].

To avoid these difficulties, it is possible to obtain results through analytical methods that generate simple equations that represent the structural deflection. Analytical methods may be considered as a complementary tool to the numerical ones, allowing quick calculations for a wide range of variation of parameters, without considering complex configurations [8]. In these analytical models, the soil is modelled with simple elastic stiffness elements as elastic springs. Winkler model is the simplest soil model and has been used by many investigators and by Deck and Singh (2010) [7] to address the question of the building deflection induced by ground movements and the assessment of Δ/Δ_0. The Winkler model is compared to the continuum model, as it will be shown in the next chapters, and this comparison provides comparable results.

1. Analytical modeling

Talking about analytical modeling of soil-structure interaction, two parts have to be distinguished: the soil and the structure.
In the various studies of the SSI, the structure is usually modeled by one or more beams (Euler-Bernoulli or Timoshenko) or framed structures, while the ground is modeled by different models, the simplest is the Winkler model. The widely used analytical models to represent the soil and the structure are presented below.

a) Soil modeling

(1) Winkler model

Winkler (1867) [72] assumed that the ground reaction at each point under the foundation is proportional to the deflection of the foundation at this point. This hypothesis amounts to modeling the ground by a juxtaposition of elastic springs. The proportionality constant of these springs is known as the soil reaction modulus K [N/m^3].

$$p(x) = \boldsymbol{K}\, w(x) \qquad \textit{Eq. II-3}$$

Where p(x) and w(x) represent the ground reaction and displacement respectively.

The evaluation of the soil reaction modulus K differs in the literature from one model to another. The proposed methods for estimating K values are based either on in-situ tests (plate test, consolidation test, CBR test, etc.) or on empirical relationships or theoretical relationships. By considering empirical

and theoretical relationships, laboratory and in-situ soil compression tests indicate that deformations are proportional to applied forces, as long as the test load does not exceed a certain limit. Eq. II-3 can therefore be only applied when there are small charges causing small deformations.

Determining the K value of the soil under the foundation is not simple since it does not depend only upon the nature of the soil, but also upon the dimensions of the loaded area and the foundation type. To simplify its evaluation, the soil reaction modulus can be considered as mainly dependent upon the mechanical parameters of soil (soil stiffness (Es), Poisson's ratio (υ)) and mechanical and geometrical parameters of the structure (EI, L and B) [8]. In fact, many expressions were developed to calculate this parameter. However, none of these can represent precisely the soil with all its complexity.

Biot (1937) [74] proposed a theoretical expression of the K modulus based on the study of a beam of infinite length, of known width B and subjected to a punctual force. He found the solution of this beam for the case where it rests on a half infinite elastic space (parameters Es, υ), and for the case where it rests on an elastic ground modeled by the springs of Winkler (parameter K). Biot (1937) suggested that the soil reaction modulus K can be expressed by the following equation:

$$\mathbf{K} = \frac{\mathbf{0.95}\,\boldsymbol{Es}}{\boldsymbol{B}(\mathbf{1}-\boldsymbol{v}^{\mathbf{2}})}\left[\frac{\boldsymbol{B}^{\mathbf{4}}\boldsymbol{Es}}{\boldsymbol{EI}(\mathbf{1}-\boldsymbol{v}^{\mathbf{2}})}\right]^{\mathbf{0.108}} \qquad \textit{Eq. II-4}$$

The configuration considered by Biot (infinite beam over an infinite half-space) was also studied by Vesic (1963) [73] who was looking to adjust the displacement between theoretical and analytical solutions and suggested Eq. II-5 for the determination of the reaction modulus. Vesic has shown that this solution overestimates the bending moments in the beam of the order of 6% on average and underestimates the movements and reactions by a maximum of 10%. He also observed that Winkler's hypothesis is practically satisfied in this special case.

$$\mathbf{K} = \frac{\mathbf{0.65}\,\boldsymbol{Es}}{\boldsymbol{B}(\mathbf{1}-\boldsymbol{v}^{\mathbf{2}})}\sqrt[\mathbf{12}]{\frac{\boldsymbol{B}^{\mathbf{4}}\boldsymbol{Es}}{\boldsymbol{EI}}} \qquad \textit{Eq. II-5}$$

Drapkin (1955) [75] proposed another formula for calculating the soil reaction modulus:

$$\mathbf{K} = \frac{\mathbf{0.65}\,\boldsymbol{Es}}{\boldsymbol{B}(\mathbf{1}-\boldsymbol{v}^{\mathbf{2}})} \qquad \textit{Eq. II-6}$$

On the other hand, Henry (1986) [77] proposed Eq. II-7, while Klopple and Glock (1970) [76] proposed Eq. II-8.

$$\mathbf{K} = \pi\,\frac{\boldsymbol{Es}}{\mathbf{2}\boldsymbol{B}(\mathbf{1}-\boldsymbol{v}^{\mathbf{2}})\boldsymbol{log}(\boldsymbol{L}/\boldsymbol{B})} \qquad \textit{Eq. II-7}$$

$$\mathbf{K} = \frac{\mathbf{0.65}\,\boldsymbol{Es}}{\boldsymbol{B}(\mathbf{1}-\boldsymbol{v}^{\mathbf{2}})} \qquad \textit{Eq. II-8}$$

According to Houlsby *et al.* (2005) [78], the Winkler model is simple and combines well with numerical and analytic methods. Despite the simplicity and efficiency of the model proposed by Winkler, it has two major disadvantages. First, it does not take into account the interaction between

the springs, which amounts to neglecting the vertical shear in the soil. As a result, a discontinuity of movement is created between the loaded area and the unloaded area under the foundation. Second, it does not take into account the plasticity that can occur in the field.
Several researchers have therefore proposed modifications of the Winkler model to make it more efficient by adding elements to introduce interaction between springs such as flexural elements (Hetényi (1946) [79], shear layers (Pasternak (1954) [80]), membranes under constant tension (Filonenko-Borodich, (1940) [81]). These models have another parameter that characterizes the interaction between the springs.

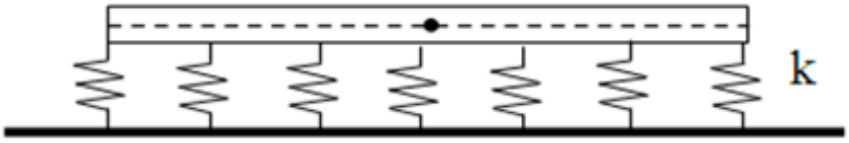


Fig. II.13 Representation of Winkler model.

(2) Filonenko-Borodich model

Filonenko-Borodich (1940) proposed a new model based on the Winkler model to provide continuity of movement between individual Winkler springs by connecting them to a thin membrane under constant tension (Fig. II.14). Taking into account the equilibrium of the membrane-spring system, then for a 2D problem the soil compaction associated with a distributed load is given by the following equation:

$$p(x)=K\,w(x) - T\,w''(x) \qquad \textit{Eq. II-9}$$

Where w is the soil displacement, K is the soil reaction modulus and T is the soil modulus of Filonenko-Borodich. So, it takes two parameters K and T to characterize this model.

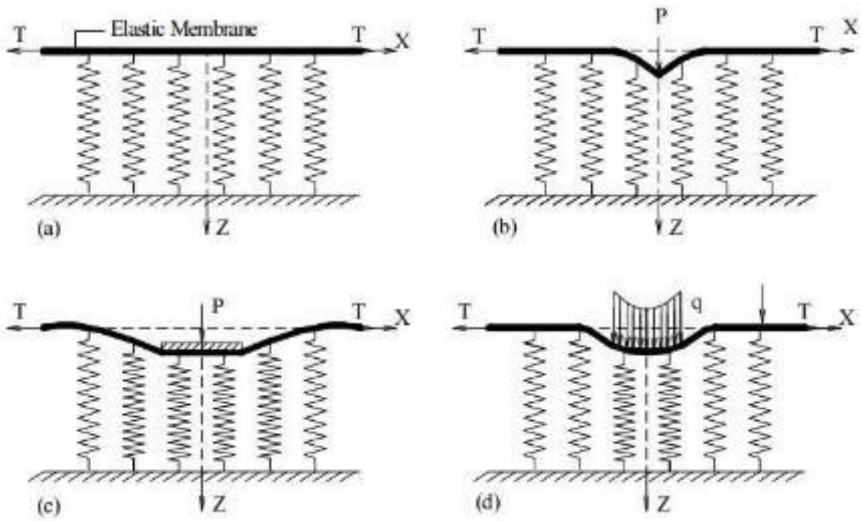


Fig. II.14 Deformation of the Filonenko-Borodich model, (a) ground without load, (b) point load, (c) point load on a stiff foundation and (d) distributed load Filonenko-Borodich (1940).

(3) Pasternak model

Pasternak (1954) also proposed a model based on the Winkler model. He hypothesized that there would be a shearing interaction between the springs, which can be accomplished by connecting the springs to a horizontal incompressible layer that deforms only in the direction of the transverse shear (Fig. II.15). Deformations and forces maintain equilibrium in the shear layer described by a Pasternak Gp modulus.
The relation between the contact pressure and the settlement of the ground, according to Pasternak, can be expressed by the following equation:

$$p(x)=K_p\, w(x) - G_p\, w''(x) \qquad \textit{Eq. II-10}$$

It should be noted that the value of the Pasternak Gp shear modulus is not the same as the soil shear modulus Gs which is defined by the following equation:

$$G_s=Es/(2(1-\nu)) \qquad \textit{Eq. II-11}$$

If Gp is different from 0, then Kp is necessarily different from Winkler modulus K; if Gp = 0, the Pasternak model is the same as the Winkler model and Kp = K.

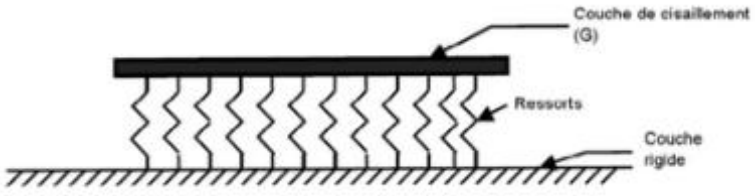


Fig. II.15 Pasternak Model

Pasternak proposed a test to find the shear modulus Gp. In the absence of experimental measurement, there are very few formulas for estimating this parameter. A new approach to estimate this parameter has been proposed by Basmaji *et al.* (2017) [8].
The proposed methodology depends on the adjustment of the ground displacement calculated by two models: the first one is based on the theory of elasticity, and the second one is based on the equations of the considered model (Pasternak).
The results were synthesized in the form of charts to facilitate their use. These parameters depend on the Young's soil modulus, the deformable soil thickness and the length of the loaded zone.
These results were validated by comparing several analytical theoretical cases with numerical models. The results showed an acceptable consistency between the results.

(4) Model of Hetényi

In the model proposed by Hetényi (1946), the interaction between the independent springs of the Winkler model is done by means of an elastic plate. The response function for this model is given by the following equation:

$$p(x)=K\, w(x) - [(Eh^3)/(12(1-\nu^2))]\, w^{(4)}(x) \qquad \textit{Eq. II-12}$$

With E the modulus of elasticity of the plate, h the height of the plate and ν the Poisson's ratio of the material constituting the plate.

(5) Kerr foundation

A shear layer is introduced in the Winkler foundation and the spring constants above and below this layer is assumed to be different as per this formulation (Kerr (1964) [82]). Fig. II.16 *Kerr foundation.* shows the physical representation of this mechanical model where k1 is the spring constant of the first layer; k2 is the spring constant of the second layer and G the shear modulus of the shear layer.

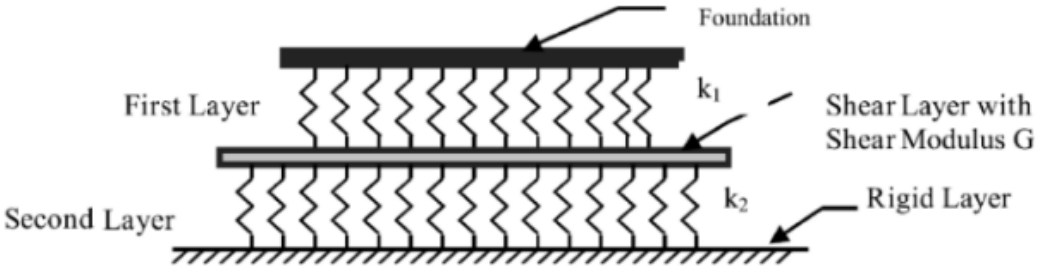


Fig. II.16 Kerr foundation.

(6) Interactive/coupled springs

As shown in Fig. II.17, Klar *et al*. (2008) [83] proposed the homogeneous continuum to represent the soil through sliders which are rigid-perfectly plastic elements with upper and lower limit forces that introduce plasticity. The homogeneous continuum is modelled with coupled vertical and horizontal springs that interact with each other. Slippage and gap formation are modelled by decoupled sliders in the horizontal and vertical directions, respectively. The displacement vector of the foundation, u, is given by:

$$u = u^c + u^{ip} \qquad \textit{Eq. II-13}$$

where u^c is the soil continuum displacement and u^{ip} the plastic interface displacement.

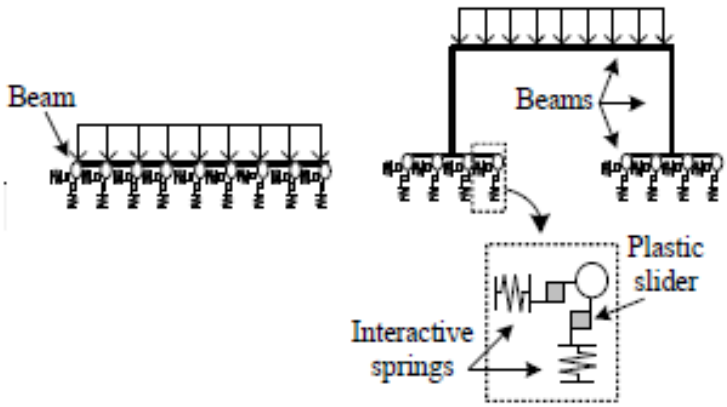


Fig. II.17 Interactive/coupled springs.

b) Structure modeling

(1) Euler-Bernoulli elastic beam

As shown in Fig. II.18, the analytical approaches developed to study soil-structure interaction phenomena generally model the building by an Euler-Bernoulli elastic beam of length "L", height "H", width "B" and Young's modulus "E". The beam is solicited by a uniform vertical load "q" and an unknown variable distribution "p (x)" which is the ground reaction. The deflection equation of the beam (without taking into account the effect of shear in the beam) is a second-order differential equation:

$$y''(x) = -M(x)/EI \qquad \textit{Eq. II-14}$$

where y (x) is the vertical displacement (positive downwards) (Fig. II.19*: Sign conventions adopted for the soil-structure interaction model.*
), M (x) the bending moment and EI the stiffness of the beam.

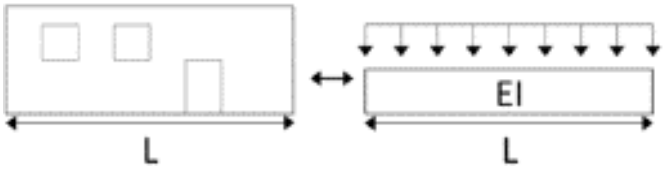


Fig. II.18: Building modeled by an elastic Euler-Bernoulli beam.

The differential equation characteristic of the frame is described by the following equation:

$$y^{(4)}(x) = (q - p(x))/EI \qquad \textit{Eq. II-15}$$

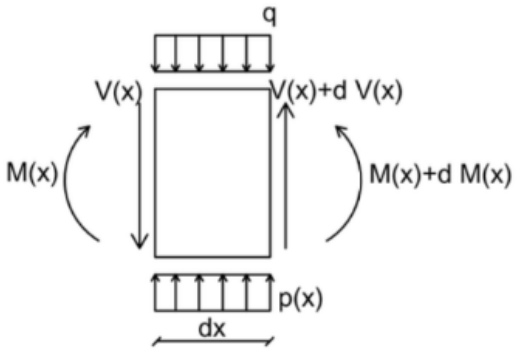


Fig. II.19: Sign conventions adopted for the soil-structure interaction model.

(2) Multi-stage framework

The multi-stage solution framework proposed by Klar *et al*. (2008) [83] is also used to model the structure in the literature where two-dimensional structures composed of Euler-Bernoulli elastic beams can be implemented, while self-weight and service loads are modelled by uniform loads distributed at

the beam axes of the superstructure. The structure is assumed orthogonal to the longitudinal tunnel axis as shown in the below figure.

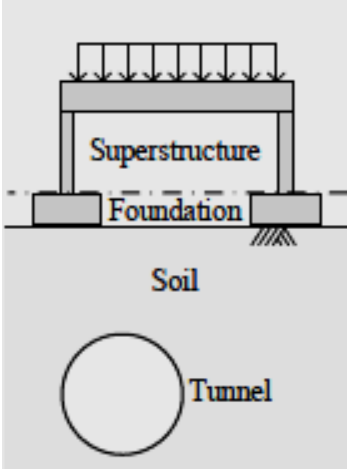


Fig. II.20: Multi-stage frame superstructure model.

(3) Timoshenko beam

One of the analytical approaches developed to study soil-structure interaction phenomena is to model the building by a Timoshenko beam in order to consider the shear deformation and rotational bending effects. As for the Euler-Bernoulli beam, a forth differential equation characterizes the beam deflection, as per the following equation:

$$EIy^{(4)}(x) = (q(x) - \frac{EI}{KAG}q^{(2)}(x)) \qquad \textit{Eq. II-16}$$

where A is the cross section area, E is the elastic modulus, G is the shear modulus, I is the second moment of area, K is the Timoshenko shear coefficient that depends on the beam geometry and q(x) is a distributed load.

Franza & DeJong (2017) presented a simplified elastic method to assess tunneling-induced deformation of simple beams, frame structures and bridges on shallow foundations (either continuous foundation or individual footings), as shown in the below figure:

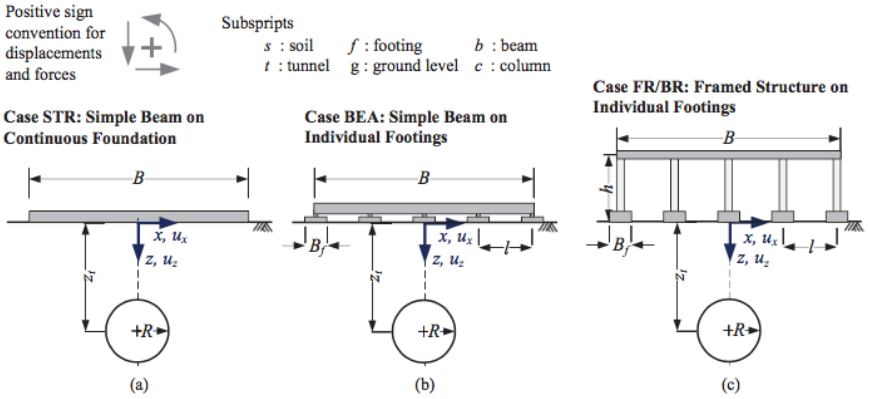


Fig. II.21: Studied configurations and used notations

According to them, the following conclusions were made:

- The foundation response to tunneling of framed structures involves a complex rotational and translational displacements.
- Simple beam structures on both continuous foundations or individual footings are sensitive to tunneling in terms of flexural deformations.
- However, modeling the structure with equivalent beam elements represent a useful preliminary assessment tool for the structural response. In particular, this tool could be used as an intermediate step prior to 3D coupled numerical modelling, when design charts based on the modification factor (which is the transmission ratio) approach are not available.

Consequently, to provide a simplified probabilistic preliminary evaluation that could be used by engineers and designers, to have a reliable assessment of the rate of the ground movement that is transmitted to structures (transmission ratio), modeling the structure by an equivalent beam can be considered as a useful tool.

2. Numerical modeling

Finite element method and finite difference method have proven to be powerful tools in modelling soil-structure interaction problems. Burland *et al.* (1977) [65] assessed the risk of damage to buildings due to tunneling and excavation and argued that neglecting the effect of the SSI would lead to an overestimate of the structural damage. Potts and Addenbrooke (1997) [6] studied numerically the influence of a circular tunnel with a diameter d = 4.146 m, located at two depths of H = 20 and 34 m, on different structures. They used a 2D numerical modeling, considering a nonlinear elastic behavior perfectly plastic for the soil, where the structure was modeled by a beam with bending stiffness EI and axial stiffness EA. Due to the fact that the transmission rate of free-field deflection Δ/Δ_0 is calculated for different values of ground and structure properties, in order to cover a large extent of relative stiffness, Potts and Addenbrooke defined the relative stiffness between the ground and the structure in bending ρ* and the axial stiffness α* as follows:

$$\rho^*_{\text{Potts}} = \frac{16EI}{EsL^4} \qquad \textit{Eq. II-17}$$

$$\alpha^* = \frac{EA}{Es(L/2)} \qquad \textit{Eq. II-18}$$

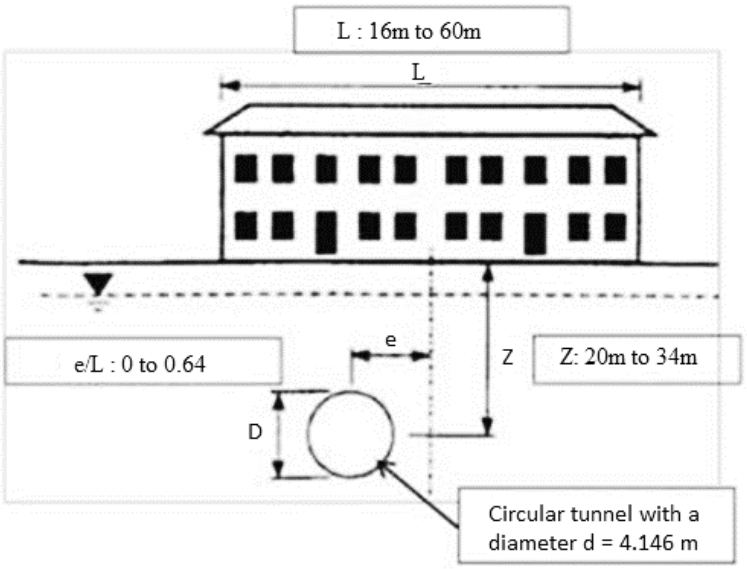


Fig. II.22 Geometry of the problem of the numerical analysis of Potts and Addenbrooke (1997)[6].

With e the distance between the tunnel and the building centerlines and Es the Young's modulus of the ground, it can be seen that α* is dimensionless (EA [N.m^2/m]) whereas the unit for ρ_{potts}* is m^{-1}, since the unit of EI is kN.m^2/m.

For each analysis, a slump profile and a horizontal displacement profile are generated.

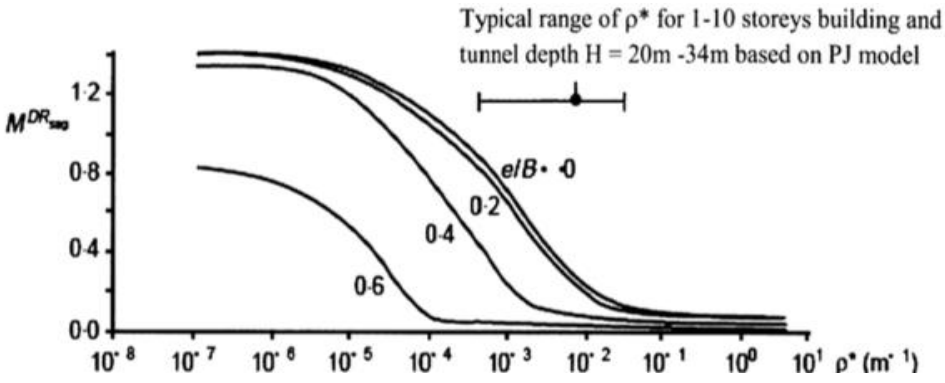


Fig. II.23 M_{sag}^{DR} deflection transmission rate (equivalent to Δ / Δ_0) versus the relative stiffness ρ (Potts and Addenbrooke (1997))[6].*

M^{DR}_{sag} is the transmission rate of the deflection, it is equivalent to Δ/Δ_0. One could expect to observe a deflection rate strictly less than or equal to 1, which is not the case of the results shown in Fig. II.23.

Franzius *et al*. (2004) [41] studied the influence of building weight (Fig. II.24). They found that this influence is relatively slight compared to the results of Potts and Addenbrooke (1997) [6]. They proved that the building stiffness controls the reduction of soil movement transmitted to the building (Figure 1-25).

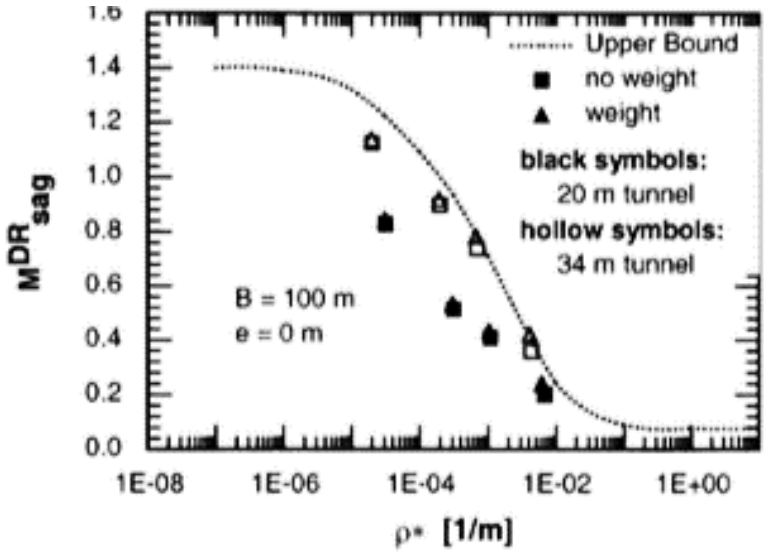


Fig. II.24 Results of Franzius et al. (2004)[41], showing the influence of building weight and building stiffness in comparison with the Potts and Addenbrooke curve (1997)[6].

On the other hand, Franzius *et al.* (2006) [40], found that the relative stiffness relation of Potts and Addenbrooke (1997) [6] overestimates the influence of the length of the building L, and that the depth of the tunnel is not taken into account in the relation of the relative stiffness of Potts and Addenbrooke. He proposed a new relationship of relative stiffness that takes into account the depth of the tunnel:

$$\rho^*_{\text{Franzius}} = \frac{EI}{EsHBL^2} \qquad \textit{Eq. II-19}$$

Where EI is the building stiffness (KN.m^2), L is the length of the building, B is its width (which is parallel to the tunnel axis), and H (or Z) is the depth of the tunnel. The new Franzius results, based on this definition of relative stiffness are shown in Fig. II.25. The expression of the relative stiffness in this equation is without unit.

In this figure, the depth of tunnel is involved in the calculation of the deflection transmission, which was neglected by Potts and Addenbrooke (1997) [6].

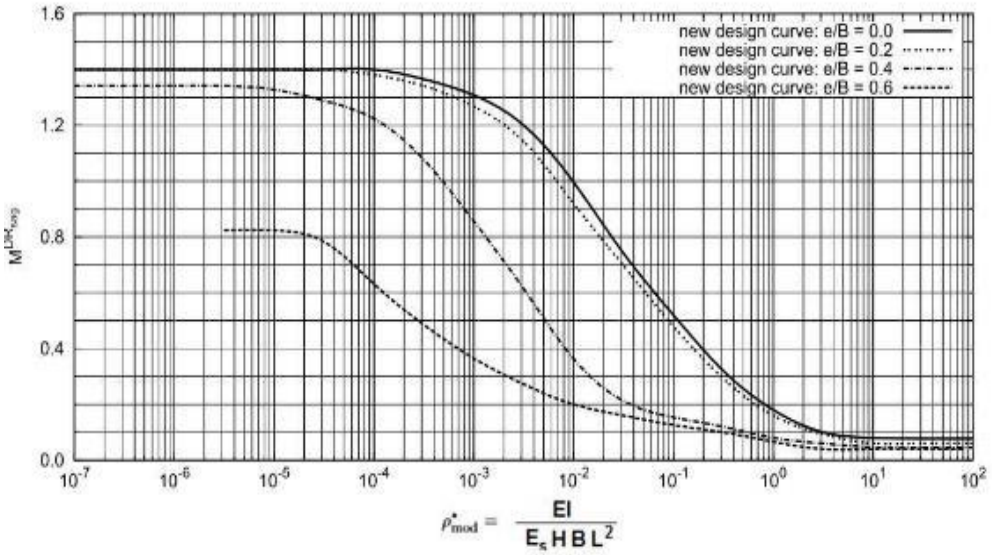


Fig. II.25 Deflection transmission rate in relation to the relative stiffness defined by Franzius et al. (2006)[40].

This relative stiffness was redefined by Goh and Mair (2011) [9] who proposed the following relationship. This relationship looks like the relationship defined by Eurocode 7 to estimate relative stiffness:

$$\rho^*_{\text{Mair}} = \frac{EI}{EsL^3} \qquad \textit{Eq. II-20}$$

Mair's relation is one of the most used relationships in the field; however it gives values of the transmission ratio that are higher than 1 which is contradictory to its definition. This relation is without unit since the unit of EI is kN.m^2/m and the building stiffness is calculated per meter.

Mair (2013) [44] retraced the numerical results of Potts and Addenbrooke (1997) and Franzius *et al.* according to his equation and compared them to experimental results. He found that the results can be grouped together as shown in Fig. II.26. Mair (2013) [44] observed that the transmission of deflection will be 1 when the relative stiffness defined by this equation is less than 10^{-4}, and 0 when this parameter is greater than 1.

On the other hand, Goh (2010) [43] has exploited results from several publications describing actual measurements for several buildings that have suffered ground movements as a result of underground work such as Mair and Taylor (2001) [36], Standing *et al.* (2002) [38], Viggiani and Standing (2002) [39], Withers (2001) [37], Dimmock and Mair (2008) [42] and Goh and Mair (2011) [9]. He was able to calculate the deflection transmission rate for these real cases based on the new relative stiffness relationships proposed by Goh and Mair (2011) [9].

The upper and lower limits of the actual results are shown in Fig. II.27. A comparison with Fig. II.26 shows that the results are close. Although consistent, these two results show that there is a great deal of uncertainty in the value of the transmission rate. As an example, it can be observed that for a relative stiffness of 0.01, it is found that the transmission rate of the deflection is between 0.2 and 0.8, which corresponds to a very large interval that is related to the presence of various sources of uncertainties.

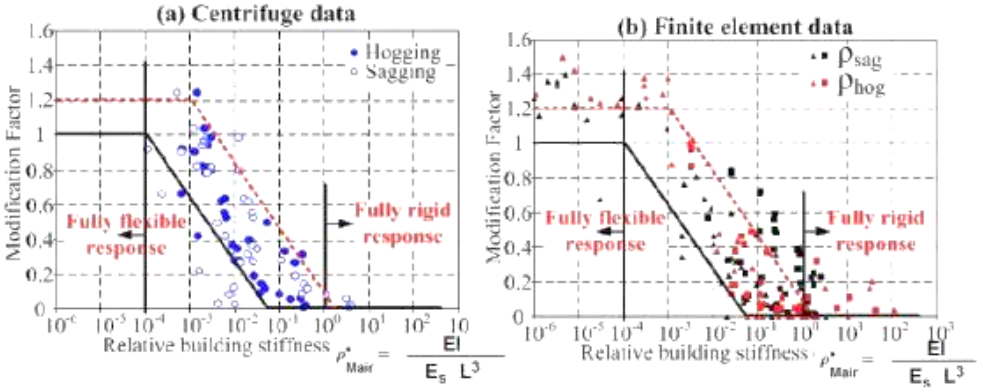


Fig. II.26 Numerical and experimental results showing the transmission rate of deflection in relation to relative stiffness according to Mair (2013) [44].

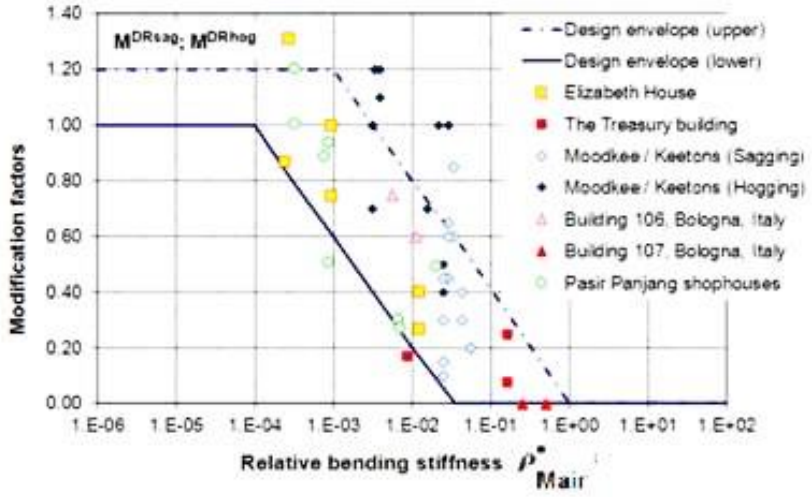


Fig. II.27 Empirical results showing the transmission rate of deflection in relation to relative stiffness according to Goh (2010)[43] and Goh and Mair (2011)[9].

3. Experimental modeling

Several physical models have been developed to analyze the effect of ground movements of different origins (tunnels, mines, excavations and mine collapses). Laefer (2001) [84], Caudron (2007) [53], Farrell *et al*. (2014) [58], Hor (2012) [51] and Nghiem (2015) [52] and others conducted research to develop physical models for the purpose of observing the influence of tunnel digging or surface mine subsidence, especially when there are buildings.

Hor (2012) [51] realized a study in INSA-Lyon and INERIS with the objective to predict the building deformations by taking the influence of the soil-structure interaction into consideration. This was achieved by performing parametric studies using an experimental approach by means of a 3D small-scale physical model under earth gravity condition. In particular the effect of building position, building weight, and relative stiffness of building and underlying soil were investigated in the soil-structure interaction study.

A Fontainebleau sand was used to represent the soil and a model in polycarbonate was used to represent a two-story masonry house (prototype). The prototype walls were masonry and the foundations were strip reinforced concrete footings embedded to the depth of 0.9 m. It contained bags of lead balls to represent the loads on the foundations (Fig. II.28).



Fig. II.28 The model polycarbonate tray type with overloading of lead balls placed in small bags to ensure good load distribution during testing.

Ngheim (2015) [52] from Grenoble University and INERIS considered the same case studied by Hor in 2012 with the objective of improving the building modeling. A second model was made of silicone since silicone shows more flexural stiffness (+ 17%) and less axial stiffness (-95%) than polycarbonate structures. The model is elastic and flexible and the results obtained were more consistent with reality. The silicone model thus appears to be a good solution for the study of soil-structure interaction but it is not representative of the initial prototype, a masonry house.

A third model combining silicone foundation and sugar block structural element is done (Fig. II.29). When applying the similarity conditions, it is noted that the height of the part of the silicone foundation is large (4 cm) in comparison to that of the walls (6 cm) which does not respect the proportion of the prototype. In addition, the dimensions of the sugar blocks are large compared to those of the actual bricks. Also, this model represents masonry with sharp joints which corresponds to a lack of cohesion between the joints. The cohesion has not been introduced and this appears difficult to achieve for the sugar blocks.



Fig. II.29 Model combining silicone foundation and sugar block structural element.

This experiment highlights the importance of the soil-structure interaction to evaluate the vulnerability of structures subjected to ground movements. The presence of the structure has modified the ground surface movements which confirmed the significant role of the relative stiffness between the structure and the soil. Also, the soil-structure interaction is variable depending on the position of the structure; the ground movements are mostly influenced by a structure centered on the axis of the tunnel (at the center of the ground curvature).

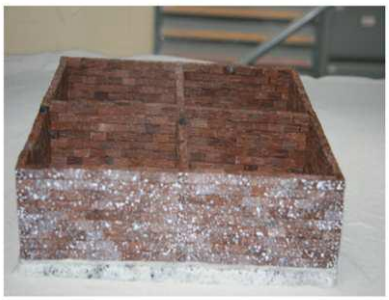


Fig. II.30 Ngheim (2015) model.

Ngheim (2015) [52] modelled the ground by the sand of Fontainebleu; for the building, the foundations are made of silicone and the walls are constructed in blocks of wood (Fig. II.30). He compared three materials to be used for walls (sugar, magnet, and wood) and presented the advantages and disadvantages as shown in the below table:

Table II-2. Advantages and disadvantages of the 3 considered materials by Ngheim (2015) [52].

	Sugar blocks	**Ferrite magnetic blocks**	**Wooden blocks**
Advantages	- Easy to find - Economical - Sufficient stiffness for the reduced scale	- Easy to manufacture according to the desired dimensions - Magnetic forces can be used to represent the cohesion of the joints	- The most massive wood found is the Azobe wood, having a weight close to a real brick - The blocks can be manufactured according to the desired dimensions
Disadvantages	- Cohesion between the joints - The minimum dimensions of the available sugar pieces that are still too large compared to the similarity conditions	- Specific weight is 5 times higher than that of a clay brick whereas the similarity imposes a factor of 1 - Magnetic forces are much greater than the cohesion of the joints and the model of the structure becomes extremely rigid	- Their disadvantages are limited compared to other materials.

Farrell *et al*. (2014) [58] carried out centrifuge tests at Cambridge University to investigate the response of surface structures to tunneling in sands. As shown in Fig. II.31, the ground was modelled by sand and the building by aluminum beams of varying stiffness. These tests were carried out under plane strain conditions at 75 g with 6.15m diameter tunnel and 8.25m sand cover. The sand was poured using an automatic sand pourer, allowing a uniform distribution of sand. The model tunnel was formed using a brass mandrill with an outer latex rubber lining. The resulting annulus between the two is filled

with water until an 82 mm diameter cylinder is obtained. So, plane strain conditions are obtained. During the test, volume losses are imposed by withdrawing the fluid from the tunnel using a piston and a motor driven actuator system. Volume losses are imposed in 0.1% increments and are determined from the ratio of the volume of fluid withdrawn to the volume of the tunnel. Digital photos were taken at each 0.1% increment, so the displacement can be measured to be related to a specific volume loss. Model structures were constructed from aluminum beams of varying thickness with a constant width (B=400mm). Each structure was placed symmetrically about the tunnel axis. A rough interface was modelled by gluing fraction E sand to the base of the structure [58].

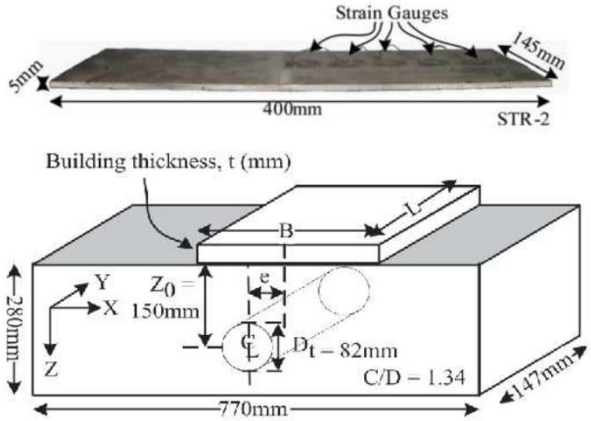


Fig. II.31 Building representation by the physical model (Farrell et al. (2014) [58]).

They found that the modification to settlement distortions is a function of both the building and the soil stiffness, in addition to the geometric parameters.

The results of the experimental studies show that estimating modification factors (transmission ratio), were found to provide moderate results to the calculated values using design charts proposed by analytical and numerical models. This shows that the design charts can be reasonably applied to practical tunneling and ground movements' projects.

4. Comparison of various SSI field data, analytical, numerical and experimental studies

A comparison is made between Mair (2013) [44] envelope and the results of various SSI studies (analytical, numerical, etc.) that also evaluate the transmission of ground movements to structures (Deck & Singh (2010) [7]; Basmaji *et al.* (2017) [8] and Franza *et al*., (2019) [5] (Fig. II.32). However, each study is based on a set of hypotheses that does not allow the generalization of the obtained results:

1. Mair (2013) [44] envelope is based on physical centrifuge modelling of building response to tunneling and his results are compared with both, the finite element analyses reported by Potts and Addenbrooke (1997) [6] and Franzius *et al.* (2006) [40], and the field data of building performance done by Goh (2010) [43].
2. Deck & Singh (2010) [7] analytical model is based on Euler–Bernoulli beam sitting on vertical springs as per the Winkler model. They plotted their results using their own definition of the

relative stiffness that is based on the Winkler coefficient of subgrade reaction (Winkler parameter k).

In fact, they defined the relative stiffness ratio ρ* by Eq. II-21 characterized by the Winkler parameter k and the structure width B. This equation is comparable to other relative stiffness ratios defined in the literature; it presents the advantage of being a non-dimensional parameter (EI [N.m^2], K [N/m^3]) and suitable to have a synthetic representation of Δ/Δ_0 based on Winkler model.

$$\rho^* = \frac{EI}{kBL^4} \qquad \textit{Eq. II-21}$$

In order to make the comparison between Deck & Singh (2010) model, based on their own relative stiffness ratio, and other models, Vesic (1963) formula (Eq. II-5) is used to define values for k in the case of a foundation with length L, width B (with L>B) and a ground characterized by a Young's modulus Es and a Poisson's ratio υ. In this case B is taken equal to 1m, which approximatively corresponds to the width of a building foundation. Noting that various formulas link the Winkler modulus to the soil Young modulus (as discussed previously), Vesic's formula is chosen since it takes into account the presence of a beam (through the "EI" term) contrary to other formulas.

3. Basmaji *et al.* (2017) [8] developed a new approach to assess the transmission ratio and the building response to differential settlements, considering the influence of shear deformation. Their model is based on both, Pasternak and Winkler soil models. For both soil models, a methodology has been implemented to justify the parameters values, k (Winkler parameter) and Kp and Gp (Pasternak parameters), as a function of the elastic properties of the soil, the thickness of the compressive ground layer and the building length. Their methodology considered Flamant's theoretical solution of induced vertical settlement to adjust the displacement for Pasternak and Winkler methods in order to justify the parameters values for both methods.
4. Franza *et al.* (2019) [5] methodology is based on elastic and elastoplastic continuum solutions that consider the structure as an equivalent simple beam, assuming that the free-field settlement is given by a standard Gaussian curve (contrary to other models that give elastic solutions based on a polynomial free-field settlement). They proposed a formulation that accounts for the change in settlement trough shape and compared it with numerical, experimental and field data from previous research.

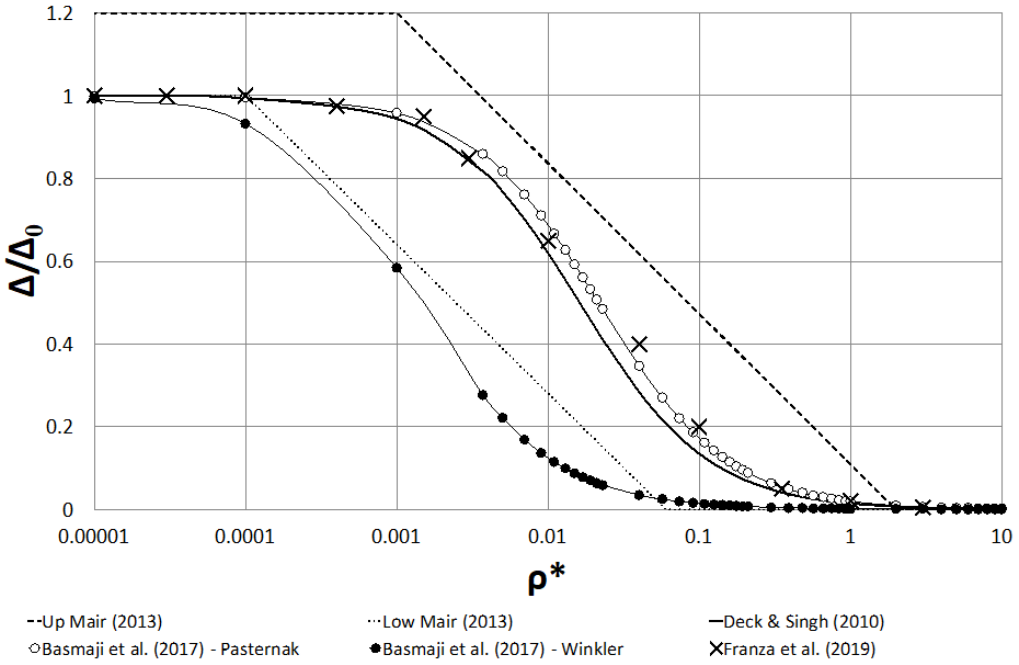


Fig. II.32 Comparison between various SSI models.

As shown in the picture above, even-tough the results of SSI studies are globally consistent in the literature, the comparison shows a large margin of discrepancy in the estimation of the transmission of the ground movements to structures. An important portion of this discrepancy may be explained by the influence of uncertainties [8, 14]. In fact, Deck & Singh (2010) [7]; Pasternak-Basmaji *et al.* (2017) [8]; and Franza *et al*. (2019) [5] analytical models present comparable results. Thus, these three models can be reasonably used to evaluate the transmission ratio; however, in comparison with numerical and experimental results and with empirical observations, the margin of discrepancy may reach ± 0.3 in the estimation of Δ/Δ_0. Consequently, this thesis aims to investigate the influence of uncertainties affecting the estimation of Δ/Δ_0 and propose a coefficient that considers their influence on the prediction of the structure response.

II.3 Uncertainties affecting the transmission of ground movements

1. Uncertainties Categories

The evaluation of the transmission ratio Δ/Δ_0 shows a significant margin of discrepancy that may be interpreted as the consequence of the uncertainties that affect its estimation. Various studies have focused on the treatment of uncertainty in geotechnical structures [85, 86]. Uncertainties that are related to SSI properties can fall into three major categories [87]:

1. Natural variability that is associated with the “inherent” randomness of natural processes, manifesting the variability over time (temporal variability), over space (spatial variability), or over both time and space. For example, the spatial variability of the soil stiffness under the building falls under this category.

2. Knowledge uncertainty that is attributed to lack of data or of information about events and processes, or lack of understanding of physical laws that limit the ability to model the real case. It is just a more common description of epistemic uncertainty.
3. Model uncertainty that corresponds to the degree to which a chosen mathematical model accurately reproduces reality. For example, the uncertainty related to the structure modeled by an Euler-Bernoulli beam characterized by one homogeneous value of its stiffness falls under this category.

2. Uncertainties Modeling

On the other hand, the majority of studies represent uncertainty by a probability theory, thus assuming that ignorance of soil-structure properties is of a random nature [88]. It is important to note that a useful tool is to develop a meta-model in order to quantify the influence of uncertainties relating the variability of these parameters to the transmission of the ground movement. In fact, since a probabilistic study requires a significant number of simulations, and the analytical approaches are based on a set of complex equations with the corresponding complex conditions to be solved involving time and computation constraints, meta-modeling is considered as an effective technique to evaluate the variability of parameters

The "basic random variables theory" may be used to model the uncertainty of the SSI properties through the Monte-Carlo simulations. This method compels the effect of the uncertainties on the input data of a model to determine the effect of a certain uncertainty on the result obtained by this model. To use the Monte-Carlo method, it is necessary to have probability distribution functions with corresponding characteristics (normal, lognormal distribution, etc.) for the input data [89]. Therefore, the developed approach for approximating the SSI parameters uncertainties is done by using estimates based on published values which are conveniently expressed in terms of the coefficient of variation (COV).

3. Confidence Intervals

Confidence intervals contain the true values of the unknown output considering the variability of the input parameters. El Kahi *et al.* [90] took the SSI parameters variability into consideration and they developed confidence intervals that contain the true values of the unknown transmission ratio versus the relative stiffness. The desired level of confidence is set between 70 and 95% and practicing engineers can directly refer to these intervals in their design considering these uncertainties affecting the SSI. A level of confidence of 70% corresponds to considering $\pm \sigma$ which may be risky; however, a 95% level of confidence corresponds to $\pm 2\sigma$.

On the other hand, model uncertainties (model and knowledge uncertainties such as the settlement shape, the building position, etc.) were also evaluated by El Kahi *et al.* [90] using a coefficient A that is correlated to the deterministic approach. For practical purposes, this coefficient can be used by engineers and designers when evaluating the transmission of ground movements to structures taking into consideration these uncertainties.

4. Sensitivity Analyses

To quantify the relative importance of each input parameter of a model on the variability and uncertainty of responses, a sensitivity analysis (SA) method is selected. In order to compare the results according to various sensitivity analysis approaches, various methods can be evaluated that correspond to local or global methods (Table II-3).

Table II-3 Comparison between local and global methods.

Local methods	**Global methods**	
- Evaluate the change in output as each parameter is individually varying by fixing all other parameters	- Quantify the contribution of each input parameter on the variability of the response in the entire domain of variation	
One-Way Sensitivity Analysis	**Sobol Indices**	**McKay Method**
- Monte-Carlo simulations - Evaluate the mean μ and the standard deviation σ of the output	- Sampling is based on Monte-Carlo simulations - Not valid if there is a dependence between input variables (various studies developed Sobol method to consider the parameters dependence [25]) - Consider the interaction between the input parameters through first, intermediate and total indices	- Sampling is based on Replicated-Latin Hypercube Sampling - Valid even if there is a dependence between input variables - Characterized by the first order sensitivity index estimating the variance of the output produced by the influence and the variation of an input parameter - Relatively rapid results compared to Sobol

1. One-way sensitivity analysis using probabilistic distributions which examines the effect of the variability of the input on the output. Consequently, this local sensitivity test examines the change in output as each parameter is individually varying according to its mean μ (Eq. II-22), standard deviation σ (Eq. II-23), and distribution function, so it can take into account the parameter variability and the associated influence on model output [91].

$$\mu = \frac{1}{n}\sum_{i=1}^{n} x_i \qquad \textit{Eq. II-22}$$

$$\sigma = \sqrt{\frac{\sum_{i=1}^{n}(x_i - \mu)^2}{n-1}} \qquad \textit{Eq. II-23}$$

2. Sobol method which is a common SA technique based on variance. It is characterized by its indices such as the first order and the total indices: the first-order sensitivity Si represents the variance of the output Y, as a function of the input parameter Xi ($var\ (E\ [Y|Xi]$)). The total

order index STi measures the contribution to the output variance of Xi ($var(X_i\ [Y|X_{-i}])$ is the variance of model outputs that results from all except the ith parameter), including all variances caused by its interactions with other input variables. If the differences between the first order indices and the total indices are significant, it means that the effect of the interactions between the variables is not negligible and it can then be useful to estimate the indices of intermediate orders [89].

$$S_i = \frac{var(E\ [Y|X_i])}{var\ (Y)} \quad \textit{Eq. II-24}$$

$$ST_i = \frac{E_{X_{-i}} var(X_i\ [Y|X_{-i}])}{var\ (Y)} \quad \textit{Eq. II-25}$$

3. McKay's (1995) method for estimating first order sensitivity indices which is based on replicated-Latin Hypercube Sampling (r-LHS). This technique consists of creating r replications of each sample of size N obtained by the LHS method and for each random input parameter Xi. If the input parameters are considered as independent, the replications can be obtained by randomly and independently switching the N values of each variable [89]. The first-order sensitivity index associated with each variable Xi is obtained by fixing the values $x_{i,j}^k$ for all the replications k = 1 … r (r is the total number of replications) such that $x_{i,j}^1 = x_{i,j}^2 = \cdots = x_{i,j}^r = x_{i,j}^*$ for all $1 \le j \le N$. The samples $y_{i,j}^k = \text{f}(x_{1,j}^k, \dots, x_{i,j}^*, \dots, x_{p,j}^k = x_{i,j}^*)$ given by the conditional law of $Y|Xi = x_{i,j}^*$ can thus be evaluated. The conditional and non-conditional averages can respectively be estimated by:

$$E\langle Y|X_i = x_{i,j}^*\rangle = \bar{y}_{i,j} = \frac{1}{r}\sum_{k=1}^{r} y_{i,j}^k \quad \textit{Eq. II-26}$$

$$E(y) = \bar{y} = \frac{1}{n}\sum_{j=1}^{n} \bar{y}_{i,j} \quad \textit{Eq. II-27}$$

The sensitivity index of the variable Xi can be estimated by:

$$S_i = \frac{r\sum_{j=1}^{n}(\bar{y}_{i,j} - \bar{y})^2}{\sum_{j=1}^{n}\sum_{k=1}^{r}(y_{i,j}^k - \bar{y})^2} \quad \textit{Eq. II-28}$$

In the following, a demonstrative example is presented to show the procedure of local and global sensitivity analysis methods [93]. The selected trial function is Eq. II-29

$$f(x) = x_1 + x_2 {x_3}^2 \quad \textit{Eq. II-29}$$

Steps for the one-way sensitivity analysis implementation [91]:

1. Select the total number of simulations to be performed.
2. Select the parameters for sensitivity analysis. In this case these are x_1, x_2 and x_3
3. Assume ranges for test variables: x_1 = [0,1000]; x_2 = [0,100]; and x_3= [0,10]

4. Choose a distribution for each of the parameters. In this case a normal distribution is chosen for all three parameters with $\mu_{x_1} = 500$, $\mu_{x_2} = 50$, $\mu_{x_3} = 5$ and a similar coefficient of variation, COV=10%.
5. For each parameter (x_1, x_2 and x_3), evaluate the mean μ and the standard deviation σ of $f(x)$ as per Eq. II-22 and Eq. II-23 by fixing the values of all except that parameter.
6. Compare the standard deviation σ of $f(x)$ for each evaluation

Steps for Sobol implementation [89]:

1. Repeat the first 4 steps of the the one-way sensitivity analysis
2. Compute the variance of the first order index for each parameter by fixing the values of that parameter and varying the remaining parameters as per Eq. II-24.
3. Compute total sensitivity effects for the every parameter using Eq. II-25 by evaluating the variance of the mean of the output conditionally to all variables except that parameter. It is then estimated as per the first index, except that instead of varying all the variables except the evaluated parameter, this parameter is the only one varying.

Steps for McKay implementation [89]:

1. Repeat the first 4 steps of the the one-way sensitivity analysis
2. From an N-sample created according to the Latin hypercube sampling plan, create r replications by independently and randomly permuting the N values of each variable. The combination of these r replications will give N × r samples for each variable.
3. Compute the variance of the McKay index for each parameter as per Eq. II-28.

The trial function was calculated for 10,000 iterations and the effects of the parameters are shown in Table II-4.

Table II-4. Sensitivity analysis results.

	One-Way Method $\mu(f(x))$	One-Way Method $\sigma(f(x))$	Sobol Method $S_{i(Sobol)}$	Sobol Method $ST_{i(Sobol)}$	McKay Method $S_{i(McKay)}$
x_1	1750.77	49.9181	0.028	0.029	0.0304
x_2	1753.05	126.971	0.187	0.193	0.187
x_3	1761.28	247.629	0.774	0.782	0.757

It was found that parameter $x_1$was the least sensitive parameter and x_3 was found to be the most sensitive parameter. x_3 has around 5 times higher effect than x_1 and around 2 times higher effect than x_2. This is clearly revealed by comparing the standard deviation σ of the one-way method. Also, for Sobol and McKay methods, since they are based on the variance σ^2, it is found that $\sqrt{S_{i(x_3)}} \approx 2\sqrt{S_{i(x_2)}} \approx 5\sqrt{S_{i(x_1)}}$.

In terms of Sobol total effects, it is also shown that the total indices of are quite close to first order indices, then there is not much interaction going on between parameters.

II.4 Conclusion

Based on the literature, taking the soil structure interaction into account is fundamental to evaluate the transmission of ground movements to structures. This chapter has presented a synthesis of the knowledge on various elements establishing the basis of this thesis: the free-field ground movements, their sources and their effects on buildings, the structure response, behavior and damage, the different approaches used to evaluate this phenomenon and the uncertainties affecting the transmission process and their evaluation.
In the next sections, an exhaustive study is presented of the identification and the evaluation of uncertainties through five papers. As shown in Fig. II.33, the transmission of ground movements to structures is a process full of uncertainties that can affect:

- The first step, between the source (mining, tunneling, etc.) and the free-field response: These uncertainties may be related to the source by itself (considering tunneling for example, the construction procedure and multiple stages duration, rate of deconfinement, evaluation of volume loss) or to the soil geology and mechanical properties, etc.
- The second step, the transmission of movement between the soil and the structure due to the SSI: Various uncertainties may be presented that are related either to the approach (analytical (equations, simplified hypotheses, SSI representative model, etc.), experimental (scale factor, material choice, etc.)), either to the model conditions (building position, soil profile, etc.), either to the knowledge (spatial variability of soil and building stiffness, etc.) either to the variability of parameters (probabilistic distribution of SSI parameters).
- The third step, the structure response and damage: These uncertainties are mainly related to the damage evaluation methods and post-damage variation of SSI properties.

Since the level of damage depends mainly on the transmission of ground movements due to the SSI, this study focuses on the second step, shown in Fig. II.33.
To evaluate the structural response to ground movements, the determination of the deflection transmission ratio is the key parameter used in this study. In particular, an exceptional concern is given to the cases of masonry structures subjected to mining subsidence settlement, since the risks due to mining subsidence extend over large regions of the Lorraine iron basin, where two thousand hectares of urbanized areas and twelve thousand hectares of non-urbanized areas were affected by this risk in the year 2000 [61]. This ratio strongly depends on SSI characteristics and modeling [92]. The uncertainties related to these parameters affect the estimation of the transmission ratio. Consequently, different sources of uncertainties that need to be considered are evaluated in the next chapters.

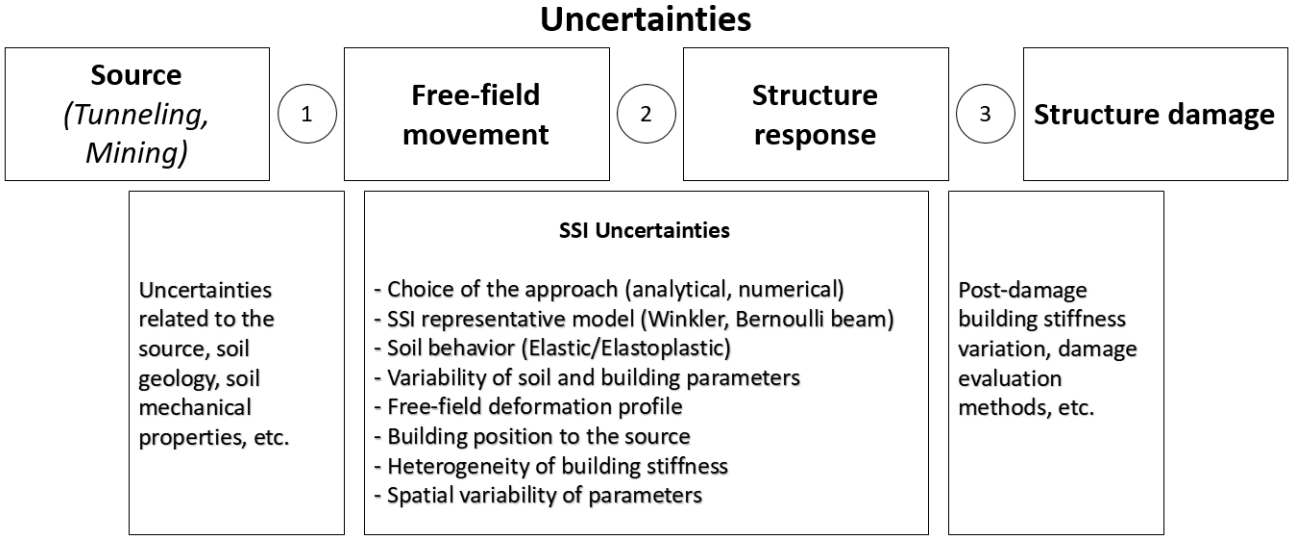


Fig. II.33: Uncertainties affecting the transmission of ground movements due to SSI.

II.5 References

[1] Soots P. Le phénomène des affaissements miniers et la prévention de ses consequences dommageables. *Cahier du CSBT*, 1969, 96, Cahier 836.

[2] Kawulok M. The protection of existing buildings subjected to large ground movements - *Proc. of the 4th int. conf. on ground movement and structures.* Pentech press (Londres), 1992, pp. 344-355.

[3] Niemic. Annulation des conséquences des déformations de la surface consécutives à une exploitation souterraine (traduit du polonais : "Usuwanie skutkow deformacji terenu powstalych w wyniku prowadzenia eksploatacji podzienmnej") - Konferencja naukowo techniczna, 2001.

[4] Haji, K., Marshall, A., & Franza, A. Mixed empirical-numerical method for investigating tunneling effects on structures. *Tunnelling and Underground Space Technology*; 2018, 73: 92-104.

[5] Franza, A., Ritter, S. & Dejong, M. Continuum solutions for tunnel-building interaction and a modified framework for deformation prediction. *Géotechnique;* 2019: 1-15.

[6] Potts, D. & Addenbrooke, T. A structure's influence on tunneling-induced ground movements. *Proceedings of the Institution of Civil Engineers – Geotechnical Engineering*; 1997, 125: 109–125.

[7] Deck, O. & Singh, A. Analytical model for the prediction of building deflections induced by ground movements. *International Journal for Numerical and Analytical Methods in Geomechanics*; 2010, 36: 62-84.

[8] Basmaji, B., Deck, O., & Alheib, M. Analytical model to predict building deflections induced by ground movements. *European Journal of Environmental and Civil Engineering*; 2017, 10: 1-23.

[9] Goh K.H. & Mair R.J. Building damage assessment for deep excavations in Singapore and the influence of building stiffness. *Geotech. Eng. J. SEAGS AGSSEA* 2011, 42 (3).

[10] Aissaoui, K. Amélioration de la prévision des affaissements dans les mines à l'aide des approches empiriques, numériques et analytiques-*Doctorate thesis, Institut National Polytechnique de Lorraine, Nancy, France*; 1999.

[11] Farrell R.P. et Mair R.J., (2012). Centrifuge modelling of the response of buildings to tunnelling. In: Seward, L. (Ed.), Physical Modelling in Geotechnics, *Proceedings of the 7th International Conference on Physical Modelling in Geotechnics, Vol. 2. CRC Press, Zurich, Switzerland*, 2012, pp. 549–554.

[12] Hassoun, M., Villard, P., Alheib, M. & Emeriault, F. Soil Reinforcement with Geosynthetic for Localized Subsidence Problems: Experimental and Analytical Analysis. *International Journal of Geomechanics*. 2018, 18 (10).

[13] National Coal Board - Subsidence engineer's handbook, 1975.

[14] ElKahi, E., Khouri, M., Deck, O., Rahme, P., & Mehdizadeh, R. Studying the Influence of Uncertainties on the Transmission of Ground Movements Affecting the Soil-Structure Interaction. *10èmes journées Fiabilité des Matériaux et des Structures, Bordeaux, France*; 2018.

[15] Deck, O. Étude des conséquences des affaissements miniers sur le bâti. *Doctorate Thesis, École des Mines Nancy*; 2002.

[16] Saeidi, A. La vulnérabilité des ouvrages soumis aux aléas mouvements de terrains : développement d'un simulateur de dommages-*Doctorate thesis, Institut National Polytechnique de Lorraine, Nancy, France*; 2010.

[17] Wagner H., Schümann E.H.R. - Surface effects of total coal-seam extraction by underground mining methods - *J.S. Afr. Inst. Min. Metall*., 1991, 91 (7), pp.221-231.
[18] Dias, D. Renforcement du front de taille des tunnels par boulonnage - etude numerique et application a un cas reel en site urbain. *Doctorate Thesis,Institut national des sciences appliquees de Lyon*, 1999.
[19] Kratzsch H. Mining Subsidence Engineering, Springer-Verlag, 1983.
[20] G. Everling and O. Jacobi, "Longwall mining in Germany: Rock pressure and design of mine layouts," *Proceedings of the 6th International Strata Control Conference*, Nos. 1 and 2, 1977.
[21] Konak, Onargan, Aksoy, Kose, Tatar, Pamukcu. Determination of immediate roof at mines of the Kutahya-Omerler coal basin, Turkey. *Journal of Mining Science*, 2006, 42 (2).
[22] Sahua, Lokhandeb. An Investigation of Sinkhole Subsidence and its Preventive Measures in Underground Coal Mining. *Procedia Earth and Planetary Science*. 2015 (11) pp. 63-75.
[23] El Kahi, E., Deck, O., Khouri, M., Mehdizadeh, R. & Rahme. P. Étude de l'influence de la plasticité du sol sur la transmission des mouvements du sol affectant l'interaction sol-structure. *Revue Française de Géotechnique*. 2018, 156, 4.
[24] Broms, Bennermark. Stability of clay at vertical opening. *Journal of the Soil Mechanics and Foundations Division*, 1967, 93(1):71–94.
[25] Franza. Tunnelling and its effects on piles and piled structures, *Doctorate Thesis, University of Nottingham*, 2016.
[26] Leca, E., New, B., and Reporter, G. Settlements induced by tunneling in Soft Ground. *Tunnelling and Underground Space Technology*, 2007 22(2):119–149.
[27] Mair, R. J. Centrifugal modelling of tunnel construction in soft clay. PhD Thesis Cambridge University, 1979.
[28] Kimura, T. and Mair, R. J. Centrifugal testing of model tunnels in soft clay. *Proceedings of the 10th international conference on soil mechanics and foundation engineering*, 1981:319–322.
[29] Davis, E. H., Gunn, M. J., Mair, R. J., and Seneviratine, H. N. (1980). The stability of shallow tunnels and underground openings in cohesive material. *Géotechnique*, 1980, 30(4):397–416.
[30] Mair, R. J. and Taylor, R. N. Theme lecture: Bored tunnelling in the urban environment. In *14th International conference on soil mechanics and foundation engineering*, Hamburg. Balkema, 1999 pages 2353–2385.
[31] Potts, D. M. Behaviour of lined and unlined tunnels in sand. *Ph.D. thesis, Cambridge University*, 1976.
[32] Loganathan, N. and Poulos, H. G. Analytical prediction for tunneling-induced ground movements in clays. *Journal of Geotechnical and Geoenvironmental Engineering*, 1998, 124(9):846–856.
[33] Rowe, R. and Kack, G. A theoretical examination of the settlements induced by tunnelling: four case histories. *Canadian Geotechnical Journal*, 1983, 20(2):299–314.
[34] Marshall, A. M. Tunnelling in sand and its effect on pipelines and piles. *Ph.D. Thesis, Cambridge University*, 2009.
[35] Zhou, B. Tunnelling-induced ground displacements in sand. *Ph.D. Thesis, University of Nottingham*, 2014.
[36] Mair, R. J. and Taylor, R. N. (2001). Elizabeth House: settlement predictions. In Building Response to Tunnelling: Case Studies from Construction of the Jubilee Line Extension, 2001 (1), pages 195–215, London, United Kingdom. Thomas Telford.
[37] Withers A.D. (2001). Surface displacement at three surface reference sites above twin tunnels through the Lambeth Group. Chapter 37 of:Burland, J.B., Standing, J.R. & Jardine, F.M. Building response to tunneling. 2001 (2).
[38] Standing JR. Elizabeth House, Waterloo, Building response to tunnelling: case studies from the Jubilee Line Extension, London: volume 2: case studies, Editors: Burland, Standing, Jardine, Publisher: CIRIA and Thomas Telford, 2002: 547-612.
[39] Viggiani G. and Standing JR. The Treasury, Building response to tunnelling: case studies from the Jubilee Line Extension, London: volume 2: case studies, Editors: Burland, Standing, Jardine, Publisher: CIRIA and Thomas Telford, 2002: 401-432.
[40] Franzius, J., Potts, D. & Burland, J. The response of surface structures to tunnel construction. *Proceedings of the Institution of Civil Engineers, Geotechnical Engineering*; 2006, 159: 3–17.
[41] Franzius J.N., Potts D.M., Addenbrooke T.I. and Burland J.B. The influence of building weight on tunnelling-induced ground and building deformation. *Soil Found*. 2004 (1), 25–38.
[42] Dimmock P. and Mair R. Effect of building stiffness on tunnelling-induced ground movement. *Tunnelling and Underground Space Technology*, 2008, 438–450.
[43] Goh K. Response of Ground and Buildings to Deep Excavations and Tunnelling-*Doctorate Thesis, University of Cambridge*, 2010.

[44] Mair, R. Tunneling and deep excavations: Ground movements and their effects. *Proceedings of 15th European conference on soil mechanics and geotechnical engineering geotechnics of hard soils – weak rocks*; 2013, 4: 39-70.

[45] Peck, R. 1969. Deep excavations and tunnels in soft ground. *Proceedings of the 7th International Conference on Soil Mechanics and Foundation Engineering, Mexico City, State of the Art Volume*; 1969: 225–290.

[46] Pinto, F. and Whittle, A. J. Discussion of "Elastic solution for tunneling-induced ground movements in clays" by K. H. Park. International Journal of Geomechanics, 2006, 6(1):72–73.

[47] Neaupane K.M and Adhikari N.R. Prediction of tunnelling-induced ground movement with the multi-layer perceptron - Tunelling and Underground Space Technology 2006, 21: 151-159.

[48] Serratrice J.F. et Magnan J.P. Analyse des tassements de surface pendant le creusement du tunnel nord de la Traversée Souterraine de Toulon, *Bulletin des laboratoires des Ponts et Chaussées*, 237, mars-avril 2002, pp. 5- 36.

[49] Fayad, A. Modélisation numérique et analytique de la montée de cloche des carrières à faible profondeur. Etude de l'interaction sol-structure due aux mouvements de terrains induits par des fontis. *Thèse, Institut National Polytechnique de Lorraine, France, 2004*.

[50] Vachat J. Les désordres survenant dans les carrières de la région parisienne. *Mémoire de diplôme d'ingénieur CNAM, Paris*, 1982.

[51] Hor B. Évaluation et réduction des conséquences des mouvements de terrains sur le bâti : approches expérimentale et numérique, *Thèse INSA Lyon, France*, 2012.

[52] Nghiem L. Evaluation des dommages induits par des mouvements de terrain sur des structures en maçonnerie à l'aide de la modélisation physique. *Thèse de Doctorat – INERIS*, 2015.

[53] Caudron M. Etude expérimentale et numérique de l'interaction sol-structure lors de l'occurrence d'un fontis. *Thèse de Doctorat - INSA – Lyon – France*, 2007.

[54] Quoc Viet Do (2010) - Impacts des mouvements de terrains sur une structure type « maison individuelle ; modélisation de l'interaction sol-structure pour l'évaluation de la vulnérabilité du bâti – *Thèse - Université Paris Est*, 2010.

[55] Cui Y. and Kimura M. Model test and numerical analysis methods in tunnel excavation problem. *Soils and Foundations*, 2010, 50(6), 915-923.

[56] Dyne L. The prediction and occurrence of chimney subsidence in southwestern Pennsylvania. *Master Thesis from Virginia Polytechnic Institute and State Faculty*, 1998.

[57] Proust A. (1964). Etude sur les affaissements miniers dans le bassin du nord et du pas de calais. *Revue de l'industrie minérale*, 1964(.64), pp. 6-13.

[58] Farrell, R., Mair, R., Sciotti, A., and Pigorini, A. Building response to tunnelling. *Soils and Foundations*, 2014 54(3):269–279.

[59] Kwiatek, J. Protection des constructions sur les terrains miniers (traduction du polonnais). Titre original "Ochrona obiektow budowlanych na terenach gomiczych". *Publication du G.I.G., Katowice*, 1998.

[60] Giardina, G., Graaf, A., Hendriks, M., Rots, J. & Marini, A. Numerical analysis of a masonry façade subject to tunnelling-induced settlements. *Engineering Structures*; 2013, 54: 234-247.

[61] Serhal, J., Deck, O., Alheib, M., Chehade, F. & Abdelmassih, D. Damage of masonry structures relative to their properties: Development of ground movement fragility curves. *Engineering Structures*; 2016, 113: 206-219.

[62] Shahin H., Nakai T. Hinokio M. Kurimoto T. and Sada T. Influence of surface loads and construction sequence on ground response due to tunnelling. *Soils and Foundations*, 2004, 44:71–84.

[63] Soots P. Le phénomène des affaissements miniers et la prévention de ses consequences dommageables. Cahier du CSBT (96, Cahier 836), 1969.

[64] Arcamone J. Méthodologie d'étude des affaissements miniers en exploitation totale et partielle. *Thèse de doctorat, Institut National Polytechnique de Lorraine*, 1980.

[65] Burland J.B., Broms B.B., and De Mello V.F.B. Behaviour of foundations and structures. *9 th Int. Conf. on soil mechanics and foundations engineering*, 1977. 495 – 546.

[66] Geddes J.D. Structural design and ground movements. Ground movement and their effects on structures, *Surrey University Press, edited by Attewell and Taylor*, 1984.

[67] Boscardin M.D. and Cording E.J. Building response to excavation-induced settlement. *Journal of Geotechnical Engineering*, 1989, 115(1): 1–21.

[68] Mair, R. J., Taylor, R. N., Burland, J. B., and Taylor, R. N. Prediction of ground movements and assessment of risk of building damage due to bored tunnelling. In Mair, R. J. and Taylor, R. N., editors, *Proceedings of the International*

Symposium on Geotechnical Aspects of Underground Construction in Soft Ground, 1996, 713–718, London, United Kingdom. Balkema, Rotterdam.

[69] Attewell P.B. and Yeates J. Tunnelling in soil. Ground movements and their effects on structures, *Surrey Univ. Press. (Ed. Attewell et Taylor)*, 1984.

[70] Burland J.B. and Wroth C.P. Settlement of buildings and associated damage. Conference on the Settlement of Structures, Pentech Press, Cambridge, London, 1974. 611–654.

[71] Neuhaus E. H. A.B.C. de la construction des maisons d'habitation en zones d'affaissements miniers. Editions Eyrolles, traduit par SOOTS, 1965.

[72] Winkler E. Die lehhre von der eiastizitat und Festigkeit (on elasticity and fixity). Dominicus, Prague, 1867, 182.

[73] Vesic. Beams on Elastic Subgrade and Winkler's Hypothesis. *Proceedings of the 5th International Conference on Soil Mechanics and Foundation Engineering*; 1963, 845-850.

[74] Biot. Bending of an infinite beam on an elastic foundation. *Journal of Applied Mechanics*; 1937.

[75] Drapkin. Grillage beams on elastic foundations. *Proc. ASCE*; 1955.

[76] Klöppel & Glock. Theoretische und Experimentelle Untersuchungen zu den Traglastproblemen Biegeweicher, in die Erde Eingebetteter. Institutes für Statik und Stahlbau der Technischen Hochschule Darmstadt; 1970.

[77] Henry. The Design and Construction of Engineering Foundations. Chapman & Hall; 1986.

[78] Houlsby, G.T. and Byrne, B.W. Design Procedures for Installation of Suction Caissons in Clay and Other Materials. Proc. ICE, *Geotechnical Eng*., 2005. 158 No. GE2, pp 75–82.

[79] Hetényi M. Beams on elastic foundation; theory with applications in the fields of civil and mechanical engineering. *Ann Arbor, The University of Michigan Press*, 1946.

[80] Pasternak P.L. On a new method of analysis of an elastic foundation by means of two constants. Moscow, URRS, 1954.

[81] Filonenko-Borodich M.M. (1940). Some approximate theories of the elastic foundation, Universiteta Mechanika 1940, 46, 3-18.

[82] Kerr A. On the determination of foundation model parameters, J. Geotech. Eng., 111, 1985, (11), 1334–1340.

[83] Klar, A. and Marshall, A. M. (2008). Shell versus beam representation of pipes in the evaluation of tunneling effects on pipelines. Tunnelling and Underground Space Technology, 23(4):431–437.

[84] Laefer DF. Prediction and Assessment of Ground Movement and Building Damage Induced by Adjacent Excavation. *Ph.D. Thesis, University of Illinois at Urbana-Champaign, Urbana, III*, 2001.

[85] Schweiger & Peschl. Basic Concepts and Applications of Random Sets in Geotechnical Engineering. *Probabilistic Methods in Geotechnical Engineering*; 2007, 491(1): 113-126.

[86] Giasi, Masi & Cherubini. Probabilistic and fuzzy reliability analysis of a sample slope near Aliano. *Engineering Geology*; 2003, 67(3-4): 391-402.

[87] Baecher, B. & Christian, J. Reliability and statistics in geotechnical engineering. John Wiley & Sons; 2003.

[88] Piegay. Optimisation multi-objectif et aide a la decision pour la conception robuste-*Doctorate Thesis, Université de Bordeaux*; 2015.

[89] Jacques, J. Pratique de l'analyse de sensibilité : comment évaluer l'impact des entrées aléatoires sur la sortie d'un modèle mathématique. Université de Lille; 2011.

[90] El Kahi, E., Deck, O., Khouri, M., Mehdizadeh, R. & Rahme. P. Comportement des ouvrages soumis à des mouvements de terrain en tenant compte des incertitudes. *37èmes Rencontres de l'AUGC, école d'ingénieur Polytech Nice Sophia, 19 au 21 juin 2019*; 2019.

[91] Kala, Z. Sensitivity assessment of steel members under compression. *Engineering Structures*; 2009, 31(6): 1344-1348.

[92] Jahangir E. Phénomènes d'interaction sol-structure vis-à-vis de l'aléa retrait gonflement pour l'évaluation de la vulnérabilité des ouvrages. *Thèse de Doctorat, Université Lorraine*, 2012.

[93] Bilal, Nasir, Implementation of Sobol's Method of Global Sensitivity Analysis to a Compressor Simulation Model. *International Compressor Engineering Conference*. Paper 2385, 2014.

III. Thesis overview

The target of this chapter is to present a detailed abstract of the thesis that summarizes the sequence of targets set and the main results obtained in each paper. Since the objective of every paper is unique, the target of this chapter is to present a global vision that links these papers issued separately in order to reach the final target of the thesis.

The objective of this thesis is to consider the impact of uncertainties affecting the evaluation of the transmission of ground movements to structures. Based on the literature, an effective way to evaluate the transmission is by evaluating the transmission ratio, Δ/Δ_0, that depends upon the relative stiffness.

Since an uncertainties study requires a significant number of simulations, the analytical approach may be considered as the fundamental approach used is this study, allowing quick calculations for a wide range of variation of parameters. Then, a numerical and an experimental approach is evaluated as a complementary tool to validate some of the analytical results. As presented in the previous chapter, since the Deck & Singh (2010) simplified analytical approach (Euler-Bernoulli beam sitting on vertical springs) provides moderate results of the transmission ratio Δ/Δ_0 compared to others, and the results vary between 0 and 1 which fits well with the definition of the maximum free-field deflection ($\Delta \leq \Delta_0$), this thesis has proceeded by considering Deck & Singh (2010) analytical model. Furthermore, this analytical model has been completed with a numerical model, using Plaxis 2D, to validate its use, as it will be shown in the next chapters.

III.1 Thesis plan

Based on the literature, the evaluation of the transmission ratio Δ/Δ_0 shows a significant margin of discrepancy between the various developed models that may be interpreted as the consequence of the uncertainties that affect its estimation. Various studies have focused on the treatment of uncertainty in geotechnical structures. Uncertainties that are related to SSI properties can fall into three major categories:

1. Natural variability that is associated with the “inherent” randomness of natural processes.
2. Knowledge uncertainty that is attributed to lack of data or of information about events and processes.
3. Model uncertainty that corresponds to the degree to which a chosen mathematical model accurately reproduces reality.

This thesis has identified and investigated the influence of significant sources of uncertainties. Results reveal the effect of considering these uncertainties, and specify their influence on the parameters that are used to evaluate the transmission of ground movements to structures associated with the SSI. Five papers are presented; every paper investigates the influence of a particular uncertainty, as shown in Table III-1.

Table III-1. Presentation of chapters

Chapter	Title	Type	Status
IV	Simplified probabilistic evaluation of the variability of soil-structure interaction parameters on the elastic transmission of ground movements	Journal paper	Under review (*Engineering Structures*)
V	Influence of uncertainties on the evaluation of building deflections induced by ground movements	Journal paper	Under review (*European Journal of Environmental and Civil Engineering*)
VI	A new simplified meta-model to evaluate the transmission of ground movements to structures integrating the elastoplastic soil behavior	Journal paper	Accepted (*Structures*)
VII	Influence of Spatial Variability of Soil Properties on Structures Response	Conference paper	Published (*Proceedings of the 29th European Safety and Reliability Conference*)
VIII	Experimental evaluation of the stiffness variability of masonry structures affecting the transmission of ground movements	Conference paper	Under Submission (*11èmes journées de fiabilité des matériaux et structures, JFMS 2020*)

III.2 Presentation of Chapter IV. Simplified probabilistic evaluation of the variability of soil-structure interaction parameters on the elastic transmission of ground movements

The impact of the variability of the main SSI parameters on the prediction of the structure response is evaluated in this paper through a probabilistic approach. The “basic random variables theory” is used to model the uncertainty of the SSI properties using the Monte-Carlo simulations. This method imposes the uncertainties on the input data of the model to determine the effect of each parameter on the result obtained by this model. To use the Monte-Carlo method, it is necessary to have probability distribution functions (normal, lognormal distribution, etc.) with their corresponding characteristics for the input data. The developed approach, for approximating the SSI parameters uncertainties, is based on using estimates obtained from published values that are conveniently expressed in terms of the coefficient of variation (COV).

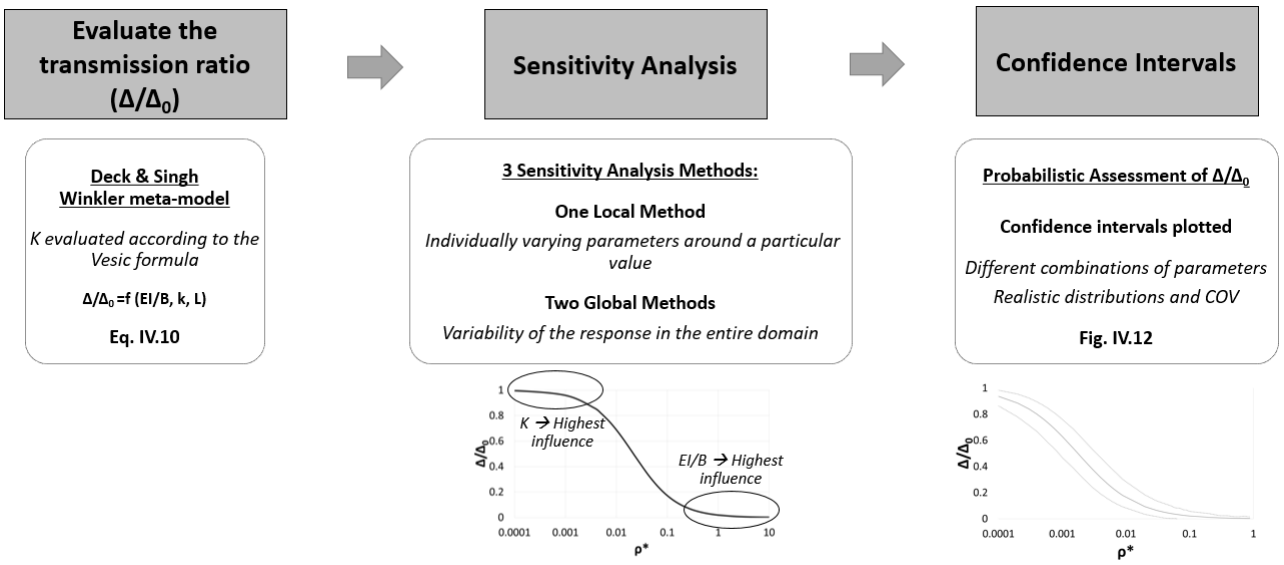


Fig. III.1: Graphical abstract of Chapter IV.

A meta-model is developed that represents the deterministic results of the transmission of the ground movement versus the relative stiffness and more precisely versus the SSI parameters EI/B, L and K (Fig. III.1*: Graphical abstract of Chapter IV.*
). This meta-model, based on Deck & Singh (2010) model, is validated by an elastic finite element model (FEM) presented in this paper that intends to fully reproduce the elastic conditions of Deck & Singh (2010) analytical approach.

Then, a sensitivity analysis (SA) is performed using local and global methods: (a) One local method (One-way sensitivity analysis) is performed to evaluate the impact of variability on the output around a particular value of each input parameter. (b) Two global methods (Sobol and McKay) are applied to evaluate the contribution of each input parameter on the response in the entire domain of variation. These two global methods present differences with respect to the sampling techniques and the evaluation of the dependence between the input variables. In addition, Sobol method evaluates the existence of a possible interaction between input variables.

SA results reveal that Δ/Δ_0 highly depends upon the variability of the SSI parameters, upon their probability distribution function and their COV.

- A first approach is performed by considering a uniform distribution of each parameter over its entire distribution range. The target is to get a global overview of the influence of parameters in the considered distribution range of parameters. Results show that L has the highest influence, but its influence is comparable to the influence of EI/B and K (approximately 1.5 times higher effect). In addition, in this approach, the effect of EI/B is higher than K, since its range of variation is higher.
- A second approach is performed by considering a normal distribution of each parameter with the same COV. The target is to assess the parameter having the highest influence from a mathematical point of view. Results show that L has the highest influence, which is 4 times higher than the influence of EI/B and K.
- A third approach is performed by considering a normal distribution of each parameter with realistic COV defined in the literature. The target is to evaluate the parameter that has the highest influence considering both, mathematical influence and realistic variability. This

approach is performed in the perspective of an operational use of the deterministic results of Δ/Δ_0.

According to the third approach, it was found that the effect of every parameter varies according to the considered ρ* value. Globally, the effect of EI/B increases with the increasing values of the relative stiffness ρ*; however, the effect of K increases when ρ* decreases.
The variability of L is limited (COV=5%) compared to the one of EI/B and K (COV=40%) according to the literature. Thus, L has the lowest influence of L for the entire variation range of ρ*. On the other hand, for low ρ* values, K has the highest influence, while for high ρ* values EI/B has the highest influence. For intermediate ρ* values, EI/B and K have nearly the same effect.
Finally, confidence intervals are developed analytically and validated numerically by considering the variability of the SSI parameters. A range of results of Δ/Δ_0 is associated with every value of the relative stiffness by considering a level of confidence that is set between 70 and 95%. These confidence intervals provide a simplified probabilistic evaluation that can be directly adopted by engineers for design purposes during preliminary stages to assume a Δ/Δ_0 value, to have an efficient assessment of the rate of the ground movement that is transmitted to structures when considering the uncertainties related to the estimation of SSI parameters.

III.3 Presentation of Chapter V. Influence of uncertainties on the evaluation of building deflections induced by ground movements

Based on Deck & Singh model, an accurate prediction of the structure response to the ground movements requires a well-characterization of uncertainties related to the SSI conditions and parameters. Fig. III.2 summarizes the main hypotheses considered in the Deck & Singh model that can be considered as significant sources of uncertainties based on the literature. This paper aims to evaluate the effect of these uncertainties using a deterministic approach. Then, a coefficient A will be proposed to consider the influence of these uncertainties while evaluating the transmission of ground movements to structures (Δ/Δ_0) by defining a variation interval.

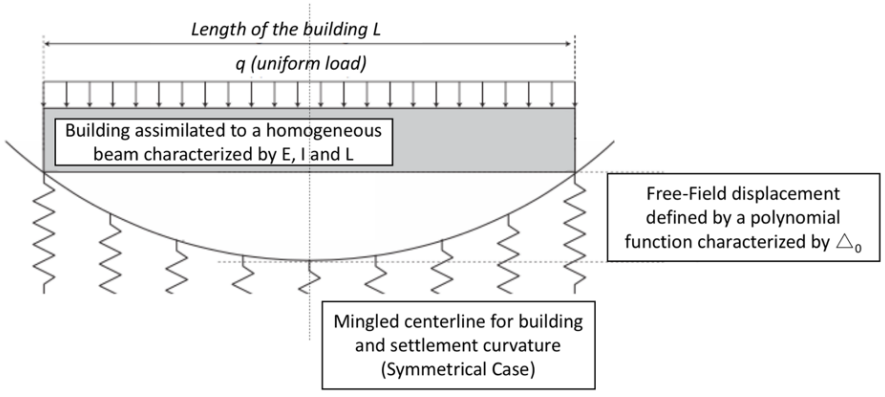


Fig. III.2: Main hypotheses considered in the Deck & Singh methodology (2010).

Consequently, a paper is presented, based on Deck & Singh Δ/Δ_0 analytical curve, to investigate the effect of various significant uncertain factors on Δ/Δ_0 related to the model and geometrical conditions and properties:

- The free-field ground movement profile
- The building position to the soil curvature
- The longitudinal variability of the structure stiffness caused by the heterogeneity of structural materials and openings (doors, windows, etc.).

These uncertainties are evaluated in the literature, and a significant discrepancy is shown indicating their influence. However, these studies considered particular SSI cases and parameters, and their results cannot be generalized for a wide range of SSI parameters. This paper aims to propose a modification factor A for operational use, to evaluate the influence of these uncertainties on the transmission ratio $(\Delta/\Delta_0)_{uncertainties} = A(\Delta/\Delta_0)_{Deck\&Singh}$. This coefficient covers the whole range of SSI parameters and varies between A_{min} and A_{max}. When these values are close to 1, the effect of uncertainties is negligible; however, when A_{min} and A_{max} are distant from 1, these uncertainties have a significant influence.

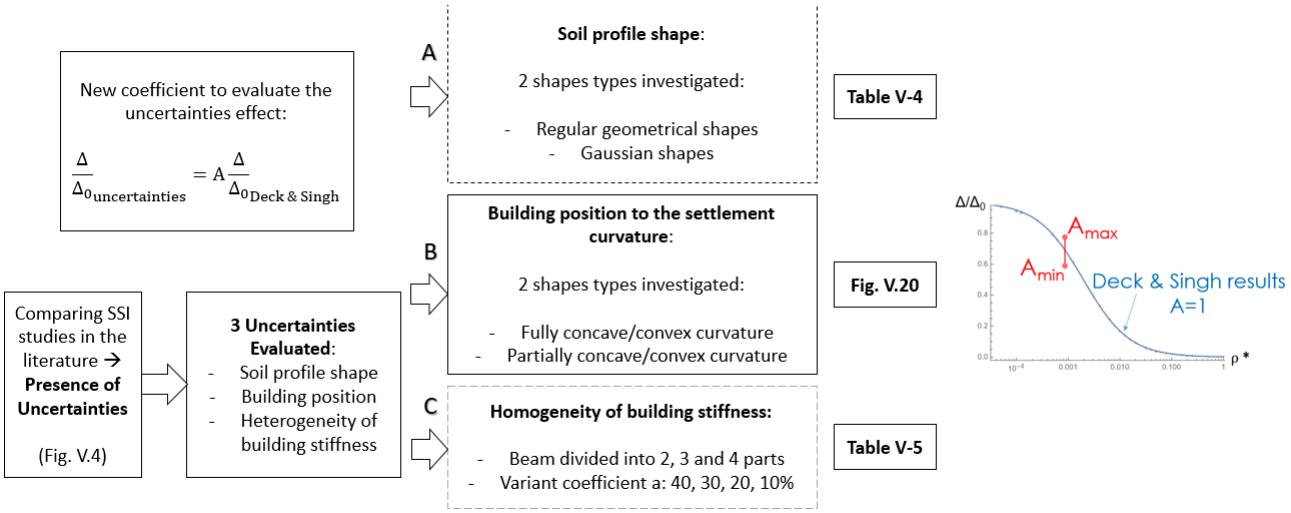


Fig. III.3: Graphical abstract of Chapter V.

As shown in Fig. III.3*: Graphical abstract of Chapter V.*
, the work done in this paper can be summarized as follows:

a- The effect of the free-field ground movement form was studied by taking several continuous shapes (polynomial, trapezoidal, sinusoidal, triangular and side triangular), one discontinuous shape (rectangular) and a Gaussian form of the free-field ground movement. Their results are plotted together for comparison purposes.

i. First, for the continuous cases, all curves have globally similar results with the usual analytical models curves. For an equivalent stiffness ratio, the results of maximum transmission ratio are slightly different.

ii. Second, the discontinuous shape does not follow a one-line curve as the continuous shapes even-though it respects the overall curvature, and the transmission ratio associated with

the relative stiffness values presents a significant difference.

iii. Third, for the Gaussian shape, the comparison of the structure and the curvature lengths shows a significant influence of this uncertainty, consequently, the horizontal distance between the settlement inflection point and the building centerline has an important influence on the results. Four cases are considered ($L_{building} << L_{curvature}$; $L_{building} >> L_{curvature}$; $L_{building} \approx L_{curvature}$; $x_{building\ end} = x_{inflection\ point}$) and results show that for a structure having a comparable length with the curvature, Δ/Δ_0 have globally similar values to the Deck & Singh polynomial model.

b- The building position to the settlement curvature was studied by considering two cases:

i. A building distant from the inflection point: the structure deflection presents a fully concave/convex curvature. The effect of the concavity and convexity of the free-field ground movement is examined according to the several deformation shapes. Results show that, with respect to the condition of no interpenetration and continuous contact between the soil and the structure, the concave and convex shapes give exactly the same results of the deflection transmission ratio Δ/Δ_0 versus the relative stiffness ρ^*.

ii. An inflection point of the free-field movement that is close or under the structure: the structure may be partially concave and convex, and its position highly affects the prediction of Δ/Δ_0. Continuous and discontinuous approaches are considered and results reveal that the worst case corresponds to the case where the curvature center coincides with the building centerline which overestimates the structure response.

c- The influence of openings, heterogeneity of structural material, etc. manifested by the stiffness variation in the structure is investigated. Various beam stiffness partitions are applied to the model; each partition is characterized by its own stiffness obtained by increasing or decreasing the stiffness value by certain percentage. All of these partitions and variations are compared to the homogeneous case where the whole building has one stiffness value. Results indicate that the evaluation of the movement transmission depends upon the stiffness variation and a difference is shown between the homogeneous and the heterogeneous case.

d- Finally, a new equation that considers the influence of every uncertainty is proposed using tables and figures (Table V-4 and 5 and Fig V.20 of this paper) based on the Deck & Singh deflection transmission ratio. This equation can be directly adopted by engineers for design purposes to assume a Δ/Δ_0 value when considering these uncertainties.

III.4 Presentation of Chapter VI. A new simplified meta-model to evaluate the transmission of ground movements to structures integrating the elastoplastic soil behavior

After evaluating the uncertainties affecting the evaluation of Δ/Δ_0 considering elastic conditions, a new paper is presented whose purpose is to integrate the soil elastoplasticity while investigating the response of a structure sitting on a soil subjected to a ground movement. Analytical and numerical approaches are applied to examine the effect of the non-linear soil behavior. The analytical approach is based on modified Winkler and Pasternak elastic models under the assumption of limiting the soil reaction by its bearing capacity ; the numerical approach is based on finite element models, using Plaxis 2D that consider an elastoplastic soil behavior.

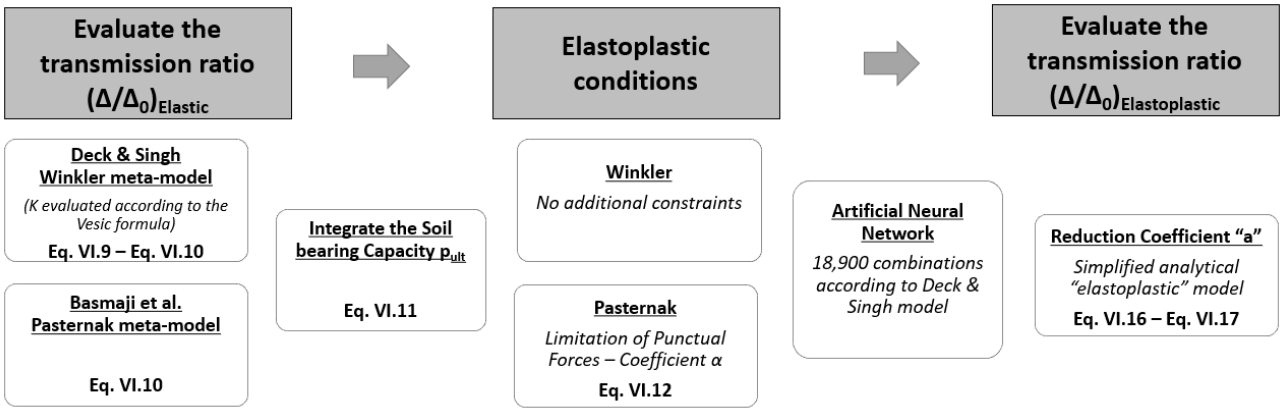


Fig. III.4: Graphical abstract of Chapter VI.

As shown in Fig. III.4*: Graphical abstract of Chapter VI.*

, simplified equations are initially proposed to evaluate the elastic transmission ratio $(\Delta/\Delta_0)_{Elastic}$ for (a) Deck & Singh (2010) Winkler model coupled with Vesic formula and (b) Basmaji et al. (2017) Pasternak approaches. These two approaches are validated by elastic numerical finite element models and numerical, experimental and field data results from previous research. Then, the influence of soil plasticity on the transmission ratio Δ/Δ_0 is investigated by integrating the soil bearing capacity p_{ult} that corresponds to a limited value for the ground reaction p (x). Results show a significant difference in the transmission ratio between the elastic and the elastoplastic soil behavior. The elastic behavior results create an envelope that engulfs the elastoplastic results.

Considering plasticity with the Pasternak model involves difficulties because this model implies the presence of a punctual reaction at the building edge. To overcome these difficulties, a coefficient α is imposed to locally modify the shear modulus Gp and limit the maximum admissible punctual forces. To find the value of α, it is required to check the statistical balance and the equivalence between the sum of the reactions and loads applied to the beam for every combination. Thus, the proposed procedure applied for Pasternak model is time consuming and presents difficulties to be generalized. On the other hand, the proposed procedure applied for Winkler model (Deck & Singh model coupled with Vesic formula) does not show constraints and is validated by finite element-models.

Based on Deck & Singh Winkler model, a new meta-model is proposed that associates the elastic with the elastoplastic results of the transmission of the ground movement ($(\Delta/\Delta_0)_{Elastoplastic}$); the statistical meta-model is realized using artificial neural networks based on 18,900 combinations of SSI parameters and soil bearing capacities p_{ult}. A reduction coefficient "a" is computed so that $(\Delta/\Delta_0)_{Elastoplastic} = a\,(\Delta/\Delta_0)_{Elastic}$.

In conclusion, to improve the investigation of the structure response to ground movements and the evaluation of its damage, the effect of a significant SSI factor, the soil elastoplastic behavior, can be directly evaluated via the proposed simplified meta-model that is based on the elastic values of $(\Delta/\Delta_0)_{Elastic}$. To reduce time and calculation difficulties, this paper proposes simple equations that are sufficient and can be directly used by geotechnical engineers and designers to consider the elastoplastic soil behavior and evaluate transmission of ground movements to structures.

III.5 Presentation of Chapter VII. Influence of Spatial Variability of Soil Properties on Structures Response

The variability of SSI parameters is investigated in the previous study without considering geostatistical conditions. Another paper is presented to evaluate the influence of spatial variability (SV) of soil properties on structures response. As shown in figure below, this paper develops a probabilistic study through an analytical approach developed by Mathematica coupled with random field of the ground Young's modulus to evaluate the uncertainties related to the soil spatial variability affecting the transmission of movements caused by various sources (tunneling, mines, sinkholes, etc.) to nearby structures. The random field is computed with the Sequential Gaussian Simulation (SGS) procedure (using GOCAD software), based on given variograms with specific correlation length and variance of the soil modulus. In fact, the soil is assimilated to a juxtaposition of elastic springs, characterized by a different stiffness value for every spring. 108 combinations of the soil modulus mean value, structure stiffness, length and correlation length are considered; for every combination, a flexible, intermediate and stiff structures are assessed. Results reveal the effect of considering the soil spatial variability on the transmission ratio that specifies the building behavior in response to the ground movement. They revealed that, for a heterogeneous soil (small correlation length), the properties compensate each other so that the final effect becomes similar to the case where there is no SV. However, when the correlation length increases, the soil becomes homogeneous and the SV influence is more important.

A coefficient α is proposed to characterize the SV effect, so that $(\Delta/\Delta_0)_{\text{with SV}} = \alpha\ (\Delta/\Delta_0)_{\text{without SV}}$.

The influence of the beam stiffness, the beam length and the mean value of the soil modulus is separately investigated. At last, for most of the cases, this study indicates that the spatial variability of soil properties has a moderate influence on the buildings response to excavation-induced ground movements.

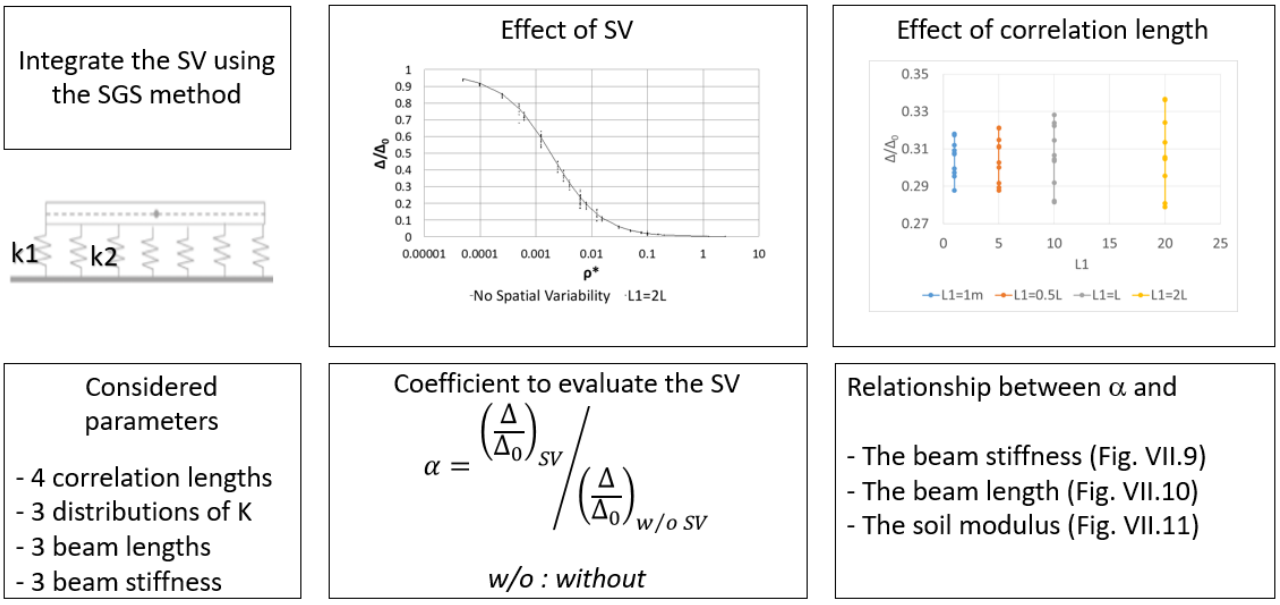


Fig. III.5: Graphical abstract of Chapter VII.

III.6 Presentation of Chapter VIII. Experimental evaluation of the stiffness variability of masonry structures affecting the transmission of ground movements

Finally, a fifth paper is presented whose target is to realize experimental tests to investigate the stiffness variability of masonry structures. In fact, the variability of stiffness highly impacts the evaluation of the buildings response to ground movements due to the soil-structure interaction as shown in the results of the sensitivity analyses of the second paper. In fact, the building stiffness has a crucial and decisive influence that impact also the confidence intervals that were set to be used by engineers and designers when evaluating the transmission of ground movements.
In this paper, the variability of the behavior of masonry structures and particularly their stiffness is investigated experimentally by evaluating stress-strain curves. As shown in the figure below, four walls are considered presenting the same relation between brick, mortar, and masonry strengths and conditions.
Results show a significant variability between the evaluated stiffness, while theoretically the same value is expected. The standard deviation and the mean value are evaluated, resulting a COV of 37.7%, which validated the value considered analytically in the previous studies of 40%.

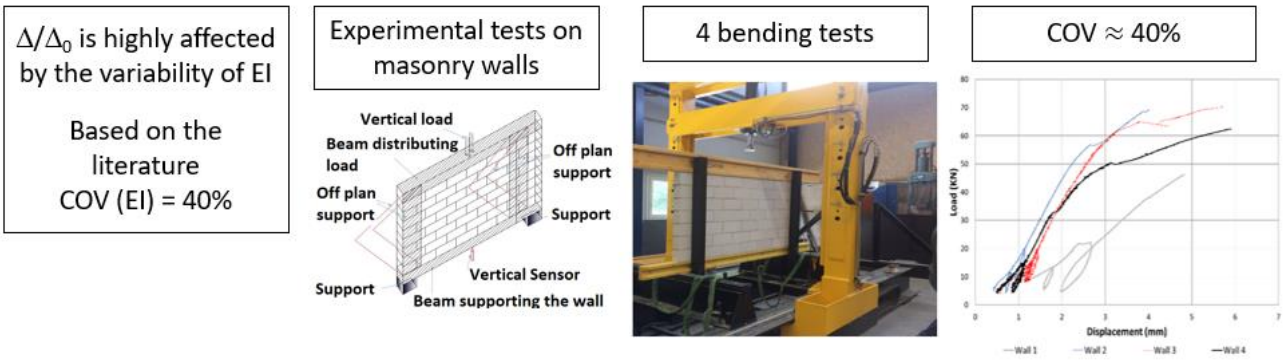


Fig. III.6: Graphical abstract of Chapter VII.

III.7 Presentation of Annex 1-4

In addition to these 5 papers, 4 annexes are presented to introduce some additional work done in this thesis and submitted in other papers not added to this manuscript, or papers that are under preparation. For example, a complementary part of the plasticity paper is mentioned in Annex 1 that summarizes a part of the scientific collaboration realized with the Polytechnic University of Madrid. A mobility grant has been associated to this thesis from Lorraine University of Excellence to realize this collaboration for three months (September-November, 2019). During this period spent in Madrid, a comparison has been done between the SSI analytical models developed in the literature by:

1- Deck & Singh that is based on Winkler model.
2- Franza *et al.* (2019) that is based on Continuum model.

Comparison results reveal that Winkler model provides moderate results even if its use may be criticized for some restrictions.

In addition, an extension to the paper is realized with the Polytechnic University of Madrid, considering a continuum model. An artificial neural network is done to evaluate the influence of plasticity and gap formation for sagging and hogging mines, in addition to the influence of eccentricity for the tunneling induced movements. Results reveal that, for the continuum model, a high number of parameters are needed which leads to a high number of neurons to evaluate the structure response.

Furthermore, an extension to the model and geometric uncertainties paper is mentioned in Annex 3 that shows the results presented in the JFMS-2018 (10èmes journées Fiabilité des Matériaux et des Structures - Bordeaux, 27-28 Mars 2018), to investigate the influence of some relevant parameters on the same free-field ground form; for example, the influence of the gap position generated by the variation of the gap form due to the ground displacement. Results reveal the effect of the gap position and shape (rectangular or trapezoidal approach) on the beam deflection.

Lastly, the influence of equivalent stiffness on the behavior of buildings subjected to soil settlements is evaluated numerically and a paper whose results are shown in Annex 4 was presented in the ESREL-2019 conference (Proceedings of the 29th European Safety and Reliability Conference). In order to separately investigate the effect of every parameter (beam length, beam stiffness, partition type and variant coefficient) on the stiffness ratio, and consequently on the equivalent stiffness, error bars are evaluated; these represent one standard deviation of uncertainty around the mean value of EI_{eq}/EI_{ref} (stiffness ratio) for the considered sets of parameters (EI_{eq} and EI_{ref} are the equivalent and the reference stiffness values respectively).

IV. Simplified probabilistic evaluation of the variability of soil-structure interaction parameters on the elastic transmission of ground movements

This paper is currently under review in the *Engineering Structures* journal.

Simplified probabilistic evaluation of the variability of soil-structure interaction parameters on the elastic transmission of ground movements

Elio EL KAHI[12*], Olivier DECK[1], Michel KHOURI[2], Rasool MEHDIZADEH[1], Pierre RAHME[2]

[1] *Lorraine University, CNRS, CREGU, GeoRessources laboratory, Ecole des Mines de Nancy, Campus Artem, CS14234, 54042 Nancy Cedex, France*

[2] *Faculty of Engineering, Lebanese University, Roumieh, Mount-Lebanon, Lebanon*

IV.1 Abstract

An efficient probabilistic approach is presented to consider the uncertainty related to the evaluation of the transmission of ground movements to structures considering the influence of the variability of the soil-structure interaction (SSI) parameters (namely the building stiffness EI/B, the soil modulus k and the structure length L). These movements can be produced by tunnels excavation, sinkholes, mining subsidence, etc. This probabilistic approach aims to quantify the relative importance of the variability of the main SSI parameters on the structure response via a sensitivity analysis (SA). The structure response is evaluated using analytical and numerical models. The analytical model is applied using Mathematica where the structure is modeled by an elastic Euler-Bernoulli beam and the soil by a combination of elastic springs as per the Winkler model. The numerical model is developed using Plaxis 2D coupled with the programming tool Python for a significant number of numerical simulations to validate the analytical results obtained. The objective is to evaluate the impact of the parameters variability which are assumed to be of a random nature. To avoid time and computation difficulties, a simplified analytical meta-model that reflects the structure response is proposed. Based on this meta-model, the SA is performed using three selected procedures, one local and two global, namely, one-way analysis, Sobol and McKay respectively. Results reveal the contribution of each input parameter on the variability of the response using various sampling techniques, such as random Monte-Carlo Simulations (MCS) and Latin Hypercube Sampling (LHS). Accordingly, the effect of EI/B increases with the increasing values of the relative stiffness (ρ*); however, the effect of k increases when ρ* decreases. Results also reveal the influence of the variability of the main SSI parameters on the rate of the ground movement that is transmitted to structures; confidence intervals are set and can be used by engineers and designers when evaluating the induced building damage in response to the transmission of ground movements taking into consideration these uncertainties.

IV.2 Keywords

Confidence intervals, sensitivity analysis, uncertainties, soil-structure interaction, meta-model, analytical, numerical approach.

IV.3 Introduction

1. Background

Ground movements may have different sources such as the influence of nearby excavations (tunnels) and the presence of underground voids such as mining subsidence, sinkhole, etc. As shown in Figure 1, these movements are characterized by vertical and horizontal displacements with other effects (ground curvature, slope, etc.) that cause differential soil settlement under the building and may lead to major damage [1, 2]. However, the transmission of ground movements to structures may be considerably affected by the soil-structure interaction phenomenon which is strongly dependent upon the stiffness of the structure as well as that of the soil [3].

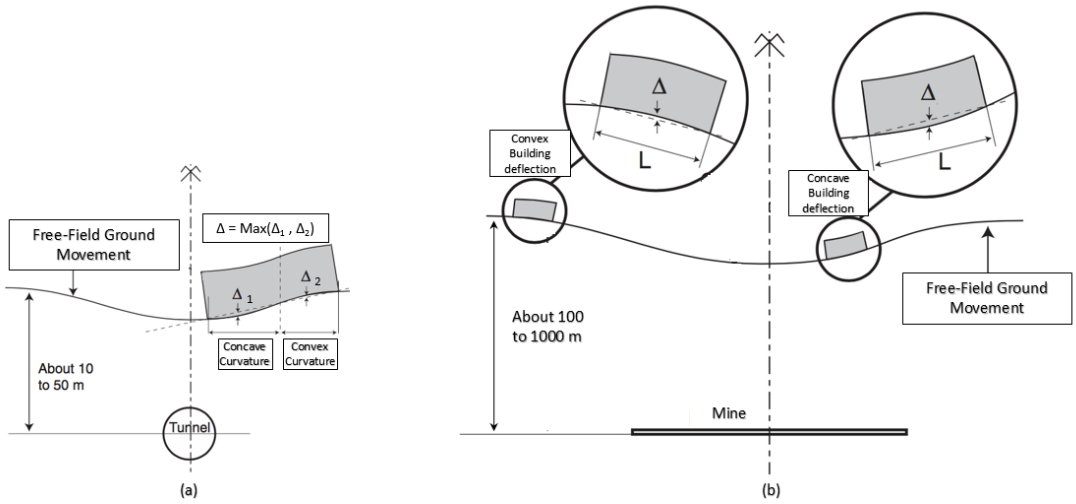


Fig. IV.1. Building deflection caused by ground movements: (a) Case of tunneling. (b) case of underground mine.

As shown in Figure 1, considering a quasi-static framework, the free-field ground movement represents the soil displacement produced by the source (tunnel, mine, etc.), without taking into account the influence of possible constructions on the surface. In the presence of an existing structure, the free-field ground movement is partially or totally transmitted to the building which may result in a structural or functional damage.

By neglecting the impact of the interaction between the soil and the structure (SSI), the free-field ground movements are integrally transmitted to the building. Under this assumption, Δ_0 indicates the maximum deflection of the building. It represents the maximum free-field deflection under the building that is totally transmitted to it. Δ_0 depends upon the ground radius of curvature R and the building length L (Figure 2). The estimation of R or Δ_0 is not the object of this paper. For movements of mining origin, Deck (2002) [44] has grouped empirical formulas for describing surface subsidence. For movements induced by tunnels excavation, the formula of Peck (1969) [45] is commonly used. In both cases, the order of magnitude of the free-field movements is variable, with radii of curvature varying from hundreds of meters to a few kilometers. For a building of 20m of length, these curves are then associated with building deflections of millimetric to centimeter order [14].

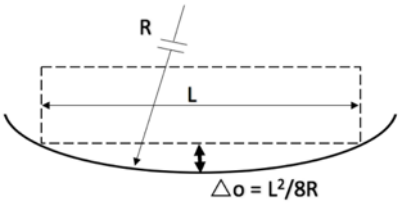


Fig. IV.2 Free-field deflection Δ_0.

By considering the impact of the SSI, the ground movement may be partially transmitted to the structure which results in a building deflection characterized by its maximum value Δ with $\Delta \leq \Delta_0$. Consequently, as shown in Figure 3, if the structure is stiff, it can resist the ground movement and the induced deformation is limited ($\Delta < \Delta_0$); if it is flexible, then it perfectly follows the soil settlement ($\Delta = \Delta_0$).

For a symmetrical free-field movement with respect to the structure, the deflection Δ corresponds to the maximum differential settlement under the building. For the non-symmetrical free-field movement case, Δ represents the maximum deflection of the building whether the structure has a concave or a convex deformation (Figure 1-a). The Δ / L ratio, called the deflection rate, is frequently used to assess the behavior of structures subjected to differential settlement and evaluate their damage [4, 5].

The objective of this paper is to evaluate the structure response to the ground movement through the deflection transmission ratio, defined as Δ/Δ_0, which is used to quantify the rate of movement transmitted to the building.

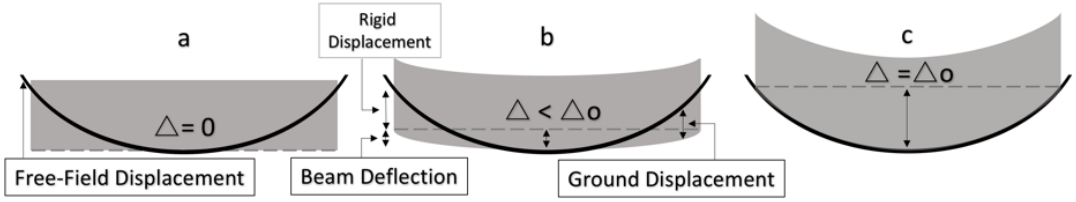


Fig. IV.3. Behavior of structures subjected to ground movement. (a) High-stiffness structure on soft ground. (b) Intermediate ground and structure stiffness. (c) Flexible structure on stiff ground.

2. Literature review

Different methods (analytical, numerical, experimental, etc.) have been developed to predict the building deflection in response to the ground movements [4-14, 49-52]. With the exception of empirical methods that are based on observations of real existing structures, these methods do not consider a specific study of a particular case but they are generally applied to simplified structures, such as elastic 2D beams, in order to assess the global trend of ground movements induced phenomena. The response of particular cases, presenting complex structural configurations, remains hardly predictable and thus, engineers need to carry out their 3D numerical modelling, which is time-consuming, during preliminary design stages [2].

Previous research on the SSI subject addresses the question of building stiffness compared to ground stiffness, which is known as "relative stiffness". It suggests to assess the transmission ratio Δ/Δ_0 as a function of a relative stiffness parameter ρ* between the soil and the structure [5-7].
Most of this research relies on Eq. (1) to evaluate the relative stiffness parameter ρ*. Their definition depends upon the structure length L, inertia I (per linear meter), Young's modulus E and the soil Young's modulus Es. Eq. (1) has the advantage of being non-dimensional and of being well adapted to the synthetic representation of Δ/Δ_0.

$$\rho^* = \frac{EI}{EsL^3} \tag{1}$$

a) Comparison of analytical, numerical, experimental and field data results from previous research

Mair (2013) [15] compared the transmission ratio versus the relative stiffness results, derived from the finite-element analyses of Potts and Addenbrook (1997) [7] and Franzius *et al*. (2006) [16]. He also considered the results of finite element parametric analyses done by Goh (2010) [17], of deep excavations in soft clay on adjacent buildings, using the Modified Cam Clay soil model. The comparison of these studies shows that the obtained results fall into a relatively narrow envelope known as Mair envelope (Figure 4).

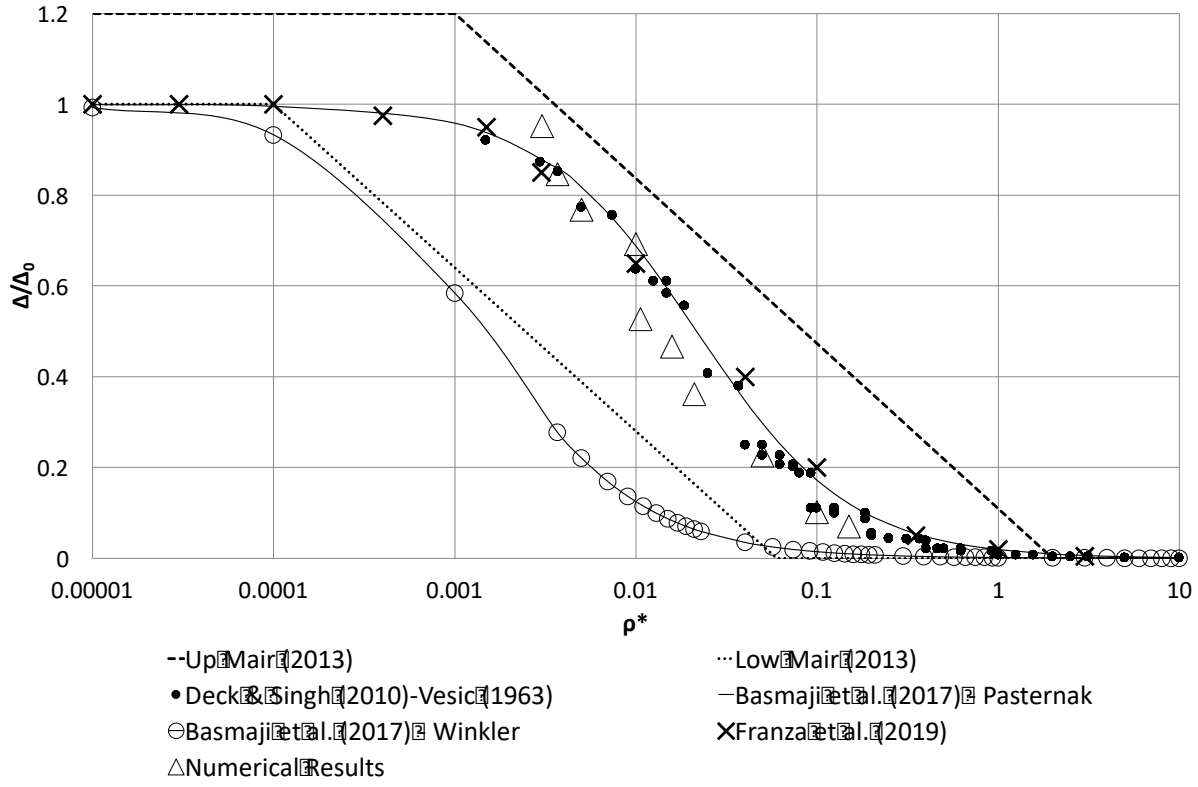


Fig. IV.4. Comparison between Mair (2013); Deck & Singh (2010); Pasternak-Basmaji *et al*. (2017); Winkler-Basmaji *et al*. (2017), Franza *et al*. (2019) results and numerical (Plaxis 2D) results.

This paper compares Mair (2013) envelope to the results of various SSI studies (analytical, numerical, etc.) that also evaluate the transmission of ground movements to structures (Deck & Singh (2010);

Basmaji *et al*. (2017) and Franza *et al*. (2019)) (Figure 4). However, each study is based on a set of hypotheses that does not allow the generalization of the obtained results:

a. Mair (2013) [15] envelope is based on physical centrifuge modelling of building response to tunneling and their results are compared with both, (a) the finite element analyses reported by Potts and Addenbrooke (1997) and Franzius *et al.* (2006), and (b) the field data of building performance reported by Goh (2010).
b. Deck & Singh (2010) [5] analytical model is based on Euler–Bernoulli beam sitting on vertical springs as per the Winkler model. They plotted their results using their own definition of the relative stiffness that is based on the Winkler reaction modulus (Winkler parameter k).
   In fact, they defined the relative stiffness ratio ρ* by Eq. (2) characterized by the Winkler parameter k and the structure width B. This equation is comparable to other relative stiffness ratios defined in the literature. It also presents the advantage of being non-dimensional and suitable to have a synthetic representation of Δ/Δ_0 based on Winkler model.

$$\rho^* = \frac{EI}{kBL^4} \tag{2}$$

   In order to make the comparison between Deck & Singh (2010) model, based on their own relative stiffness ratio, and other models, Vesic (1963) [28] formula (Eq. (3)) is used. Eq. (3) defines k values as a function of the beam length L, width B (with L>B) and the ground characterized by a Young's modulus Es and a Poisson's ratio υ. In this case, B is taken equal to 1m. Noting that various formulas link the Winkler modulus to the soil Young's modulus [28-32], Vesic's formula is chosen since it takes into account the presence of a beam (through the "EI" term) contrary to other formulas.

$$\mathrm{k} = \frac{0.65}{B}\sqrt[12]{\left(\frac{EsB^4}{EI}\right)}\frac{Es}{(1-\nu^2)} \tag{3}$$

c. Basmaji *et al*. (2017) [4] developed a new approach to assess the transmission ratio and the building response to differential settlement, considering the influence of shear deformation. Their model is based on both, Pasternak and Winkler soil models. For both soil models, a methodology has been implemented to justify the parameters values, k (Winkler parameter) and Kp and Gp (Pasternak parameters), as a function of the elastic properties of the soil, the thickness of the compressive ground layer and the building length. Their methodology considered Flamant's theoretical solution of induced vertical settlement, to adjust the displacement for Pasternak and Winkler methods and justify the parameters values for both methods.
d. Franza *et al*. (2019) [2] methodology is based on elastic and elastoplastic continuum solutions that consider the structure as an equivalent simple beam, assuming that the free-field settlement is given by a standard Gaussian curve, contrary to other models that give elastic solutions based on a polynomial free-field settlement. In addition, the structure is connected to vertical and horizontal coupled springs that model the elastic homogeneous half-space continuum, the soil, while other models assimilate the soil to a juxtaposition of elastic vertical springs. Also, Franza

et al. (2019) proposed a formulation that accounts for the change in settlement trough shape and compared it with numerical, experimental and field data from previous research.

b) Comparison with a finite-element model

This paper develops an elastic finite element model (FEM) to compare the results of previous studies in the literature with a set of numerical simulations. The objective of the FEM is to model the ground curvature induced by ground movements and calculate the elastic transmission ratio of the free-field deflection. In fact, Basmaji *et al.* (2017) [6] and Deck & Singh (2010) [7] validated their analytical elastic results with numerical models; however, they considered an elastoplastic ground behavior in their numerical studies, and they modeled the subsidence by a uniformly distributed load imposed on the lower boundary. On the contrary, the numerical model presented in this paper intends to fully reproduce the elastic conditions in order to well verify the effectiveness of the previous elastic analytical results. Subsequently, this FEM model considers a linear elastic ground behavior. By considering a linear behavior, a generalized rupture of the ground at the level of the lower boundary is avoided [47]. A ground curvature is obtained that allows a suitable comparison between the FEM calculations and the analytical ones. Note that the FEM generates a horizontal deformation; however, this deformation does not have a significant influence on the deflection transmission ratio.
The numerical model is performed with a finite element software (Plaxis 2D) under the plane strain hypothesis. The model consists of an elastic soil layer, 125 m thick and 800 m long, with a building located at the center (Figure 5). A fine mesh is used for soil elements and the subsidence is imposed without adding a uniform load on the lower boundary. For the boundary conditions, the horizontal displacement is fixed on the right and left boundaries and the vertical displacement is fixed only at the bottom boundary right and left sides (L1) while the central region of the bottom boundary is free.
The soil Poisson's ratio ν is 0.3 and the unit weight is 20 KN/m^3. The structure is modeled by a beam that is loaded with a vertical uniformly distributed load q.

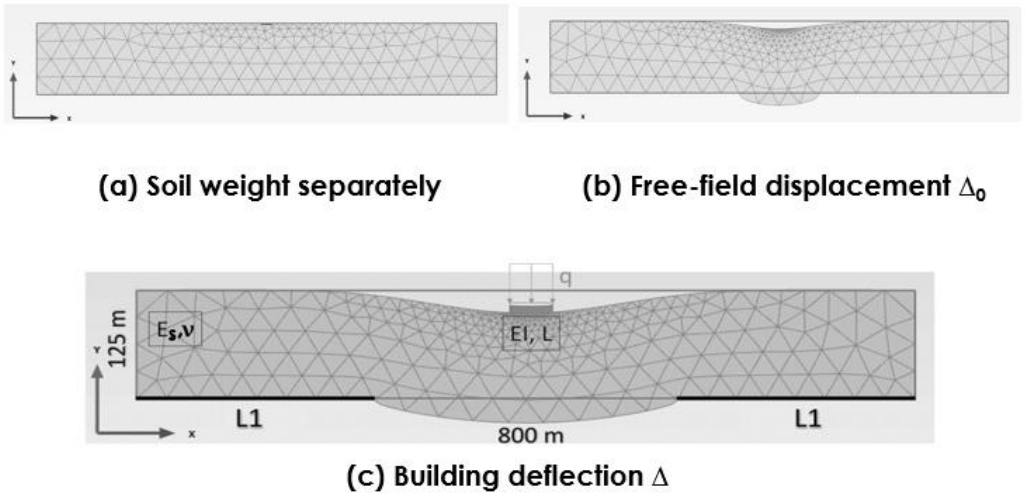


Fig. IV.5. Description of the finite element model used to compare analytical results of the deflection transmission ratio with numerical results.

Three computations are performed as follows:

(a) A first computation is performed by fixing the vertical displacement on all the lower boundary in order to generate the initial ground situation under the soil weight. All the evaluated displacements are then set to zero.
(b) A second computation is performed by fixing the vertical displacement on L1 (on both sides), without considering the structure, in order to assess the free-field displacement Δ_0 of the subsidence. Δ_0 is evaluated and the displacements are set to zero.
(c) A third computation is performed with the precense of both the structure (with the vertical uniformly distributed load) and the subsidence in order to assess the final building deflection Δ considering the soil-structure interaction.

The equivalence between the FEM and the analytical solution is maintained as follows:

- A linear elastic soil behavior is considered that is equivalent to the elastic analytical approaches (Winkler, etc.).
- A value of L1 is selected in order to reach a value of Δ_0 in the FEM that is equivalent to the one of the analytical model (Figure 5).
- Mechanical properties and buildings dimensions are chosen so that values are identical with the ones considered in the analytical approach (q, EI and L).

As shown in Figure 4, a set of 10 simulations are performed that cover the distribution range of the relative stiffness ρ^*, for different values of EI/B, Es, L, q and Δ_0. Globally, numerical results presented in Figure 4 are superimposed with the curve of the transmission ratio calculated with the models of (a) Deck & Singh (2010) using Winkler model combined with Vesic (1963) formula, (b) Basmaji et al. (2017) using Pasternak model and (c) Franza *et al*. (2019) continuum model. Therefore, these three models can be reasonably used to evaluate the transmission ratio.

3. Presence of uncertainties

As shown in Figure 4, even-tough the results of SSI studies are globally consistent in the literature, the comparison shows a large margin of discrepancy in the estimation of the transmission of the ground movements to structures. An important portion of this discrepancy may be explained by the influence of uncertainties [1, 4, 18]. In fact, Deck & Singh (2010); Pasternak-Basmaji *et al*. (2017); and Franza *et al*. (2019) analytical models present comparable results that were validated by the FEM (Figure 4) and can be reasonably used to evaluate the transmission ratio. However, in comparison with numerical and experimental results and with empirical observations of Mair (2013), the margin of discrepancy may reach ± 0.3 in the estimation of Δ/Δ_0. Consequently, this paper aims to investigate the influence of uncertainties affecting the estimation of Δ/Δ_0, define confidence intervals identifying the discrepancy of results and identify the factors presenting the highest influence on the prediction of the structure response.

Various studies have focused on the treatment of uncertainties in geotechnical structures and SSI phenomenon [20-22], these can fall into three major categories [23]:

a. Natural variability that is associated with the “inherent” randomness of natural processes.
b. Knowledge uncertainty that is attributed to lack of data or information.

c. Model uncertainty that corresponds to the degree to which a chosen mathematical model accurately reproduces reality.

By considering the variability of the main SSI parameters, this paper combines the three categories. The "basic random variables theory" is used to model the uncertainty of the SSI properties through the Monte-Carlo simulations. This method imposes the uncertainties on the input data of the model to determine the effect of each parameter on the result obtained by this model. To use the Monte-Carlo method, it is necessary to have probability distribution functions (normal, lognormal distribution, etc.) with their corresponding characteristics for the input data [24, 25]. The developed approach for approximating the SSI parameters uncertainties is based on using estimates obtained from published values that are appropriately expressed in terms of the coefficient of variation (COV).

4. Simplified probabilistic approach

Since the Deck & Singh (2010) analytical model (Euler-Bernoulli beam sitting on elastic vertical springs) is a simplified approach that provides moderate results of the transmission ratio Δ/Δ_0 compared to others (Figure 4), and the results vary between 0 and 1 which fits well with the definition of the maximum free-field deflection ($\Delta \leq \Delta_0$), this study will proceed by considering this approach.

However, Deck & Singh (2010) simplified approach presents numerous model uncertainties and their results may be affected by various uncertain factors. These factors include the structure equivalent stiffness, particularly for structures with significant wall openings, the geometric and the geological characteristics and the mechanical properties of the soil in addition to the characteristics related to the source by itself that may affect the free-field deflection shape [48].

For example, Franza & DeJong (2017) [10] presented a simplified elastic method to assess tunneling-induced deformation by investigating simple beams, frame structures and bridges on shallow foundations (either continuous foundation or individual footings). They revealed the effect of this uncertainty, however, results indicated that modeling the structure with equivalent beam elements represent a useful preliminary assessment tool for the structural response since the maximum transmission ratio difference does not exceed 0.05 [10].

On the other hand, ElKahi *et al*. (2018) [19] studied the influence of the free-field deflection shape based on the Deck & Singh analytical model; they considered different geometrical profiles (Gaussian, Trapezoidal, Sinusoidal, Triangular, Polynomial, etc.). All of these shapes are characterized by the same value of the maximum free-field deflection Δ_0 except for the dissymmetrical side triangular case where it goes to $2\Delta_0$, to be compared to a convex symmetrical triangular case characterized by Δ_0 at the two ends. Also, since the Gaussian curve depends upon the curvature length and the horizontal position of the inflection point, a configuration that considers $L_{building} \approx L_{curvature}$ and an inflection point located at 0.3 L is evaluated.

As shown in Figure 6, results vary slightly from one shape to another and the influence of this uncertainty on the prediction of the deflection transmission ratio Δ/Δ_0 is limited, the relative difference between $\Delta/\Delta_{0\,(Deck\ \&\ Singh)}$ polynomial shape and Δ/Δ_0 for other shapes does not exceed 10%.

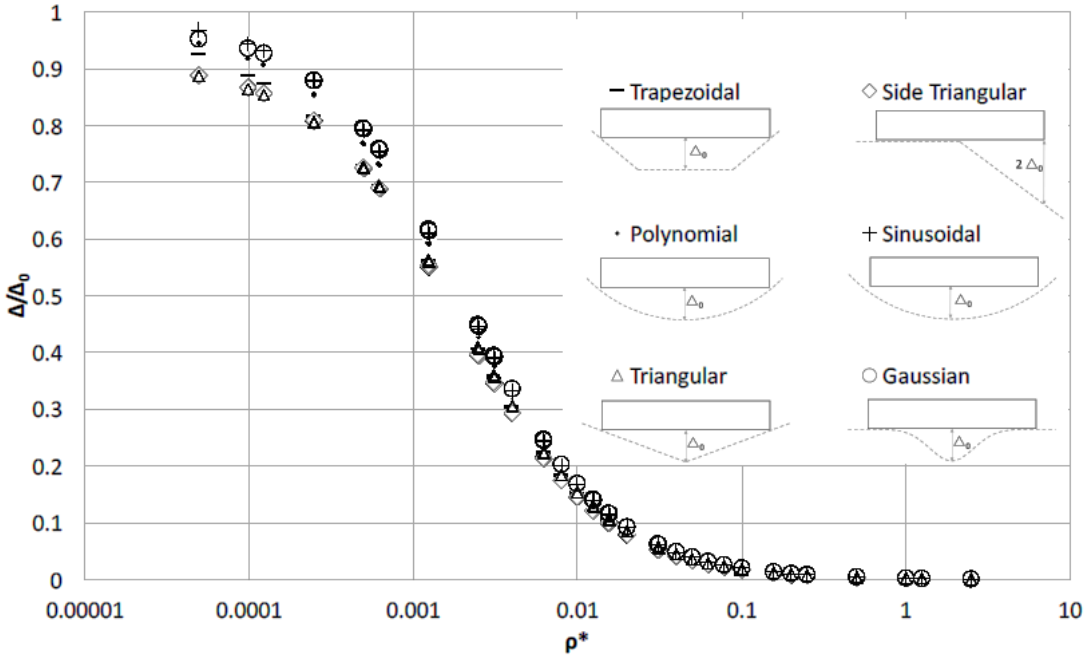


Fig. IV.6. Deflection transmission ratio Δ/Δ_0 versus the relative stiffness ρ^* for different forms of free-field ground movements.

Consequently, a polynomial shape may be used to represent the free-field profile. On the other hand, this "model" uncertainty may partially explain the discrepancy in the results shown in Figure 4, but it has to be added to other uncertainties in order to improve the prediction of the transmission ratio.
Other model uncertainties may also affect the prediction of the transmission ratio. However, these uncertainties correspond to particular cases, presenting complex configurations where a 3D numerical modelling has to be carried out. However, this paper aims to provide a simplified probabilistic evaluation that can be used by engineers and designers during preliminary design stages, to have an efficient assessment of the rate of the ground movement that is transmitted to structures. This requires a comprehensive analysis of the variability of the main SSI parameters and their impact on the structure response which constitutes a useful tool to evaluate risks associated with the impact of ground movements on nearby existing structures [13, 14].
Since a probabilistic study requires a significant number of simulations, and the Deck & Singh analytical approach is based on a set of forth differential equations with the corresponding boundary conditions (Eq. (5) and Eq. (6) defined in the next sections) involving time and computation constraints, meta-modeling is considered as an effective technique to evaluate the variability of parameters [24-26]. A simplified meta-model representing the transmission of the ground movement as a function of the relative stiffness is evaluated. Analytical and numerical confidence intervals are then set and sensitivity analysis are evaluated to quantify the effect of the variability of SSI parameters on the transmission of ground movements.

IV.4 Procedure and modeling

Various approaches have been used to study the behavior of structures subjected to differential settlement. These can be gathered into five main groups [27]: numerical, empirical, semi-empirical,

physical and analytical. Since the objective of this paper is to develop an uncertainties study, an analytical approach, based on Deck & Singh (2010) model, is used first, due to the fact that analytical modeling allows rapid results to be obtained for a large variation range of model parameters and sensitivity studies. A numerical model is then applied to compare the analytical results to a set of numerical simulations.

1. Analytical modeling

The Deck & Singh (2010) analytical approach models the building sitting on an elastic soil, by an elastic Euler-Bernoulli beam of length L, width B, inertia I and Young's modulus E (Figure 7). The work is developed in linear meter considering that B=1 m. In both research and practice, it is common to simplify the structures to equivalent linear elastic beams to decrease computational costs during initial assessment. Generally equivalent beams are identified by matching the bending stiffness EI [4-6, 10, 14-16].

By assessing the transmission ratio, Deck & Singh (2010) approach aims to evaluate the movement that the building must resist before suffering significant damage. Thus, the choice of an elastic building behavior corresponds to the objective of ensuring building safety because if the building does not suffer significant damage, its behavior may be assumed elastic [5]. Ground is thus modelled with an elastic behavior; this choice is consistent with ensuring building safety, because an elastoplastic soil behavior would lead to a decrease in the apparent ground stiffness and a decrease in the estimated transmission ratio [4]. Thus, a simplified correlation is proposed by ElKahi *et al.* (2018) [14], based on Deck & Singh elastic model, to evaluate the transmission ratio (Δ/Δ_0) for an elastoplastic soil (Eq. (4)).

$$\frac{\Delta}{\Delta_0}(Elastoplastic) = \alpha\frac{\Delta}{\Delta_0}(Elastic) \qquad \text{with } (0 \leq \alpha \leq 1) \tag{4}$$

Where α is a coefficient that depends upon the SSI parameters and the soil bearing capacity.

The beam is loaded by a uniform vertical load q. The differential equation of the building displacement y(x) can be written as follows:

$$y^{(4)}(x) = \frac{q - p(x)}{EI} \tag{5}$$

Where p(x) is the soil reaction. The soil is modeled by a juxtaposition of elastic springs characterized by their modulus k as per the Winkler model. Considering w(x) the ground displacement, p(x) can be written as follows:

$$p(x) = k.\,w(x) \tag{6}$$

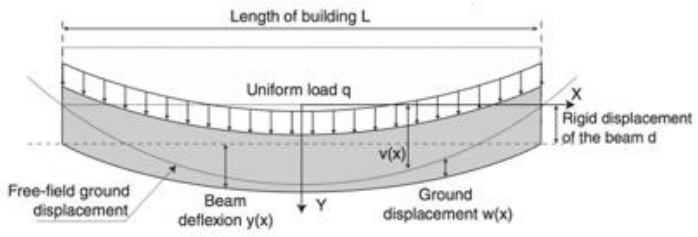


Fig. IV.7. Presentation of the SSI parameters.

If v(x) represents the free-field ground displacement, y(x) and d represent the building deflection and rigid vertical displacement respectively, the condition of no interpenetration is given by:

$$y(x) + d = v(x) + w(x) \tag{7}$$

The characteristic differential equation of the beam deflection of Eq. (5) can then be written as follows:

$$y^{(4)}(x) = \frac{q - k.(y(x) + d - v(x))}{EI} \tag{8}$$

To solve the problem, six boundary conditions are used; the building deflection, the bending moment and the shear force at the beam extremities (from both sides) are equal to zero.

According to the considered cases, the equilibrium of the system may lead to a tension zone under the building having no physical meaning and which can be interpreted as the occurrence of a detachment between the ground and the building. This particular case is not considered in this paper. Therefore, it is verified that the solutions obtained are all characterized by values of p (x) > 0 over the entire length of the building. To represent the free-field ground movement, the polynomial function v(x) is used:

$$v(x) = \Delta_0 \left(1 - \frac{4x^2}{L^2}\right) \tag{9}$$
$$For \ -L/2 < x < L/2$$

2. Development of the meta-model

An analytical model is developed by investigating 2700 cases by considering the combinations of all possible values mentioned in Table 1, for the considered model parameters.

Table IV-1. Model parameters.

Symbol (Unit)	**Description**	**Values**
L(m)	Beam Length	10, 20, 30
q (KN/m)	Beam Load	100, 200, 300, 400
EI/B(GN.m^2/m)	Beam Stiffness	20, 50, 100, 250, 500
k (MPa/m)	Ground Stiffness	20, 50, 100, 250, 500
R(m)	Free-Field Ground Radius of Curvature	250, 500, 750, 1000, 1500, 2000, 3000, 4000, 5000

The building length is taken between 10 and 30 m to model small and intermediate buildings [5]. The beam loading represents the building self-weight and service loading. 100 kN/m is approximately the weight of a 5 m high wall with a thickness of 0.5 m with service loading, 200 kN/m is approximately the weight of a 10 m high wall with a thickness of 0.5 m and 400 kN/m is roughly the weight of a whole building with three 5 m tall walls with a thickness of 0.5 m including service loading.

The beam bending stiffness EI is between 20 and 500 GN.m^2. The smallest value represents the stiffness of a 0.5 m masonry wall thickness with 5 m height and a 3000 MPa equivalent Young's modulus for the masonry. The largest value represents the stiffness of a 0.2 m thick concrete wall, 12 m tall with a 20000 MPa equivalent Young's modulus.

The ground stiffness values vary between 20 and 500 MPa according to Eq. (3), for values of soil Young modulus between 40 MPa (soft ground) and 500 MPa (stiff ground) and a Poisson's ratio of 0.3. The free-field ground radius of curvature is set between 250 and 5000m to represent a wide range of scenarios. Results of the analytical model are shown in Figure 8.

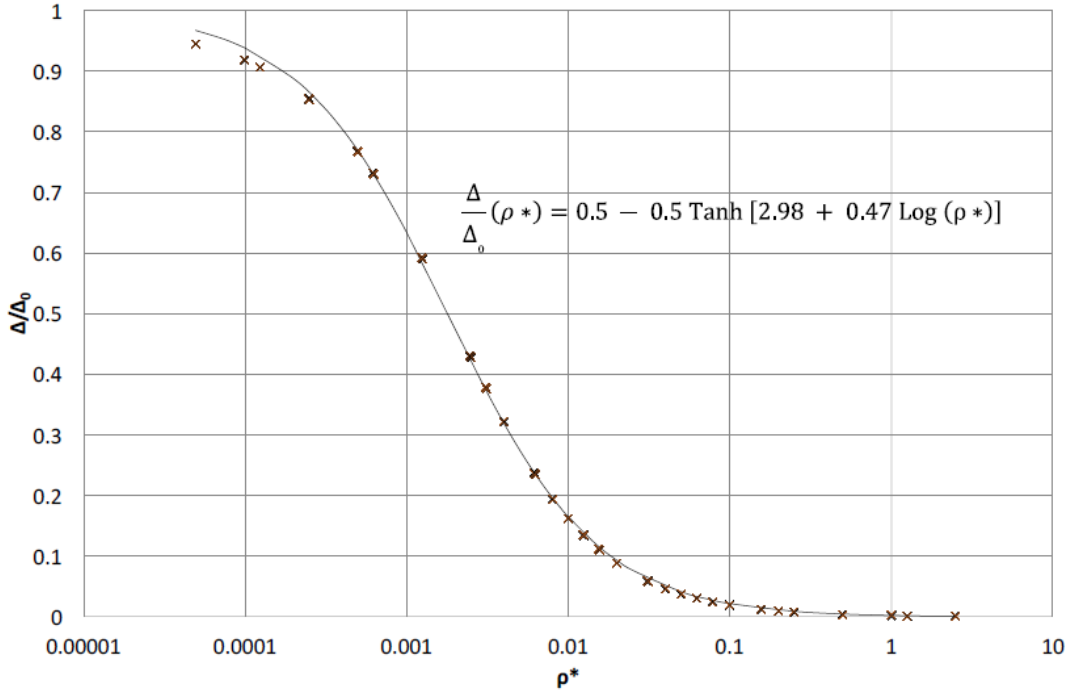


Fig. IV.8. Development of an analytical meta-model for the deflection transmission ratio Δ/Δ_0 versus the relative stiffness ratio ρ*.

To avoid time and computation difficulties while investigating the influence of the variability of the main SSI parameters on the transmission of the ground movement, an analytical meta-model is developed based on the analytical results. According to this meta-model, the deflection transmission ratio curve is assumed to respect Eq. (10) that fits the analytical results of Figure 8.

$$\frac{\Delta}{\Delta_0}(\rho*) = 0.5\left[1 - \mathrm{Tanh}[2.98 + 0.47\mathrm{Log}(\rho*)]\right] \quad (10)$$

3. Sensitivity analysis methods

To quantify the relative importance of each input parameter of a model, on the variability and uncertainty of responses, sensitivity analysis (SA) methods have to be developed. Three SA methods are evaluated: one local method that evaluates the impact of variability on the output around a particular value of each input parameter (other inputs are fixed); two global methods that quantify the contribution of each input parameter on the variability of the response in the entire domain of variation (Sobol and McKay) (Table 2).

Table IV-2. Comparison between local and global methods.

Local methods	**Global methods**	
- Evaluate the change in output as each parameter is individually varying by fixing all other parameters	- Evaluate the influence of every input parameter on the variability of the response in the entire domain of variation (all parameters varying together)	
One-Way Sensitivity Analysis	**Sobol Indices**	**McKay Method**
- Monte-Carlo simulations - Evaluate the mean μ and the standard deviation σ of the output	- Sampling based on Monte-Carlo simulations - Not valid if there is a dependence between input variables (various studies developed Sobol method to consider the parameters dependence [25]) - Consider the interaction between the input parameters through first, intermediate and total indices	- Sampling based on Replicated-Latin Hypercube Sampling - Valid even if there is a dependence between input variables - Characterized by the first order sensitivity index estimating the variance of the output produced by the influence and the variation of an input parameter - Relatively rapid results compared to Sobol

- One-way sensitivity analysis (Local method): This test examines the change in output as each parameter is individually varying, while other input parameters are fixed, according to its mean and standard deviation σ values, in addition to the associated distribution function. Thus, this method considers the input parameter variability and the associated influence on model output [33].
- Sobol and McKay (Global methods): The difference between these two global methods used in this paper is that Sobol is not valid when there is a dependence between input variables contrary to McKay's method. Another difference between these two global methods is related to the sampling techniques. The first method (Sobol) is based on the random Monte-Carlo simulations (MCS) that generates, by random and arbitrary draws, a large number of values respecting the distributions of the associated random variables. The second method (McKay) is based on the replicated Latin Hypercube Sampling (r-LHS) that consists on subdividing the variation domain of each random variable into N equal-probability sub-intervals. A uniform random sampling is then performed within each sub-interval [24, 25]. Furthermore, McKay is generally characterized by the first order sensitivity indices S_i that estimate the variance of the output (Δ/Δ_0) produced by both, the influence and the variation of a given "independent" input parameter (SSI parameter). However, Sobol's method is characterized by different indices such as the first order and the total indices: the first-order sensitivity index S_i is also based on the variance of the output for every input parameter. However, the total order index ST_i assesses the sensitivity of the variance of the output with respect to the standalone (independent) and every interaction of the considered factor with other input factors. If the differences between the first order indices and the total indices are significant, it means that the effect of the

interactions between the variables is not negligible and it can then be useful to estimate the indices of intermediate orders [25].

Consequently, this paper investigates the impact of the variability of the SSI parameters on predicting the structure response (Δ/Δ_0) in the entire domain of variation of ρ*. Local SA are evaluated to assess the influence of the variability of each input parameter separately, for specific values of ρ*, for particular combinations of EI/B, L and k, based on Eq. (10). Global SA are evaluated in order to quantify the variability of all parameters in the entire domain of variation, and to check the absence of interaction and/or dependence between the SSI parameters (based on the considered equation (Eq. (10))), using different sampling techniques.

IV.5 Results and discussion

1. Sensitivity analysis results

To conduct a sensitivity analysis (SA), numerous iterations should be developed according to a particular sampling method. The three considered SA (local and global) are based on the MCS sampling method (random MCS and r-LHS) that requires a minimum number of iterations.
According to the random MCS sampling method, the evaluation of results becomes better as the number of iterations increases [34]. This number is selected based on an acceptable approximation with an admissible potential error. Thus, the number of iterations is steadily increased until getting a mean value of the output result that is relatively stable (COV<10^{-5} %). In this paper, 50,000 iterations are studied using the MCS method while evaluating the SA.
On the other hand, the number of replications has to be more than 20 while applying the r-LHS sampling method [24]. The number of replication applied in this study is 50, and the considered number of LHS segments is 100.

The influence of the variability of the main SSI parameters (EI/B, L and k) on Δ/Δ_0 is investigated according to three approaches shown in Figure 9, with the range of variation described in Table 1.

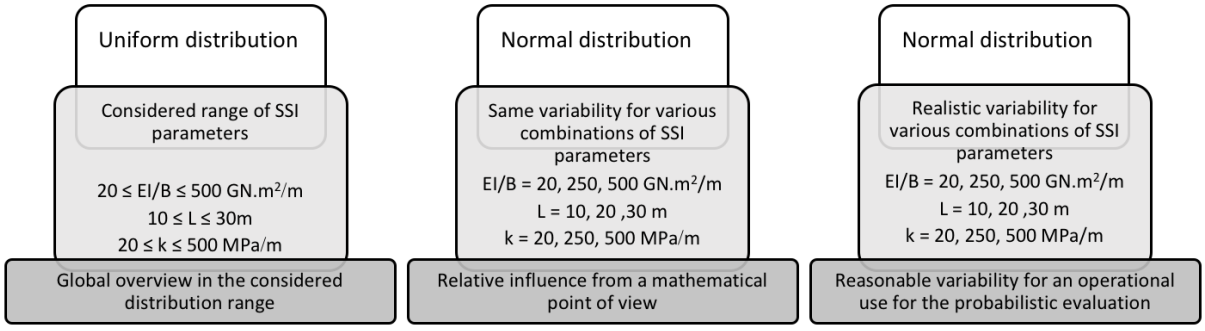


Fig. IV.9. Three approaches to evaluate the influence of the variability of SSI parameters on Δ/Δ_0

To highlight the relative influence of each parameter in comparison with others, a coefficient A is introduced to normalize the influence of every parameter according to the influence of L. For Sobol and McKay methods, since they are based on the variance σ^2, the square root of the indices are compared, and A is defined as follows:

$$A\,(\sigma)j = \frac{\sigma_{(\frac{\Delta}{\Delta_0})j}}{\sigma_{(\frac{\Delta}{\Delta_0})L}} \tag{11}$$

$$A\left(S_{i(Sobol)}\right)j = \frac{\sqrt{S_{i(Sobol)_j}}}{\sqrt{S_{i(Sobol)_L}}} \tag{12}$$

$$A\left(S_{Ti(Sobol)}\right)j = \frac{\sqrt{S_{Ti(Sobol)_j}}}{\sqrt{S_{Ti(Sobol)_L}}} \tag{13}$$

$$A\left(S_{i(McKay)}\right)j = \frac{\sqrt{S_{i(McKay)_j}}}{\sqrt{S_{i(McKay)_L}}} \tag{14}$$

Where j is an SSI parameter (EI/B, k or L).

The three considered approaches are the following:

a) First approach: Uniform distribution and global parameters range

In this approach, the entire range of variation is considered to get a general overview of the variability of the SSI parameters. To consider the global parameters range, the local one-way sensitivity method cannot be applied since all parameters are varying simultaneously in the entire domain of variation. Thus, SA are evaluated according to the global methods for a uniform distribution, according to the chosen variation range of the SSI parameters (Table 1): $20 \leq EI/B \leq 500$ GN.m^2/m, $10 \leq L \leq 30$ m and $20 \leq k \leq 500$ MPa/m.

Results presented in Table 3 reveal that EI/B gives higher effect than k, but the effect of L is higher than both in the considered range of variation of the SSI parameters. Sobol and McKay methods give comparable results with $S_{i(k)} \leq S_{i(EI/B)} \leq S_{i(L)}$. Results also reveal that the difference between the Sobol first and total indices is not significant; consequently, the effect of the interaction between the SSI parameters can be neglected.

Table IV-3. Model parameters Effect of the SSI parameters on Δ/Δ0 (First approach with a uniform distribution for all SSI parameters).

	$\mathbf{S_{i(Sobol)}}$	$\mathbf{A\left(S_{i(Sobol)}\right)}$	$\mathbf{ST_{i(Sobol)}}$	$\mathbf{A\left(ST_{i(Sobol)}\right)}$	$\mathbf{S_{i(McKay)}}$	$\mathbf{A\left(S_{i(McKay)}\right)}$
EI/B	0.244	0.69	0.272	0.69	0.227	0.68
k	0.184	0.60	0.228	0.63	0.165	0.58

L	0.511	1.00	0.572	1.00	0.491	1.00

Consequently, as shown in Table 3, since there is no dependence and no interaction between the input parameters, the results of these two global methods are comparable; therefore, this paper will proceed next by evaluating the McKay indices that provide relatively rapid results compared to Sobol.

b) Second approach: Normal distribution and particular local values of parameters with same COV

In this approach, a given value is fixed for every SSI parameter (EI/B, L and k) making the use of local SA methods appropriate. Normal distributions are considered with the same COV of 10%. Sensitivity analysis are evaluated for 27 combinations of EI/B, L and k using the mid, maximum and minimum values of the considered range of parameters: EI/B = 20, 250, 500 GN.m^2/m; L = 10, 20, 30 m; k = 20, 250, 500 MPa/m. Table 4 presents the results corresponding to one of the combinations presented in Figure 9, the combination of the mid-values of the considered range of variations (Table 1.
Table 4 shows that all the local and the global methods give relatively the same result since local combinations are considered around particular values of the relative stiffness. EI/B and k have nearly the same effect, while L has a 4 times higher effect.
Having the same probability distribution function and the same COV for all the variables, the obtained results can be justified by Eq. (2) where L has the power 4. Thus, by considering the same variability for the three SSI parameters, L has the highest influence in the meta-model equation (Eq. (10)), consequently, from a mathematical point of view, L is the parameter presenting the highest influence. This approach is equivalent to the evaluation of the first differential equation Eq. (10), according the EI/B, L and k.

Table IV-4. Effect of the SSI parameters on Δ/Δ_0 (Second approach with a normal distribution having COV = 10% for each parameter) – Combination of EI/B=250 GN.m^2/m, L=20 m and k=250 MPa/m.

	Local $\boldsymbol{\mu(\frac{\Delta}{\Delta_0})}$	**Local** $\boldsymbol{\sigma(\frac{\Delta}{\Delta_0})}$	$\mathbf{A(\sigma)}$	$\mathbf{S_{i(McKay)}}$	$\mathbf{A(S_{i(McKay)})}$
EI/B	0.234	0.017	0.26	0.052	0.24
k	0.233	0.016	0.25	0.055	0.25
L	0.236	0.065	1.00	0.871	1.00

It is important to note that the other combinations of EI/B, k and L were evaluated and gave similar results to those obtained for the combination shown in Table 4. Results indicate that the variability of L has the highest effect on Δ/Δ_0 in the entire domain of variation of ρ^*, with considering the same COV for all the variables.
Consequently, in absolute terms and from a mathematical point of view, L is the parameter having the highest influence on the variability of Δ/Δ_0.

c) Third approach: Normal distribution with realistic variability of parameters for various local values

This approach considers a normal distribution of each parameter with different but realistic coefficient of variation (COV) noting that the probabilistic distribution type may be different [23] which may affect the results. This approach aims to evaluate the parameter that has the highest influence considering both, mathematical influence and realistic uncertainty, corresponding to a suitable variability for every parameter. This last analysis is performed in the perspective of an operational use of Figure 8. Sensitivity analysis are evaluated for the 27 combinations considered in the first approach. The realistic COV for each parameter, which are considered for the third approach in this paper, are the following:

a. For L: from the perspective of evaluating its value, L can be determined from plans, aerial photos, or in situ measurements. A descriptive investigation done by Kimathi (2016) [35], shows a 5% COV on the structure length. Based on engineering judgment, this value seems to be logical to adopt in this study when considering the uncertainty of the equivalent length of L, particularly for geometrically irregular structures.
b. For EI/B: considering a 1m width beam, only the uncertainty of EI is investigated. First, the variability of the inertia I is investigated. The structure is simplified by an equivalent linear elastic beam. However, this approach results in equivalent regular beams presenting numerous uncertainties related to the bending and the shear deformability with respect to the target building. These uncertainties are associated with the difference in the evaluation of various factors like the inertia between regular and irregular structures. Various studies suggest a procedure to identify an equivalent beam stiffness for structures with openings aiming to match the total structure stiffness. This might effectively capture the effect of openings in a simplified manner, but presents a significant uncertainty that needs more thorough understanding of the effect of the non-regularity of the structure geometrical and mechanical properties, particularly its inertia [2]. Second, this uncertainty must be combined with the evaluation of the Young's modulus E that presents its own variability. A developed experimental investigation of the variability of concrete durability properties [36] found that the elastic modulus E can follow a normal distribution with a COV that does not exceed 10%. Knowing that this study is more focused on masonry structures, it was observed from data collection of published experimental work on masonry structures that the COV of E is around 20% [37-39]. Thus, by combining the variability of E and I, a final COV(EI)=40% was assumed to be realistic.
c. For k: since Winkler assumes that all springs under the structure are characterized by the same soil modulus (k), this paper considers the variability of k without propagating geostatistical conditions. However, a preliminary study was realized by El Kahi et al. (2019) [46] to evaluate the influence of the soil spatial variability on the transmission ratio. A modified Winkler model is considered, with a juxtaposition of elastic springs characterized by a particular modulus value (k) for every spring, according to the SGS (Sequential Gaussian Simulation) method. Results revealed that various factors affect the transmission ratio while considering the geostatistical conditions, such as the soil homogeneity (correlation length), the building length,

etc. However, they revealed that the margin of discrepancy does not exceed ± 0.05 in the estimation of Δ/Δ_0 by considering the spatial variability.

Besides the soil spatial variability, the variability in the evaluation of the k value is investigated. In addition to the expression suggested by Vesic (1963) (Eq. (3)), many others were developed as well [28-32, 40-42]. However, none of these can represent precisely the soil with all its complexity and its variability [43]. Vesic (1963) expression, considered in this study (Eq. (3)) depends upon four parameters (Es, EI, B and υ). In order to determine the variability of k, the corresponding COV and probability distribution function are assigned to these four parameters:

- The variability of the structure width B is not considered (B=1m).
- Based on the above, EI follows a normal distribution with COV(EI) = 40%.
- Based on the literature [23, 26, 34, 43], a normal distribution can be assigned to Es and υ with COV(Es)=40% and COV(υ)=5%.

Nine combinations of these parameters, with the corresponding COV and probability distribution function, are considered, as presented in Table 5, with 50,000 iterations for each combination as per the Monte Carlo Simulation (the variability of the structure width B will not be considered).

Table IV-5. Various combinations considered for the calculation of the variability of k.

k = f(EI,Es,v,B)				
	EI ($GN.m^2$)	Es (MPa)	v	B (m)
Possible Values	20 100 500	20 100 500	0.3	1
Distribution Function	Normal	Normal	Normal	NA
COV	40%	40%	5%	NA
9 Combinations of f(EI,Es,v,B) are considered - 50,000 Iterations for each (normal distribution for each parameter)				

Results show a COV of the Winkler parameter k of around 40% for all of the combinations, which validates the fact the k depends mainly upon the soil Young's modulus Es [43], as shown in Vesic (1963) formula (Eq. (3)), and its variability follows the variability of Es.

A first analysis is done with mean values of EI/B=250 $GN.m^2/m$, L=20 m and k=250 MPa/m that correspond to the mid-values of the studied range of variations (Table 1). Since McKay method provides a good assessment of the results, only McKay indices are shown in Table 6.

Table IV-6. Effect of the SSI parameters on Δ/Δ_0 (Third approach with a normal distribution for all SSI parameters and COV = 40% for EI/B and k; COV = 5% for L) – Combination of EI/B=250 $GN.m^2/m$, L=20 m and k=250 MPa/m.

	$S_{i(McKay)}$	$A(S_{i(McKay)})$
EI/B	0.584	3.4
k	0.253	2.2

L	0.050	1.0

Results show that EI/B is the parameter that has the highest effect and k has more influence than L for all the considered SA methods. The relative influence for EI/B is around 3.4 while it is around 2.2 for k.
In order to have a global overview, the 27 combinations for SSI parameters (EI/B, L and k) mentioned in Figure 9 are considered and the effect of their variability on Δ/Δ_0 is evaluated. Figure 10 shows the relative influence according to McKay indices ($A(S_{i(McKay)})$) for different relative stiffness values obtained by different combinations of the SSI parameters.

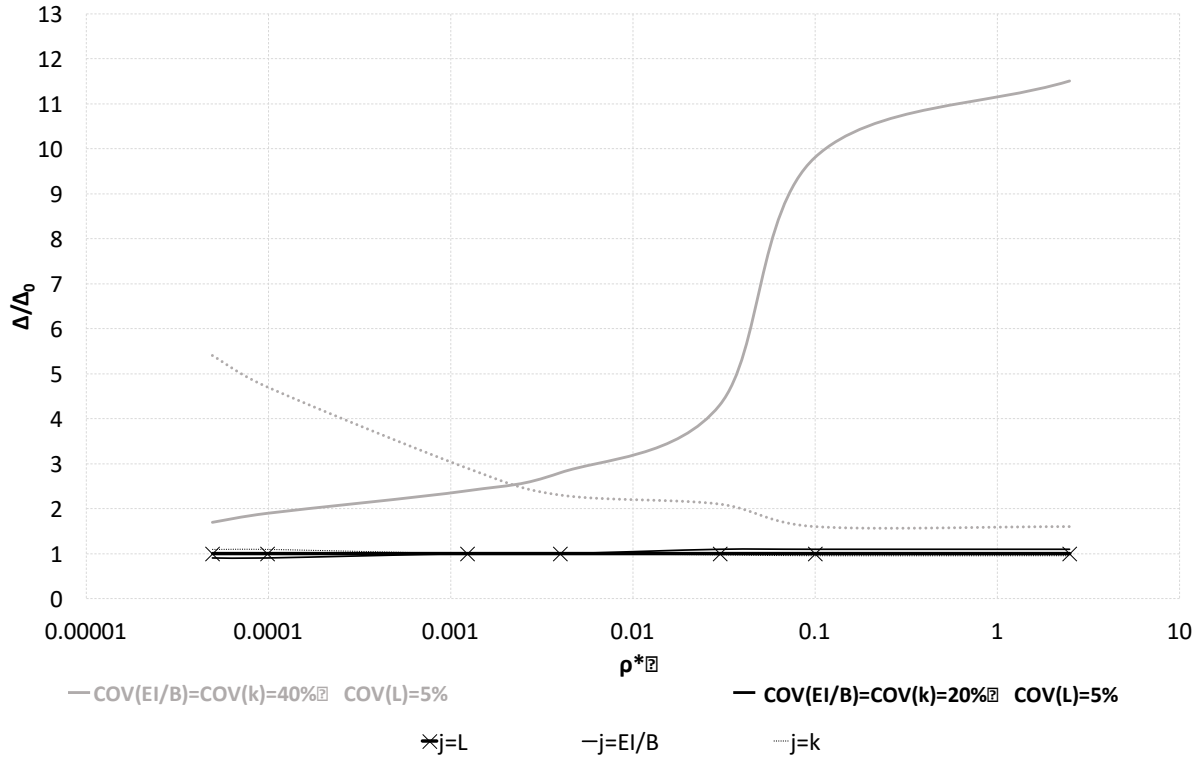


Fig. IV.10. Relative influence $A(S_{i(McKay)})$ of each parameter on Δ/Δ_0 for various relative stiffness values.

Even-though the overall effect is nearly the same, results differ according to the relative stiffness and the mean values of the SSI parameters. Globally, the effect of EI/B increases with the increasing values of the relative stiffness ρ* (Figure 10). However, the effect of k decreases when ρ* increases. This is attributed to the fact that the variability of L (5%) is limited compared to the one of EI/B and k (40%). Consequently, since ρ* (Eq. (2)) is proportional to EI/B and inversely proportional to k, these results are justified. For low relative stiffness values ($\rho^* \leq 0.001$), k has the highest influence ($A \geq 5.0$), while for high ρ* values ($\rho^* \geq 0.01$), EI/B has the highest influence ($A \geq 5.0$). For intermediate ρ* values ($0.001 \leq \rho^* \leq 0.01$), EI/B and k have nearly the same effect $2.0 \leq A \leq 3.0$. Therefore, the influence of EI/B and k are inversely proportional with varying the value of ρ*.
According to the considered distribution range of SSI parameters, ρ* is reaching high values corresponding to low values of Δ/Δ_0 that are highly sensitive to the variability of parameters allowing the high values of $A(S_{i(McKay)})_{EI/B}$ ($A(S_{i(McKay)})_{EI/B} \geq 10$ for $\rho^* > 1$).

On the other hand, seeking to have a more accurate estimation of the transmission of the ground movement, the COV of EI/B and k can be reduced to 20%. The corresponding results are presented in Figure 10.

It is observed that by decreasing the COV, the relative influence for both EI/B and k decreases. $A(S_{i(McKay)})$ for COV(EI/B,k)=20% is lower than $A(S_{i(McKay)})$ for COV(EI/B,k)=40%, for EI/B and k. As shown in Figure 10, the results of the relative influence of the three parameters are nearly the same in the second case (close to 1). These results are associated to Eq. (2) where L has the power 4. Even-though its variability is limited to a COV of 5% while it is 20% for EI/B and k, but they (EI/B and k) have the power 1.

Thus, by considering a 40% COV for EI/B and k, the influence of their variability dominates that of the length L, while by considering a COV of 20% for EI/B and k, the influence of the 3 SSI parameters variabilities is comparable.

2. Confidence intervals of Δ/Δ_0 versus ρ*

By considering SSI parameters variability, a confidence interval is plotted in order to allow a probabilistic assessment of Δ/Δ_0 instead of the deterministic one shown in Figure 8. For different combinations of the parameters, corresponding to their mean values with realistic COV, a MCS with 50,000 iterations is developed. Results allow to plot the confidence interval of Δ/Δ_0 versus ρ*.

Nine curves are plotted in Figure 11, the middle one corresponds to the mean value of Δ/Δ_0 and is strictly equal to the deterministic curve of Figure 8. Four of the curves correspond to the results for a COV(EI/B)=COV(k)=40% and COV(L)=5%, by considering one standard-deviation (30% probability of exceeding the value), or 2 standard-deviations (5% probability of exceeding the value). Similarly, four curves of Figure 11 that correspond to the results for a COV(EI/B)=COV(k)=20% and COV(L)=5% are presented in order to show the influence of a reduction of the parameters variability if additional investigations are done.

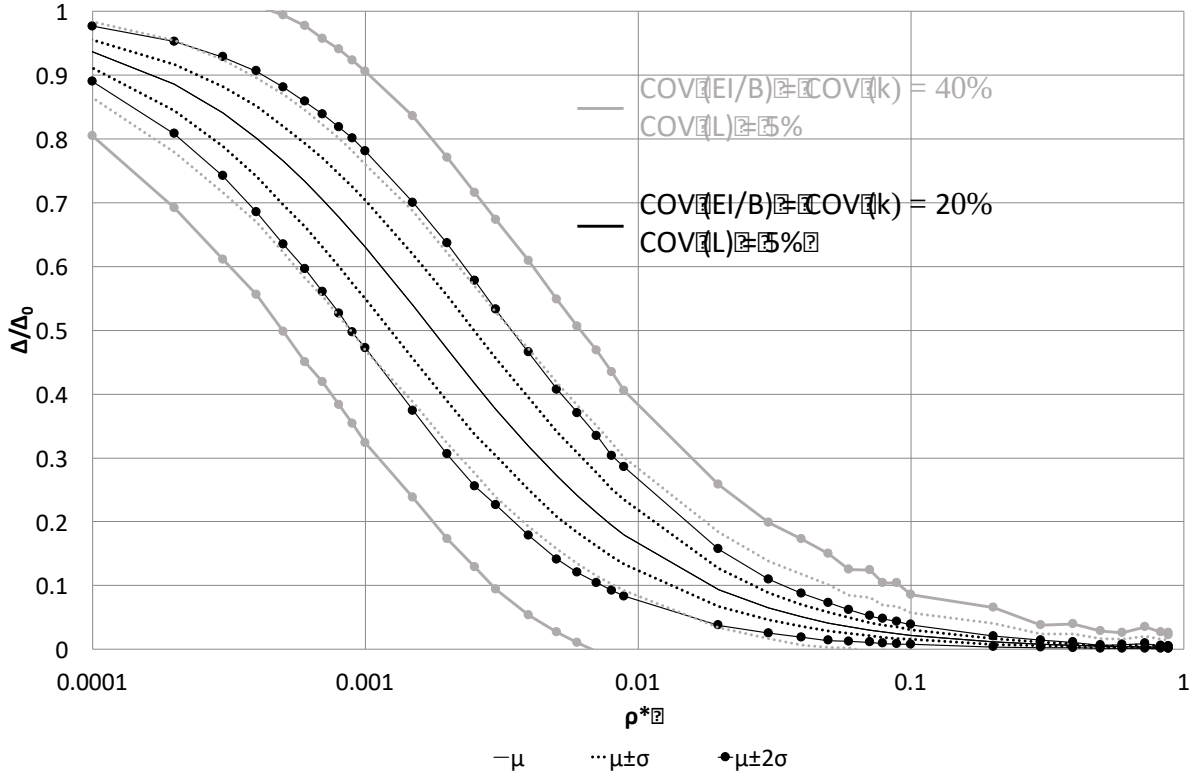


Fig. IV.11. Confidence intervals of the transmission ratio Δ/Δ_0 versus the relative stiffness ρ^*.

Thus, to consider the uncertainties related to the estimation of SSI parameters and their variability, Figure 11 shows a simplified evaluation of Δ/Δ_0 though the evaluated confidence intervals.

3. Comparison with Finite Element Models

One of the objectives of this paper is to numerically evaluate the confidence intervals of Δ/Δ_0. A significant number of simulations has to be evaluated. To do so, a remote scripting interface is added to Plaxis, this interface that is based on the Python language, allows to control both the input and output of Plaxis program via an external Python handler.

Consequently, three particular cases are chosen that cover the distribution range of the relative stiffness corresponding numerically to Δ/Δ_0 of 0.102, 0.467 and 0.768 (Figure 4). For every case 1,000 simulations are evaluated according normal distributions of L (COV=5%) and EI/B and k (COV=40%). In this particular process, serious computational difficulties are involved, which proves the advantage of using an analytical approach to evaluate the parameters variability.

The mean value and standard-deviation are calculated for every case, and results are shown in Figure 12. Globally, numerical confidence intervals evaluated with 1,000 iterations for each of the 3 particular cases fit-well with the analytical confidence intervals results. Consequently, the analytical approach seems to be sufficient to predict the confidence intervals of the transmission ratio taking the SSI parameters variability into consideration.

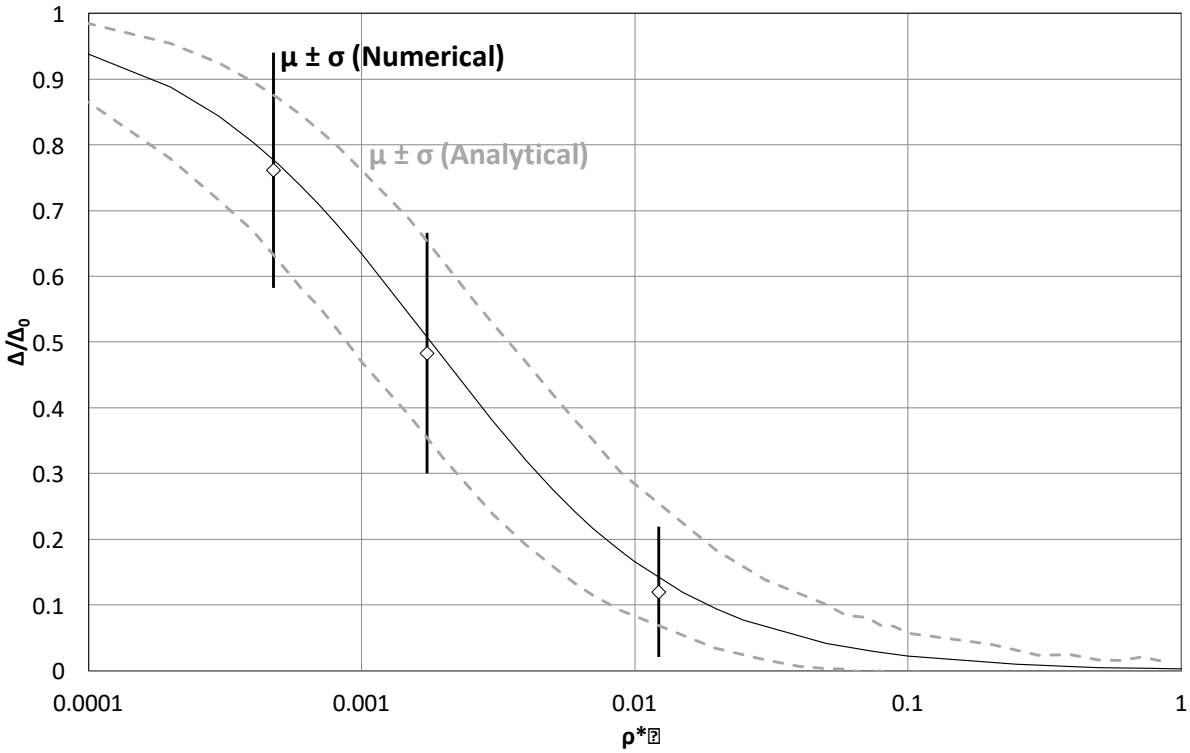


Fig. IV.12. Comparison between the analytical confidence intervals and the numerical confidence intervals evaluated for the 3 particular cases, 1,000 numerical simulations for each case.

IV.6 Conclusions

A large margin of discrepancy is shown between different SSI methods presented in the literature to evaluate the transmission of the ground movements to structures. This discrepancy may be explained by the influence of uncertainties. This paper aims to investigate the uncertainties affecting the prediction of the structure response to ground movements, through an analytical approach, taking into account the variability of the SSI parameters.

This paper suggests a simplified meta-model (Eq. (10)) to evaluate the transmission of the ground movement to structures. This equation depends upon the relative stiffness, upon the SSI parameters (EI/B, k and L). This meta-model corresponds to Deck & Singh (2010) analytical approach that is based on elastic Euler–Bernoulli beam sitting on elastic vertical springs as per the Winkler model. This approach presents moderate results in comparison with other analytical, numerical, experimental and field data results. In addition, this approach is validated by an elastic finite element model (FEM) presented in this paper that intends to fully reproduce the elastic conditions of Deck & Singh (2010) analytical approach.

Then, a sensitivity analysis (SA) is performed using local and global methods: (a) One local method (One-way sensitivity analysis) is performed to evaluate the impact of variability on the output around a particular value of each input parameter. (b) Two global methods (Sobol and McKay) are applied to evaluate the contribution of each input parameter on the response in the entire domain of variation. These two global methods present differences with respect to the sampling techniques and the

evaluation of the dependence between the input variables. In addition, Sobol method evaluates the existence of a possible interaction between input variables.

SA results reveal that Δ/Δ_0 highly depends upon the variability of the SSI parameters, upon their probability distribution function and their COV.

- A first approach is performed by considering a uniform distribution of each parameter over its entire distribution range. The target is to get a global overview of the influence of the parameters in the considered distribution range. Results show that L has the highest influence; its influence is comparable to the influence of EI/B and k (approximately 1.5 times higher effect). In addition, in this approach, the effect of EI/B is higher than k, since its range of variation is higher (Table 3).
- A second approach is performed by considering a normal distribution of each parameter with the same COV. The target is to assess the parameter having the highest influence from a mathematical point of view. Results show that L has the highest influence, which is 4 times higher than the influence of EI/B and k (Table 4).
- A third approach is performed by considering a normal distribution of each parameter with realistic COV defined in the literature. The target is to evaluate the parameter that has the highest influence considering both, mathematical influence and realistic variability. This approach is performed in the perspective of an operational use of the deterministic results of Δ/Δ_0 shown in Figure 8.

According to the third approach, it was found that the effect of every parameter varies according to the considered ρ* value. Globally, the effect of EI/B increases with the increasing values of the relative stiffness ρ*; however, the effect of k increases when ρ* decreases.

The variability of L is limited (COV=5%) compared to the one of EI/B and k (COV=40%) according to the literature. Thus, L has the lowest influence of L for the entire variation range of ρ* (Figure 10). On the other hand, for low ρ* values, k has the highest influence, while for high ρ* values EI/B has the highest influence. For intermediate ρ* values, EI/B and k have nearly the same effect.

Finally, confidence intervals are developed analytically and validated numerically by considering the variability of the SSI parameters. A range of results of Δ/Δ_0 is associated with every value of the relative stiffness by considering a level of confidence that is set between 70 and 95% (Figure 11). These confidence intervals provide a simplified probabilistic evaluation that can be directly adopted by engineers for design purposes during preliminary stages to assume a Δ/Δ_0 value, to have an efficient assessment of the rate of the ground movement that is transmitted to structures when considering the uncertainties related to the estimation of SSI parameters.

IV.7 Acknowledgement

The work presented in this paper was supported by a research grant from Lorraine University of Excellence and the National Council for Scientific Research-Lebanon (CNRS-L) and the Lebanese University.

IV.8 References

[1] Serhal, J., Deck, O., Alheib, M., Chehade, F. & Abdelmassih, D. Damage of masonry structures relative to their properties: Development of ground movement fragility curves. *Engineering Structures*; 2016, 113: 206-219.

[2] Franza, A., Ritter, S. & Dejong, M. Continuum solutions for tunnel-building interaction and a modified framework for deformation prediction. *Géotechnique;* 2019: 1-15.

[3] Zhang, J., Chen, J., Wang, J. & Zhu, Y. Prediction of tunnel displacement induced by adjacent excavation in soft soil. *Tunnelling and Underground Space Technology*; 2013, 36: 24-33.

[4] Basmaji, B., Deck, O., & Alheib, M. Analytical model to predict building deflections induced by ground movements. *European Journal of Environmental and Civil Engineering*; 2017, 10: 1-23.

[5] Deck, O. & Singh, A. Analytical model for the prediction of building deflections induced by ground movements. *International Journal for Numerical and Analytical Methods in Geomechanics*; 2010, 36: 62-84.

[6] Son, M. & Cording, E. Evaluation of building stiffness for building response analysis to excavation-induced ground movements. *Journal of Geotechnical and Geoenvironmental Engineering*; 2007, 133: 995-1002.

[7] Potts, D. & Addenbrooke, T. A structure's influence on tunneling-induced ground movements. *Proceedings of the Institution of Civil Engineers – Geotechnical Engineering*; 1997, 125: 109–125.

[8] Haji, K., Marshall, A., & Franza, A. Mixed empirical-numerical method for investigating tunneling effects on structures. *Tunnelling and Underground Space Technology*; 2018, 73: 92-104.

[9] Giardina, G., Marini, A., Hendriks, M., Rots, J., Rizzardini, F. & Giuriani, E. Experimental analysis of a masonry façade subject to tunnelling-induced settlement. *Engineering Structures*; 2012, 45: 421-434.

[10] Franza, A. & DeJong, M. A simple method to evaluate the response of structures with continuous or separated footings to tunnelling–induced movements. *Congress on Numerical Methods in Engineering, Valencia, Spain*; 2017, 919-931.

[11] Saeidi, A. La vulnérabilité des ouvrages soumis aux aléas mouvements de terrains : développement d'un simulateur de dommages-Doctorate thesis, Institut National Polytechnique de Lorraine, Nancy, France; 2010.

[12] Giardina, G., Graaf, A., Hendriks, M., Rots, J. & Marini, A. Numerical analysis of a masonry façade subject to tunnelling-induced settlements. *Engineering Structures*; 2013, 54: 234-247.

[13] Fu, J., Yu, Z., Wang, S. & Yang, J. Numerical analysis of framed building response to tunnelling induced ground movements. *Engineering Structures*; 2018, 158: 43-66.

[14] El Kahi, E., Deck, O., Khouri, M., Mehdizadeh, R. & Rahme. P. Étude de l'influence de la plasticité du sol sur la transmission des mouvements du sol affectant l'interaction sol-structure. *Revue Française de Géotechnique*. 2018, 156, 4.

[15] Mair, R. Tunneling and deep excavations: Ground movements and their effects. *Proceedings of 15th European conference on soil mechanics and geotechnical engineering geotechnics of hard soils – weak rocks*; 2013, 4: 39-70.

[16] Franzius, J., Potts, D. & Burland, J. The response of surface structures to tunnel construction. *Proceedings of the Institution of Civil Engineers, Geotechnical Engineering*; 2006, 159: 3–17.

[17] Goh K. Response of Ground and Buildings to Deep Excavations and Tunnelling-Doctorate Thesis, University of Cambridge, 2010.

[18] Saeidi, A., Deck, O. & Verdel, T. Development of building vulnerability functions in subsidence regions from empirical methods. *Engineering Structures*; 2009, 31: 2275-2286.

[19] ElKahi, E., Khouri, M., Deck, O., Rahme, P., & Mehdizadeh, R. Studying the Influence of Uncertainties on the Transmission of Ground Movements Affecting the Soil-Structure Interaction. *10èmes journées Fiabilité des Matériaux et des Structures, Bordeaux, France*; 2018.

[20] Schweiger & Peschl. Basic Concepts and Applications of Random Sets in Geotechnical Engineering. *Probabilistic Methods in Geotechnical Engineering*; 2007, 491(1): 113-126.

[21] Giasi, Masi & Cherubini. Probabilistic and fuzzy reliability analysis of a sample slope near Aliano. *Engineering Geology*; 2003, 67(3-4): 391-402.

[22] Castaldo, P., Gino, D., Bertagnoli, G. & Mancini, G. Partial safety factor for resistance model uncertainties in 2D non-linear finite element analysis of reinforced concrete structures. *Engineering Structures*; 2018, 176: 746-762.

[23] Baecher, B. & Christian, J. Reliability and statistics in geotechnical engineering. John Wiley & Sons; 2003.

[24] Jacques, J. Pratique de l'analyse de sensibilité : comment évaluer l'impact des entrées aléatoires sur la sortie d'un modèle mathématique. Université de Lille; 2011.

[25] Piegay. Optimisation multi-objectif et aide a la decision pour la conception robuste-Doctorate Thesis, Université de Bordeaux; 2015.

[26] Giardina, G., Hendriks, M. & Rots, J. Sensitivity study on tunnelling induced damage to a masonry façade. *Engineering Structures*; 2015, 89: 111-129.

[27] Aissaoui, K. Amélioration de la prévision des affaissements dans les mines à l'aide des approches empiriques, numériques et analytiques-Doctorate thesis, Institut National Polytechnique de Lorraine, Nancy, France; 1999.

[28] Vesic. Beams on Elastic Subgrade and Winkler's Hypothesis. *Proceedings of the 5th International Conference on Soil Mechanics and Foundation Engineering*; 1963, 845-850.
[29] Biot. Bending of an infinite beam on an elastic foundation. *Journal of Applied Mechanics*; 1937.
[30] Drapkin. Grillage beams on elastic foundations. *Proc. ASCE*; 1955.
[31] Klöppel & Glock. Theoretische und Experimentelle Untersuchungen zu den Traglastproblemen Biegeweicher, in die Erde Eingebetteter. Institutes für Statik und Stahlbau der Technischen Hochschule Darmstadt; 1970.
[32] Henry. The Design and Construction of Engineering Foundations. Chapman & Hall; 1986.
[33] Kala, Z. Sensitivity assessment of steel members under compression. *Engineering Structures*; 2009, 31(6): 1344-1348.
[34] Sudret. Meta-models for structural reliability and uncertainty quantification. *Asian-Pacific Symposium on Structural Reliability and its Applications, Singapore*; 2012, 1-24.
[35] Kimathi, N. Investigation into estimation of building projects variation contract period. University of Nairobi, 2016.
[36] Aït-Mokhtar, A., Torrenti, M., Benboudjema, F., Capra, B., Carcasses, M., Colliat, J., Cussigh, F., Larrard, T., Lataste, J., Poyet, S. Experimental investigation of the variability of concrete durability properties. *Cement and Concrete Research;* 2013, 45 : 21-36.
[37] Sykora & Holicky. Evaluation of Compressive Strength of Historic Masonry Using Measurements. *Advanced Materials Research*; 2014, 923: 213-216.
[38] Parisi & Augenti. Uncertainty in Seismic Capacity of Masonry Buildings. *Buildings*; 2012: 218-230.
[39] Dymiotis & Gutlederer. Allowing for uncertainties in the modelling of masonry compressive strength. *Construction and Building Materials*; 2002, 16: 443-452.
[40] Sadrekarimi & Akbarzad. Comparative Study of Methods of Determination of Coefficient of Subgrade Reaction. *Electronic Journal of Geotechnical Engineering*; 2009.
[41] Matsubara & Hoshiya. Soil Spring Constants of Buried Pipelines for Seismic Design. *Journal of Engineering Mechanics*; 2000, 126(1).
[42] Terzaghi, K. Evaluation of coefficient of subgrade reaction. *Geotechnique*; 1955, 5(4): 297-326.
[43] Imanzadeh. Effects of uncertainties and spatial variation of soil and structure properties on geotechnical design. Cases of continuous spread footings and buried pipes-Doctorate Thesis, Université Bordeaux; 2013.
[44] Deck, O. Étude des conséquences des affaissements miniers sur le bâti. Doctorate Thesis, École des Mines Nancy; 2002.
[45] Peck, R. 1969. Deep excavations and tunnels in soft ground. *Proceedings of the 7th International Conference on Soil Mechanics and Foundation Engineering, Mexico City, State of the Art Volume*; 1969: 225–290.
[46] El Kahi, E., Deck, O., Khouri, M., Mehdizadeh, R. & Rahme. P. Influence of Spatial Variability of Soil Properties on Structures Response. *Proceedings of the 29th European Safety and Reliability Conference*; 2019.
[47] El Kahi E., Deck, O., Khouri, M., Mehdizadeh, R., Rahme, P. A new simplified meta-model to evaluate the transmission of ground movements to structures integrating the elastoplastic soil behavior. *Structures*, 2020, 23: 324–334.
[48] Fatahi, B., Tabatabaiefar, S. & Samali, B. Soil-structure interaction vs Site effect for seismic design of tall buildings on soft soil. *Geomechanics and Engineering*, 2014, 6(3): 293-320.
[49] Fatahi, B. & Tabatabaiefar, S. Effects of Soil Plasticity on Seismic Performance of Mid-Rise Building Frames Resting on Soft Soils. *Advances in Structural Engineering*, 2016, 17(10): 1387-1402.
[50] Far, H. Advanced computation methods for soil-structure interaction analysis of structures resting on soft soils. *International Journal of Geotechnical Engineering*. 2019, 13(4): 352-359.
[51] Fatahi, B., Tabatabaiefar, S. & Samali, B. Finite difference modelling of soil-structure interaction for seismic design of moment resisting building frames. *Australian Geomechanics Journal,* 2012, 47(3):113-120.
[52] Tabatabaiefar, S. & Clifton T. Significance of considering soil-structure interaction effects on seismic design of unbraced building frames resting on soft soils. *Australian Geomechanics Journal,* 2016, 51(1): 55-64.

V. Influence of uncertainties on the evaluation of building deflections induced by ground movements

This paper is currently under review in the *European Journal of Environmental and Civil Engineering*.

Influence of uncertainties on the evaluation of building deflections induced by ground movements

Elio EL KAHI[12*], Olivier DECK[1], Michel KHOURI[2], Rasool MEHDIZADEH[1] and Pierre RAHME[2]

[1] *Lorraine University, CNRS, CREGU, GeoRessources laboratory, Ecole des Mines de Nancy, Campus Artem, CS14234, 54042 Nancy Cedex, France;*

[2] Faculty of Engineering, Lebanese University, Roumieh, Mount-Lebanon, Lebanon

V.1 Abstract

The objective of this paper is to investigate the influence of uncertainties affecting the evaluation of building-relevant deflections induced by tunneling or mining subsidence. Based on a Winkler model coupled with an elastic Euler-Bernoulli beam, an analytical approach is applied to evaluate the influence of important sources of uncertainties related to the Soil-Structure Interaction (SSI) conditions and properties, namely, the free-field ground movement profile, the building position to the settlement curvature and the variability of the structure stiffness caused by the heterogeneity of structural materials and openings (doors, windows, etc.). The analytical approach is then validated by numerical finite element models that are applied using Plaxis 2D. Results reveal the discrepancy in the structure response by considering these uncertainties in the entire domain of variation of the SSI parameters. For an operational use, a coefficient A is proposed; this coefficient can be used by engineers and designers when evaluating the building damage induced by the transmission of ground movements to structures taking into consideration these uncertainties.

V.2 Keywords:

Soil-Structure Interaction; Uncertainties; Ground movements; Building deflection; Analytical approach; Numerical models.

V.3 Introduction

1. Background

Ground movements may have different sources such as the influence of nearby excavations (tunnels) [1, 2] and the presence of underground voids such as mining subsidence, sinkhole, etc. [3, 4]. Mining subsidence and tunneling-induced ground movements are characterized by vertical and horizontal displacements with other effects (ground curvature, slope, etc.) that cause differential soil settlement under the building and may lead to major damage [5, 6]. As shown in Fig. 1, the free-field ground movement represents the soil displacement produced by the source (tunnel, mine, etc.), without taking into account the influence of possible constructions on the surface. In the presence of an existing structure, the free-field ground movement is partially or totally transmitted to the building which may result in a structural or functional damage [7].

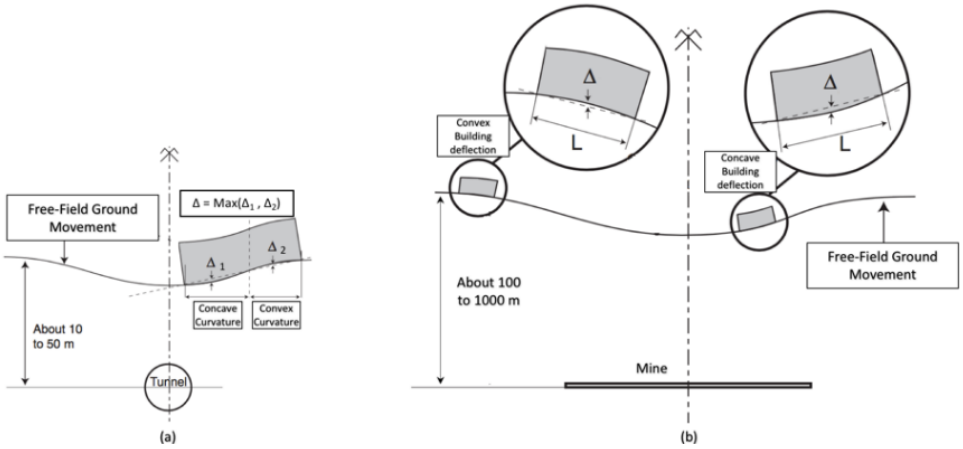


Fig. V.1: Building deflection caused by ground movements.

By neglecting the impact of the interaction between the soil and the structure (SSI), the free-field ground movements are integrally transmitted to the building. Under this assumption, Δ_0 represents the maximum deflection of the building. Assuming that free-field ground motion is symmetrical and roughly circular under the building, Δ_0 represents the maximum free-field deflection under the building (for an integrally transmitted movement); it depends upon the ground radius of curvature R and the building length L (Fig. 2). By considering the impact of the SSI, the ground movement may be partially transmitted to the structure which results a building deflection characterized by its maximum value Δ with $\Delta \leq \Delta_0$. Consequently, as shown in Fig. 3, if the structure is stiff, it can resist the ground movement and the induced deformation is limited ($\Delta < \Delta_0$); if it is flexible, then it perfectly follows the settlement of the soil ($\Delta = \Delta_0$) [8, 9]. The soil settlement produced by the free-field ground movements affects the structure behavior, the induced loads in the structural members may change and can cause structural damage [9]. The amount of redistribution of loads depends upon the stiffness of the structure and the load-settlement characteristics of the soil. The Δ/L ratio, called the deflection rate, is frequently used to assess the behavior of structures subject to differential settlement and evaluate their damage [10].
The objective of this paper is to evaluate the uncertainties affecting the structure response to the ground movement through the deflection transmission ratio, defined as Δ/Δ_0 that is used to quantify the rate of movement transmitted to the building.

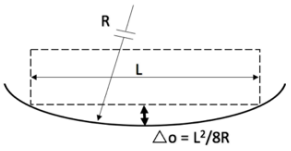


Fig. V.2: Free-field deflection Δ_0.

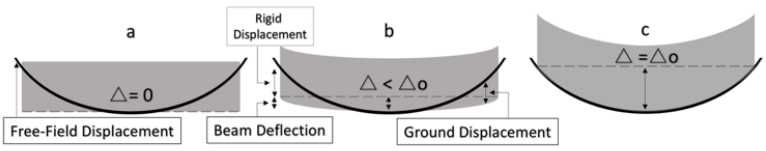


Fig. V.3: Behavior of structures subjected to ground movement. (a) High-stiffness structure on soft ground. (b) Intermediate ground and structure stiffness. (c) Flexible structure on stiff ground.

2. Literature review

Different methods (analytical, numerical, experimental, etc.) have been developed to predict the building deflection in response to the ground movements [1, 9, 11-13]. Except empirical methods based on observations of real existing structures, all of these methods do not consider a specific study of a particular case but they are applied to simplified structures, such as beams, in order to assess the

global trend of ground movements induced phenomena. Consequently, previous research on this subject addresses the question of building stiffness compared to ground stiffness, which is known as "relative stiffness", and suggests to assess the transmission ratio Δ/Δ_0 as a function of a relative stiffness parameter ρ* between the soil and the structure [1, 9, 12]. Most of these studies rely on Eq. 1 to evaluate the relative stiffness parameter ρ* based on the structure length L, inertia I* (per linear meter), Young's modulus E and soil Young's modulus Es. Eq. 1 has the advantage of being non-dimensional and of being well adapted to the synthetic representation of Δ/Δ_0.

$$\rho^* = \frac{EI^*}{EsL^3} \qquad \textit{Eq. V-1}$$

a) Comparison of analytical, numerical, experimental and field data results from previous research

Mair (2013) [7] compared the transmission ratio, derived from the finite-element analyses of Potts and Addenbrook (1997) [1] and Franzius et al. (2006) [14], against the relative stiffness. Also, he considered the results of finite element parametric analyses, of deep excavations in soft clay on adjacent buildings, using the modified cam clay soil model done by Goh (2010) [15]. The comparison of these studies shows that the obtained results fall into a relatively narrow envelope known as Mair (2013) [7] envelope (Fig. 4).

This paper compares Mair (2013) [7] envelope to the results of various SSI studies (analytical, numerical, etc.) that also evaluate the transmission of ground movements to structures (Deck & Singh (2010) [9]; Basmaji *et al*. (2017) [11] and Franza *et al*. (2019) [5]) (Fig. 4). However, each study is based on a set of hypotheses that does not allow the generalization of the obtained results:

a- Mair (2013) [7] envelope is based on physical centrifuge modelling of building response to tunneling and their results are compared with both, the finite element analyses reported by Potts and Addenbrooke (1997) [1] and Franzius et al (2006) [14], and the field data of building performance Goh (2010) [15].

b- Deck & Singh (2010) [9] analytical model is based on Euler–Bernoulli beam sitting on vertical springs as per the Winkler model. They plotted their results using their own definition of the relative stiffness that is based on the Winkler coefficient of subgrade reaction (Winkler parameter k).

In fact, they defined the relative stiffness ratio ρ* by Eq. 2 characterized by the Winkler parameter k and the structure width B. This equation is comparable to other relative stiffness ratios defined in the literature; it presents the advantage of being a non-dimensional parameter and suitable to have a synthetic representation of Δ/Δ_0 based on Winkler model.

$$\rho^* = \frac{EI}{kBL^4} \qquad \textit{Eq. V-2}$$

In order to make the comparison between Deck & Singh (2010) model, based on their own relative stiffness ratio, and other models, Vesic (1963) [16] formula (Eq. 3) is used to define values for k in the case of a foundation with length L, width B (with L>B) and a ground characterized by a Young's modulus Es and a Poisson's ratio υ. In this case B is taken equal to 1m, which approximatively corresponds to the width of a building foundation. Noting that various formulas link the Winkler modulus to the soil Young modulus [16-20], Vesic's formula is chosen since it takes into account the

presence of a beam (through the "EI" term) contrary to other formulas.

$$k = \frac{0.65}{B}\sqrt[12]{\left(\frac{EsB^4}{EI}\right)}\frac{Es}{(1-\nu^2)} \qquad \textit{Eq. V-3}$$

c- Basmaji et al. (2017) [11] developed a new approach to assess the transmission ratio and the building response to differential settlement, considering the influence of shear deformation. Their model is based on both, Pasternak and Winkler soil models. For both soil models, a methodology has been implemented to justify the parameters values, k (Winkler parameter) and Kp and Gp (Pasternak parameters), as a function of the elastic properties of the soil, the thickness of the compressive ground layer and the building length. Their methodology considered Flamant's theoretical solution of induced vertical settlement, to adjust the displacement for Pasternak and Winkler methods and justify the parameters values for both methods.

d- Franza et al. (2019) [5] methodology is based on elastic and elastoplastic continuum solutions that consider the structure as an equivalent simple beam, assuming that the free-field settlement is given by a standard Gaussian curve, contrary to other models that give elastic solutions based on a polynomial free-field settlement. In addition, the structure is connected to vertical and horizontal coupled springs that model the elastic homogeneous half-space continuum, the soil, while other models assimilate the soil to a juxtaposition of elastic vertical springs. Also, Franza et al. (2019) proposed a formulation that accounts for the change in settlement trough shape and compared it with numerical, experimental and field data from previous research.

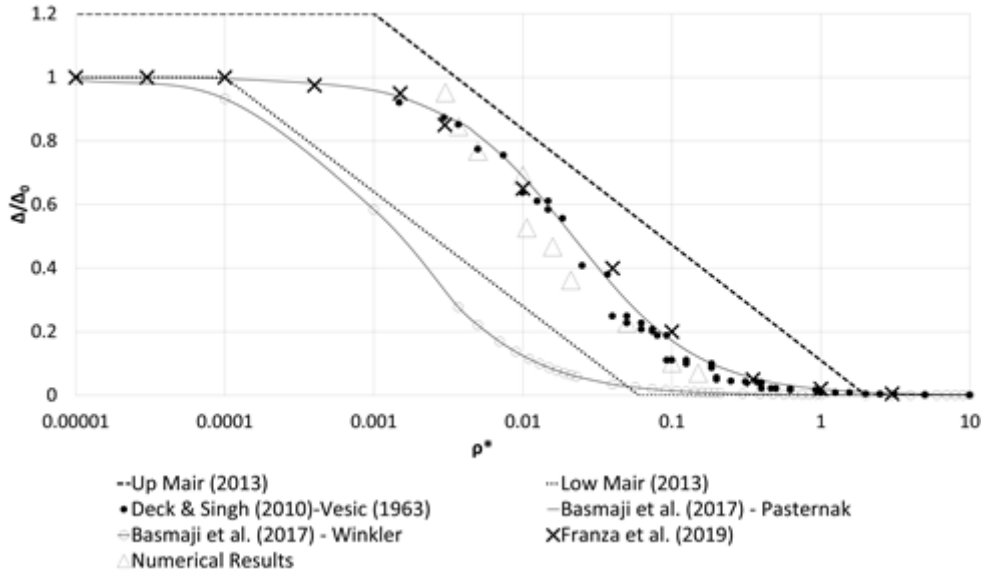


Fig. V.4: Comparison between Mair (2013); Deck & Singh (2010); Pasternak-Basmaji *et al*. (2017); Winkler-Basmaji *et al*. (2017), Franza *et al*. (2019) results and numerical (Plaxis 2D) results.

b) Comparison with a finite-element model

This paper develops an elastic finite element model (FEM) to compare the results of previous studies in the literature with a set of numerical simulations. The objective of the FEM is to model the ground curvature induced by ground movements and calculate the elastic transmission ratio of the free-field deflection. In fact, Basmaji et al. (2017) [11] and Deck & Singh (2010) [9] validated their analytical elastic results with numerical models; however, they considered an elastoplastic ground behavior in their numerical studies, and they modeled the subsidence by a uniformly distributed load imposed on

the lower boundary. On the contrary, the numerical model presented in this paper intends to fully reproduce the elastic conditions in order to well verify the effectiveness of the previous elastic analytical results. Subsequently, this FEM model considers a linear elastic ground behavior. By considering a linear behavior, large deformations and large mass losses that occur near the lower limit are avoided which allows the convergence of calculations and the accuracy of results.

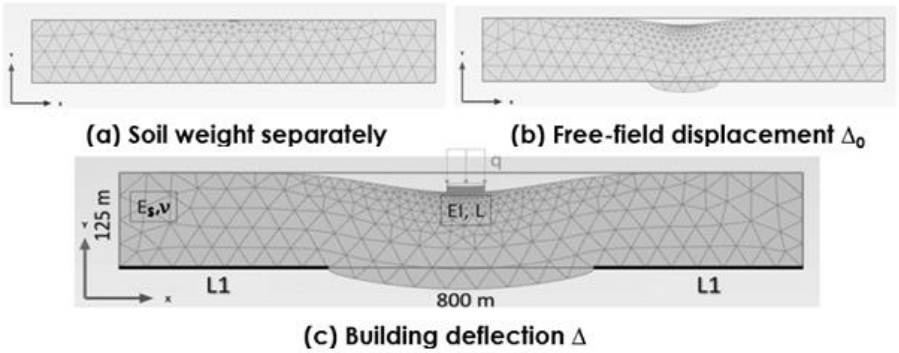


Fig. V.5: Description of the finite element model used to compare analytical results of the deflection transmission ratio with numerical results.

The numerical model is performed with a finite element software (Plaxis 2D) under the plane strain hypothesis. The model consists of an elastic soil layer, 125 m thick and 800 m long, with a building located at the center (Fig. 5). A fine mesh is used for soil elements and the subsidence is imposed without adding a uniform load on the lower boundary. For the boundary conditions, the horizontal displacement is fixed on the right and left boundaries and the vertical displacement is fixed only at the bottom boundary right and left sides (L1) while the central region of the bottom boundary is free. The soil Poisson's ratio ν is 0.3 and the unit weight is 20 KN/m3. The structure is modeled by a beam that is loaded with a vertical uniformly distributed load q.

Three computations are performed as follows:

a- A first computation is performed by fixing the vertical displacement on all the lower boundary in order to generate the initial ground situation under the soil weight. All the evaluated displacements are then set to zero.

b- A second computation is performed by fixing the vertical displacement on L1 (on both sides), without considering the structure, in order to assess the free-field displacement Δ_0 of the subsidence. Δ_0 is evaluated and the displacements are set to zero.

c- A third computation is performed with the presence of both the structure (with the vertical uniformly distributed load) and the subsidence in order to assess the final building deflection Δ considering the soil-structure interaction.

The equivalence between the FEM and the analytical solution is maintained as follows:

a- A linear elastic soil behavior is considered equivalent to the elastic analytical approaches (Winkler, etc.).

b- A value of L1 is selected in order to reach a value of Δ_0 in the FEM that is equivalent to the one of the analytical model (Fig. 5).

c- Mechanical properties and buildings dimensions are chosen so that values are identical with the

ones considered in the analytical approach (q, EI and L).

As shown in Fig. 4, a set of 10 simulations are performed that cover the distribution range of the relative stiffness ρ*, for different values of EI/B, Es, L, q and Δ_0. Globally, numerical results presented in Figure 4 are superimposed with the curve of the transmission ratio calculated with the models of (a) Deck & Singh (2010) using Winkler model combined with Vesic (1963) formula, (b) Basmaji et al. (2017) using Pasternak model and (c) Franza et al. (2019) continuum model. Therefore, these three models can be reasonably used to evaluate the transmission ratio.

3. Presence of uncertainties

As shown in Fig. 4, even-tough the results of SSI studies are globally consistent in the literature, the comparison shows a large margin of discrepancy in the estimation of the transmission of the ground movements to structures. An important portion of this discrepancy may be explained by the influence of uncertainties [11, 18]. In fact, Deck & Singh (2010); Pasternak-Basmaji *et al*. (2017); and Franza *et al*. (2019) analytical models present comparable results that were validated by the FEM (Fig. 4) and can be reasonably used to evaluate the transmission ratio. However, in comparison with numerical and experimental results and with empirical observations of Mair (2013), the margin of discrepancy may reach ± 0.3 in the estimation of Δ/Δ_0.Consequently, this paper aims to investigate the influence of uncertainties affecting the estimation of Δ/Δ_0 and propose a coefficient that considers their influence on the prediction of the structure response. In fact, the transmission ratio may be affected by various uncertain factors, namely the structure equivalent stiffness, particularly for structures with significant wall openings, the geometric and the geological characteristics and the mechanical properties of the soil, in addition to the characteristics related to the source by itself that may affect the free-field deflection shape.

a- In both research and practice, it is common to simplify the structure to equivalent linear elastic beams to decrease computational costs during initial assessment. Generally equivalent beams are identified by matching the bending stiffness EI [14, 22]. However, this approach results in equivalent beams with a lower building deformation. Son & Cording (2007) [12] investigated the equivalent bending and shear stiffness of masonry structures, taking into account the anisotropy of the masonry units and the percentage of window openings, while evaluating the building response to induced ground movements. Pickhaver et al. (2010) [23] suggested a procedure to identify an equivalent Timoshenko beam for bearing wall structures with openings aiming to match the total structure stiffness (both bending and shear contributions). Comparing the results of these studies, a discrepancy is shown revealing the influence of the uncertainty related to the heterogeneity of structure properties on the transmission ratio. This paper aims to investigate and characterize through a coefficient A the influence of this uncertainty on Δ/Δ_0.
b- Structural response is affected by the shape of the settlement curve under the builidng [24]. This curve depends upon the building position to the source of ground movement. Based on numerical calculations in 2D, Potts & Addenbrooke (1997) [1] investigated the effect of the tunnel excavation position and their results revealed an important difference in the structural response by varying this parameter. In addition, Franza et al. (2018) [24] investigated the impact of the tunneling free-field inflection point location on the structure response and their results showed that the interaction

mechanism varied for low and high values of tunnel-structure eccentricity and the difference of the building deflection may reach 50% for various horizontal positions of the inflection point. The impact of the uncertainty of the soil settlement profile and its location compared to the structure position is evaluated in this paper for various settlement shapes and building positions.

4. Choice of an analytical approach

Among the approaches developed to study the SSI phenomenon, only numerical methods offer great flexibility for taking into account the complexity of the SSI conditions [1]. Although it is relatively simple to consider complex soil behavior and structure configuration (heterogeneity of properties, non-symmetrical settlement profile, etc.) in numerical models, their use may be criticized by the justification of the numerical values of all parameters and conditions. In addition, numerical models present difficulties to generalize results, because of the need to reproduce the same scenario numerous times, by varying a particular SSI parameter in each repetition to cover the extent of the variation range of all parameters. Thus, they can be considered as time-consuming processes for uncertainties analyses, considering the elevated number of iterations required [9]. To avoid these difficulties, it is possible to obtain results through analytical methods that develop simple equations to represent the structural deflection. Analytical methods may be considered as a complementary tool to the numerical ones, allowing quick calculations for a wide range of variation of parameters.

Since the Deck & Singh (2010) [9] simplified analytical approach (Euler-Bernoulli beam sitting on vertical springs) provides moderate results of the transmission ratio Δ/Δ_0 compared to others (Fig. 4), and the results vary between 0 and 1 which fits well with the definition of the maximum free-field deflection ($\Delta \leq \Delta_0$), this paper will proceed by considering Deck & Singh (2010) analytical approach.

Based on Deck & Singh Δ/Δ_0 analytical curve, the effect of various significant uncertain factors on Δ/Δ_0 related to the model and geometrical conditions and properties is investigated, in particular, the free-field ground movement profile, the building position to the soil curvature and the variability of the structure stiffness caused by the heterogeneity of structural materials and openings (doors, windows, etc.). These uncertainties are evaluated in the literature [1, 12, 14, 22-44], and a significant discrepancy is shown indicating the influence of these uncertainties. However, these studies considered particular SSI cases and parameters, and their results cannot be generalized for a wide range of SSI parameters. This paper aims to propose a coefficient A for operational use, this coefficient that covers the whole range of SSI parameters, evaluates the influence of these uncertainties on the transmission ratio (Δ/Δ_0).

On the other hand, to validate the analytical results, numerical finite element models are applied for particular cases of SSI conditions and parameters, to investigate the influence of uncertainties affecting the structure response to ground movements, particularly the transmission ratio (Δ/Δ_0).

V.4 Procedure and modeling

Analytically, to characterize the transmission of ground movements to structures, the “elastic springs” approach applied under the diaphragm walls domain can be used to represent the SSI conditions [11, 21]. An illustrative case is the analytical approach developed by Deck and Singh (2010) [9]. This study combines the Winkler model that represents the soil by a juxtaposition of elastic springs characterized by their parameter K (soil reaction modulus) with an elastic Euler-Bernoulli beam to study the

transmission ratio of free-field movement to structures.

Winkler model assumes that the reaction of the soil at each point under the foundation is proportional to the deflection of the foundation at this point. Considering that p(x) and w(x) represent the ground reaction and displacement respectively, Winkler model is evaluated using Eq. V-4 (Fig. 5):

$$p(x) = Kw(x) \qquad \textit{Eq. V-4}$$

On the other hand, the building is assimilated to an elastic Euler-Bernoulli beam of length L, width B, inertia I and Young's modulus E. This beam is loaded by an external uniform vertical load q and by the ground reaction p(x) producing a bending moment M(x) (Fig. 8). The deflection of the beam y(x) is determined using Eq. V-5:

$$y^{(4)}(x) = \frac{q - p(x)}{EI} \qquad \textit{Eq. V-5}$$

Considering that the displacements of the ground and the building are in static equilibrium, it follows that there is a continuous contact between the ground and the beam. As illustrated in Fig. 8, the building undergoes a rigid vertical displacement d with a deflection y(x). If v(x) represents the free-field ground displacement, the condition of no interpenetration is given by Eq. 6. Consequently, the characteristic differential equation of the beam deflection is given by Eq. 7.

$$y(x) + d = v(x) + w(x) \qquad \textit{Eq. V-6}$$

$$y^{(4)}(x) = \frac{q - K_w(y(x) + d - v(x))}{EI} \qquad \textit{Eq. V-7}$$

To solve the problem, six boundary conditions are used [9]. The building deflection (y), bending moment (y'') and shear force (y''') are equal to zero at the extremities of the beam (-L/2 and L/2).



Fig. V.6: Winkler model.

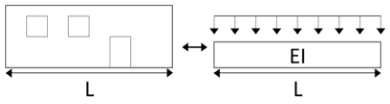


Fig. V.7: Building modeled by an elastic Euler-Bernoulli beam.

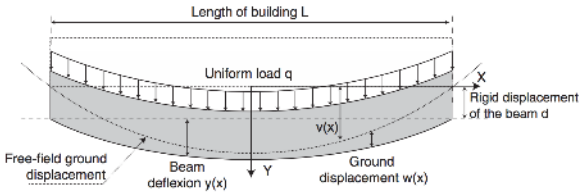


Fig. V.8: Displacements of the ground and the building under conditions of static equilibrium

V.5 Results & Discussion

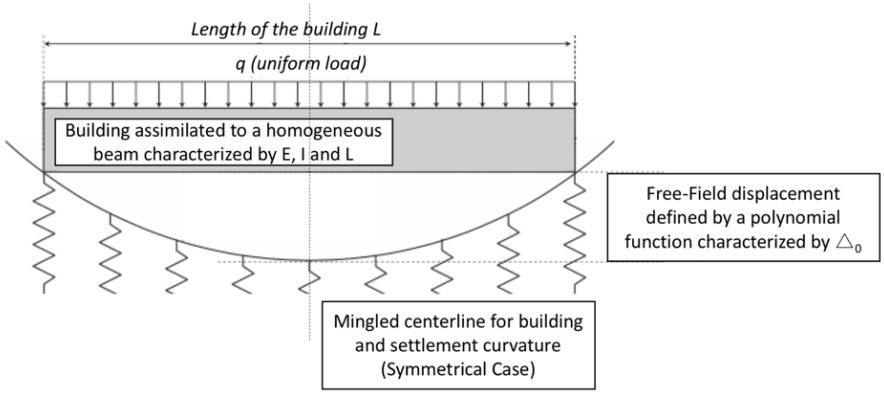


Fig. V.9: Main hypotheses considered in the Deck & Singh methodology (2010).

Based on Deck & Singh model, an accurate prediction of the structure response to the ground movements requires a well-characterization of uncertainties related to the SSI conditions and parameters. Fig .9 summarizes the main hypotheses considered in the Deck & Singh model that can be considered as significant sources of uncertainties based on the literature. The present paper aims to evaluate the effect of these uncertainties and then, a coefficient A will be proposed to consider the influence of these uncertainties while evaluating the transmission of ground movements to structures (Δ/Δ_0).

1. Free-field shape

a) Regular geometrical shapes

Deck & Singh (2010) used a polynomial equation (Eq. V-8) to represent the free-field ground movements shape.

$$v(x) = \Delta_0 \, (1\text{-}4x^2 / L^2) \quad for \quad -L/2 < x < L/2 \qquad Eq.\ V\text{-}8$$

However, geotechnical models are associated with considerable uncertainty of settlement estimation [25]. To check this uncertainty, 5 continuous forms (polynomial, triangular, side triangular, trapezoidal and sinusoidal) and 1 discontinuous form (rectangular) are considered analytically with the same free-field maximal deflection Δ0 (Fig. 10, Fig. 11 and Table 1). Also, a comparison with a Gaussian shape (that is detailed in the next section), for a configuration of $L_{building} \approx L_{curvature}$ and an inflection point located at 0.3 L is evaluated. It is worth to note that the maximum free-field deflection Δ_0 is the same for all these shapes except for the dissymmetrical side triangular case where it goes to $2\Delta_0$ to be compared to a convex symmetrical triangular case characterized by Δ_0 at the two ends. Since all except the side triangular case presented in Fig. 10 are symmetrical, solving the problem for these cases, involves exactly the same variables and equations as the second-order polynomial function presented in Eq. V-8. However, the side triangular case (Fig. 10) is different because of its dissymmetry; it involves another variable, and a condition of no interpenetration different from Eq. V-8. In fact, the rigid displacement for this case is not the same all along the beam. It is important however to consider two different rigid displacements in each of the two beam extremities, d1 for the left extremity and d2 for the right one. The condition of no interpenetration in this case is given by Eq. V-9.

$$(d1 + d2)/2 + x \, (d2 - d1)/L \; + y(x) = v(x) + w(x) \qquad Eq.\ V\text{-}9$$

Table V-1: Regular geometrical free-field movement shapes functions.

Polynomial	*(Deck & Singh model)*		
Sinusoidal	$v(x) = \Delta_0 \, cos(x \, \pi / L)$	for –L/2 < x < L/2	*Eq. V-10*
Triangular	$v(x) = \Delta_0 \, (1 - \frac{2\|x\|}{L})$	for –L/2 < x < L/2	*Eq. V-11*
Trapezoidal	$v(x) = \Delta_0$ $v(x) = 5.\Delta_0 \frac{(-\|x\| + L/2)}{L}$	for |x| < 3L/10 for 3L/10 ≤ |x|	*Eq. V-12*
Side Triangular	$v(x) = 0$ $v(x) = (4.x.\Delta_0) \, /L$	for x < 0 for 0 ≤ x	*Eq. V-13*
Rectangular	$v(x) = \Delta_0$ $v(x) = 0$	for |x| < 2L/10 for 2L/10 ≤ |x|	*Eq. V-14*

To cover a wide range of SSI parameters for various values of the relative stiffness ρ*, an analytical model is developed by investigating 2700 cases for each shape (by considering the combination of all possible values for the considered parameters), as mentioned in Table 2.

Table V-2: Model parameters

Symbol (Unit)	Description	Values
L(m)	Beam Length	10, 20, 30
q (KN/m)	Beam Load	100, 200, 300, 400
EI(GN.m²)	Beam Stiffness	20, 50, 100, 250, 500
KB(MPa)	Ground Stiffness	20, 50, 100, 250, 500
R(m)	Free-Field Ground Radius of Curvature	250, 500, 750, 1000, 1500, 2000, 3000, 4000, 5000

The building length was taken between 10 and 30 m to model small and intermediate buildings [9]. The beam loading represents the building self-weight and service loading. Therefore, 100 kN/m is approximately the weight of a 5 m high wall, with a thickness of 0.5 m with service loading; 200 kN/m is approximately the weight of a 10 m high wall with a thickness of 0.5 m and 400 kN/m is about the weight of a whole building with three 5 m tall walls with a thickness of 0.5 m including service loading. The beam bending stiffness EI is between 20 and 500 GN.m^2. The smallest value represents the stiffness of a 0.5 m masonry wall thickness with 5 m height and a 3000 MPa equivalent Young's modulus for the masonry. The largest value represents the stiffness of a 0.2 m thick concrete wall, 12 m tall with a 20000 MPa equivalent Young's modulus. Vesic (1963) formula (Eq. 3) is used to define values for K. The ground stiffness values Es vary between 20 and 500 MPa for values of soil Young modulus between 40 MPa (soft ground) and 500 MPa (stiff ground) and a Poisson's ratio of 0.3. The free-field ground radius of curvature is set between 250 and 5000m to represent a wide range of scenarios.

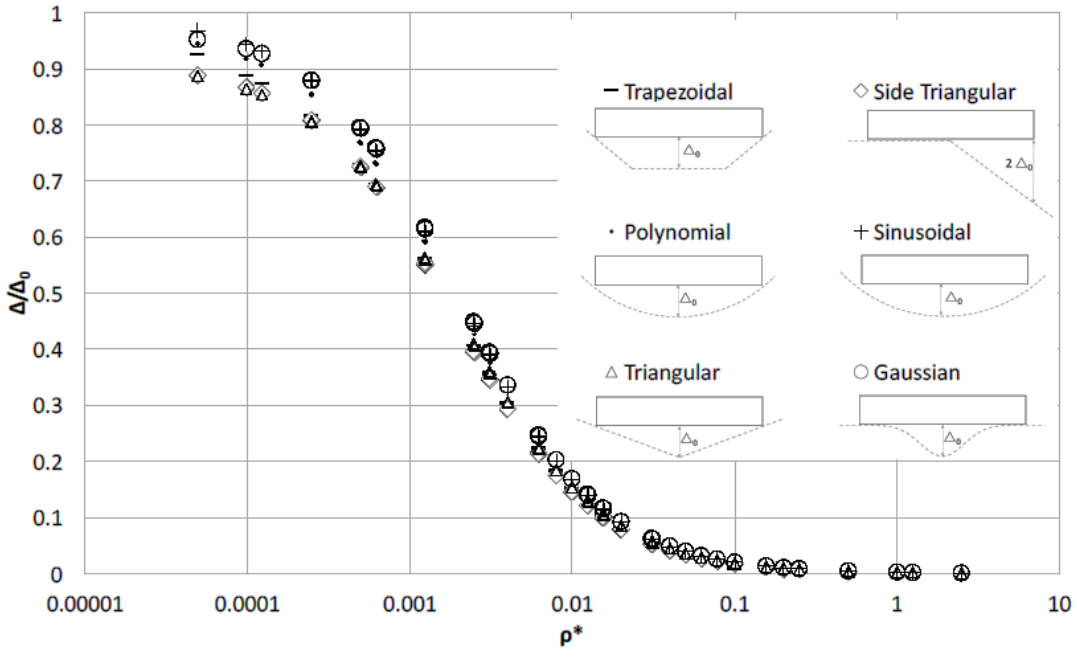


Fig. V.10: Deflection transmission ratio Δ/Δ_0 versus the relative stiffness ρ* for different continuous regular geometrical shapes of free-field ground movements.

Fig. 10 and Fig. 11 show the results of the investigated deformation shapes for the free-field ground movement using Mathematica given the values of parameters defined in Table 2. The global trend of the transmission ratio is approximately the same for all the shapes and reach their maximum values as the relative stiffness ratio ρ* decreases (flexible structures on stiff ground). As shown in Fig. 10, for each continuous regular geometrical shape, the curve of the deflection transmission ratio versus the relative stiffness curve is similar to the curve corresponding to the Deck & Singh polynomial function of Eq. V-8 for the free field ground movement. However, for an equivalent stiffness ratio, the results of the maximum transmission ratio vary slightly from one shape to another. The highest values are obtained for the sinusoidal form, while the lowest values are for the triangular form. Nevertheless, the difference between the results of these curves is always less than 15% with a maximal absolute difference of Δ/Δ_0 equal or less than 0.1 which is not very significant for flexible structures on stiff ground (low values of ρ*). It is worth to note that the triangular and the side triangular shapes give very close results with the variation of ρ*. The trapezoidal form gives close results to the polynomial function for small values of ρ*, but it joins the curve of the triangular and the side triangular forms above ρ* = 0.0002.

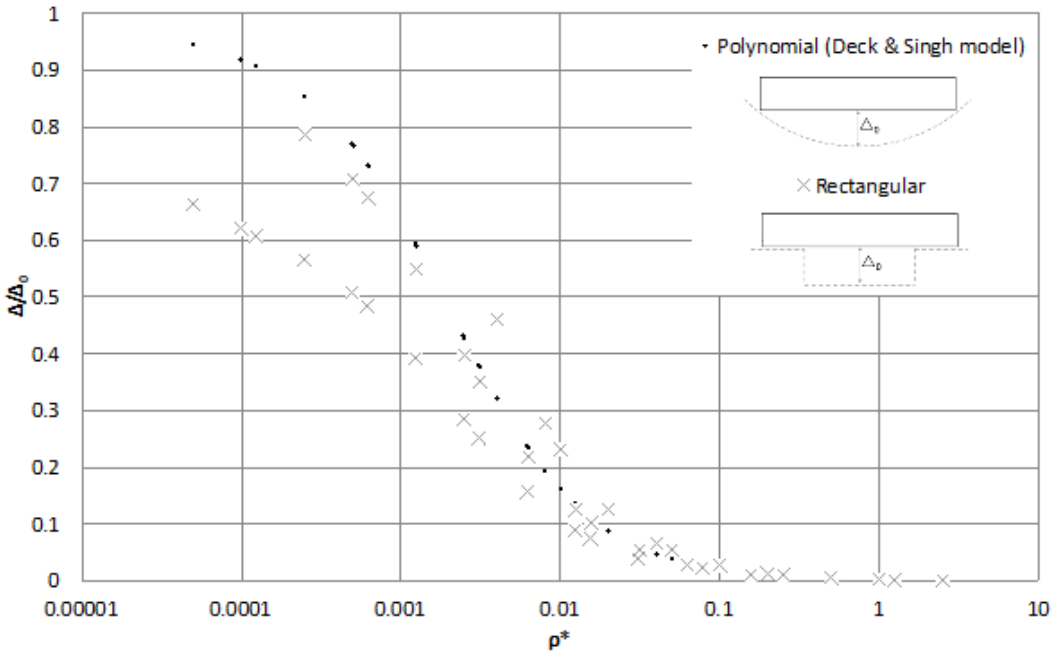


Fig. V.11: Δ/Δ_0 versus ρ* for the discontinuous shape in comparison with the polynomial shape.

As shown in Fig. 11, for the discontinuous shape, the results do not show a "one-line curve" such as the continuous regular geometrical shapes, but they show a range of points that respects the overall curvature of the continuous cases. Thus, for nearly the same value of the relative stiffness ρ*, 2 results of Δ/Δ_0 are presented. This can be associated to the ultimate discontinuity between 0 and Δ_0 in the rectangular free-field shape which may lead to a significant difference in the behavior between a flexible and a stiff building even if the relative stiffness ρ* is nearly the same. Practically, an accurate evaluation of the discontinuous shape requires the approach of framed structures with columns/piers on separated footings in order to consider the significant differential horizontal displacements they undergo because of tunneling, which are associated with a bending deformation of first level of columns/piers rather than an overall axial deformation of the structure [26]. Additionally, for a discontinuous shape, a complex combination of rotational and translational displacements (consisting

of both vertical and horizontal movements) can occur for separated footings of framed structures which is not illustrated in the beam approach [27]. In comparison with the continuous shape, the difference between the continuous and discontinuous shapes can reach 40% for low values of relative stiffness.

b) Gaussian shape with other configuration

Various researches have considered the free-field shape induces by ground movements through a standard Gaussian curve (particularly for tunneling) displayed in Eq. V-15 [24, 28-29].

$$v(x) = u_{z,max} \exp(-x^2/2i^2) \quad for \quad -L/2 < x < L/2 \qquad Eq.\ V\text{-}15$$

Where x is the horizontal spatial coordinate, $u_{z,max}$ is the maximum settlement that depends upon the tunnel radius and volume loss and i is the horizontal distance of the settlement trough inflection point to the tunnel centerline.

Since the Gaussian curve depends upon the horizontal position of the inflection point, 2 configurations are considered in this paper (Fig. 12): (a) Case 1: i = 0.6 (L/2) and (b) Case 2: i = 0.2 (L/2).

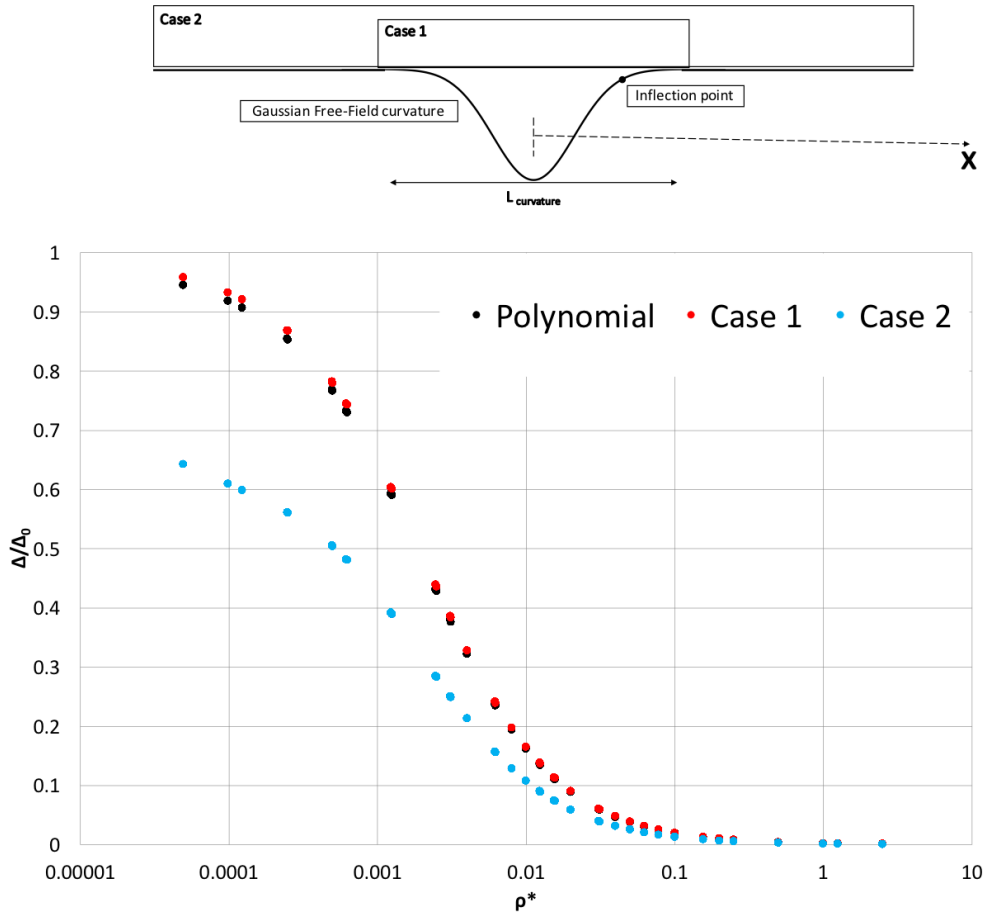


Fig. V.12: Δ/Δ_0 versus ρ* for the Gaussian shape, for various configurations of the Gaussian shape in comparison with the polynomial shape.

As shown in Fig. 12, for the Gaussian shape, the overall form of Δ/Δ_0 curve is similar to the Deck & Singh curve, however, the structure length compared to the curvature length has an important role.

a- For the case 1, $L_{building} \approx L_{curvature}$ the results are very close to Deck & Singh model with the variation of ρ*. This case is presented in Fig. 10.

b- For the case 2, $L_{building} >> L_{curvature}$, a significant portion of the building is subjected to a relatively "flat" soil settlement; consequently, Δ/Δ_0 results are significantly lower than the Deck & Singh results.

2. Building position to the settlement curvature

Previous discussed shapes (Fig. 10, Fig. 11 and Fig. 12) consider the building centerline mingled with the one of the free-field curvature (even the dissymmetrical side triangular case subjected to $2\Delta_0$ indirectly represents a symmetrical convex triangular case characterized by Δ_0 at the two ends). However, as shown in Fig. 1, for real cases, the building may be distant from the curvature center and inflection point which affects the structure response. Two cases are distinguished:

a- Fully concave/convex curvature, where the building is distant from the inflection point (Case of mines) as shown in Fig. 1(b).

b- Partially concave/convex curvature, where the inflection point of the free-field settlement is close or under the structure (Case of tunnels) as shown in Fig. 1(a).

a) Fully concave/convex curvature

Considering an important curvature length and a building that is distant from the inflection point, induce a fully concave or convex curvature under the building. Thus, all cases considered in Fig. 10, Fig. 11 and Fig. 12 are concave. On the other hand, to investigate the difference with the convex curvatures, sinusoidal, triangular, trapezoidal, side triangular, rectangular and Gaussian for convex shape deformation profiles are compared with concave shape profiles. Following the hypothesis of the continuous contact between the ground and the beam, the results of the concave form coincide with that of the convex form for all considered forms (sinusoidal, triangular, trapezoidal, side triangular, rectangular and Gaussian).

Numerical finite element models are applied to validate the concavity/convexity analytical results. As shown in Fig. 13, a vertical uniform load is applied on the bottom boundary to impose a convex curvature; its value is fixed depending on Δ_0 value. The target is to get a comparable Δ_0 in both cases, concave and convex soil curvatures. Fig. 13 shows the results in comparison with the same concave investigated cases; results reveal that having a comparable value of Δ_0, the transmission ratio Δ/Δ_0 of the concave form coincide with that of the convex form.

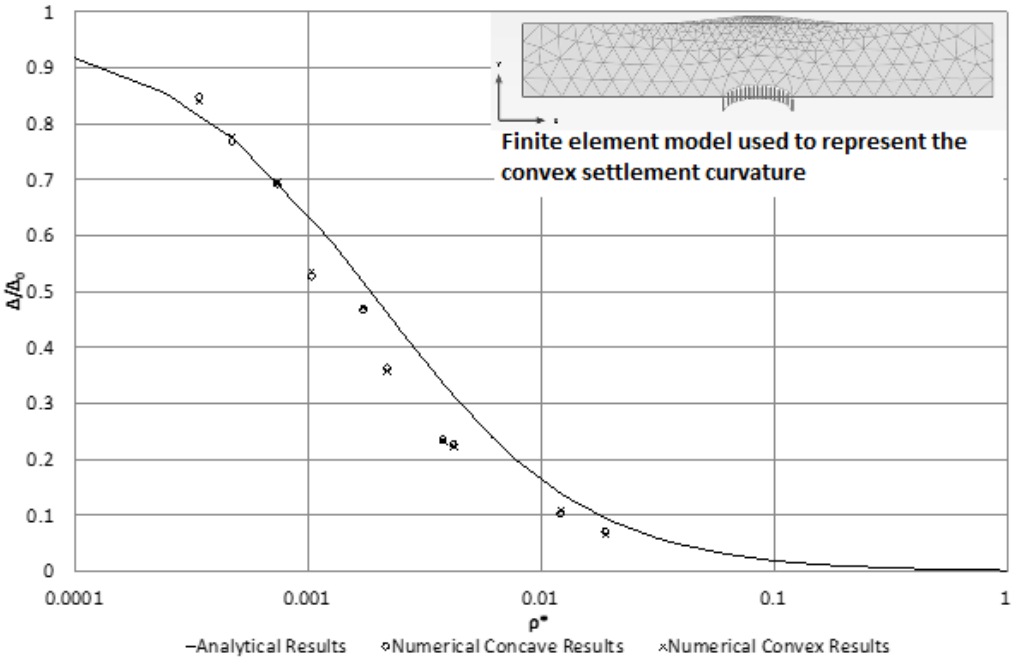


Fig. V.13: Results of the numerical comparison between concave and convex soil curvatures for the deflection transmission ratio.

b) Partially concave/convex curvature.

For ground movements caused by tunneling in particular, the horizontal dimension of the building is typically similar to that of the ground subsidence ($L_{curvature} \approx L_{building}$). The building may straddle the concave and convex curvatures. It is important to note that the deformation Δ represents the maximum deflection of the building whether the beam has a concave or a convex deformation. As shown in Fig. 1, if one part of the building has concave curvature and the other part is convex, then Δ represents the maximum between these two values. This paper considers this uncertainty by applying a continuous and a discontinuous approach, as shown in Fig. 14 and Fig. 15, where "a" is the length of the gap located underneath the structure. A non-dimensional parameter, x0 = a/L, is considered to plot the results ($L_{curvature} \approx L_{building}$).

Considering the Case 3 of Fig. 12, Fig. 16 shows the results for different values of x0 between 0 and 1 and different values of ρ* between 0.0005 and 0.1. It is important to note that Δ is not always located under the center of the building; it depends upon the value of x0. Results for a continuous shape (Fig. 16) show two maximums for a value of x0≈0.4 and x0=1 and two minimums for x0=0 and x0≈0.65. This behavior corresponds to a change in the building curvature. At first, for small values of x0, the whole building takes a convex curvature. It reaches a maximum value for x0≈0.4, then the building undergoes simultaneously a concave and convex curvature on two distinct parts. For a value of x0≈0.65, both curvatures (concave and convex) are comparable and counterbalance. For a greater value, the building is mainly of fully concave curvature when the building center is mingled with the curvature center. For a discontinuous shape (Fig. 16), a quite symmetrical behavior is obtained with two maximums for x0≈0.25 and x0≈0.8 and 3 minimums for x0=0, 0.5 and 1. Explanation of this evolution is comparable to the evolution of the continuous shape. In contrast with the continuous shape, the two extreme positions (x0=0 and 1) are here similar and correspond to a building lying on a flat

ground.



Fig. V.14: Influence of building position – Continuous shape.

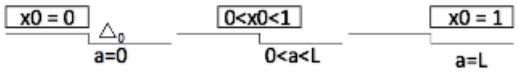


Fig. V.15: Influence of building position – Discontinuous shape.

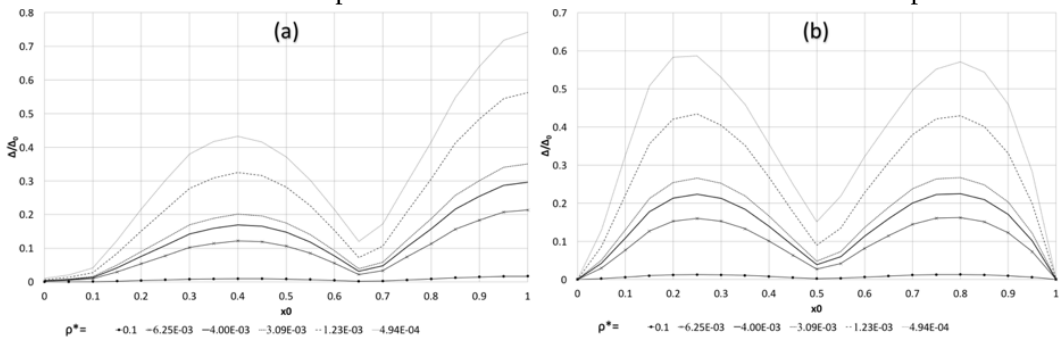


Fig. V.16: Transmission ratio Δ/Δ0 versus the building position: (a)-Continuous approach, (b) Discontinuous Approach.

3. Homogeneity of building stiffness

As Son & Cording (2007) [12] revealed the effect of the anisotropy of the masonry units and the percentage of window openings on the building response, the variability of the building stiffness is considered as an additional source of uncertainty in this study. The presence of openings (windows, doors, etc.), the existence of interior walls, and the heterogeneity of structural materials in addition to the effect of the third dimension are the cause of a stiffness variation along the building. Since the building is assimilated to a beam characterized by one unique stiffness value in the original model, this variation is a source of uncertainty that has to be assessed. Considering a stiffness value EI, this uncertainty is considered by subdividing the building into different portions with a local stiffness value EI_i = (1 + a/100) EI, where the variant coefficient a is a percentage of variation. Four values are considered for a: 40%, 30%, 20% and 10%, and the building is divided into 2, 3 or 4 portions so that the weighted arithmetic mean value EI_{mean} (Eq. V-16) remains constant and equal to EI.

$$EI_{mean} = \frac{1}{L}\sum_{i=1}^{n}(EI_i L_i) = EI \qquad \textit{Eq. V-16}$$

Where n is the number of portions.

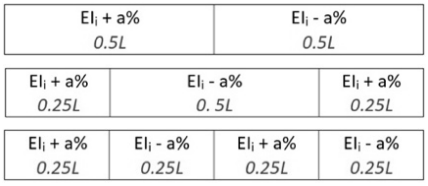


Fig. V.17: Beam divided into 2, 3 or 4 parts.

The transmission ratio Δ/Δ_0 is computed for all the cases (Fig. 17) and compared with the one homogeneous case that is computed with a uniform value EI= EI_{mean}. Preliminary results reveal that both the number of portions and the value of the variant coefficient have a significant influence on the prediction of the transmission ratio. The difference, between the homogenous and the heterogeneous

case, is higher for a=40% than for a=10%, consequently, the increase of the variant coefficient increases the impact of this uncertainty. Consequently, the variability of the building stiffness related to the presence of openings, existence of interior walls, heterogeneity of structural materials, etc., affects the analytical prediction of the transmission of the ground movement. A discrepancy is shown between the values of Δ/Δ_0 for the heterogeneous and the homogeneous case that is based on one equivalent stiffness value. A possible way to minimize the discrepancy is to define a more efficient equivalent stiffness. Three formulas are tested: the geometric mean, the minimal value, and the last one the maximal value (Table 3).

Table V-3: Different possible homogeneous stiffness definitions for the building

Geometric mean	Maximum Value	Minimum Value
$EI_{geo} = \sqrt[n]{EI_1 . EI_2 \dots EI_n}$	$EI_{max} = Max[EI_1 \dots EI_n]$	$EI_{min} = Min[EI_1 \dots EI_n]$
Eq. V-17	*Eq. V-18*	*Eq. V-19*

As shown in Fig. 18, for a beam divided into two parts, the homogeneous case underestimates the exact solution of the transmitted deflection based on EI_{mean}, EI_{max} and EI_{geo} definitions and overestimates the results compared to the EI_{min} definition. However, the EI_{min} and EI_{max} definitions present a large difference with the homogeneous case since they present an extreme case where the transmission ratio is evaluated for a relative stiffness that corresponds to the one of an entirely flexible or stiff structure. Referring to the homogeneous case curve, an accurate estimation is to consider the Δ/Δ_0 value of this curve that corresponds to the EI_{mean} since the value of the relative stiffness ρ^* for the heterogeneous case based on EI_{mean} is the same the one of the homogeneous case.

On the other hand, comparing the results to a beam divided into three and four parts, a=40%, a slight difference in the transmitted deflection is observed between the two, three and four parts cases based on EI_{mean} definition; the highest results are for a three parts beam, since the middle portion of this beam, that is less stiff, is subjected to the highest soil settlement. The lowest results are for the four parts beam, since the stiffness is compensated between two short portions of the beam which makes it comparable to the homogeneous case. Consequently, for a beam divided into two, three and four parts, the homogeneous case underestimates the exact solution of the transmitted deflection based on the EI_{mean} definition. The effect of heterogeneity of building stiffness is also investigated numerically. As shown in Fig. 19, the 10 simulations evaluated in Fig.4 are compared to heterogeneous beams evaluated numerically. Globally, numerical results fit well with the analytical ones and the homogeneous case underestimates the exact solution of the transmitted deflection; in addition, the highest results of Δ/Δ_0 are for a three parts beam, the intermediate ones are for a two parts beam and the lowest are for the four parts beam.

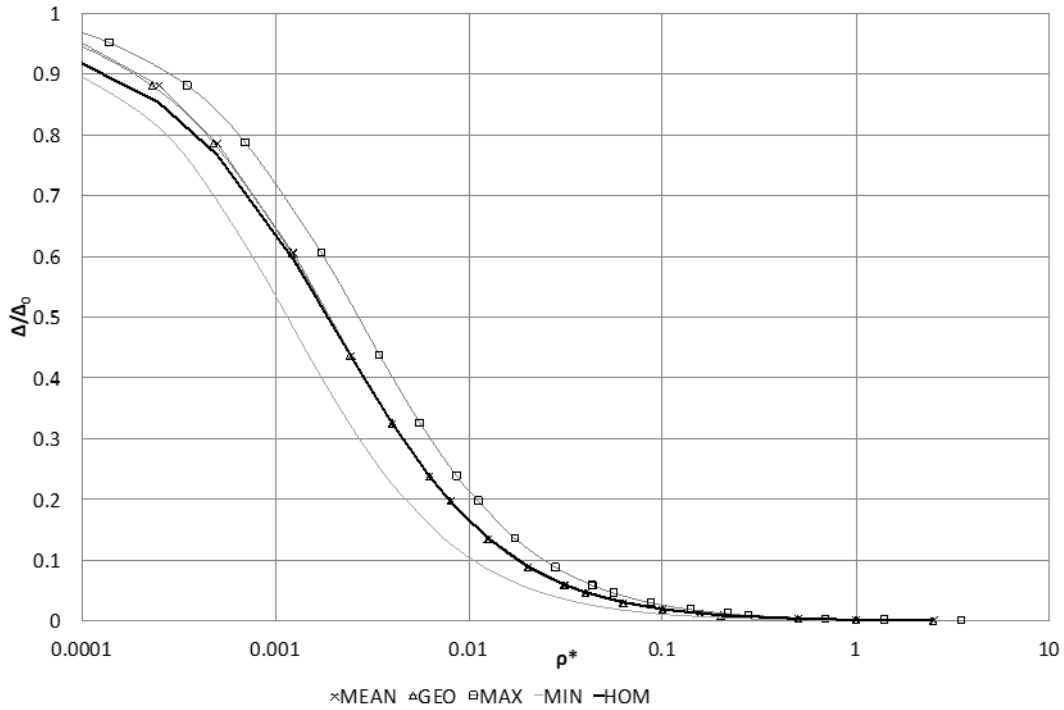


Fig. V.18: Comparison of the deflection transmission ratio versus the relative stiffness for different possible homogeneous stiffness definitions for a beam divided into two parts for a=40%.

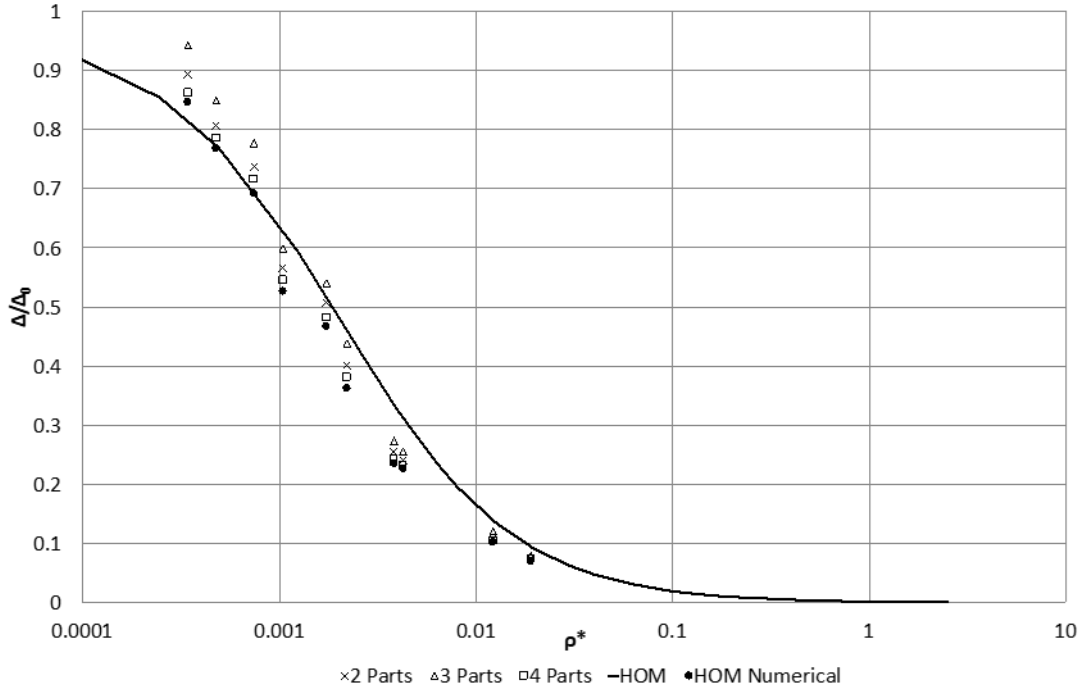


Fig. V.19: Numerical evaluation of Δ/Δ_0 versus ρ^* for different for a beam divided into two, three and four parts for a=40%.

4. A new coefficient to evaluate the influence of uncertainties on the transmission ratio

To assess the influence of the considered uncertainties (free-field shape, building position and homogeneity of building stiffness) on the evaluation of the structure response, a new equation that

quantifies the effect of every uncertainty can be proposed, based on the Deck & Singh deflection transmission ratio, using a coefficient A as follows:

$$\frac{\Delta}{\Delta_0} = A\ \frac{\Delta}{\Delta_0}(\text{Deck \& Singh}) \qquad \textit{Eq. V-20}$$

Thus, a practical way of evaluating uncertainties affecting building deflections induced by ground movements is to consider the Deck & Singh analytical curve of Fig.4 coupled with Eq. V-20.

a) Free-field shape

As shown in Fig. 10, Fig. 11 and Fig. 12, the free-field shape uncertainty affects the Deck & Singh Δ/Δ_0 curve that is based on the polynomial model (Eq. V-9).

a- For the continuous regular geometrical shapes, results vary slightly from one shape to another. The relative difference between Δ/Δ_0 (Deck & Singh) and Δ/Δ_0 for other shapes does not exceed 10%; the highest negative and positive relative differences are obtained with the triangular and sinusoidal forms respectively (≈ -10% and +5% respectively). For the discontinuous shape, a significant influence is obtained in the structure response. The relative difference can reach 40% for low values of relative stiffness, so the prediction of the building defection based on Deck & Singh model presents a large margin of uncertainty which makes this model less-adapted for the evaluation of these shapes. Framed structures with columns/piers on separated footings are more-adapted since they can undergo significant differential horizontal displacements, which are associated with a bending deformation of first level of columns/piers rather than an overall axial deformation of the structure [26]. Additionally, a discontinuous shape may lead to a complex combination of rotational and translational displacements (consisting of both vertical and horizontal movements) which can occur for separated footings [27]. However, based on the literature, ground movements, like tunneling and mining subsidence, usually induce continuous settlements; an ultimate discontinuity is rarely presented but can be revealed instead by an important inflection according to the Gaussian shape.

b- For the Gaussian shape, the inflection point position with respect to the curvature centerline is one of the significant sources of uncertainties that affects the evaluation of building deflections induced by ground movements. For $L_{building} << L_{curvature}$ or $L_{building} \approx L_{curvature}$, Δ/Δ_0 results are very close to Deck & Singh model with the variation of ρ*. The relative difference does not exceed 5%. However, for $L_{building} >> L_{curvature}$ or a position that corresponds to an inflection point located at the building end, the relative difference may exceed the 40%.

Based on Eq. V-20, Table 4 shows the proposed values of the coefficient A, considering the free-field shape uncertainty.

Table V-4: Proposed values of the coefficient A, considering the free-field shape uncertainty.

	Regular Continuous Shapes	Regular Discontinuous Shapes	Gaussian Shape	
			$L_{building} << L_{curvature}$ $L_{building} \approx L_{curvature}$	$L_{building} >> L_{curvature}$ $x_{building\ end} \approx x_{inflection\ point}$
A	$0.9 \leq A \leq 1.05$	$0.6 \leq A \leq 1.4$	$1 \leq A \leq 1.05$	$0.6 \leq A \leq 0.7$

b) Building position to the settlement curvature

When the building is far distant from the inflection point, the structure deflection presents a fully concave/convex curvature. As shown in Fig. 13, there is no difference between the concave and convex curvatures having the same maximum free-field deflection Δ_0. On the other hand, if the inflection point is close or under the structure, the structure may be partially concave and convex, as shown in Fig. 1. For this case, the building position to the settlement curvature uncertainty highly affects the Deck & Singh Δ/Δ_0 curve. Fig. 16 shows the effect of this uncertainty considering a continuous and a discontinuous approach for particular values of the relative stiffness.
To normalize the results, an abacus is presented in Fig. 20. Based on Eq. V-20, the coefficient A can be evaluated using Fig. 20 to consider the relative influence of the building position for continuous and discontinuous approaches.

c) Homogeneity of building stiffness

By assimilating the structure to a homogeneous beam, the effect of the heterogeneity of the building stiffness is neglected. As shown in Fig. 18, Deck & Singh Δ/Δ_0 curve that is based on a homogeneous beam, underestimates the heterogeneous building response. The response depends upon various factors, such as the distribution of the non-equivalent stiffness portions within the building, the proportion of stiffness variation, etc. Table 5 shows the relative difference (RD) and the proposed values of the coefficient A, considering the heterogeneity of building stiffness.

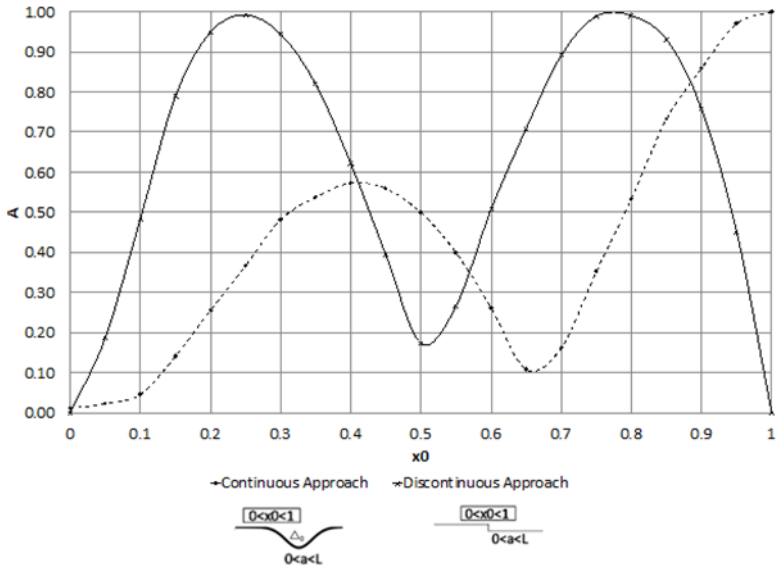


Fig. V.20: Abacus of the coefficient A to evaluate the relative influence of the building position for continuous and discontinuous approaches.

Table V-5: Maximum relative difference and proposed values of the coefficient A considering the heterogeneity of building stiffness.

	Beam divided into 2 parts				Beam divided into 3 parts				Beam divided into 4 parts			
a (%)	40	30	20	10	40	30	20	10	40	30	20	10
RD (%)*	10.60	9.62	7.59	4.43	11.77	10.12	7.75	4.46	10.08	9.32	7.49	4.43
A	$1.04 \leq A \leq 1.11$				$1.04 \leq A \leq 1.12$				$1.04 \leq A \leq 1.10$			

* RD (%) = Relative Difference (%) = Max [($\Delta/\Delta_0(\rho^*_i) - \Delta/\Delta_0(\rho^*_{mean})$)/ $\Delta/\Delta_0(\rho^*_i)$]

V.6 Conclusions & Perspectives

This paper investigates the influence of significant sources of uncertainties (free-field deformation profile, building position to the settlement curvature and homogeneity of building stiffness) on the evaluation of the transmission of the ground movements affecting the soil-structure interaction through an analytical approach coupled with numerical finite element models. The work done in this paper can be summarized as follows:

a- By comparing various studies in the literature, the prediction of structures response to ground movements shows a margin of discrepancy that is associated to the influence of uncertainties. Based on the Deck & Singh analytical model, three significant sources of uncertainties are considered:

a-1. The free-field shape: Deck & Singh defined the free-field profile by a polynomial function characterized by Δ_0.

a-2. The building position to the curvature center: previous models used to consider symmetrical cases where the building centerline is mingled with the one of the soil settlement.

a-3. The homogeneity of building properties: The building is usually assimilated to a homogeneous beam, while modeling the SSI parameters, which neglects the influence of openings (doors, windows), the existence of interior walls, the heterogeneity of structural materials in addition to the effect of the third dimension.

b- The effect of the free-field ground movement form was studied by taking several continuous shapes (polynomial, trapezoidal, sinusoidal, triangular and side triangular), one discontinuous shape (rectangular) and a Gaussian form of the free-field ground movement. Their results are plotted together for comparison purposes.

b-1. First, for the continuous cases, all curves have globally similar results with the usual analytical models curves. For an equivalent stiffness ratio, the results of maximum transmission ratio are slightly different.

b-2. Second, the discontinuous shape does not follow a one-line curve as the continuous shapes even-though it respects the overall curvature, and the transmission ratio associated with the relative stiffness values presents a significant difference.

b-3. Third, for the Gaussian shape, the comparison of the structure and the curvature lengths shows a significant influence of this uncertainty. Results show that for a structure having a comparable length with the curvature, Δ/Δ_0 have globally similar values to the Deck & Singh polynomial model.

c- The building position to the settlement curvature was studied by considering two cases:

c-1. A building distant from the inflection point: the structure deflection presents a fully concave/convex curvature. The effect of the concavity and convexity of the free-field ground movement is examined according to the several deformation shapes. Results show that, with respect to the condition of no interpenetration and continuous contact between the soil and the structure, the concave and convex shapes give exactly the same results of the deflection transmission ratio Δ/Δ_0 versus the relative stiffness ρ^*.

c-2. An inflection point of the free-field movement that is close or under the structure: the structure may be partially concave and convex, and its position highly affects the prediction of Δ/Δ_0. Continuous and discontinuous approaches are considered and results reveal that the worst case corresponds to the case where the curvature centre coincides with the building centreline which overestimates the structure response.

d- The influence of openings, heterogeneity of structural material, etc. manifested by the stiffness variation in the structure is investigated. Various beam stiffness partitions are applied to the model; each partition is characterized by its own stiffness obtained by increasing or decreasing the stiffness value by certain percentage. All of these partitions and variations are compared to the homogeneous case where the whole building has one stiffness value. Results indicate that the evaluation of the movement transmission depends upon the stiffness variation and a difference is shown between the homogeneous and the heterogeneous case.

e- Finally, a new equation that considers the influence of every uncertainty is proposed using tables and figures based on the Deck & Singh deflection transmission ratio. This equation can be directly adopted by engineers for design purposes to assume a Δ/Δ_0 value when considering these uncertainties.

V.7 Acknowledgement

The work presented in this paper was supported by a research grant from Lorraine University of Excellence and the National Council for Scientific Research-Lebanon (CNRS-L) and the Lebanese University.

V.8 References

[1] Potts, D. & Addenbrooke, T. A structure's influence on tunneling-induced ground movements. *Proceedings of the Institution of Civil Engineers – Geotechnical Engineering*; 1997, 125: 109–125.

[2] Rachdi, S., Jahangir, E., Tijani, M. & Rouabhi, A. (2019) Tunnelling-induced surface settlement: on the choice of soil constitutive model, *European Journal of Environmental and Civil Engineering*, DOI: 10.1080/19648189.2019.1639078

[3] Cai, Y., Verdel, T. & Deck, O. (2017) Using plane frame structural models to assess building damage at a large scale in a mining subsidence area, *European Journal of Environmental and Civil Engineering*, DOI: 10.1080/19648189.2017.1379911

[4] Saeidi, A., Deck O. & Verdel T. (2015) An extension of analytical methods for building damage evaluation in subsidence regions to anisotropic beams, *European Journal of Environmental and Civil Engineering*, 19:6, 756-772, DOI: 10.1080/19648189.2014.969386

[5] Franza, A., Ritter, S. & Dejong, M. Continuum solutions for tunnel-building interaction and a modified framework for deformation prediction. *Géotechnique;* 2019: 1-15.

[6] Bitarafan, M. & Vahdani, R. (2018) Assessing the effect of soil-structure interaction on damage indices of reinforced concrete frames, *European Journal of Environmental and Civil Engineering*, DOI: 10.1080/19648189.2018.1482789

[7] Mair, R. Tunneling and deep excavations: Ground movements and their effects. *Proceedings of 15th European conference on soil mechanics and geotechnical engineering geotechnics of hard soils – weak rocks*; 2013, 4: 39-70.

[8] ElKahi, E., Khouri, M., Deck, O., Rahme, P., & Mehdizadeh, R. Studying the Influence of Uncertainties on the Transmission of Ground Movements Affecting the Soil-Structure Interaction. *10èmes journées Fiabilité des Matériaux et des Structures, Bordeaux, France*; 2018.

[9] Deck, O. & Singh, A. Analytical model for the prediction of building deflections induced by ground movements. *International Journal for Numerical and Analytical Methods in Geomechanics*; 2010, 36: 62-84.

[10] Serhal, J., Deck, O., Alheib, M., Chehade, F. & Abdelmassih, D. Damage of masonry structures relative to their properties: Development of ground movement fragility curves. *Engineering Structures*; 2016, 113: 206-219.

[11] Basmaji, B., Deck, O., & Alheib, M. Analytical model to predict building deflections induced by ground movements. *European Journal of Environmental and Civil Engineering*; 2017, 10: 1-23.

[12] Son, M. & Cording, E. Evaluation of building stiffness for building response analysis to excavation-induced ground movements. *Journal of Geotechnical and Geoenvironmental Engineering*; 2007, 133: 995-1002.

[13] Haji, K., Marshall, A., & Franza, A. Mixed empirical-numerical method for investigating tunneling effects on structures. *Tunnelling and Underground Space Technology*; 2018, 73: 92-104.

[14] Franzius, J., Potts, D. & Burland, J. The response of surface structures to tunnel construction. *Proceedings of the Institution of Civil Engineers, Geotechnical Engineering*; 2006, 159: 3–17.

[15] Goh K. Response of Ground and Buildings to Deep Excavations and Tunnelling-Doctorate Thesis, University of Cambridge, 2010.

[16] Vesic. Beams on Elastic Subgrade and Winkler's Hypothesis. *Proceedings of the 5th International Conference on Soil Mechanics and Foundation Engineering*; 1963, 845-850.

[17] Biot. Bending of an infinite beam on an elastic foundation. *Journal of Applied Mechanics*; 1937.

[18] Drapkin. Grillage beams on elastic foundations. *Proc. ASCE*; 1955.

[19] Klöppel & Glock. Theoretische und Experimentelle Untersuchungen zu den Traglastproblemen Biegeweicher, in die Erde Eingebetteter. Institutes für Statik und Stahlbau der Technischen Hochschule Darmstadt; 1970.

[20] Henry. The Design and Construction of Engineering Foundations. Chapman & Hall; 1986.

[21] El Kahi, E., Deck, O., Khouri, M., Mehdizadeh, R. & Rahme. P. Étude de l'influence de la plasticité du sol sur la transmission des mouvements du sol affectant l'interaction sol-structure. *Revue Française de Géotechnique*. 2018, 156, 4.

[22] Bilotta, E., A. Paolillo, G. Russo, & S. Aversa (2017). Displacements induced by tunnelling under a historical building. *Tunnelling and Underground Space Technology* 61, 221–232.

[23] Pickhaver, J., H. Burd, & G. Houlsby (2010). An equivalent beam method to model masonry buildings in 3D finite element analysis. *Computers & Structures* 88(19), 1049–1063.

[24] Franza, A., Acikgoz, S. & DeJong M.J. Linear models for the evaluation of the response of beams and frames ttunnelling. *9th NUMGE Conference on Numerical Methods in Geotechnical Engineering*. DOI: 10.1201/9781351003629-161

[25] Khademian, A., Abdollahi, H., Bagherpour, R & Faramarzi, L. (2017). Model uncertainty of various settlement estimation methods in shallow tunnels excavation; case study: Qom subway tunnel. *Journal of African Earth Sciences*. 134. 10.1016/j.jafrearsci.2017.08.003.

[26] Goh, K. H. & R. J. Mair (2014). Response of framed buildings to excavation-induced movements. *Soils and Foundations* 54(3), 250–268.

[27] Franza, A. & DeJong, M. A simple method to evaluate the response of structures with continuous or separated footings to tunnelling–induced movements. *Congress on Numerical Methods in Engineering, Valencia, Spain*; 2017, 919-931.

[28] Mair, R. J. & R. N. Taylor (1997). Theme lecture: Bored tunnelling in the urban environment. *14th International conference on soil mechanics and foundation engineering, Hamburg*, pp. 2353–2385. Balkema.

[29] Mair, R. J., R. N. Taylor, & A. Bracegirdle (1993). Subsurface settlement profiles above tunnels in clay. *Geotechnique* 43(2), 315–320.

VI. A new simplified meta-model to evaluate the transmission of ground movements to structures integrating the elastoplastic soil behavior

This paper is accepted in the *Structures* journal.

A new simplified meta-model to evaluate the transmission of ground movements to structures integrating the elastoplastic soil behavior

Elio EL KAHI[12*], Olivier DECK[1], Michel KHOURI[2], Rasool MEHDIZADEH[1], Pierre RAHME[2]

[1] *Lorraine University, CNRS, CREGU, GeoRessources laboratory, Ecole des Mines de Nancy, Campus Artem, CS14234, 54042 Nancy Cedex, France*
[2] *Faculty of Engineering, Lebanese University, Roumieh, Mount-Lebanon, Lebanon*

VI.1 Abstract

Many buildings may suffer damage due to ground movements associated to underground excavations like tunneling, mines or urban excavations. The level of damage depends upon the rate of ground movements transmitted to structures that is affected by the Soil-Structure Interaction (SSI) conditions and parameters such as the soil elastoplastic behavior. The purpose of this paper is to integrate the soil elastoplasticity while investigating the response of a structure sitting on a soil subjected to a ground movement. Analytical and numerical approaches are applied to examine the effect of the non-linear soil behavior. The analytical approach is based on modified Winkler and Pasternak elastic models under the assumption of limiting the soil reaction by its bearing capacity ; the numerical approach is based on finite element models, using Plaxis 2D that consider an elastoplastic soil behavior. Results display the discrepancy in the structural response between considering an elastic or an elastoplastic soil behavior. Based on a significant number of iterations, the artificial neural network technique is used to propose a new simplified meta-model that integrates the soil elastoplasticity to evaluate the transmission of ground movements to structures. In addition, a procedure, which can be used by engineers and designers, is developed to evaluate the transmission ratio for any structure sitting on any type of soil.

VI.2 Keywords

Meta-model, elastoplastic soil behavior, Pasternak model, Winkler model, soil-structure interaction, ground movements, artificial neural network.

VI.3 Introduction

Ground movements designate a sequence of soil displacements, of natural or anthropogenic origin such as shrink-swell phenomenon of clayey soils, influence of nearby excavations (tunnels) and presence of underground voids such as mining subsidence and sinkholes. These ground movements are responsible of the soil settlements and displacements. The soil displacement may occur even in the absence of any structure on top of it; this case represents the free-field ground movement. Conversely, if the soil is underneath an existing structure, the ground movement is transmitted to the building foundations (Figure 1). An important parameter is the stiffness and the building stiffness could be underestimated if it is only based on the foundation geometry. Consequently, the building with its foundation is assimilated to a beam with an equivalent stiffness. The computed deflection represents

the deflection transmitted to both the building and its foundation which may cause a structural damage [1, 2]. It is not proper to consider that these movements in the free-field are transmitted entirely to the building since the transmission may be considerably affected by the soil-structure interaction (SSI) phenomenon which is strongly dependent upon the structure and the soil conditions and the associated parameters [3-5].

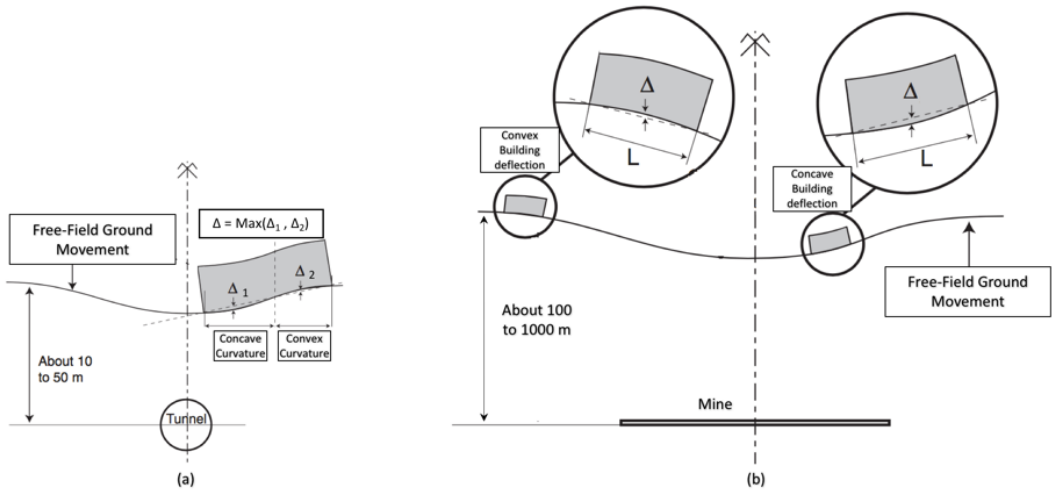


Fig. VI.1. Building deflection caused by ground movements: (a) Case of tunneling. (b) Case of underground mine.

By neglecting the impact of the interaction between the soil and the structure, the free-field ground movements are integrally transmitted to the building. Under this assumption, Δ_0 represents the maximum deflection of the building. Assuming that the free-field ground movement is symmetrical and roughly circular under the building, Δ_0 represents the maximum free-field deflection under the building (for an integrally transmitted movement); it depends upon the ground radius of curvature R and the building length L (Figure 2).

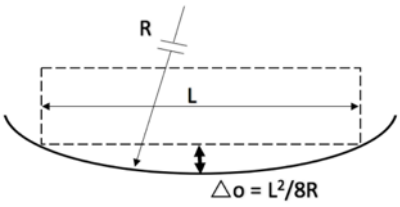


Fig. VI.2. Free-field deflection Δ_0.

By considering the impact of the SSI, the soil, located under an existing structure and subjected to a ground movement, will influence the structure differently due to the interdependence of the mechanical behavior between the soil under the foundations and the structure sitting on these foundations. This interdependence is strongly dependent on the stiffness of the structure as well as that of the soil [2, 4, 6]. Due to the influence of the SSI, the ground movement may be partially transmitted to the structure which results in a building deflection characterized by its maximum value Δ with $\Delta \leq \Delta_0$. As shown in Figure 3, if the structure is stiff, it can resist the ground movement and the induced transmitted deflection is limited ($\Delta < \Delta_0$); if it is flexible, then it perfectly follows the settlement of the soil and $\Delta = \Delta_0$.

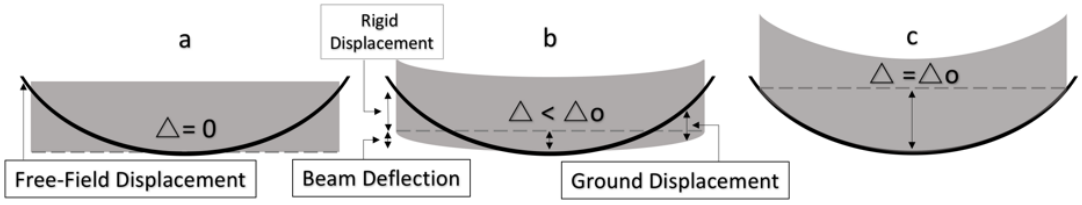


Fig. VI.3. Behavior of structures subjected to ground movement. (a) High-stiffness structure on soft ground. (b) Intermediate ground and structure stiffness. (c) Flexible structure on stiff ground.

For a symmetrical free-field movement with respect to the structure, the deflection Δ corresponds to the maximum differential settlement under the building. For a non-symmetrical free-field movement case, Δ represents the maximum deflection of the building, whether the structure has a concave or a convex deformation (Figure 1-a).

The Δ / L ratio, called the deflection rate, is frequently used to assess the behavior of structures subject to differential settlement and to evaluate their damage [6, 7]. Since the damage depends upon the rate of movement transmitted to the building, the structure response to the ground movement is usually evaluated through the deflection transmission ratio, defined as Δ/Δ_0 [8, 9].

Different methods (analytical, numerical, experimental, empirical field data results) have been developed to predict the building deflection in response to the ground movements [6-15]. Except empirical methods that are based on observations of real existing structures, all of these methods do not consider a specific study of a particular case but they are applied to simplified structures, such as beams, in order to assess the global trend of ground movements induced phenomena.

Among the approaches developed to study the SSI phenomenon, only numerical methods offer great flexibility for taking into account the complexity of the SSI conditions [11, 16]. Although it is relatively simple to consider complex soil and structure behaviors in numerical models, their use may be criticized by the justification of the numerical values of all parameters and conditions. In addition, numerical models present difficulties to generalize results, because of the need to reproduce the same scenario numerous times, by varying a particular SSI parameter in each repetition to cover the extent of the variation range of all parameters. Thus, they can be considered as time-consuming processes [7].

To avoid these difficulties, it is possible to obtain results through analytical methods that develop simple equations that represent the structural deflection. Analytical methods may be considered as a complementary tool to the numerical ones, allowing quick calculations for a wide variation range of parameters, without considering complex configurations [6]. In these analytical models, the soil is modelled with simple elastic stiffness elements as elastic springs. Winkler model is the simplest soil model and has been used by many investigators and by Deck and Singh (2010) [7] to address the question of the building deflection induced by ground movements and the assessment of Δ/Δ_0. Such a SSI model can be criticized because it neglects any interaction between the springs and because it assumes a purely elastic behavior of the ground [17]. As a consequence, it does not take into account the influence of soil settlement outside the loaded area, which leads to discontinuities in the settlement

profile when the applied load is also discontinuous; the displacements of the soil outside the building are supposed null, which is not correct. Basmaji et al. (2017) [6] developed a similar SSI model by replacing the Winkler by Pasternak model in order to introduce some interactions between the springs (Figure 4). This SSI model corrects some critical points of the previous one, but it does not take into consideration the soil elastoplastic behavior.

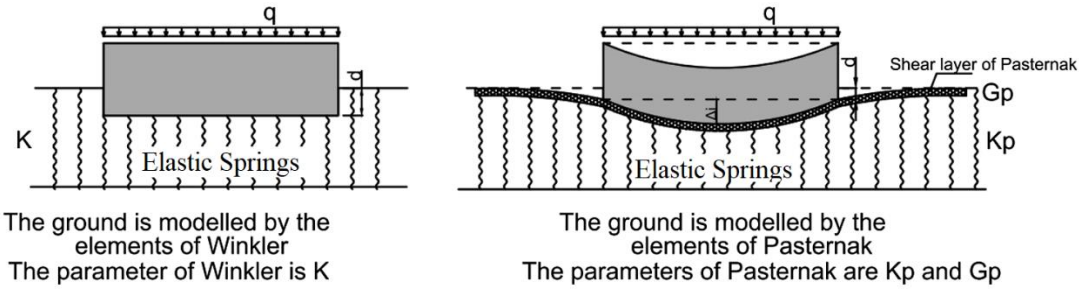


Fig. VI.4. Structure on a soil modelled analytically with the one parameter Winkler's elastic model or the two parameters Pasternak's elastic model [6].

Thus, soil analytical models do not take into account the influence of the soil elastoplastic behavior even-though this factor significantly affects the transmission of ground movements to structures [6-9]. As shown in Figure 5, the target of this paper is to investigate the influence of soil elastoplasticity on the transmission of ground movements affecting the soil-structure interaction. Based on the elastic analytical models, a simplified elastoplastic meta-model is proposed, via statistical regressions, to evaluate the structural response. A modification is added to the analytical elastic models that assimilate the soil to a juxtaposition of elastic springs; the modification incorporates elastoplastic conditions based on the soil bearing capacity. Results of the analytical approach are then compared to the results obtained by numerical finite element models. In order to generalize the obtained results, a large database of the deflection transmission ratio is evaluated for different combinations of the SSI parameters and the soil bearing capacity. Based on this database, a new correlation is proposed to evaluate the transmission of ground movements to structures considering the elastoplastic soil behavior, in an effort to improve the investigation of the structure response to ground movements.

Step 1 $(\Delta/\Delta_0)_{Elastic}$		**Step 2** **Elastoplasticity**		**Step 3** **Validation**		**Step 4** **Reduction Coefficient**
Evaluate the transmission ratio $(\Delta/\Delta_0)_{Elastic}$ analytically based on soil elastic models.	→	Incorporate elastoplastic conditions based on the soil bearing capacity	→	Validate the analytical results by the numerical finite element models.	→	Generalize the results of the transmission ratio $(\Delta/\Delta_0)_{Elastoplastic}$ by considering the soil elastoplastic behavior through a reduction coefficient.

Fig. VI.5. Diagram representing the study plan.

VI.4 Procedure & Modeling

Previous research on this subject addresses the question of building stiffness compared to ground stiffness, which is known as "relative stiffness", and suggests to assess the transmission ratio Δ/Δ_0 as a function of a relative stiffness parameter ρ* between the soil and the structure [7, 11, 18].
Most of these studies rely on Eq. (1) to evaluate the relative stiffness parameter ρ* based on the structure length L, inertia I, Young's modulus E and the soil Young's modulus Es. Since it is a 2D study done per linear meter (EI [N.m^2/m]), Eq. (1) has the advantage of being non-dimensional and of being well adapted to a synthetic representation of Δ/Δ_0.

$$\rho* = \frac{EI}{EsL^3} \qquad (1)$$

In order to propose a simplified meta-model that evaluates the transmission ratio Δ/Δ_0 as a function of the relative stiffness ρ*, an appropriate SSI model has to be considered. While there is a significant number of SSI models proposed in the literature [6-8, 10-11, 18-23], a comparison between two elastic models, representing the transmission ratio Δ/Δ_0 versus the relative stiffness ρ* for a wide variation range of SSI parameters, is performed.

1. Elastic Deck & Singh SSI analytical model

Deck and Singh (2010) [7] developed a SSI analytical model to calculate the deflection transmission ratio Δ/Δ_0 as a function of the ground and building mechanical properties. As shown in Figure 6, the building is assimilated to an elastic Euler–Bernoulli beam and the ground is represented by the Winkler model, which consists on assimilating the soil to a juxtaposition of vertical springs characterized by their stiffness K without any interaction between them. Considering that p(x) and w(x) represent the ground reaction and displacement respectively, Winkler model is evaluated using Eq. (2). The ground is modelled with an initial shape corresponding to Δ_0 and a polynomial equation v(x) (Eq. (3)) that represents the free-field movement shape. The final building deflection Δ is then calculated based on the final position and deformation of the beam required to get a static equilibrium under its own weight q and the vertical ground reaction p(x) (Eq. (4)).

$$p(x) = Kw(x) \qquad (2)$$

$$v(x) = \Delta_0 (1-4x^2/L^2) \quad for \quad -L/2 < x < L/2 \qquad (3)$$

$$y^{(4)}(x) = \frac{q - p(x)}{EI} \qquad (4)$$

Where L and EI are the building length [m] and elastic stiffness [N.m2/m] (since it is a 2D study done per linear meter).

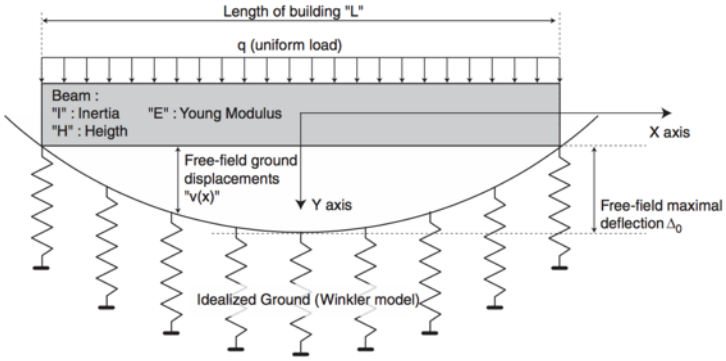


Fig. VI.6. Deck & Singh (2010) analytical model for the SSI and the building deflection induced by ground

movements.

On the other hand, Deck & Singh (2010) [7] introduced their own relative stiffness definition to plot the results of Δ/Δ_0 (Eq. (5)) that is suitable to the Winkler model, since the ground stiffness is defined with the Winkler parameter K instead of Es used in Eq. (1).

$$\rho * (Deck\ \&\ Singh) = \frac{EI}{KL^4} \quad (5)$$

Where K is the Winkler elastic modulus [N/m^3].

This equation is comparable to other relative stiffness ratios defined in the literature; it presents the advantage of being a non-dimensional parameter and suitable to have a synthetic representation of Δ/Δ_0 based on Winkler model. In order to show the consistency between Eq. (1) and Eq. (5), Vesic (1963) [24] formula (Eq. (6)) is used to define values for K in the case of a foundation with length L, width B (with L>B) and a ground characterized by a Young's modulus Es and a Poisson's ratio υ. In this case B is taken equal to 1m, which approximatively corresponds to the width of a building foundation. Noting that various formulas link the Winkler modulus to the soil Young modulus [24-28], Vesic formula is chosen since it takes into account the presence of a beam (through the "EI" term) contrary to other formulas.

$$K = \frac{0.65Es}{B(1-\nu^2)} \sqrt[12]{\frac{EsB^4}{EI}} \quad (6)$$

Figure 7 shows the Deck & Singh (2010) results for the transmission ratio plotted against the relative stiffness ρ*(Deck & Singh) defined in Eq. (5). A comparison is done between the Δ/Δ_0 values evaluated according to specific values of K and Δ/Δ_0 values evaluated according to specific values of Es and converted to K according to Vesic formula (Eq. (6)). The difference between the results is slight (Figure 7) which validates the consistency between Eq. (1) and Eq. (5) using Vesic formula.

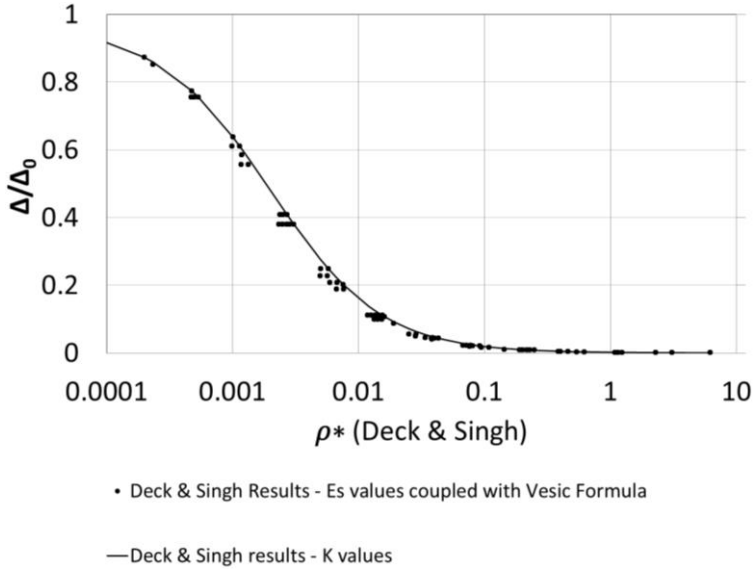


Fig. VI.7. Results of the deflection transmission ratio Δ/Δ_0 versus the relative stiffness ratio ρ*(Deck & Singh) obtained for K values and for Es values coupled with Vesic formula.

2. Elastic Basmaji et al. SSI analytical model

Based on Deck & Singh (2010) model, Basmaji et al. (2017) [6] developed their analytical model where the soil is represented by the Pasternak model, a two parameters soil model that takes into account the interaction between adjacent springs, in addition to the influence of shear deformation in the soil (Figure 4). The two parameters are the shear modulus Gp, and the stiffness modulus Kp. The soil reaction can be written as follows:

$$p(x) = K_P.B.w(x) - G_P.B.w''(x) \quad (7)$$

When Gp is taken to be zero, the Pasternak model is equivalent to the Winkler model. The Winkler parameter K is used instead of Kp. It should be noted that if a given geotechnical problem is modelled with each of the two models, i.e., Pasternak and Winkler, the values of Kp and K will be different, unless Gp is assumed to be equal to zero [6].

As shown in Figure 4, due to the influence of the shear layer, Pasternak model displays a differential settlement under the building without any discontinuities contrary to Winkler model that displays a uniform settlement with a discontinuity at the edge. Thus, when a local force F acts on a point (x) of a soil modelled by Pasternak model, the slope curve w'(x) presents a discontinuity. Conversely, any discontinuity of w'(x) must be associated to a local force. To overcome this problem, Eq. (7) must be completed with Eq. (8).

$$F = w'_{left}(x) - w'_{right}(x) \quad (8)$$

Where w'_{left} and w'_{right} are the limit of the first derivatives of w(x) for x_0- and x_0+ respectively and F is the associated local force (Figure 8).

To highlight the effect of the shear deformation, Basmaji et al. (2017) compared Pasternak and Winkler models. In order to make a suitable comparison, the transmitted ratio Δ/Δ_0 has to be plotted versus the same definition of the relative stiffness ρ*. To do so, the parameters used in the soil models have to be calculated according to the same methodology in order to correspond to the same soil in terms of Young's modulus and Poisson's ratio. Due to the lack of existing analytical relations to assess the two parameters used in the Pasternak's model (Gp and Kp), Basmaji et al. (2017) [6] implemented a new methodology based on Flamant's theoretical solution of induced vertical settlement. They adjusted the displacement for both methods according to Flamant's theoretical solution in order to justify the parameter values for Winkler and Pasternak. Consequently, they proposed abacuses to select the Winkler and Pasternak values based on the half width of the loaded zone and the thickness of the compressive ground for Es = 1MPa and ν = 0.3. However, the comparison of the transmitted ratio Δ/Δ_0 versus the relative stiffness ratio ρ* defined in Eq. (1), between Pasternak and Winkler models, reveal a discrepancy between both methods which is related to the influence of shear deformation into the soil (Figure 10).

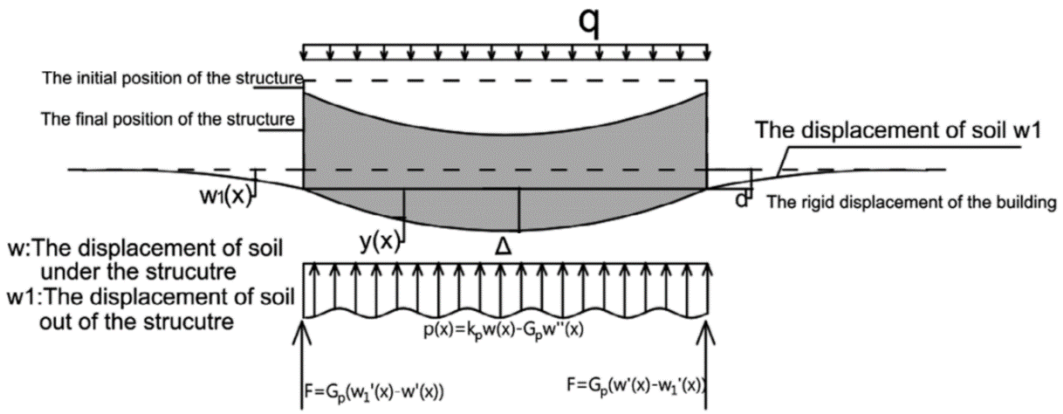


Fig. VI.8. Definition of parameters used to model the beam deflection according to Pasternak model [6].

3. Validation of elastic analytical models

A significant number of SSI models (analytical, numerical, experimental, etc.) were proposed in the literature. In order to investigate the influence of soil elastoplasticity on the transmission of ground movements, the elastic analytical models have to be validated, since a simplified elastoplastic meta-model will be proposed based on the elastic analytical results. Two validation techniques are evaluated in this paper: (a) Validation with a finite-element model; (b) Validation with numerical, experimental and field data results from previous research.

a) Validation with a finite-element model

A finite element model (FEM) is developed to compare the elastic analytical results with a set of numerical simulations. The objective of the FEM is to model the ground curvature induced by ground movements and calculate the transmission ratio of the free-field deflection. In fact, Basmaji et al. (2017) [6] and Deck & Singh (2010) [7] validated their analytical results with numerical models; however, they considered an elastoplastic ground behavior in their studies, and they modeled the subsidence by a uniformly distributed load imposed on the lower boundary. On the contrary, the numerical model presented in this paper intends to fully reproduce the analytical conditions in order to well verify the effectiveness of the analytical results. Subsequently, this FEM model considers an elastic ground behavior and the subsidence is imposed without adding a uniform load on the lower boundary.

The numerical model is performed with a finite element software (Plaxis 2D) under the plane strain hypothesis. The model consists of an elastic soil layer, 125 m thick and 800 m long, with a building located at the center (Figure 9). For the boundary conditions, the horizontal displacement is fixed on the right and left boundaries and the vertical displacement is fixed only at the bottom boundary right and left sides (L1) while the central region of the bottom boundary is free. So, to model the subsidence and the free-field displacement, the length of L1 is selected in order to reach a value of Δ_0 that is equivalent to the analytical model.

The soil Poisson's ratio ν is 0.3 and the unit weight is 20 KN/m^3. The structure is modeled by a beam that is loaded with a vertical uniformly distributed load q. Mechanical properties and buildings dimensions are chosen in order to get values that are identical to the ones considered in the analytical approach (EI and L).

(a) A first computation is performed by fixing the vertical displacement on all the lower boundary in order to generate the initial ground situation under the soil weight; all the evaluated displacements are then set to zero.

(b) A second computation is performed by fixing the vertical displacement on L1, without considering the structure, in order to assess the free-field displacement Δ_0 of the subsidence; Δ_0 is evaluated and the displacements are set to zero.

(c) A third computation is performed with the precense of both the structure (with the vertical uniformly distributed load) and the subsidence in order to assess the final building deflection Δ considering the soil-structure interaction.

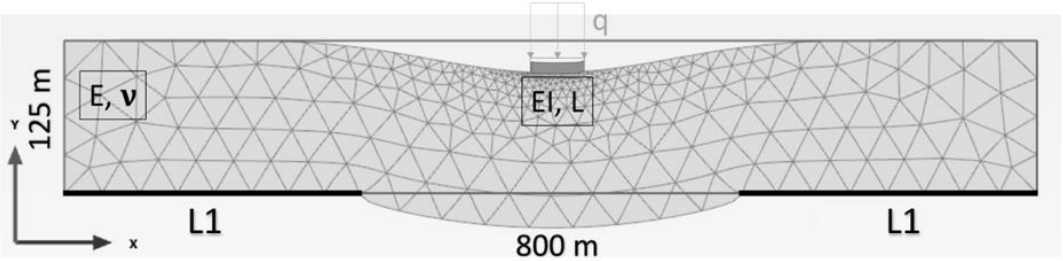


Fig. VI.9. Description of the finite element model used to compare analytical results of the deflection transmission ratio with numerical results.

A set of 10 simulations are performed that cover the distribution range of the relative stiffness ρ*, for different values of EI/B, Es, L, q and Δ_0. Globally, numerical results presented in Figure 10 are superimposed with the curve of the transmission ratio calculated with the elastic analytical models of Deck & Singh (2010) Winkler model combined with Vesic (1963) formula and Basmaji et al. (2017) with Pasternak model; consequently, these two analytical approaches seem to be sufficient to predict the trend of the transmission ratio.

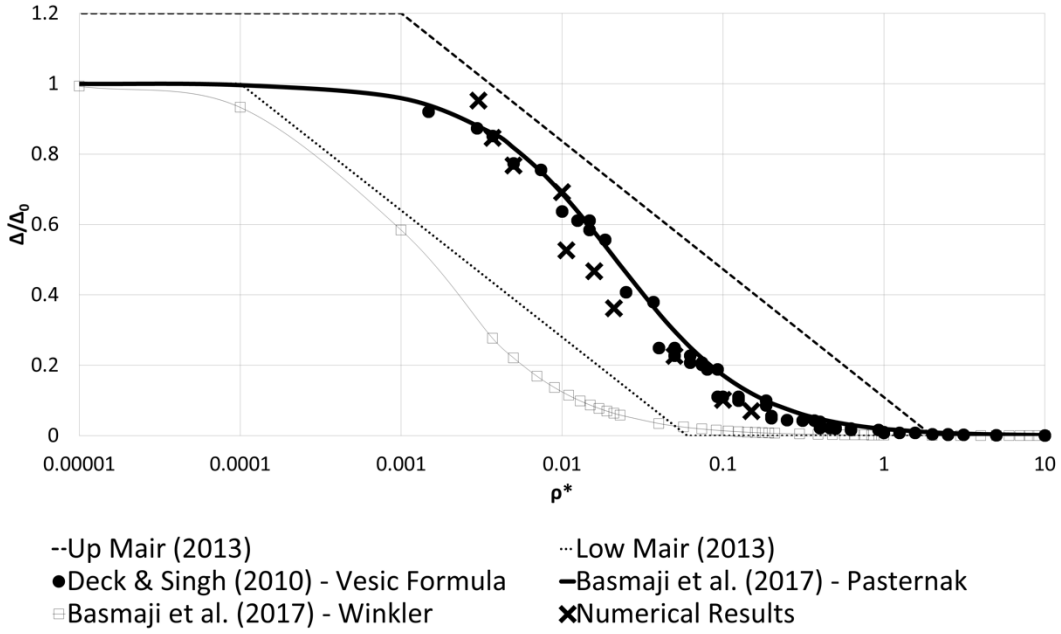


Fig. VI.10. Comparison between Mair (2013); Deck & Singh (2010); Pasternak-Basmaji *et al*. (2017); Winkler-Basmaji *et al*. (2017) and numerical results.

b) Validation with numerical, experimental and field data from previous research

In addition to the finite-element model validation, Mair (2013) [2] envelope is used to validate the elastic analytical results. In fact, Mair (2013) [2] compared the transmission ratio, derived from the finite-element analyses of Potts and Addenbrook (1997) [11] and Franzius et al. (2006) [29] with respect to the relative stiffness. Also, he considered the results of the finite element parametric analyses, of deep excavations in soft clay on adjacent buildings, using the Modified Cam Clay soil model done by Goh (2010) [30]. The comparison of these studies shows that the obtained results fall into a relatively narrow envelope known as Mair (2013) [2] envelope (Figure 10).

As shown in Figure 10, the elastic analytical models of Deck & Singh (2010) with Winkler model [7] combined with Vesic (1963) formula and Basmaji et al. (2017) with Pasternak model [6] fit well within Mair (2013) envelope, while an important discrepancy is shown between these results and Basmaji et al. (2017) with Winkler model [6]. Accordingly, even-though Deck & Singh (2010) Winkler model does not consider the shear deformation and the displacement outside the building, results show that the influence of these properties is indirectly taken into consideration or compensated by evaluating the Winkler modulus according to Vesic (1963) formula. In fact, Vesic (1963) has adopted the principle of equivalence between two solutions to find the soil reaction modulus for an infinite length beam in contact with the ground, modeled by the Winkler model. The same principle has been adopted by Basmaji et al. (2017) to calculate the Pasternak parameters; it was done for the case of a distributed load applied on a length L on a soil modeled by the Pasternak model. Thus, the results of Deck & Singh (2010) Winkler model combined with Vesic (1963) formula and Basmaji et al. (2017) with Pasternak model are comparable.

VI.5 Results & Discussion

1. $(\Delta/\Delta_0)_{Elastic}$

Based on Eq. (4), the Deck & Singh analytical model is based on evaluating the deflection of the building using Euler–Bernoulli forth order differential equation. To solve the problem, six boundary conditions are used which present computation difficulties and time consumption to generalize the results for a significant number of iterations. On the other hand, as shown in Figure 8, Pasternak model presents punctual forces at the building extremities; thus, a higher number of boundary conditions is needed for Basmaji et al. (2017) model leading to additional computation time difficulties.

In order to simplify the evaluation of Δ/Δ_0, this paper proposes simple meta-model equations, based on the results shown in Figures 7 and 10, depending upon the relative stiffness ρ* parameters, namely the structure stiffness EI and length L and the soil stiffness Es that can be substituted by the soil modulus K evaluated according to the Vesic formula (Eq. (6)). A significant number of iterations of the ρ* parameters is evaluated, covering its variation range in the analytical models of Deck & Singh (2010) and Basmaji et al. (2017). Since these original models are heavy to implement and expensive in computation time, polynomial meta-models are proposed to evaluate $(\Delta/\Delta_0)_{Elastic}$. The predictability and general applicability of the equation are evaluated by comparing the predictions of these meta-models with analytical results of the original models. Thus, the meta-models allow having, in any point of the design space, an estimate of the value of the elastic transmission ratio $(\Delta/\Delta_0)_{Elastic}$ while reducing the computation time for designers and engineers. Based on Figure 7 and Figure 10, Eq. (9) and Eq. (10) correspond to $(\Delta/\Delta_0)_{Elastic}$.

$$\frac{\Delta}{\Delta_0}\text{Elastic}(\text{EI},\text{K},\text{L}) = 0.5 - 0.5\,Tanh[2.99373 + 0.46898\,(\frac{EI}{KL^4})] \quad (9)$$

(K evaluated according to the Vesic formula)

$$\frac{\Delta}{\Delta_0}(\text{EI},\text{Es},\text{L}) = 0.5 - 0.5\,Tanh[1.96633 + 0.512843\,(\frac{EI}{EsL^3})] \quad (10)$$

2. Integrate the elastoplastic soil behavior

The objective is to develop an analytical SSI model that takes into account the influence of plasticity in the soil. To consider the influence of the elastoplastic soil behavior, a comparison between the stresses applied to the soil and its bearing capacity will be used as a criterion to judge whether the soil is in a plastic state or not. If it is in a plastic state, a new relation is proposed based on assuming that the vertical stresses in the soil must not exceed the bearing capacity of the soil (Figure 11). If the applied forces exceed the soil bearing capacity, a spring continues to deform but it cannot carry any additional stress. The overloads are thus transferred to nearby springs which are still in the elastic range. The applied procedure is iterative given the nonlinear behavior of the ground.

As presented in Figure 11, at the beam edges where the constraints are greater than p_{ult} , $p(x)=p_{ult}$ is imposed. Note that, since the integral of p(x) before and after taking into account the plasticity is always equal to the external loads applied to the building, the values of p(x) are increased in the middle of the beam for the elastoplastic behavior, as shown in Figure 11.

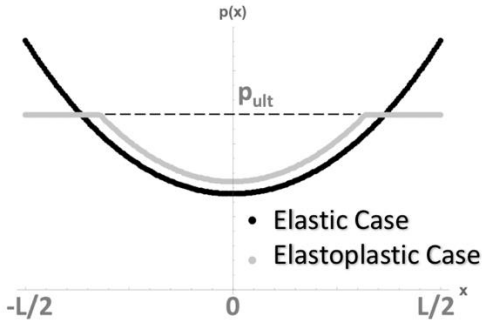


Fig. VI.11. Presentation of the applied procedure.

The concept of considering the elastoplastic soil behavior is divided into two cases (elastic and elastoplastic) as follows:

Elastic Case:	Winkler	$p(x) = K.w(x)$	*(2)*
	Pasternak	$p(x) = K_P.B.w(x) - G_P.B.w''(x)$	*(7)*
Elastoplastic Case:		$p(x) = p_{ult}$	*(11)*

Where p_{ult} is the soil bearing capacity; p_{ult} is the maximum stress that the springs can carry. First, the elastic conditions of Winkler and/or Pasternak are considered (Eq. (2) or Eq. (7)). Then, the beam deformation and the stresses applied to the ground are evaluated. Two cases are then possible:

- The stresses applied to the ground are less than p_{ult} (the soil is still in the elastic range). In this case, the maximum deformation of the building can be directly evaluated according to Winkler and/or Pasternak equations.
- Some of the stresses applied in a certain zone under the building (at the edges), known as the "plastic zone", are greater than p_{ult}. In this case, an iterative procedure is applied to find the solution in the plastic zone and determine the soil reaction based on Eq. (11).

a) Winkler model

An example is presented to show the influence of considering soil plasticity. This example is based on the model considered by Basmaji et al. (2017) [6] with an additional parameter (the soil bearing capacity), in order to integrate the elastoplastic conditions. Given a beam of unit width and length L=20m, stiffness EI=5350MN.m^2, loaded with 100KN/m, bearing capacity p_{ult}=120KN/m, Winkler reaction modulus K=3850KN/m^3 and a radius of curvature of the free field ground movement R=1500m, the solution of the problem is found by solving the equations and boundary conditions using Mathematica.

Figure 12 first shows the elastic solution for which there is no limitation on the soil reaction due to assuming an elastic behavior for the soil. For this case, the maximum displacement in the middle of the building is equal to 0.6 cm. However, at the boundaries there is an area where $p(x) > p_{ult}$, then the soil plasticity must be considered. Consequently, by applying the iterative process of resolution (Eq. (2) and Eq. (11)), it is noted that the maximum deflection of the beam Δ is reduced from 0.6 cm to

0.35 cm after considering plasticity.

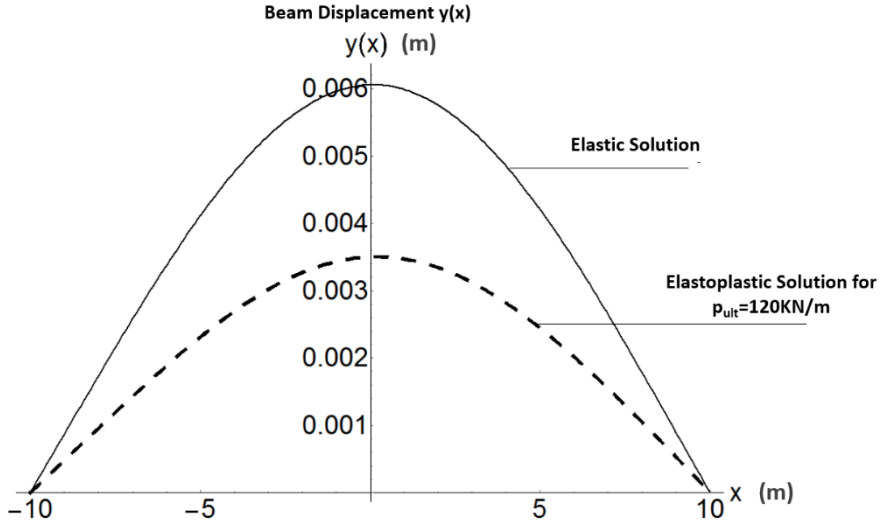


Fig. VI.12. Vertical displacements at the soil-structure interface according to the elastic and elastoplastic behavior of the ground.

b) *Pasternak model*

A procedure similar to that applied to Winkler model, to find the solution of a beam on an elastoplastic ground, is applied to find a solution for Pasternak model. However, since there is a soil displacement in Pasternak model outside the structure length L, the solution must take into account the movements of the soil throughout the whole system. The system is composed of the ground under the structure of length L, and the ground outside the structure over a length of 5L. It is assumed that the displacement of the ground at a distance of 5L from the structure is zero, this distance being infinite in the case of an analytical solution. The length 5L was chosen after numerous tests, as a reasonable compromise to obtain a satisfactory solution without an excessive computation time.

A preliminary example according to the Pasternak model has been applied and results show an inconsistency and a discontinuity in the values of the punctual forces at the building edges. According to the simulations evaluated by Mathematica, the soil reaction is concentrated in the two punctual forces generated at the building extremities. The value of F is significantly higher than the total sum of the reaction p(x) distributed under the building (Figure 8) which confirms the necessity of adding a limitation of the maximum punctual forces admissible at the building extremities. To do so, the shear modulus Gp is modified locally as per Eq. (12) so that the formula of the punctual force F shown in Figure 8 is limited by multiplying it by a coefficient α.

$$F_{lim} = \alpha \, \mathrm{Gp} \, (w'(x) - w'_1(x)) \qquad (12)$$

The criterion of validation of the results is the verification of the stability of the system (statistical equilibrium of the system) for each iteration, as per the following equation:

$$qL = \int_{-L/2}^{L/2} p(x) + 2F \qquad (13)$$

As shown in Figure 13, it is found that, without plasticity, the soil reaction p(x) decreases with the increasing values of x toward the beam edges where the punctual force F is located. However, after considering the influence of plasticity, the p(x) decreases at the beam center and increases at the beam edges in comparison with the first case. These results confirm the statistical balance and the equivalence between the sum of the reactions of p(x) and F from one side and the loads applied to the beam from the other side.

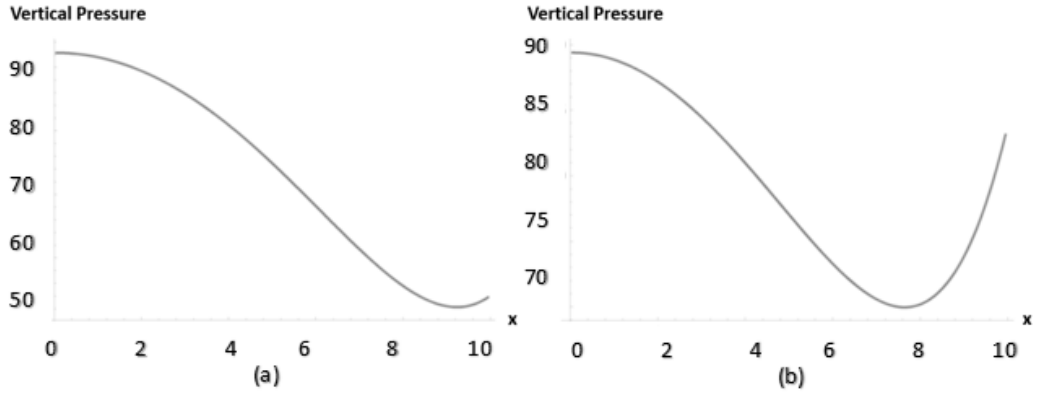


Fig. VI.13. Vertical pressure along the half beam (a) without plasticity; (b) with plasticity.

In order to find the exact value of F_{lim} , the parameter α is varied from 0.1 to 0.7 with a step of 0.1 to find the suitable value of F where the sum of the soil reaction p(x) and F is exactly equal to the loads applied to the beam. The results obtained showed that a value of α= 0.4 seems to be the most adequate for the Basmaji et al. (2017) example shown in Figure 12.

However, even-though the elastoplastic soil conditions can be integrated to the Pasternak model, the applied procedure presents several difficulties since the coefficient α has to be evaluated for every case separately and to check the system stability and the equivalence between the sum of the reactions and the applied loads by varying the value of α progressively. Thus, the process of integrating elastoplastic conditions to the Pasternak model is time consuming and presents difficulties to be generalized. Since the objective is to propose a 'generalized' meta-model that integrates the soil elastoplasticity, this paper will proceed by considering the Deck & Singh (2010) Winkler model combined with Vesic (1963) formula.

3. Validation with finite-element models

Based on the elastic finite element model explained previously, a new elastoplastic model is developed on Plaxis 2D. This model consists of dividing the soil into two layers; the upper layer of thickness h1 = 100 m is modelled as elastoplastic with a Mohr–Coulomb criterion, whereas the lower layer of thickness h2 = 25 m is assumed to be elastic. The function of the upper layer is to represent the elastoplastic conditions with a cohesion and a friction angle that vary with respect to p_{ult} value determined by the Terzaghi formula:

$$p_{ult} = cN_c + 0.5B\gamma_1 N_\gamma + (q + \gamma_2 D)N_q \qquad (14)$$

with γ_1 the soil density under the foundation, γ_2 the soil density lateral to the foundation, q the lateral vertical overload to the foundation, c the cohesion of the soil under the base of the foundation, B the width of the foundation, D the embedment depth of the foundation and N_c, N_q, $N\gamma$ the bearing capacity

factors.
The function of the lower layer (h2 = 25 m) is to avoid large deformations and large mass losses that occur near the lower limit due to the fact that such a loss could compromise the convergence of calculations and the accuracy of results; also stress-strain results are only interpreted for the upper ground layer. Considering an elastoplastic soil layer in contact with the building, a sliding interface is modelled between the ground and the structure in order to investigate only the influence of the ground curvature and not the influence of horizontal strains and the associated shear stresses induced by the subsidence. The same boundary conditions are applied and the model is realized in three stages as for the elastic case.

The set of 10 finite-element models that were generated for the elastic conditions are evaluated for elastoplastic conditions considering a particular value of the bearing capacity p_{ult} (cohesion and friction angle as per Eq. (14)) for every case. The numerical results presented in Figure 14 are superimposed with the elastoplastic analytical results of the same considered combinations of the SSI parameters (same p_{ult}, EI, K, L, q and Δ_0 values) for the transmission ratio calculated with the Deck & Singh (2010) Winkler model combined with Vesic (1963) formula. Consequently, the analytical methodology developed to consider the soil elastoplastic behavior is validated numerically and can be used to predict the value of the elastoplastic transmission ratio $(\Delta/\Delta_0)_{\text{Elastoplastic}}$.

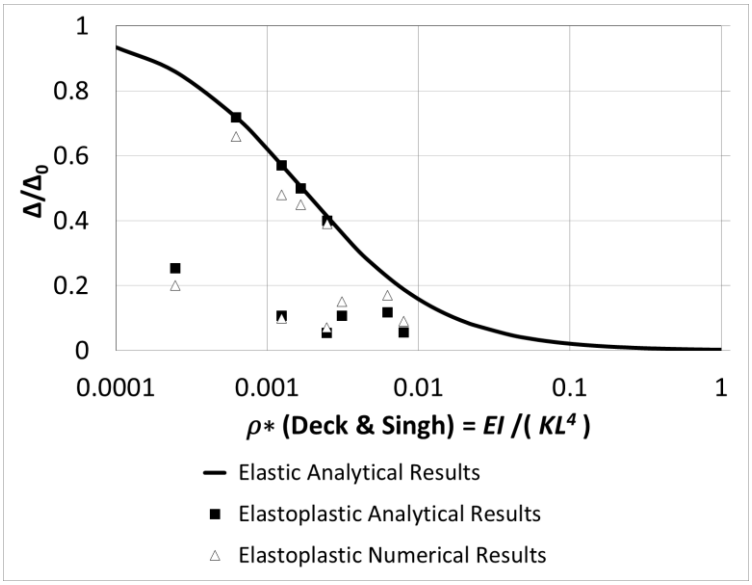


Fig. VI.14. Results of the comparison between analytical and numerical results of the deflection transmission ratio.

4. Reduction coefficient

In order to study the effect of soil plasticity on the transmission ratio Δ/Δ_0, the elastoplastic analytical model was evaluated using Mathematica, by investigating 18,900 possible combinations of p_{ult}, EI, K, L, R and q, as shown in Table 1.

The building length is taken between 10 and 30 m to model small and intermediate buildings [8]. The beam loading represents the building self-weight and service loading. 100 kN/m is approximately the weight of a 5 m high wall with a thickness of 0.5 m with service loading, 200 kN/m is approximately

the weight of a 10 m high wall with a thickness of 0.5 m and 400 kN/m is about the weight of a whole building with three 5 m tall walls with a thickness of 0.5 m including service loading.

The beam bending stiffness EI is between 20 and 500 GN.m^2. The smallest value represents the stiffness of a 0.5 m masonry wall thickness with 5 m height and a 3000 MPa equivalent Young's modulus for the masonry. The largest value represents the stiffness of a 0.2 m thick concrete wall, 12 m tall with a 20000 MPa equivalent Young's modulus.

The ground stiffness values vary between 20 and 500 MPa, according to Eq. (6), for values of soil Young modulus between 40 MPa (soft ground) and 500 MPa (stiff ground) and a Poisson's ratio of 0.3. The free-field ground radius of curvature is set between 250 and 5000m to represent a wide range of scenarios [7].

Considering that the structures are usually constructed with shallow foundations of length L and width B with L >> B, the bearing capacity can be obtained by Terzaghi's formula which depends essentially on the angle of internal friction and the cohesion of the ground under the foundation. To show the essential role that the limitation of the soil bearing capacity can have on the deflection of the building, the soil bearing capacity is considered variable between q and 4 q. Nevertheless, given the partial safety factors used in construction codes (Eurocode, etc.) for the design of the foundations at the Ultimate and Serviceability Limit States ULS and SLS (1.35 or 1.5), the considered cases (pult = Xq with X = 1, 1.5, … , 4) can be representative to approximate to standard situations [4].

Table VI-1: Model Parameters.

Symbol (Unit)	Description	Values
L(m)	Beam Length	10, 20, 30
q(KN/m)	Beam Load	100, 200, 300, 400
p_{ult}	Soil Bearing Capacity	q, 1.5q, 2q, 2.5q, 3q, 3.5q, 4q
EI(GN.m^2)	Beam Stiffness	20, 50, 100, 250, 500
K(MPa/m)	Ground Stiffness	20, 50, 100, 250, 500
R(m)	Free-Field Ground Radius of Curvature	250, 500, 750, 1000, 1500, 2000, 3000, 4000, 5000

Based on the results shown in Figure 15 for the 18,900 investigated combinations, a new relation can be proposed for the elastoplastic deflection transmission ratio using a reduction coefficient "a" as follows:

$$\frac{\Delta}{\Delta_0}(\text{Elastoplastic}) = a\ \frac{\Delta}{\Delta_0}(\text{Elastic}) \qquad (15)$$

$$\text{With } 0 \leq a \leq 1$$

If a=1, p_{ult} is not reached with the soil still in the elastic range, and there is no difference between considering an elastic or an elastoplastic soil behavior. However, when "a" decreases below 1, p_{ult} is reached. In order to establish a new correlation that evaluates "a" as a function of p_{ult}, q, R, K, EI and L, the influence of every factor on "a" is evaluated and presented in Table 2.

Table VI-2: Effect of every increasing factor on a.

Factor	Comments	a
$\mathbf{p_{ult}}\uparrow$	The soil does not reach the plastic phase and behaves as an elastic soil.	↑
q ↑	Due to static equilibrium, the soil reaction p(x) increases and may reach p_{ult} at a certain position under the structure.	↓
R ↑	The soil reaction difference at the ends of the structure is limited. The soil reaction p(x) then remains low and does not exceed p_{ult}, in most cases.	↑
K ↑	The soil reaction increases as per Winkler formula and becomes closer to p_{ult}.	↓
EI ↑	The building has more stiffness and can sink in the soil which will increase the soil reaction until reaching p_{ult}.	↓
L ↑	The structure is more flexible and the soil reaction under the structure is more homogeneous and exceeds less often p_{ult}.	↑

After evaluating 18,900 combinations (Table 1) and calculating Δ/Δ_0 for an elastic and an elastoplastic soil behavior, a new correlation (Eq. (16)) is proposed for the reduction factor "a" using artificial neural networks via JMP software which is a software used for statistical analysis.

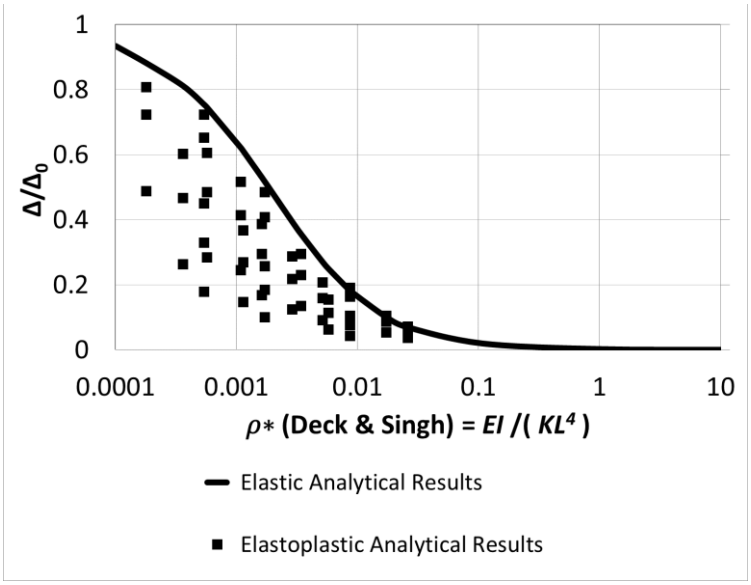


Fig. VI.15. Deflection transmission ratio Δ/Δ_0 versus the relative stiffness ρ* for elastic/elastoplastic behavior of soil for various soil bearing capacities.

To obtain the analytic expression of a, several data analyzes were performed. Attempts to express this parameter by various combinations of the model input parameters have not lead to satisfactory results. For this reason, the technique of neural networks has been used [4, 31].

The artificial neural network is composed of a collection of artificial neurons by computing a weighted sum of the inputs (18,900 combinations of p_{ult}, q, R, K, EI and L). Many variations exist in the way neurons are organized into a network, but all neural networks are composed of multiple layers; an input layer, an output layer, and intermediate layers, called hidden layers. The proposed model seeks to match the relationship between the obtained values of Δ/Δ_0 and the inputs. For good generalization performance, a balance must be found between an artificial neural network with insufficient neurons

that miss trends, and an artificial neural network with too many neurons that suffer from over fitting to the training data. The latter occurs when the minimization procedure tunes the weights in such a way that it almost perfectly captures the provided data, but is inaccurate when applied to new data, not used in the training procedure. To detect over fitting, the data is divided into three sets: a training, validation and test set. The network is built with a validation rate of 0.1 meaning that a proportion of 10% is therefore retained for validation. The final network obtained is composed of one layer and 3 neurons H1, H2 and H3 evaluated by minimizing the variance of the residues (Eq. (16)).

$$a = -7.19258 - 0.97155H1 - 0.52479H2 - 8.10706H3 \quad (16)$$

$$H1 = TanH\left(0.5\begin{pmatrix}-5.55733\\+0.00045K_w\\-0.00062R\\+0.00037q\\+0.00040p_{ult}\\+0.20247L\\+0.010897EI\end{pmatrix}\right); H2 = TanH\left(0.5\begin{pmatrix}44.10233\\+0.02106K_w\\-0.00035R\\+0.00033q\\-0.00102p_{ult}\\-1.77733L\\-0.076137EI\end{pmatrix}\right); H3 = TanH\left(0.5\begin{pmatrix}-2.44438\\+0.000078K_w\\+0.000071R\\+0.001837q\\-0.001939p_{ult}\\-0.009696L\\-0.001588EI\end{pmatrix}\right) \quad (17)$$

Figure 16 shows the actual values as a function of the expected values of the coefficient a. Thus, it is possible to visualize the residues. The coefficient of correlation is R^2 = 0.9026 and the root mean square error (RMSE) is relatively low (0.12). Figure 16 shows that the formulation of "a" has a general tendency to overestimate the large values of "a" and to underestimate the small values of "a".

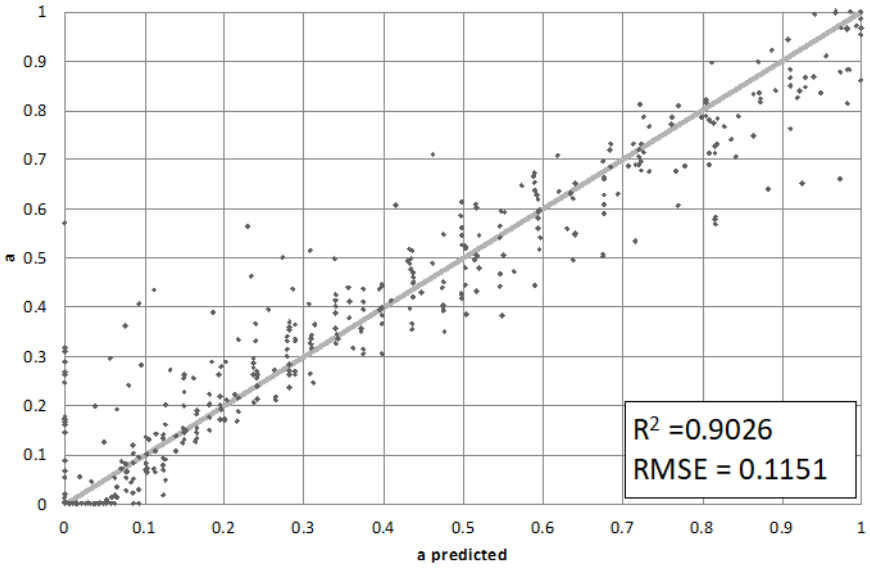


Fig. VI.16. Graph of observed values versus expected values.

It should be noted that the network has been reconstructed with other values of the validation rate (0.2 and 0.3) and the results are roughly the same, the RMSE is always close to 0 and it slightly increases with the increase of this rate. Thus, results show that the application of Eq. (16) can approximate the influence of plasticity when evaluating the transmission ratio. Consequently, this correlation can be directly adopted by the engineering society for design purposes to approximate the Δ/Δ_0 value when considering the elastoplastic behavior of the soil.

VI.6 Conclusions

This paper presents a new correlation to incorporate the elastoplastic soil behavior when evaluating the transmission of ground movements to structures induced by tunneling and mining subsidence. Based on the SSI analytical elastic approaches that are based on Pasternak and Winkler models, a new methodology is implemented that consists of limiting the soil reaction to its bearing capacity in order to consider soil elastoplastic conditions.
As shown in Figure 17, simplified equations are initially proposed to evaluate the elastic transmission ratio $(\Delta/\Delta_0)_{Elastic}$ for (a) Deck & Singh (2010) Winkler model coupled with Vesic formula and (b) Basmaji et al. (2017) Pasternak approaches. These two approaches are validated by elastic numerical finite element models and numerical, experimental and field data results from previous research. Then, the influence of soil plasticity on the transmission ratio Δ/Δ_0 is investigated by integrating the soil bearing capacity p_{ult}. Results show a significant difference in the transmission ratio between the elastic and the elastoplastic soil behavior. The elastic behavior results create an envelope that engulfs the elastoplastic results.

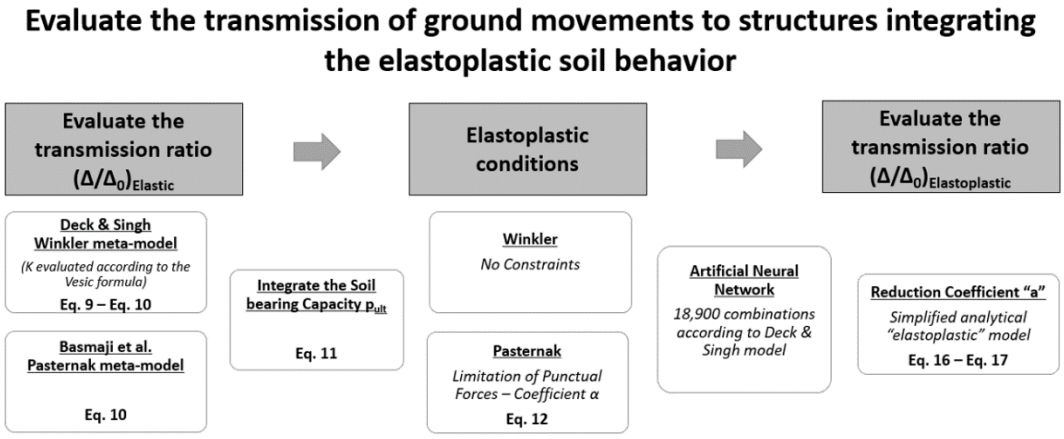


Fig. VI.17. Methodology of evaluation of the new simplified meta-model to calculate the transmission of ground movements to structures integrating the elastoplastic soil behavior.

On one hand, the proposed procedure applied for Pasternak model shows an inconsistency and a discontinuity in the values of the punctual forces at the building edges. Thus, a coefficient α is imposed to modify the shear modulus Gp locally and limit the maximum admissible punctual forces. To find the value of α, it is required to check the statistical balance and the equivalence between the sum of the reactions and loads applied to the beam for every combination. Thus, the proposed procedure applied for Pasternak model is time consuming and presents difficulties to be generalized. On the other hand, the proposed procedure applied for Winkler model (Deck & Singh model coupled with Vesic formula) does not show constraints and is validated by finite element-models.

Based on Deck & Singh Winkler model, a new meta-model is proposed that associates the elastic with the elastoplastic results of the transmission of the ground movement ($(\Delta/\Delta_0)_{Elastoplastic}$); the statistical meta-model is realized using artificial neural networks based on 18,900 combinations of SSI parameters and soil bearing capacities p_{ult}. A reduction coefficient "a" is proposed to associate the elastic ($(\Delta/\Delta_0)_{Elastic}$) with the elastoplastic ($(\Delta/\Delta_0)_{Elastoplastic}$) transmission ratios.

In conclusion, to improve the investigation of the structure response to ground movements and the evaluation of its damage, the effect of a significant SSI factor, the soil elastoplastic behavior, can be directly evaluated via the proposed simplified meta-model that is based on the elastic values of $(\Delta/\Delta_0)_{Elastic}$. To reduce time and calculation difficulties, this paper proposes simple equations (as shown in Figure 17) that are sufficient and can be directly used by geotechnical engineers and designers to consider the elastoplastic soil behavior and evaluate transmission of ground movements to structures.

VI.7 Acknowledgment

The work presented in this paper was supported by a research grant from Lorraine University of Excellence and the National Council for Scientific Research-Lebanon (CNRS-L) and the Lebanese University.

VI.8 References

[1] Mitropoulou, C., Kostopanagiotis, C., Kopanos, M., Ioakim, D. & Lagaros, N. Influence of soil–structure interaction on fragility assessment of building. Structures. 2016, 6: 85-98.

[2] Mair, R. Tunneling and deep excavations: Ground movements and their effects. *Proceedings of 15th European conference on soil mechanics and geotechnical engineering geotechnics of hard soils – weak rocks*; 2013, 4: 39-70.

[3] Anand, V. & Kumar, S. Seismic Soil-structure Interaction: A State-of-the-Art Review. *Structures*. 2018, 16: 317-326.

[4] ElKahi, E., Deck, O., Khouri, M., Mehdizadeh, R. & Rahme, P. Étude de l'influence de la plasticité du sol sur la transmission des mouvements du sol affectant l'interaction sol-structure. *Revue Française de Géotechnique*. 2018, 156, 4.

[5] Krishnamoorthy, A. & Anita, S. Soil–structure interaction analysis of a FPS-isolated structure using finite element model. *Structures*. 2016, 5: 44-57.

[6] Basmaji, B., Deck, O. & Alheib, M. Analytical model to predict building deflections induced by ground movements. *European Journal of Environmental and Civil Engineering*; 2017, 10: 1-23.

[7] Deck, O. & Singh, A. Analytical model for the prediction of building deflections induced by ground movements. *International Journal for Numerical and Analytical Methods in Geomechanics*; 2010, 36: 62-84.

[8] ElKahi, E., Khouri, M., Deck, O., Rahme, P. & Mehdizadeh, R. Studying the Influence of Uncertainties on the Transmission of Ground Movements Affecting the Soil-Structure Interaction. *10èmes journées Fiabilité des Matériaux et des Structures, Bordeaux, France*; 2018.

[9] Franza, A., Ritter, S. & Dejong, M. Continuum solutions for tunnel-building interaction and a modified framework for deformation prediction. *Géotechnique;* 2019: 1-15.

[10] Haji, K., Marshall, A. & Franza, A. Mixed empirical-numerical method for investigating tunneling effects on structures. *Tunnelling and Underground Space Technology*; 2018, 73: 92-104.

[11] Potts, D. & Addenbrooke, T. A structure's influence on tunneling-induced ground movements. *Proceedings of the Institution of Civil Engineers – Geotechnical Engineering*; 1997, 125: 109–125.

[12] Aissaoui, K. Amélioration de la prévision des affaissements dans les mines à l'aide des approches empiriques, numériques et analytiques-Doctorate thesis, Institut National Polytechnique de Lorraine, Nancy, France; 1999.

[13] Hassoun, M., Villard, P., Alheib, M. & Emeriault, F. Soil Reinforcement with Geosynthetic for Localized Subsidence Problems: Experimental and Analytical Analysis. *International Journal of Geomechanics*. 2018, 18 (10).

[14] Goh, K. & Mair, R. Building Damage Assessment for Deep Excavations in Singapore and the Influence of Building Stiffness. *Geotechnical Engineering*. 2011, 42: 1–12.

[15] Farrell, R. & Mair, R. Centrifuge modelling of the response of buildings to tunnelling. *Proceedings of the Seventh International Symposium on Geotechnical Aspects of Underground Construction in Soft Clay, Rome*. 2011, 2: 549-554.

[16] Koneshwaran, S., Thambiratnam, D. & Gallage, C. Blast Response of Segmented Bored Tunnel using Coupled SPH–FE Method. *Structures*. 2015, 58-71.

[17] Rahgozar, N., Rahgozar, N. & Moghadam, A. Controlled-rocking Braced Frame Bearing on a Shallow Foundation. *Structures*. 2018, 16: 63-72.

[18] Son, M. & Cording, E. Evaluation of building stiffness for building response analysis to excavation-induced ground movements. *Journal of Geotechnical and Geoenvironmental Engineering*; 2007, 133: 995-1002.

[19] Giardina, G., Hendriks, M. & Rots, J. Damage Functions for the Vulnerability Assessment of Masonry Buildings Subjected to Tunneling. *Journal of Structural Engineering*. 2014, 141 (9).

[20] Franza A. & DeJong M. A simple method to evaluate the response of structures with continuous or separated footings to tunnelling–induced movements. *Congress on Numerical Methods in Engineering, Valencia, Spain*; 2017: 919-931.

[21] Giardina, G., Marini, A. Hendriks, M., Rots, J. Rizzardini, F. & Giuriani, E. Experimental analysis of a masonry façade subject to tunnelling-induced settlement. *Engineering Structures*. 2012, 45: 421-434.

[22] Saeidi, A. La vulnérabilité des ouvrages soumis aux aléas mouvements de terrains : développement d'un simulateur de dommages-Doctorate thesis, Institut National Polytechnique de Lorraine, Nancy, France; 2010.

[23] Giardina, G., DeJong, M. & Mair, R. Important aspects when modelling the interaction between surface structures and tunnelling in sand. *Geotechnical Aspects of Underground Construction in Soft Ground - Proceedings of the 8th Int. Symposium on Geotechnical Aspects of Underground Construction in Soft Ground*. 2014: 263-268.

[24] Vesic. Beams on Elastic Subgrade and Winkler's Hypothesis. *Proceedings of the 5th International Conference on Soil Mechanics and Foundation Engineering*; 1963, 845-850.

[25] Biot. Bending of an infinite beam on an elastic foundation. *Journal of Applied Mechanics*; 1937.

[26] Drapkin. Grillage beams on elastic foundations. *Proc. ASCE*; 1955.

[27] Klöppel & Glock. Theoretische und Experimentelle Untersuchungen zu den Traglastproblemen Biegeweicher, in die Erde Eingebetteter. Institutes für Statik und Stahlbau der Technischen Hochschule Darmstadt; 1970.

[28] Henry. The Design and Construction of Engineering Foundations. Chapman & Hall; 1986.

[29] Franzius, J., Potts, D. & Burland, J. The response of surface structures to tunnel construction. *Proceedings of the Institution of Civil Engineers, Geotechnical Engineering*; 2006, 159: 3–17.

[30] Goh K. Response of Ground and Buildings to Deep Excavations and Tunnelling-Doctorate Thesis, University of Cambridge, 2010.

[31] Shahin, M., Jaksa, M. & Maier, H. Artificial Neural Network Applications in Geotechnical Engineering. *Australian Geomechanics*. 2001, 36: 49–62.

VII. Influence of Spatial Variability of Soil Properties on Structures Response

This paper was presented in the *29th European Safety and Reliability Conference*.

VII.1 Geostatistics background

Geostatistics are proved to be reliable and well adapted methods when dealing with gridding tasks and risk analysis in the geotechnical engineering. Compared to classical statistics, geostatistical methods take into account the spatial variability of the target parameter, in order to provide realistic spatial estimates together with a quantification of the associated uncertainty.
In the geostatistical approach, an analysis is made to evaluate the dependence of a variable in relation to itself and separated by a vector distance (Separation distance h). The magnitude of dependence can be detected by means of correlation coefficients and spatial covariance that can be expressed by a function called variogram. The semi-variogram $\gamma(h)$ is defined as half the average squared difference between points separated at distance h.
The below figure shows a variogram with nugget effect (C_0), range (A_0) (De-correlation length) and sill (C_0+C). In theory the variogram value at the origin (0 lag) should be zero. If it is significantly different from zero for lags very close to zero, then this variogram value is referred to as the nugget. This value represents the variability is due to measurement errors or errors of location of measures, either to the existence of a microstructure (small scale variability). Thus, the nugget effect is in most cases due to measurement uncertainty, which by nature does not exhibit any spatial correlation structure. The range is a distance beyond which the variogram essentially remains constant and reaches the sill value. Presumably, autocorrelation is essentially zero beyond the range. The sill is the plateau the variogram reaches at the range. If the variogram reaches a sill, the variable is stationary (its mean and variance are constant whatever the location in the space). If the variogram keeps increasing, the variable is non-stationary (the variable presents a trend, for instance its mean varies regarding the location in the space).

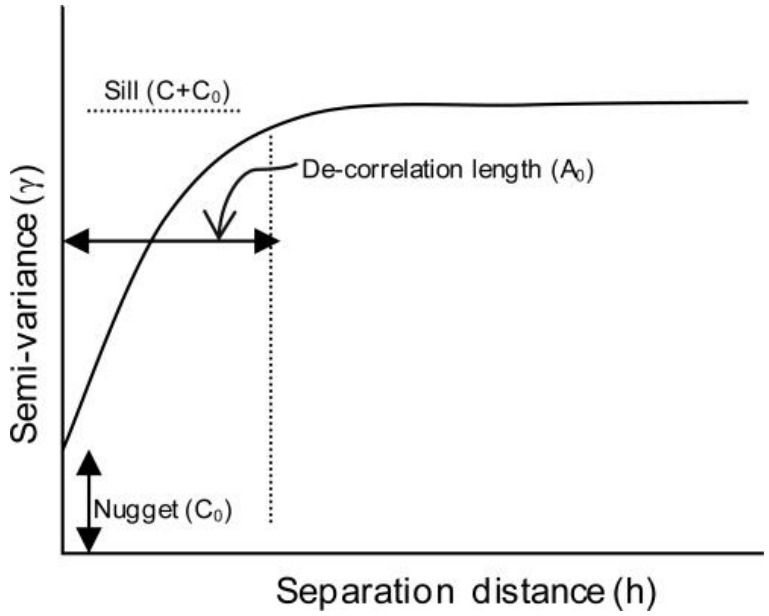


Fig. VII.0.a. Diagram of a stationary variogram.

The variogram is a basic graphic tool to support geostatistical techniques which allows quantitative representation of the variability of a regionalized phenomenon spatially [1]. In geological and geotechnical engineering, the most common models are:

- Pure nugget

- Power model (special case: the linear model)
- Spherical model
- Gaussian model
- Exponential model
- Cubic model

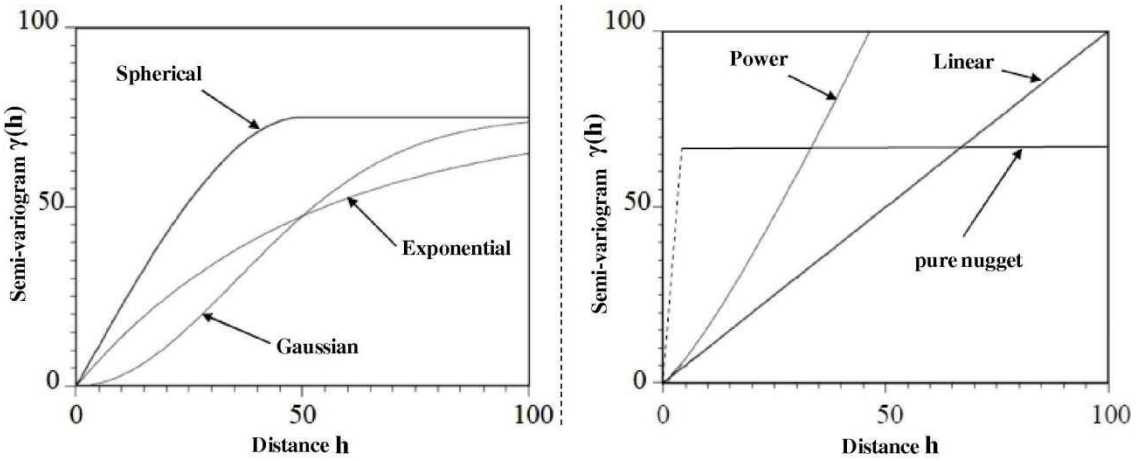


Fig. VII.0.b. Commonly used semi-variogram models with C_0 set to zero.

Every semi-variogram model is characterized by a mathematical function. For example, the exponential model respects the following equation:

$$\gamma(h) = C\left(1 - e^{\frac{-3h}{a}}\right) + C_0$$

Generally, the geostatistics allows to model a spatially continuous field values with conserving the measured values, then a random function would simulate a value at a known point. It can be useful to simulate different regionalized fields that represent several possible cases.

There are two kind of simulation: conditional and non-conditional simulations. In the event that data is available at the site being simulated, conditional simulation should be employed to ensure that the random field realizations match the data at the data locations exactly. Furthermore, all realizations pass through the known data but are random between the data sites. An unconditional simulation ignores this additional information and will lead to higher variability in the response quantities.

There are many simulation methods that can be grouped into Gaussian methods (matrix decomposition method, sequential methods, frequency, autoregressive, turning bands method, etc.) and non-Gaussian (annealing simulations, using methods in the probability field, etc.). Chilès and Delfiner (1999) [2]gave a fairly complete description of these methods. Examples of the simulation algorithms used in practice are the sequential Gaussian, the sequential indicator simulations and the local average subdivision technique [3].

The sequential Gaussian simulation (SGS) is the most commonly used technique, especially in the field of petroleum engineering. Its implementation allows the simulated values to be conditioned on a correlated variable whose value is known everywhere. If such a variable is available, this can lead to improved accuracy and precision. In this chapter, geostatistical tools are used to represent the soil spatial variability according to the SGS that will be detailed in the next paragraphs.

Influence of Spatial Variability of Soil Properties on Structures Response

EL KAHI Elio[ab], DECK Olivier[a], KHOURI Michel[b], MEHDIZADEH Rasool[a], CONIN Marianne[a] and RAHME Pierre[b]

[a]*GeoRessources, Université de Lorraine, Nancy, France.*

[b]*Faculté de Génie, Université Libanaise, Roumieh, Lebanon.*

E-mail: elio.el-kahi@univ-lorraine.fr

VII.2 Abstract

Physical and mechanical properties of soils have spatial heterogeneities whose origins come from the complexity of the involved natural geological processes that lead to their constitution. This spatial heterogeneity is associated with an uncertainty on each of the parameters usually used to quantify the natural variability that represents the soil. In addition, this spatial variability (SV) of soils may lead to differential settlements that affect the nearby buildings due to the soil-structure interaction phenomenon, causing structural and functional damages. The target of this study is to investigate the influence of natural variability of soil properties on the evaluation of the transmission of ground movements caused by tunneling and mining subsidence to nearby structures, whose consequences on structural response can be risky and dangerous. A probabilistic study is done using an analytical approach developed through Mathematica, coupled with a numerical model developed through GOCAD, to evaluate the uncertainties affecting the transmission of movements. In order to propagate geostatistical conditions to represent the soil, a modified Winkler model is developed where the soil is assimilated to a juxtaposition of elastic springs characterized by a particular stiffness value for every spring according to the SGS (Sequential Gaussian Simulation) method. Results reveal the effect of considering this uncertainty on the transmission ratio that specifies the building displacement in response to the ground movement.

VII.3 Keywords:

Spatial variability, soil heterogeneity, geostatistical conditions, movement transmission, Winkler model, uncertainties evaluation, soil structure interaction.

VII.4 Introduction

Nonlinearity, stress-dependency, anisotropy and heterogeneous nature of soils are some of the main sources of their complex mechanical behavior. Thus, one of the major challenges that faces geotechnical engineers is the need to make decisions regarding the soil parameters to be used in engineering analysis. These decisions have to be based on information that invariably has a certain degree of uncertainty [1]. On the other hand, this complex soil behavior may affect the decisions regarding the soil-structure interaction parameters while evaluating the transmission of ground movements, caused by tunneling, mining subsidence, sinkholes, etc. to nearby buildings, causing potentially their structural and functional damages [4].

In fact, several methods have been proposed to represent the soil stiffness. However, because of the modeling complications, Winkler's analytical approach has been used by many investigators to model the soil-structure interaction, instead of modeling the subsoil in all its complexity [5]. From a practical point of view, Winkler seems to be appropriate for superficial geotechnical designs. Thanks to its simplicity along with the advantage of taking into account only one parameter (the coefficient of subgrade reaction) to characterize elastic soil and structure responses under loading, the Winkler model has been extensively used to solve many soil-structure interaction problems and has given satisfactory results for many practical problems [6]. The soil reaction modulus is not an intrinsic parameter of soil; it depends on the mechanical parameters of the soil and mechanical and geometrical parameters of the structure. All of these parameters are uncertain and represent the major source of uncertainty in the output model [1]. Consequently, the objective of this paper is to investigate the influence of the spatial variability (SV) of soil properties, in particular the influence of the soil reaction modulus on the evaluation of the transmission of ground movements to structures.

VII.5 Spatial Variability (SV) and Geostatistics

Soils are geological materials formed by weathering, erosion and sedimentation processes. When transported to their present locations, soils have been subjected to various stresses and physical and chemical changes. In this context, heterogeneity is used as a synonym to SV. Consequently, the physical properties of soils vary from place to place within resulting deposits defined as SV [7]. It should be mentioned that the SV of the soil properties occurs at different scales of variability depending on the type of problem. When dealing with geotechnical structures, the inherent SV has been considered as a major source of uncertainties in soil properties. It significantly affects the performance of geotechnical structures that, under a probabilistic framework, is commonly measured by the probability of failure. Note that the determination of the mean and standard deviation of the soil property is performed using the conventional statistical analysis [8]. This analysis considers the variability of the soil property however, it does not provide its SV. Therefore, to characterize the spatial variation of a soil property (such as the coefficient of

subgrade reaction), one needs to determine the autocorrelation function and the corresponding value of the autocorrelation distance. For this purpose, an important technique that is found in the literature to identify the autocorrelation structure of a soil property is the geostatistical tools [1]. In fact, geostatistics approaches have proved to be reliable and well adapted methods when dealing with gridding tasks and risk analysis in geotechnical engineering [9]. Compared to classical statistics, geostatistical methods take into account the SV of the target parameter in order to provide realistic spatial estimates together with a quantification of the associated uncertainty. Many applications can be found in the literature: Thajeel (2017) [7], Imanzadeh (2013) [1], Sadrekarimi & Akbarzad (2009) [10], etc. Any geostatistical process begins with data quality control and analysis, thus allowing an understanding of the data prior to further steps. The variographic analysis is then performed in order to measure the SV of the data leading to a variogram computation. Afterwards, geostatistical modelling and simulation can be performed using this spatial information (variogram) [9].

While there are a number of simulation algorithms available (sequential indicator simulation, local average subdivision, etc.), Sequential Gaussian Simulation (SGS) is widely applied [1]. Its implementation allows the simulated values to be conditioned on a correlated variable whose value is known everywhere. If such a variable is available, this can lead to improved accuracy and precision. In this paper, geostatistical tools are used to represent the SV of the soil.

Sequential Gaussian Simulation

In general, conditional simulation algorithms allow uncertainty to be assessed by creating a set of realizations of the spatial distribution of a variable. Each realization is conditioned on the original data, and approximately reproduces the sample histogram and variogram. When a large number of realizations have been created, the variance of their mean value allows to calculate the estimation variance [8].

As illustrated in Table 1, the basic idea of the SGS is that the conditional distribution of the observed variable can be used for the simulation of subsequent grid points. The SGS is based on multi-Gaussian assumption of a random function model. It consists of defining a regularly spaced grid, covering the region of interest and establishing a random path through all grid nodes such that each node is visited only once in each sequence. For every grid node the normal score conditional cumulative distribution function (CCDF) is estimated according to a simple krigging system. Afterwards, a simulated value is drawn from the estimated CCDF and then added to the conditioning data set to be used for simulating other grid nodes. This procedure will be continued until all the grid nodes are simulated. The simulated normal score CCDFs then need to be back transformed to obtain the CCDFs of the considered parameter in original space. These sequential steps build up only the first realization; this sequence should be repeated with different random paths passing through all nodes for each realization. Indeed, the only difference among the several

individual simulations is the random-number seed, which initiates the simulation process and affects the random drawing of a value from the CCDF used to generate each simulated value. Therefore, in different realizations different values will be assigned to the same location [9] as shown in Table 1. Input random variables are transformed into standardized normally distributed random variables with zero means and unit variances for which different variogram characteristics are assessed. Simulated values of a standardized variable, Z, can be determined at any node of the simulation grid according to the relationship of Eq. (1):

$$Z_S(x_0) = Z^*(x_0) + R(x_0) \quad (1)$$

where $Z_S(x_0)$ is the simulated value of the variable Z at location x_0, $Z^*(x_0)$ is the krigged estimate of the variable Z at location x_0 and $R(x_0)$is a random residual.

$R(x_0)$ follows a normal distribution with zero mean and a variance equal to the krigging variance [3]. A different value of $R(x_0)$ is obtained in each realization using Monte Carlo Simulation resulting in a variation of the simulated value of the random variable ($Z(x_0)$ from one realization to another). A random path is followed to assess the value of the standardized random variable at each node of the numerical simulation grid. The simulated values across the analysis domain are then back transformed to their original probability distribution. By repeating the above procedure, several realizations of soil spatial variation across the analysis domain can be obtained.

Table VII-1. The basic idea of the sequential Gaussian simulation.

Steps of the Sequential Gaussian Simulation (SGS)
1. Transform input random variable into a standardized normally distributed (Gaussian) random variable of zero mean and unit variance.
2. Assess variogram characteristics for the standardized variable.
3. Implement Monte Carlo simulation to estimate a simulated value of the standardized variable at a certain node in the simulation grid.
4. Choose a random path through all nodes of the simulation grid.
5. For each node, search for nearby simulated nodes and use them to estimate a new simulated value of the random variable.
6. Check that new simulated values of the random variable satisfy variogram characteristics.
7. Back-transform all simulated values from its standardized form to its original probability distribution.

On the other hand, the autocorrelation function has been widely used for investigating SV in the context of geotechnical engineering (8, 11, 12). For the SV modeling, an autocorrelation distance of a property is defined as the distance within which the soil property exhibits relatively strong correlation. A large autocorrelation distance value implies that the soil property is highly correlated over a large spatial extent, resulting in a smooth variation within the soil profile. On the other hand, a small value indicates that the fluctuation of the soil property is large [10].

VII.6 Analytical Approach

To study the behavior of structures subjected to differential settlement caused by ground movements (tunneling, mining subsidence, sinkholes, etc.), various approaches have been developed. These can be gathered into five main groups [13]: numerical, empirical, semi-empirical, physical and analytical. This study uses an analytical approach and the modeling is used to allow rapid results to be obtained for a large variation range of model parameters considering the soil SV.

1. Soil & Structure Modeling

Winkler model is characterized by being a simple model to represent the soil underlying a foundation. Winkler assumes that the reaction of the soil at each point under the foundation is proportional to the deflection of the foundation at that point [6]. As shown in Figure 1, this hypothesis amounts to modeling the soil by a juxtaposition of elastic springs. The proportionality constant of these springs is known as the soil reaction modulus k. Considering that p(x) and w(x) represent the ground reaction and displacement respectively, Winkler's model is represented by Eq. (2):

$$p(x) = k.w(x) \tag{2}$$

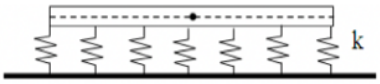


Fig. VII.1. Winkler Model.

The analytical approaches, developed to study the phenomenon of soil-structure interaction, model the building by an elastic Euler-Bernoulli beam of length L, width B, inertia I and Young's modulus E. The beam is loaded by a uniform vertical load q. The differential equation of the building displacement can be written as follows:

$$y^{(4)}(x) = \frac{q - p(x)}{EI} \tag{3}$$

Considering that the displacements of the ground and the building are in static equilibrium, it follows that there is a continuous contact between the ground and the beam. As illustrated in Figure 2, the building undergoes a rigid vertical displacement "d" with a deflection y(x). If v(x) represents the free-field ground displacement, the condition of no interpenetration is given by:

$$y(x) + d = v(x) + w(x) \tag{4}$$

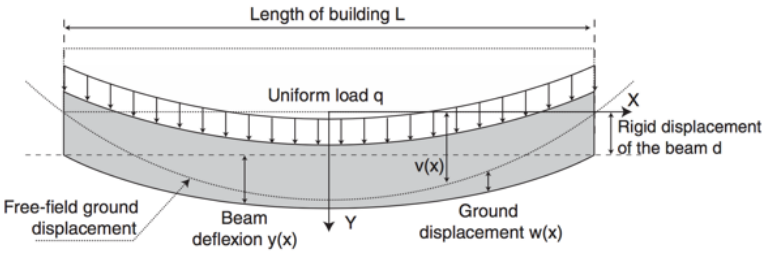


Fig. VII.2. Displacements of the ground and the building under conditions of static equilibrium.

Based on equations (2), (3) and (4), the characteristic differential equation of the beam deflection is given by Eq. (5):

$$y^{(4)}(x) = \frac{q - k.(y(x) + d - v(x))}{EI} \tag{5}$$

To solve the problem, six boundary conditions are used; the building deflection, the bending moment and the shear force at the beam extremities are equal to zero [5].

2. Transmission Ratio & Relative Stiffness

The transmission ratio is used to quantify the building damage analytically. It is the ratio of the maximum deflection of the building foundation Δ over the free-field deflection Δ_0. Considering the ground movement origin and the geological/geotechnical conditions, many methods can be used to assess the transmission ratio value. However, if one assumes that the free-field ground movement is roughly circular under the building, with a radius of curvature R (Figure 3), a geometric relationship can be determined to calculate Δ_0, by combining R with the length of the building L [4]:

$$\Delta_0 = L^2/8R \tag{6}$$

To represent the free-field ground movement, the polynomial function v(x) can be used:

$$v(x) = \Delta_0 \left(1 - \frac{4x^2}{L^2}\right) \quad For \;\; -L/2 < x < L/2 \tag{7}$$

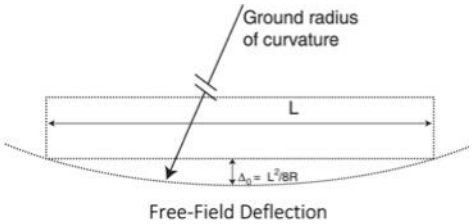


Fig. VII.3. Presentation of the free-field deflection.

The assessment of Δ is the key point because the free-field ground movements vary with the dimensions of the building. By taking the soil-structure interaction into consideration, Δ should be less than Δ_0 and the values of the transmission ratio Δ/Δ_0 are expected to be between 0 and 1.
On the other hand, to predict the building deflections by ground movements, research addresses the question of building stiffness compared to ground stiffness, which is known as "relative stiffness" [5, 14, 15].

In the literature, different stiffness ratios have been defined, and the transmission ratio of the free-field ground movements was investigated with analytical and numerical models according to the predefined stiffness ratios. However, this study considers the relative stiffness ratio ρ* defined in the analytical model of Deck & Singh (2010):

$$\rho^* = \frac{EI}{KBL^4} \tag{8}$$

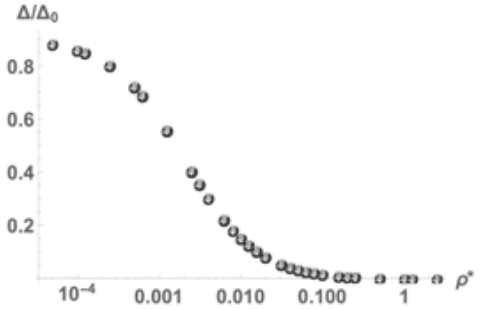


Fig. VII.4. Results of the deflection transmission ratio Δ/Δ_0 versus the relative stiffness ρ* ratio for the El Kahi *el al.* model (2018).

In Figure 4, the deflection transmission ratio is plotted against the relative stiffness; it shows that the results of the soil-structure interaction analytical model are as expected.

VII.7 Results & Discussion

The determination of the deflection transmission ratio is a key parameter used in soil-structure interaction studies. This ratio strongly depends on the soil characteristics and modeling, in particular the soil reaction modulus k [10]. In order to propagate geostatistical conditions to represent the soil, a modified Winkler model is used with a particular reaction modulus value k for every spring. To do so, GOCAD, a computer application that offers a variety of geological, geophysical and geostatistical analyses that can be performed on geological objects, is used to apply the sequential Gaussian simulations (SGS) to evaluate the spatial variability of the soil in the horizontal direction.

Table VII-2. Model Parameters.

Soil reaction modulus k		Beam Length L	
Mean Values μ (MPa/m)	20, 250, 500	Considered values (m)	10, 20, 30
Coefficient of Variation	40%	Correlation Length L1	1m, 0.5 L, L, 2L
Beam Stiffness EI (GN.m^2)		20, 250, 500	
108 combinations -10 simulations for every combination (Total: 1080 simulations)			

In this numerical software Gaussian distribution is evaluated according to an exponential variogram type. Three mean values of k and a coefficient of variation (standard-deviation/mean) of 40% (Table 2) are considered. Every distribution is associated with a value of the beam length (10, 20 or 30 m) and a considered value of the correlation length accordingly (1 m, 0.5L, L or 2L (where L is the building length)); they are used to evaluate the cases of heterogeneous, intermediate and homogeneous soil respectively. Consequently, 108 combinations of the soil reaction modulus are evaluated according to the SGS method using GOCAD; for every simulation ten simulations are applied, so confidence intervals of the transmission ratio Δ/Δ_0 can be calculated (Table 2). Note that 200 nodes are considered for every simulation which means 200 springs under the building as per the Winkler model.

Figure 5 shows the evaluated results of a simulation for the combination of μ_k = 250 MPa/m, L = 20 m and L1 = 5m. GOCAD can consequently fit these results to a theoretical variogram in order to compare the results. Consequently, an exponential variogram type is suitable to the results with a coefficient of variation of 36%, an azimuth of 4.5° and a range of 4.1m. Figure 6 shows the values of the first simulation of k for μ_k = 20 MPa/m for L = 10 m according to the four considered correlation lengths mentioned in Table 2.

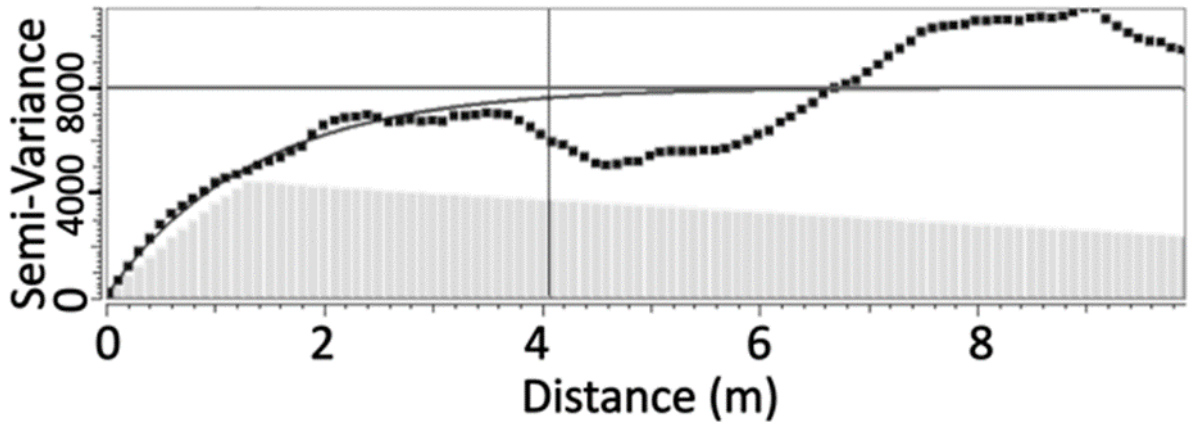


Fig. VII.5. Variogram model fitting a curve to the results.

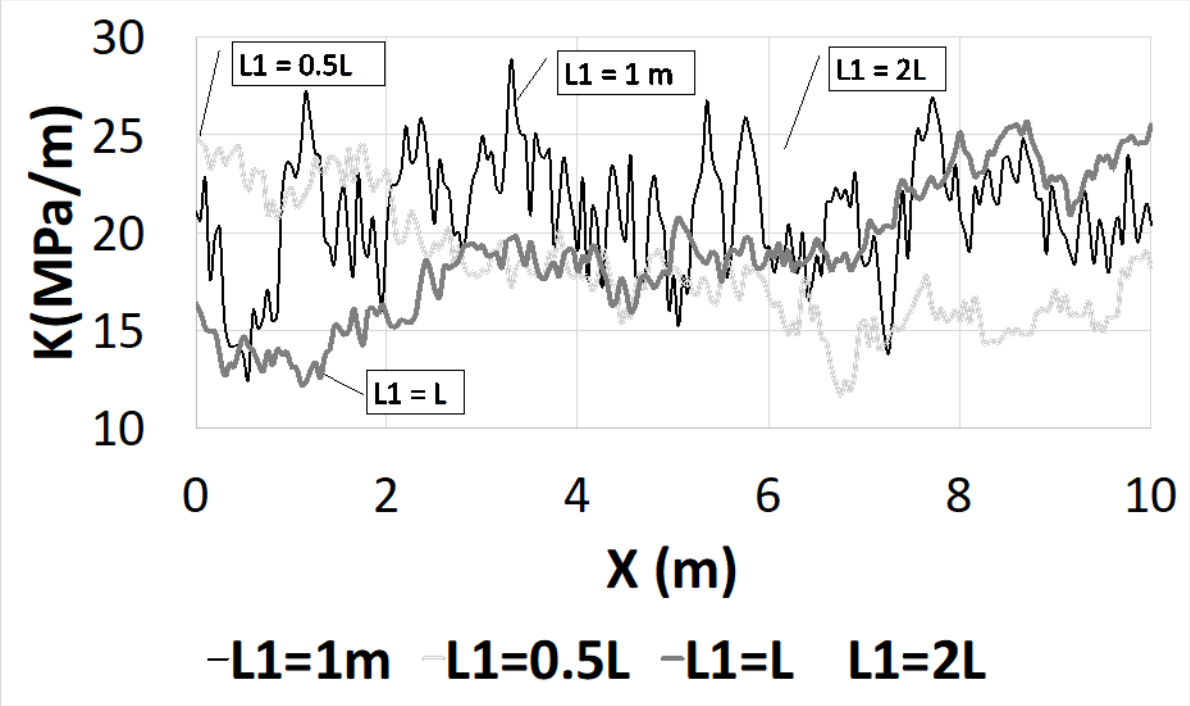


Fig. VII.6. First simulation of k distribution for μ_k = 20 MPa/m for four considered correlation lengths for L=10 m.

In determining the transmission ratio Δ/Δ_0, a radius of curvature R = 2000 m corresponding to the mid-value of the range of scenarios suggested by Deck & Singh (2010) is considered. Concerning the beam, a loading of 500 kN/m is evaluated; it represents the building self-weight and service loading. For every combination mentioned in Table 2, three values of the beam stiffness are considered: 20, 250 and 500 GN.m^2. The lowest value represents the stiffness of a 0.5 m masonry wall thickness with 5m height and a 3000 MPa equivalent Young's modulus. The largest value is approximately the stiffness of a 0.2 m concrete wall thickness, 12 m high with a 20000 MPa equivalent Young's modulus.

Figure 7 shows the results for one of the investigated correlation length (L1=2L) shown in Table 2 for different combinations of ρ* (soil reaction modulus and beam length values, μ_k = 20, 250, 500 MPa/m, L = 10, 20, 30 m, for three values of the beam stiffness (20, 250, 500 GN.m^2) using Mathematica.

Globally, for an equivalent stiffness ratio, the difference between the results of the maximum transmission ratio and the case that does not consider the geostatistical conditions is slight. To show the influence of the SV, a coefficient α is introduced representing the ratio of Δ/Δ_0results with SV $(\Delta/\Delta_0)_{SV}$ and without it $(\Delta/\Delta_0)_{w/o\ SV}$.

$$\alpha = \left(\frac{\Delta}{\Delta_0}\right)_{SV} \Big/ \left(\frac{\Delta}{\Delta_0}\right)_{w/o\ SV} \tag{9}$$

For L1=2L, the mean value of α for different combinations of EI, k and L is 0.944. For the low values of ρ^*, α is nearly equal to 1. However, when ρ^* increases, α varies significantly, even-though the absolute variation of Δ/Δ_0 is slight between the two cases (with or without SV); this is due to the low values of Δ/Δ_0 that correspond to the high values of ρ^* (Figure 4). For example, for ρ^*=2.5, for one of the simulations that corresponds to L=0.5L, the values of Δ/Δ_0 with or without SV are 14.28×10^{-4} and 7.79×10^{-4} respectively, which corresponds to an absolute difference of 6.49×10^{-4} and a value of α=1.84.

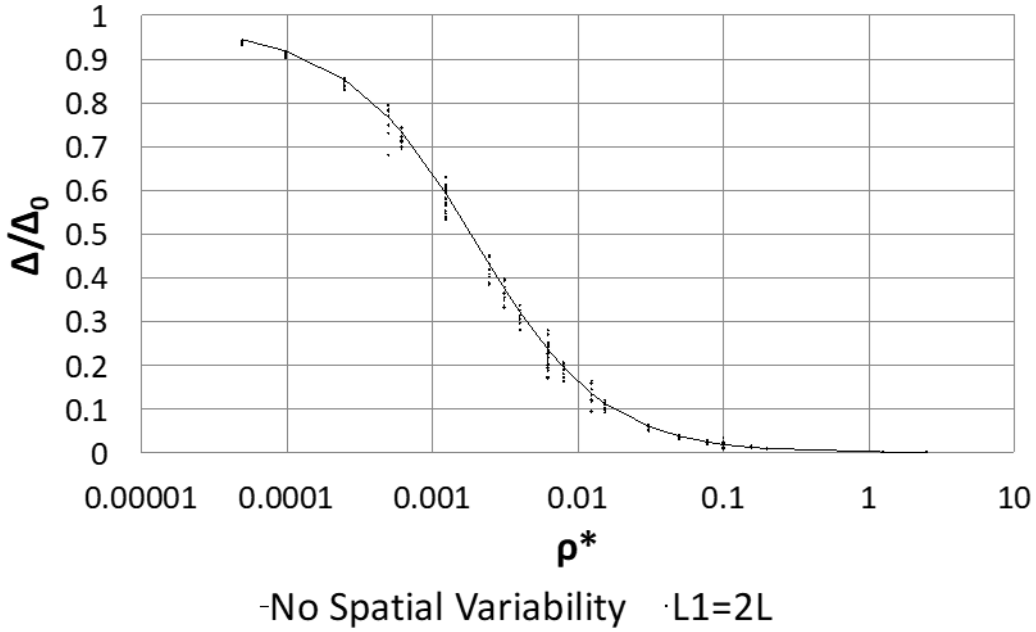


Fig. VII.7. Results of the deflection transmission ratio Δ/Δ_0 versus the relative stiffness ρ^* ratio for L1=2L.

On the other hand, considering the other correlation lengths (1m, 0.5L and L), the coefficient α value is close to 1 when the soil is highly heterogeneous (L1=1m). Consequently, the effect of the variability increases with the increase of L1 (Figure 8). In fact, for a heterogeneous soil, the different values of k compensate each other so that the final soil reaction becomes similar to the case where there is no SV. However, when L1 increases, α tends to increase farther from 1, so the effect of the SV becomes more significant. In fact, even if the soil behavior becomes more homogeneous, the modulus k characterizing the soil, tends to have the same value all along the building length; this value can be either higher of lower than the mean considered value.

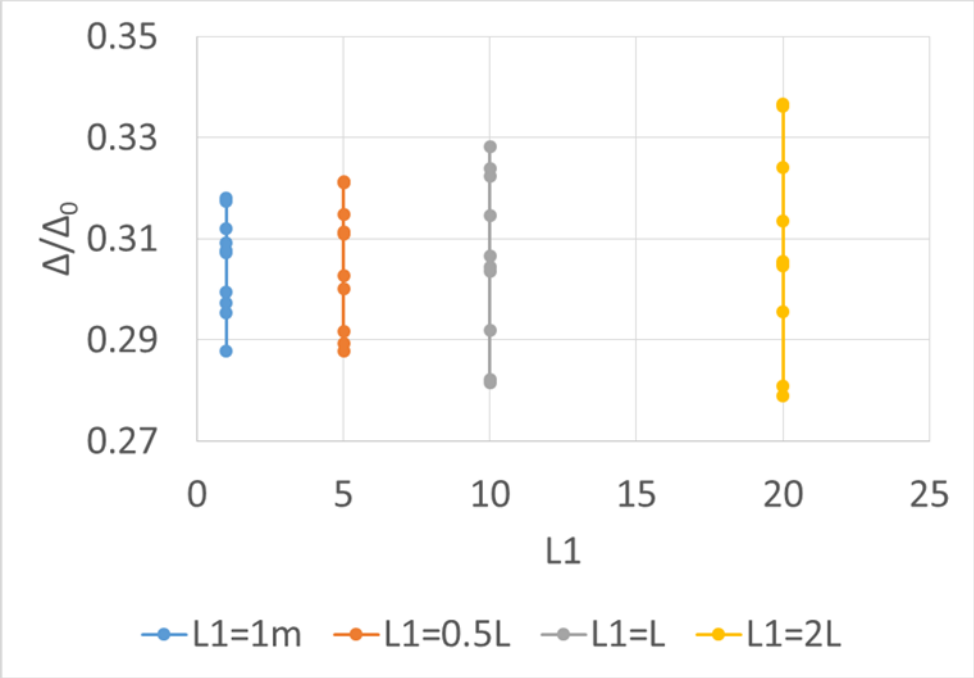


Fig. VII.8. Results of the deflection transmission ratio Δ/Δ_0 for different L1 values for L=10m, μ_k=500MPa/m and EI=20GN.m^2.

In order to separately investigate the effect of every parameter on the transmission ratio by considering the SV, and consequently the effect on the coefficient α, the error bars are evaluated; these represent one standard deviation of uncertainty around the mean value of α for the considered sets of parameters.

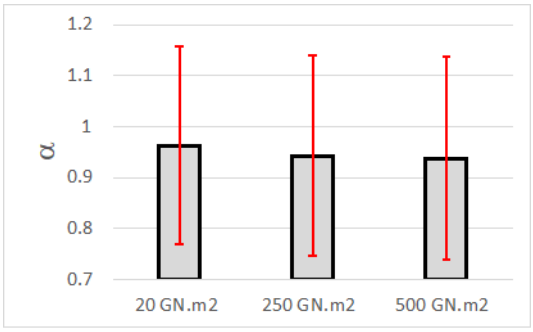


Fig. VII.9. Relationship between α and the beam stiffness.

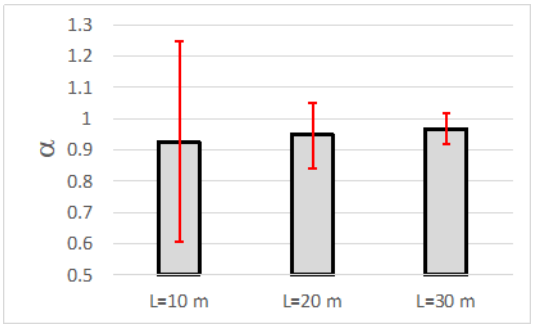


Fig. VII.10. Relationship between α and the beam length.

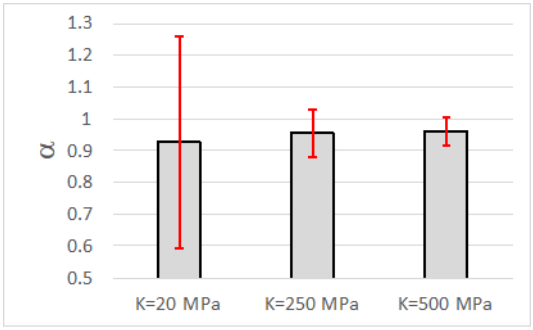


Fig. VII.11. Relationship between α and the soil modulus mean value.

Based on Figures 9-11, the following comments can be made:

- Figure 9 shows that, globally, the results are similar while varying EI value. However, results show that for a flexible beam, the transmission ratio (Δ/Δ_0) is high (close to 1) while for a stiff beam (Δ/Δ_0) is low (close to 0); therefore, having the same value α for both beams indicates that the influence of the SV on a flexible beam is more significant than that on a stiff beam.
- Figure 10 shows that the coefficient α is highly affected by the beam length. In fact, the beam length represents the length of the application of the soil reaction and its SV. In addition, the chosen values of the correlation length L1 are directly correlated to the value of L (0.5L, L and 2L). For high values of L, the mean value of α is almost equal to 1, and the standard error is low indicating that the effect of the SV is low. However, when L decreases (L=10m), the SV has a significant influence. In fact, when L decreases, ρ* increases (Eq. (8)) and α varies significantly for high ρ* values, even-though the absolute variation of Δ/Δ_0 is slight.
- Figure 11 shows that the coefficient α is also highly affected by the investigated soil modulus value. For a soft ground (k=20 MPa), SV highly affects the beam deflection, while its effect is low for a stiff ground (k=500 MPa). The influence of k can be compared to the one of L, since they both have the same effect on ρ* (Eq. (8)), even-though L is power 4 while k is power 1. However, SV is directly applied to the soil modulus, so, its effect is more significant on k; but, since L is power 4, the SV of k has the same influence on α while varying k and L.

VII.8 Conclusions & Perspectives

This paper develops a probabilistic study through an analytical approach developed by Mathematica coupled with a numerical model using GOCAD to evaluate the uncertainties related to the soil spatial variability affecting the transmission of movements caused by various sources (tunneling, mines, sinkholes, etc.) to nearby structures. A modified Winkler model is used in this study to propagate geostatistical conditions to represent the soil using the sequential Gaussian sequence method. In fact, the soil is assimilated to a juxtaposition of elastic springs, characterized by a particular stiffness value for every spring. 108 combinations of the soil modulus, structure stiffness, length and correlation length are considered; for every combination, a flexible, intermediate and stiff structures are assessed. Results reveal the effect of considering the soil spatial variability on the transmission ratio that specifies the building behavior in response to the ground movement. They revealed that, for a heterogeneous soil, the properties compensate each other so that the final effect becomes similar to the case where there is no SV. However, when the correlation length increases, the soil becomes homogeneous, but the SV influence is more important.

These results are also affected by various factors such as the soil homogeneity, the building length and the soil modulus. Thus, the impact of every parameter has been studied separately and diagrams are presented that can simplify the determination of the coefficient α that compares the results with or without spatial variability for the considered parameters. Consequently, this study indicates the significant impact that spatial variability of soil properties has on evaluating the behavior of buildings and their response to excavation-induced ground movements. However, a numerical validation has to be realized in order to endorse the proposed analytical approach. Advanced computer software, like Plaxis 3D, permit to consider the spatial variability which allows a comparison and a validation of the proposed analytical approach.
As perspectives, this study raises many questions related to the uncertainties that can affect the evaluation of the transmission of ground movements:

- Uncertainty of the applied model (Winkler): Since Winkler model does not consider the geostatistical conditions of the soil, a modification of this model is developed in this study. However, an evaluation can be made to compare Winkler to other analytical (or numerical and experimental) models that consider soil spatial variability.
- Detachment between the soil and the structure: By imposing the condition of no interpenetration and continuous contact between the soil and the structure, this study does not take into consideration the possibility of detachment between them.
- Elastoplastic soil behavior: Winkler is an elastic model that does not take into consideration the plasticity of the soil. However, plasticity has a significant role that has to be considered while evaluating the transmission of ground movements to structures.

VII.9 Acknowledgement

The work presented in this paper was supported by a research grant from the National Council for Scientific Research-Lebanon (CNRS-L) and the Lebanese University.

VII.10 References

[1] Imanzadeh, 2013. Effects of uncertainties & spatial variation of soil and structure properties on geotechnical design. Cases of continuous spread footings and buried pipes, Doctorate thesis, Université Bordeaux.

[2] Chilès JP., Blanchin R., 1995. ″Contribution of geostatistics to the control of the geological risk in civil-engineering projects: the example of the Channel Tunnel″. In Application of Statistics and Probability, Lemaire, Favre & Mébarki (eds), Blakeme, Rotterdam.

[3] Deutsch, 2002. Geostatistical reservoir modeling. Oxford University Press.

[4] Basmaji, B., Deck, O. & Heib, M., 2017. Analytical model to predict building deflections induced by ground movements. European Journal of Environmental and Civil Engineering.

[5] Deck, O. & Singh, A., 2010. Analytical model for the prediction of building deflections induced by ground movements. International Journal for Numerical and Analytical Methods in Geomechanics, 36, p. 62–84.

[6] El Kahi E., Khouri, M., Deck, O., Rahme, P., Mehdizadeh, R., (2018). Studying the influence of uncertainties on the transmission of ground movements affecting the soil-structure interaction, 10 éme journées fiabilité des materiaux et des structures – Bordeaux.

[7] Thajeel, 2017. Kriging-based Approaches for the Probabilistic Analysis of Strip Footings Resting on Spatially Varying Soils, s.l.: PhD. Thesis, University of Nantes.

[8] Baecher, B. & Christian, J., 2003. Reliability and statistics in geotechnical engineering. John Wiley & Sons.

[9] Asghari, Soltni & Amnieh, 2009. The Comparison Between Sequential Gaussian Simulation (SGS) of Choghart Ore Deposit and Geostatistical Estimation Through Ordinary Kriging. Australian Journal of Basic and Applied Sciences, 3(1), pp. 330-341.

[10] Sadrekarimi & Akbarzad, 2009. Comparative Study of Methods of Determination of Coefficient of Subgrade Reaction. Electronic Journal of Geotechnical Engineering, 14, p. 1-14.

[11] Piegay, 2015. Optimisation multi-objectif et aide a la decision pour la conception robuste, Doctorate thesis, Université de Bordeaux.

[12] Jacques, J., 2011. Pratique de l'analyse de sensibilité : comment évaluer l'impact des entrées aléatoires sur la sortie d'un modèle mathématique, Université de Lille.

[13] Aissaoui, K., 1999. Amélioration de la prévision des affaissements dans les mines à l'aide des approches empiriques, numériques et analytiques. Doctorate thesis. INPL.

[14] Potts, D. & Addenbrooke, T., 1997. A structure's influence on tunneling-induced ground movements. Proceedings of the Institution of Civil Engineers – Geotechnical Engineering, 125, p. 109–125.

[15] Son, M. & Cording, E., 2007. Evaluation of building stiffness for building response analysis to excavation-induced ground movements. Journal of Geotechnical and Geoenvironmental Engineering, 133, p. 995–1002.

VIII. Experimental evaluation of the stiffness variability of masonry structures affecting the transmission of ground movements

This paper is currently under submission in *11èmes journées de fiabilité des matériaux et structures, JFMS 2020.*

Experimental evaluation of the stiffness variability of masonry structures affecting the transmission of ground movements

EL KAHI Elio[ab], MECHLING Jean-Michel[c], KHELIL Abdelhouahab[d], DECK Olivier[a], KHOURI Michel[b], MEHDIZADEH Rasool[a] and RAHME Pierre[b]

[a]*GeoRessources, Université de Lorraine, Nancy, France.*

[b]*Faculté de Génie, Université Libanaise, Roumieh, Lebanon.*

[c]*Institut Jean Lamour, CP2S, Nancy Université, UPVM, CNRS, IUT NB, 54601 Villers-lès-Nancy, France*

[d]*Institute University of Technology, Nancy Brabois, 54601 Villers Les Nancy, France*

E-mail: elio.el-kahi@univ-lorraine.fr

VIII.1 Abstract

The objective of this study is to investigate the influence of the variability of stiffness while evaluating the buildings response to ground movements induced by tunneling, shrink-swell phenomenon of clay soils, mining subsidence, etc. Previous studies in the literature assessed the uncertainty related to the influence of the variability of the main soil-structure interaction (SSI) properties on the transmission of ground movements. Sensitivity Analyses (SA) were developed to quantify the relative importance of the variability of every SSI parameter which was assumed to be of a random nature. Various sampling techniques, were used according to suitable distribution functions with associated Coefficient of Variation (COV) for every parameter. Results of the SA revealed that the variability of the building stiffness has a crucial and decisive influence that impacts also the confidence intervals that are set to be used by engineers and designers when evaluating the transmission of ground movements. However, the choice of a suitable distribution function to represent the stiffness variability with its associated COV presents a large margin of uncertainty in the literature. While certain experimental investigations of concrete durability properties found that the stiffness E can follow a normal distribution with a COV that does not exceed 10%, it was observed from data collection of published experimental works on masonry structures that the COV of the stiffness is around 30% to 40%. Thus, experimental tests are carried out on masonry walls in in order to study the variability of the stiffness of the masonry walls subjected to a ground settlement. The results of these experimental tests are then compared to the published results in the literature to validate their use while evaluating the uncertainties affecting the transmission of ground movements.

VIII.2 Keywords:

Experimental tests, masonry structures, stiffness variability, soil settlement, soil-structure interaction.

VIII.3 Introduction

Many underground projects such as tunneling, mines and braced excavations, considered as sources of ground movements, may create various effects on overlying structures. As shown in Fig. 1, these sources will cause the soil settlement, and in the presence of an existing structure, the settlement may considerably affect the structure leading to its damage. The process in which the soil movement influences the structure response is known as SSI (Soil-Structure Interaction) [1].

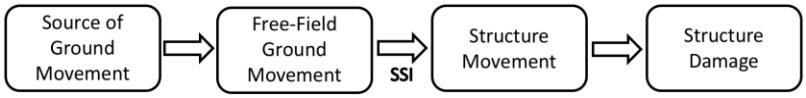


Fig. VIII.1. Diagram representing the ground movement transmission to the structures due to Soil-Structure Interaction (SSI).

The understanding of this complex phenomenon has continuously improved through several studies where many approaches have been developed to assess the SSI phenomenon, and consequently to measure the soil settlement and the deformation of the structure [2].

In fact, Farrell & Mair (2010) [3] and Ngheim (2015) [4] proposed experimental and physical approaches to study the structure response to the free field movement while Franzius *et al.* (2006) [5], Son & Cording (2007) [6], Dimmock & Mair (2008) [7], Mirhabibi & Soroush (2013) [8] and Franza & DeJong (2017) [9] used numerical approaches to study SSI. In addition, analytical approaches have been also developed by Potts & Addenbrooke (1997) [10], Deck & Singh (2010) [1], Maleki *et al*. (2010) [11], Basmaji *et al*. (2017) [12], El Kahi *et al*. (2018) [13].

However, each approach presents its own disadvantages and uncertainties, such as scale effects for reduced scale models, complex problem configuration (boundary conditions, mesh size, etc.) for numerical approaches and debatable parameters uses and choices in these approaches [12]. In addition to uncertainties related to the use of the corresponding SSI evaluation approach (experimental, numerical, etc.), parameters uncertainties may affect the investigation of SSI. These can be either related to the soil (mechanical properties, geology, soil profile deformation, etc.) either related to the structure (building stiffness, homogeneity of properties, building complex geometry and materials, etc.) [14].

A probabilistic study is developed by El Kahi *et al*. (2019) [14] by developing confidence intervals to consider the effect of the uncertainties related to the variability of every SSI parameter on the transmission of the ground movement and consequently on the behavior of structures. As shown in Fig. 2, they considered Δo the free-field maximum deflection that is produced by the ground without considering the structure, Δ the deflection of the structure produced by the transmission of the ground movement due to the SSI. Thus, the transmission ratio $\Delta/\Delta o$ is used to assess transmission of ground movements to structures. By taking the SSI into consideration, Δ should

be less than Δo and the values of the transmission ratio Δ/Δo are expected to be between 0 and 1. As shown in Fig. 3, this ratio depends upon the relative stiffness ρ* which is the structure stiffness compared to the soil stiffness. In order to develop their probabilistic study, a meta-model is evaluated representing Δ/Δo as a function of ρ*. The "basic random variables theory" is used to model the uncertainty of the SSI properties through the Monte-Carlo simulations. To use the Monte-Carlo method, it is necessary to have probability distribution functions with corresponding characteristics (normal, lognormal distribution, etc.) for the input data. Therefore, their developed approach for approximating the SSI parameters uncertainties is done by using estimates based on published values which are conveniently expressed in terms of the coefficient of variation (COV). For the structure stiffness, a developed experimental investigation of the variability of concrete durability properties [15] found that the elastic modulus E can follow a normal distribution with a COV that does not exceed 10% (Table 1).

Table VIII-1. Mechanical tests for 3 concrete mix designs: mean values, coefficient of variation and number of specimens tested for Young's modulus (E).

Site	Number	E [GPa] Mean Value	COV (%)
A1	40	46.8	6.2
A2-1	20	40.8	7.0
A2-2	20	40.8	5.4

Considering masonry structures, the stiffness variability is higher. These types of structures are used in almost all types of building construction in many parts of the world because of low cost material, good sound and heat insulation properties, easy availability, and locally available material and skilled labor. Mathematical modeling of structures with masonry walls requires the material properties and constitutive relationships of masonry and its constituents, i.e., bricks and mortar, which are not easily available because of lack of controlled experimental tests and significant variation in material properties geographically (Table 2). By collecting data from published experimental work, it was found that the COV of E is more than 20% which is around the double of the one of concrete (Sykora & Holicky (2014) [16], Parisi & Augenti (2012) [17], Dymiotis & Gutlederer (2002) [18]).

Table VIII-2. Comparison of 3 existing experimental tests in the literature to evaluate the masonry structures variability.

Ref.	COV (%)	Comments
[16]	~32	Evaluated the variability of various type of bricks and mortar joints. The mentioned value is the highest one obtained.
[17]	~20	Performed a statistical analysis of experimental data on tuff masonry selected from online database of masonry properties collected in more than 400 studies.
[18]	~ 30	Worked mainly on the compressive strength variability but a correlation is made with E.

Based on Table 2, masonry structures stiffness present a significant variability. It is important to note that these tests are performed considering different conditions of mortar specimens, brick units and masonry parameters with additional uncertainties in come relevant details such as geometric parameters (dimensions of bricks, joints openings, walls, etc.).

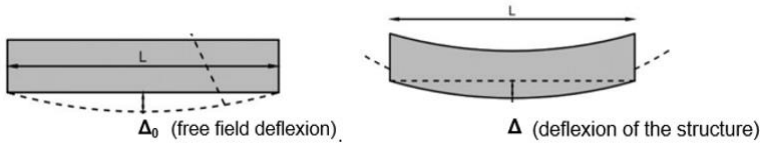


Fig. VIII.2. Presentation of the free field deflection Δo and the structure deflection Δ [14].

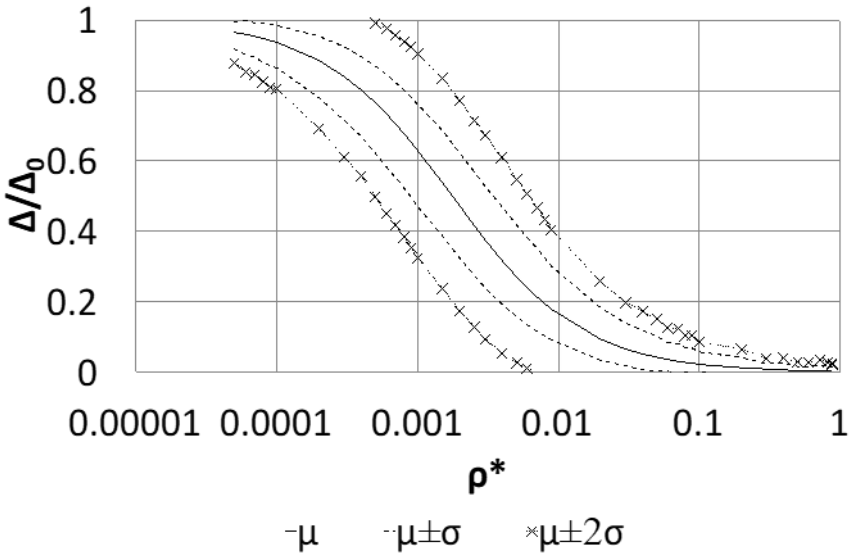


Fig. VIII.3. Confidence intervals to the curve of the transmission ratio Δ/Δ_0 versus the relative stiffness ρ* [14].

Thus, this uncertainty must be combined with that of the beam inertia I. No theoretical data have been found to clearly address this point. However, according to El Kahi *et al.* (2019) [14], it seems reasonable to consider a high value of uncertainty considering that assimilating the building to a beam is a very simple model of a reality, especially when the building is not regular. Based on engineering judgment the COV (EI) for masonry structures is taken equal to 40% in their study.
Consequently, the target of this study is to carry out tests on masonry walls in in order to study the variability of the stiffness of the masonry walls subjected to a ground settlement. The realization of experimental tests reproducing the exact conditions of settlement is not possible with the equipment available. To overcome this difficulty, based on Serhal (2016) [19] model, the experimental study is carried out on masonry structures undergoing bending loads via a gradually increasing vertical load. Four bending tests are carried out on identical masonry walls simply supported at their ends and bending under the effect of vertical loads in order to follow the variability of their stiffness. The results of these bending tests are then compared to the published results in the literature that evaluate the stiffness variability of masonry structures.

VIII.4 Procedure and Modelling

1. Masonry Structures

Masonry is typically a non-elastic, nonhomogeneous, and anisotropic material composed of two materials of quite different properties: stiffer bricks and relatively softer mortar. Under lateral loads, masonry does not behave elastically even in the range of small deformations [16]. Masonry is very weak in tension because it is composed of two different materials distributed at regular intervals and the bond between them is weak. Therefore, masonry is normally provided and expected to resist only the compressive forces. To reproduce the settlement conditions, the experimental study is carried out on masonry structures undergoing bending tests through a progressively increasing vertical load. The bending tests are performed on a wall simply supported at both ends. The evolution of the slope of the curve connecting the vertical force applied to the displacement at mid-span of the beam (maximum deflection) is used to determine the stiffness of the wall. The results of these tests are compared to models evaluated in the literature (Table 2).

2. Characterization of constituent materials

a) Mortar

The same type of mortar is used for the 4 considered walls. Based on Serhal (2016) [19] model, the first type of mortar used in his study, which is a mortar that had to be resistant, is considered in the current study. This type is representative of a modern masonry. In addition, the mortar had a low consistency in order to be implemented in the joints of the wall.



Fig. VIII.4. Wall built horizontally.



Fig. VIII.5. Prismatic mortar test (4*4*16) manufactured to test the characteristics of the considered formulation of manufactured mortar.

The wall is built flat horizontally (molded joints), and not vertically according to the traditional technique (Fig. 4). The manufacture and characterization of the mortar type were carried out at Department of Civil Engineering of the IUT (University Institute of Technology) Nancy - Brabois. The mortar is made using cement, sand, fines (filler), water and fluidifiers. The properties of the mortar formulation was studied by bending and compression tests performed on prismatic test pieces of dimensions 4*4*16 cm^3, as shown in Fig. 5. The sand used for the mixtures is a siliceous sand (0/5 mm alluvial sand) from Moselle. It was sieved to bring it back to the 0/2 particle size fraction. The filler used is of type “Bétocarb P2 (OMNYA)”, which is pure limestone brocated from “Maxé sur Vaize-55”. The mortar is obtained by mixing with a CEM II / B42.5R cement (Cement Calcia, Rombas-57 plant), drinking water and possibly a superplasticizer (Chrysofluid Premia 310). The fluidity of the mixtures was tested with the LCL type mortar maniabilimeter according to standard NF P 18-452, EN 413-2. It makes it possible to compare the respective dynamic maniabilities of the mixtures, which are expressed by a flow time in seconds. The mortars are poured into 4*4*16 cm^3 prismatic molds to study their mechanical strength.

The demolding is carried out 7 days after manufacture and the test pieces were placed in a humid environment (relative humidity = 95%) first at 20 ° C and then at 40 ° C to accelerate the increase in resistance (acceleration of the test). The 4*4*16 cm^3 molds were weighed empty then filled, allowing the density of the fresh mortars to be calculated and the respective contents of occluded air to be calculated (deduced from the ratio between theoretical and experimental fresh densities). The constituents of the used mortar formulation (F2) is presented in Table 3. Note that, theoretically, it has not been planned to use superplasticizer, but in order to ensure the speed of the tests, superplasticizer is added for the manufactured formula. The limited use of the superplasticizer does not have an influence on the final mechanical properties [19]. The constituents are presented for one cubic meter of mortar. As shown in Fig. 6, a 3-point bending test (0.05 MPa / sec. Stress rise rate) and pure compression (1.5MPa / sec. Rate) according to EN 196-1 is done for mortar specimens. The bending and compression tests are carried out successively on the 4*4*16 cm^3 test pieces. In other words, each test piece is first tested in flexural traction according to the principle of three-point bending. After rupture, both parts of the test piece are tested in compression. Table 4 shows the results of one of the three-point compression and bending tests on the mortar blocks used.

Table VIII-3. Composition of the manufactured mortar formula.

	1 m^3	
	M	V
	Kg	L
Cement C	295.3	93.7
Water W	242.7	242.7
Sand 0/2	1456.3	568.2
Filler F	157.0	60.4
Superplasticizer SP	0	0
Air occluded	-	35.0
Theoretical fresh density	2151	1000.0
W/C	0.82	
Experimental SP	2.5	
Fluidity LCL (sec.)	4.4	
Theoretical fresh density	2201	

b) Blocks of cellular concrete

The construction elements used are the cellular concrete blocks (Fig. 7). Cellular concrete is a building material for structural work. Made from raw materials such as water, sand, cement, powder or aluminum paste, it traps a large proportion of air which gives it good properties in terms of thermal insulation. Cellular concrete, in the form of a block, is used in particular for the construction of buildings, in particular individual houses. It consists of about 64% siliceous quartz sand, 21% cement, 15% lime, 0.05% aluminum paste or powder, 1% gypsum and water. Thus, with 1 m^3 of raw material, about 5 m^3 of finished product is manufactured, i.e. a block composed of 20% of material and 80% of air (valid for a density block of 400 Kg / m3). Its compressive strength is around 5MPa. Its flexural strength is about 1/3 of its compressive strength [20]. The cellular concrete blocks used in the construction of the test walls is small blocks cut into dimensions of 25 cm x 12 cm x 7 cm (Fig. 7).

Table VIII-4. Results of three-point compression and bending tests.

	Mass g	Rt MPa	Rc1 MPa	Rc2 MPa	
1	552	4.47	18.14	18.56	
2	552	5.15	18.89	19.85	**Rt=4.70 MPa**
3	548	4.47	17.69	19.19	
			18.72	18.72	**Rc=18.72 MPa**
Mean	550.6	4.70	18.72		

VIII.5 Results and Discussion

1. Experimental Setup

The main objective of the experimental tests is to follow the variability of the stiffness of the walls undergoing bending. The walls are 180 cm long and 80 cm high. The height of the wooden beam is 10 cm. The thickness of the system is 7 cm (Fig. 8). Serhal (2016) [19] proved that the stiffness and the height of the beam used does not affect the results, which will be detailed in the next sections. The walls were built at the IUT Nancy. It is proceeded to their construction horizontally in flat conditions. The bricks were first laid with around 10 mm open joint and the mortar poured into the joints. A disadvantage of this technique is that some joints were not completely filled with mortar. However, the influence of these two constraints is acceptable as shown in Fig.9. In addition, a second constraint was to straighten the flat-built walls and move them to equip them on the flex bench without causing damage to the joints and blocks.

To solicit the wall in flexion, it is necessary that it is on two simple supports. For this, the wall is put on a wooden support beam, and left the latter simply supported at its ends. A second identical wooden beam is placed at the top of the wall. It makes it possible to distribute the vertical load imposed on the length of the wall. A bending test is applied on the wooden beam used to characterize its behavior under a vertical load. This test will be presented in the next sections. The wall and beam support system is equipped with guides to prevent off-plane movement of the wall during the test. A vertical displacement sensor is placed under the system to measure the evolution of the system deflection as a function of the applied vertical force. Note that the sensor measures the maximum deflection.



Fig. VIII.6. Bending and compression tests of mortar specimen.

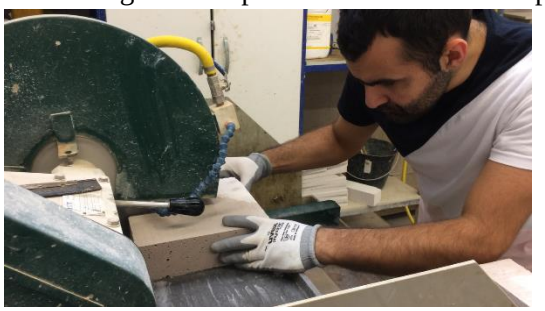


Fig. VIII.7. Cutting of cellular concrete blocks.

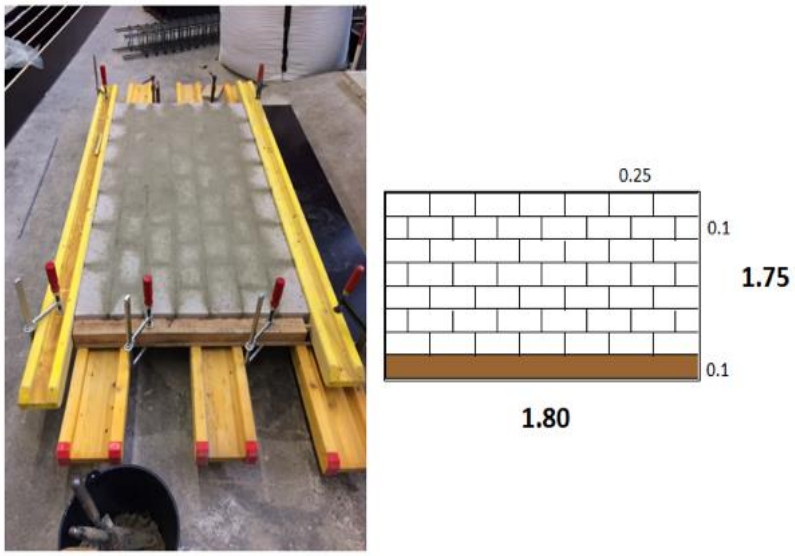


Fig. VIII.8. Geometry of masonry walls tested in the bending test and illustration of the wall.



Fig. VIII.9. Joints filled with mortar from the other side.

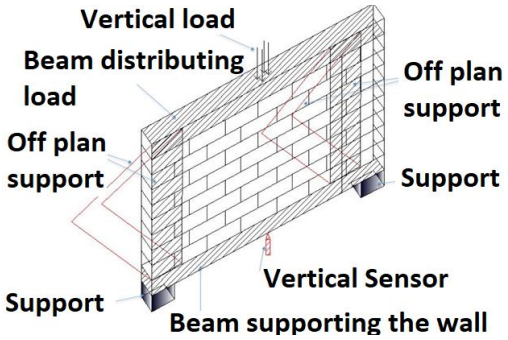


Fig. VIII.10. Geometry of masonry walls tested in the bending test and illustration of the wall.



Fig. VIII.11. System installation.

Fig.10 and Fig. 11 present the experimental setup used.

2. Characterization of the wooden beam

The target of this study is to evaluate the wall stiffness without considering the beam effect. Serhal (2016) [19] proved that the stiffness of the beam used does not affect the load - deflection curve of the wall alone. According to his study, four curves relating to the behavior of the wall alone, for the four beam stiffness were tested, they were all well combined.

Thus, the wooden beam is first tested in bending in a manner similar to the entire system. Charge-discharge cycles are therefore applied to this beam. Fig. 12 shows the installation of the beam on the bending apparatus. Fig. 13 shows the vertical force curve applied as a function of the deflection of the beam, relating to the charge-discharge cycles performed. Thus, for evaluating the wall stiffness, the system (wall and beam) stiffness is evaluated, then, the beam stiffness is deducted.



Fig. VIII.12. Bending test for the wooden beam.

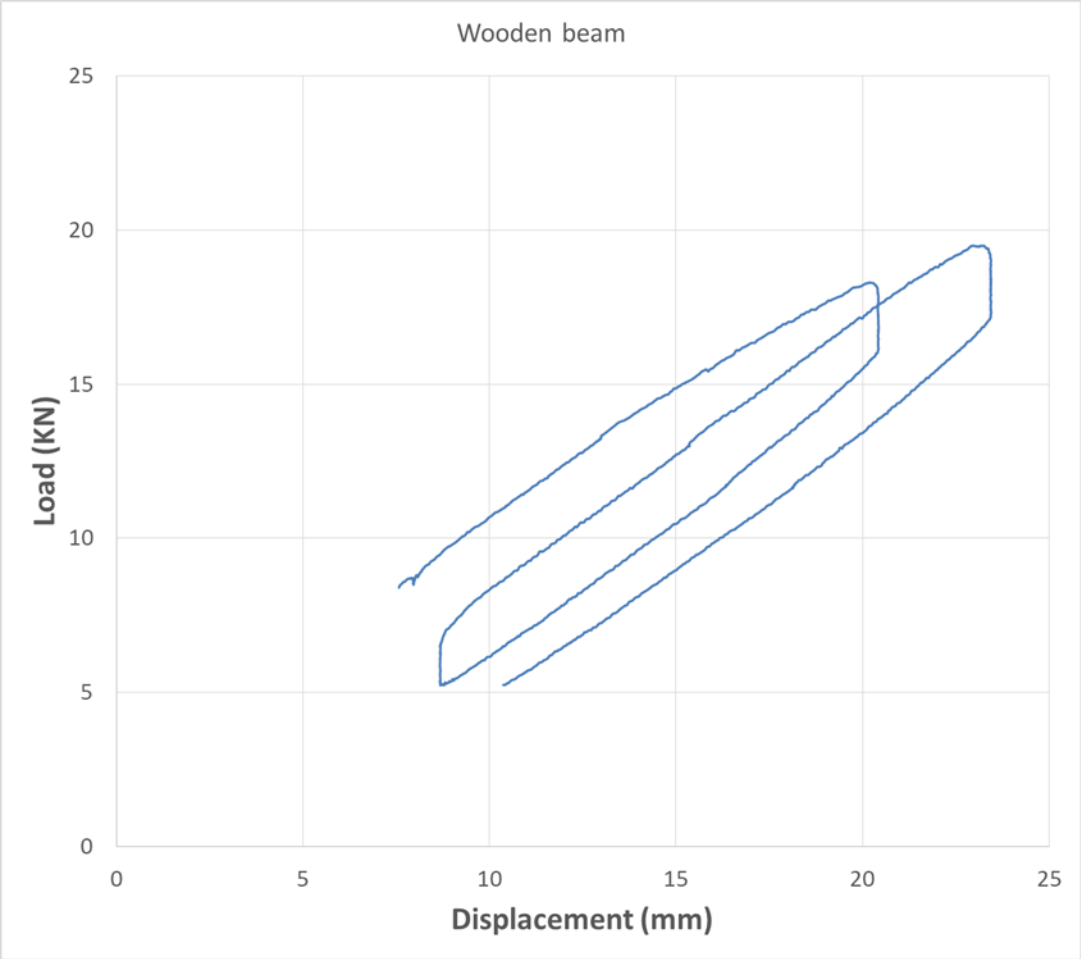


Fig. VIII.13. Vertical load versus the deflection of the beam.

3. Bending test on the whole system (wall and beam)

The test consists in applying a vertical loading by means of the cylinder with a loading speed of 0,2KN/s. The sensor underneath the system measures the displacement as a function of the applied vertical force from a vertical force of 6 KN (device sensitivity limit). The test was stopped at around 60 to 70 KN because the wooden beam was beginning to show signs of failure. During the test, a vertical main crack appears in the wall; secondary cracks appear inclined (Fig. 14). The main cracking begins to appear from a force of about 25 kN. It corresponds to a tensile rupture induced by the bending of the system. Secondary cracking appears almost superficial because it does not appear on the other side of the wall. This is probably due to the mortar joints that were not in some places completely filled with mortar.

Fig. 15 shows the results of the comparison between the four tested walls. It has been observed in the present study that a significant difference is shown between the stiffness of 4 fully identical masonry wall. The Wall 1 presents a stiffness of 7.8 KN/mm, while the Walls 2 to 4 present a comparable stiffness of around 22.5, 20.4 and 19.0 KN/mm. These values correspond to a standard

deviation of 6.6, a mean value of 17.4 and consequently a COV of 37.7% which is comparable to the results of the literature (Table 2). In fact, the 3 walls (2, 3 and 4) presenting comparable results, correspond to walls without major defect.

On the other hand, Wall 1 had to have a defect. Therefore, a COV of 40% corresponds rather to the variability which takes into account major defects. This may be the case for old masonry; for recent masonry, the variability is less (as for Walls 2, 3 and 4).



Fig. VIII.14. Cracks appearing in the wall.

VIII.6 Conclusion and perspectives

The target of this study is to realize experimental tests to investigate the stiffness variability of masonry structures. In fact, the variability of stiffness highly impacts the evaluation of the buildings response to ground movements due to the soil-structure interaction. Various sensitivity analyses done revealed that the variability of the building stiffness has a crucial and decisive influence that impact also the confidence intervals that were set to be used by engineers and designers when evaluating the transmission of ground movements.

In this study, the variability of the behavior of masonry structures and particularly their stiffness is investigated experimentally by evaluating stress-strain curves. Four walls are considered presenting the same relation between brick, mortar, and masonry strengths and conditions.

Results show a significant variability between the evaluated stiffness, while theoretically the same value is expected. The standard deviation and the mean value are evaluated, resulting a COV of 37.7%, which validated the value considered analytically in the previous studies of 40%.

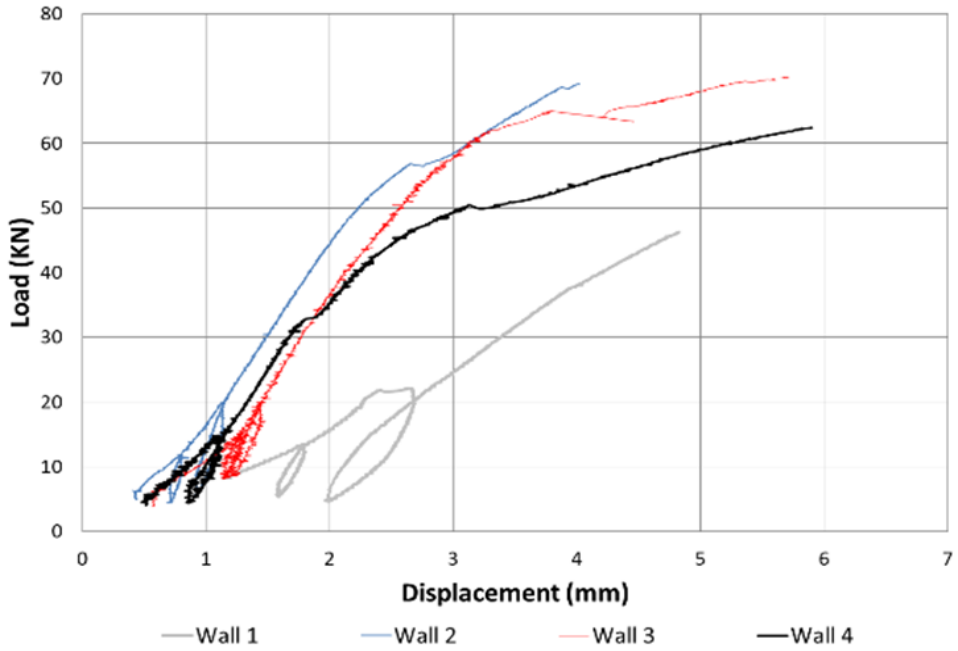


Fig. VIII.15. Comparison between the four tested walls.

However, the work presented in this study is restricted to specific conditions such as the use of masonry structures considering a particular type of bricks and mortar joints. Consequently, the obtained results based on the proposed model can be improved by other tools that constitute the perspectives of this study:

- Realize experimental tests for a higher number of walls presenting the same properties in order to check the influence of the probability of recurrence of such variability of the stiffness.
- Investigate other mortar formulas with other types of bricks and other wall and bricks dimensions in order to separately highlight the effect of every parameter on the variability of the results.
- Examine the influence of openings in these walls by introducing the effect of windows in addition to the propagation of cracks and the evolution of stiffness.
- Inspect the stiffness variability for other types of structures that may be highly affected by the transmission of ground movements such as concrete structures.

VIII.7 Acknowledgement

The work presented in this paper was supported by a research grant from Lorraine University of Excellence (LUE) the National Council for Scientific Research-Lebanon (CNRS-L) and the Lebanese University.

VIII.8 References

[1] Deck, O. & Singh, A., (2010). Analytical model for the prediction of building deflections induced by ground movements. International Journal for Numerical and Analytical Methods in Geomechanics, Volume 36, p. 62–84.

[2] Serhal, J., Deck, O., Marwan AL, H., Fadi, H., Chehade., Dalia, A., (2016) Influence des propriétés des bâtiments en maçonnerie sur les tassements différentiels admissibles, 33èmes rencontres de l'AUGC, ISABTP/UPPA, Anglet, 27 au 29 mai 2015.

[3] Farrell, R. & Mair, R. (2010). Centrifuge modelling of the response of buildings to tunnelling. In Physical modelling in geotechnics (eds S. Springman, J. Laue and L. Seward), vol. 1, pp. 549–554. Boca Raton, FL, USA: CRC Press.

[4] Ngheim L. (2015). Evaluation des dommages induits par des mouvements de terrain sur des structures en maçonnerie à l'aide de la modélisation physique. Thèse de Doctorat - INERIS.

[5] Franzius J.N., Potts D.M., Burland J.B. (2006). The response of surface structures to tunnel construction. Proceedings of the ICE-Geotechnical Engineering, 159(1): 3 – 17.

[6] Son, M., Cording, M., (2007). Evaluation of building response analysis to excavation-induced ground movements. Journal of geotechnical and geoenvironmental engineering. Vol. 133, n° 8 August I, p. 995–1002.

[7] Dimmock, S., Mair, J., (2008) Effect of building stiffness on tunnelling-induced ground movement, Tunnelling and underground space technology 23, 438-450.

[8] Mirhabibi, A., Soroush, A., (2013) Effect of building three dimensional modeling type on twin tunneling-induced ground settlement, Tunneling and underground space technology 38, 224-234.

[9] Franza A. & DeJong M. (2017). A simple method to evaluate the response of structures with continuous or separated footings to tunnelling–induced movements. Congress on Numerical Methods in Engineering, Valencia, Spain, 919-931.

[10] Potts, D.M., Addenbrooke, T.I., (1997). A structure's influence on tunneling induced ground movement. Proc. Inst. Eng. Geotech. Eng. 125 (2), 109-125.

[11] Maleki, M., Sereshteh, M., Mousivand, Bayat, M., (2010) An equivalent beam model for the analysis of tunnel-building interaction, tunneling and underground space technology 26, 524-533.

[12] Basmaji, B., Deck, O. & Heib, M., (2017). Analytical model to predict building deflections induced by ground movements. European Journal of Environmental and Civil Engineering.

[13] El Kahi E., Khouri, M., Deck, O., Rahme, P., Mehdizadeh, R., (2018). Studying the influence of uncertainties on the transmission of ground movements affecting the soil-structure interaction, 10 éme journées fiabilité des materiaux et des structures – Bordeaux.

[14] El Kahi E., Mehdizadeh, R., Khouri, M., Deck, O., Rahme, P., (2019). Sensitivity Analysis in the Transmission of Ground Movements to Structures considering the Variability of Soil-Structure Interaction Parameters, Proceedings of the 29th European Safety and Reliability Conference – Hannover, Germany.

[15] Aït-Mokhtar, Belarbi, Benboudjema, Burlion, Capra, Carcassès, Colliat. 2013. "Experimental investigation of the variability of concrete durability properties." Cement and Concrete Research.

[16] Sykora, Holicky. 2014. "Evaluation of Compressive Strength of Historic Masonry Using Measurements." Advanced Materials Research 923: 213-216.

[17] Parisi, Augenti. 2012. "Uncertainty in Seismic Capacity of Masonry Buildings." Buildings 218-230.

[18] Dymiotis, Gutlederer. 2002. "Allowing for uncertainties in the modelling of masonry compressive strength." Construction and Building Materials 16: 443–452.

[19] Serhal, (2016). Étude de la vulnérabilité des bâtiments en maçonnerie soumis à des mouvements de terrains et élaboration de critères d'évolution de leur rigidité. Doctorate Thesis. Université de Lorraine.

[20] Cellumat (2009) – Construire BBC et passif sans isolants rapports, construire durable –catalogue- France

IX. Conclusions

The purpose of this thesis is to evaluate the structure response to ground movements due to the soil structure interaction (SSI), taking uncertainties into consideration. The structural response is evaluated through the transmission ratio that calculates the rate of ground movement transmitted to the structure. This ratio depends upon the relative stiffness that represents the structure stiffness over the soil stiffness. Due to the fact that mining subsidence extend over large regions of the Lorraine iron basin, where two thousand hectares of urbanized areas and twelve thousand hectares of non-urbanized areas were affected by this risk in the year 2000, a particular concern is given to the cases of masonry structures subjected to mining subsidence settlement.
Even-though the results of the SSI studies are globally consistent in the literature, the comparison shows a large margin of discrepancy in the estimation of the structural response to the ground movements. A significant portion of this discrepancy may be explained by the influence of uncertainties.

Results of this thesis are mainly based on analytical modeling and focus on the four following uncertainties:

- Uncertainties on the value of the main geo-mechanical parameters: building length, building stiffness and ground stiffness ;
- Uncertainties on the free-field ground displacement and the building position ;
- Uncertainties on the soil or building stiffness variability ;
- Uncertainties on the ground elastoplastic behavior.

To evaluate the impact of these uncertainties and present a practical way to predict the building deflections induced by ground movements, different techniques can be used. For example, based on the deterministic results of the transmission ratio, a modification factor A, a or α (depending on the corresponding chapter) can be proposed so that $(\Delta/\Delta_0)_{\text{with uncertainties}} = A\ (\Delta/\Delta_0)_{\text{without uncertainties}}$; this coefficient is evaluated by calculating a significant number of iterations. It may be presented using a chart (an abacus) or an equation evaluated through statistical procedures like the artificial neural networks. Another technique to consider the uncertainties is to plot confidence intervals in order to allow a probabilistic assessment of the transmission ratio instead of a deterministic one.

First, this study investigates the uncertainties affecting the prediction of the structure response to ground movements taking into account the variability of the SSI parameters. Results reveal that Δ/Δ_0 highly depends upon the variability of the SSI parameters, their probability distribution function and their COV. For a uniform distribution and a normal distribution with the same COV for the 3 SSI parameters, L has the highest influence.
Studying the variability of EI/B, L and K according to a normal distribution with corresponding COV defined in the literature, it was found that the effect of every parameter varies according to

the considered ρ* value. Globally, the effect of EI/B increases with the increasing values of the relative stiffness; however, the effect of K decreases when ρ* increases.
If the variability of L is limited (COV=5%) compared to the one of EI/B and K (COV=40%), for low ρ* values, K has the highest influence, while for high ρ* values EI/B has the highest influence. For intermediate ρ* values, EI/B and K have nearly the same effect. On the other hand, by reducing the parameters variability, COV (EI/B) = COV (K) = 20%, results reveal that the influence of the SSI parameters variabilities is comparable.

Confidence intervals are then developed analytically and validated numerically by varying the SSI parameters. A range of results of $(\Delta/\Delta_0)_{\text{with uncertainties}}$ is associated with every value of the relative stiffness by considering a level of confidence that is set between 70 and 95%. These confidence intervals provide a simplified probabilistic evaluation that can be directly adopted by engineers for design purposes to assume a Δ/Δ_0 value when considering these uncertainties.

Second, based on the Winkler model coupled with an elastic Euler-Bernoulli beam, an analytical approach is applied to evaluate the influence of important sources of uncertainties related to the SSI conditions and properties, namely, the free-field ground movement profile and the building position to the settlement curvature. The analytical approach is then validated by numerical finite element models that are applied using Plaxis 2D.

The effect of the free-field ground movement profile was studied by taking several continuous shapes (polynomial, trapezoidal, sinusoidal, triangular and side triangular), one discontinuous shape (rectangular) and a Gaussian shape. For the continuous cases, the results of maximum transmission ratio are slightly different. For the discontinuous shape, the transmission ratio does not follow a one-line curve as the continuous shapes even-though it respects the overall curvature; a significant difference is shown. For the Gaussian shape, the horizontal distance between the settlement inflection point and the building centerline has a significant influence on the results. Two Gaussian cases are considered and results show that for a structure having a comparable length with the curvature, Δ/Δ_0 have globally similar values to the previous SSI models.

The building position to the settlement curvature was studied by considering two cases. The first case is that of a building distant from the inflection point where the structure deflection presents a fully concave/convex curvature. However, the concave and convex shapes give exactly the same results of the deflection transmission ratio Δ/Δ_0. The second case is when the inflection point of the free-field movement is close or under the structure, then the structure may be partially concave and convex, and its position highly affects the prediction of Δ/Δ_0. Continuous and discontinuous approaches are considered and results reveal that the worst case corresponds to the case where the curvature center coincides with the building centerline which overestimates the structure response.

For an operational use, a coefficient A is proposed; this coefficient can be used by engineers and designers when evaluating the building damage induced by the transmission of ground movements to structures taking into consideration these uncertainties.

Third, analytical and numerical approaches are also applied to investigate the response of an existing structure sitting on a soil subjected to a ground movement by integrating the soil elastoplasticity through the soil bearing capacity parameter. A new simplified meta-model is proposed to evaluate the discrepancy in the transmission ratio between considering an elastic or an elastoplastic soil behavior. This meta-model is evaluated using the neural artificial network technique based on a significant number of iterations for various SSI parameters combinations.

Forth, a study is done to investigate the influence of the natural variability of soil properties and the variability of the structure stiffness, caused by the heterogeneity of structural materials and openings (doors, windows, etc.), on the evaluation of the transmission of ground movements.

The ground variability is also considered using a random field to evaluate the Young's Modulus. Results reveal the effect of considering the soil spatial variability on the transmission ratio; for a heterogeneous soil, the properties compensate each other so that the final effect becomes similar to the case where there is no spatial variability. However, when the correlation length increases, the soil becomes homogeneous, but the spatial variability influence is more important. For an operational use, a coefficient α is proposed; this coefficient can be used by engineers and designers when evaluating the building damage induced by the transmission of ground movements to structures taking into consideration these uncertainties.

Uncertainties related to the building stiffness are investigated using two procedures. First, the structure stiffness variation is investigated by considering various beam stiffness partitions. Results indicate that the evaluation of the movement transmission depends upon the stiffness variation and a difference is observed between the homogeneous and the heterogeneous case where the homogeneous case usually underestimates the prediction of the transmission ratio. Secondly, the building stiffness variability is investigated by carrying experimental tests on masonry walls in order to study the evolution of the stiffness variability of these walls subjected to a ground settlement. Results showed a COV that is comparable to the considered values of the stiffness variation used in the evaluation of the effect of the variability of SSI parameters on the transmission ratio.

The perspectives of this thesis concern various research domains. Below are some of the perspectives:

1. Consider other sources of uncertainties that affect the first step of the transmission of ground movements between the sources and the free-field movement (uncertainties related

to the source, soil geology, soil mechanical properties, etc.) or the third step particularly the post-damage building stiffness variation, damage evaluation methods, etc.

2. Correlate the uncertainties in the prediction of the transmission ratio Δ/Δ_0 to the uncertainties related to the evaluation of the structure vulnerability. The study of the vulnerability of structures requires predicting the behavior of structures and estimating the damage they are likely to suffer as a result of ground movements of natural or anthropogenic origin. To assess the vulnerability of buildings, there are several methods, in particular, empirical methods which are based on threshold values of certain parameters of the movement of ground or building. The relative deflection Δ/L is one of the main parameters, consequently, by evaluating the uncertainties related to the prediction of the transmission ratio Δ/Δ_0, a useful tool is to consider these uncertainties while assessing the building vulnerability.
3. Consider the detachment aspect between the soil and the structure and develop the model by considering the detachment under the building. The consideration of the detachment criterion seems necessary; this criterion depends mainly upon the free-field profile (radius of curvature) and the beam load and its effect may be comparable to the one of soil plasticity. An artificial neural network may be developed, based on a significant number of simulations, to propose a coefficient that links the transmission ratio Δ/Δ_0 with and without detachment.

X. Annex 1. Comparison Winkler / Continuum

A mobility grant has been associated to this thesis from Lorraine University of Excellence to realize a scientific collaboration with the Polytechnic University of Madrid for three months (September-November, 2019). During this period spent in Madrid, a comparison has been done between the SSI analytical models developed in the literature by:

1- Deck & Singh that is based on Winkler model.
2- Franza *et al*. (2019) that is based on Continuum model (Figure 1). This model displays two advantages. First it considers interactives springs with mechanical properties that are directly calculated with the elastic properties of the ground. Secondly, it is not limited to plane strain assumption and allows to consider the third dimension with the effect of the B/L ratio (width over length ratio of the building).

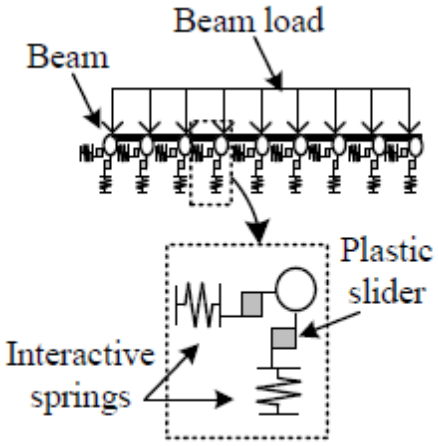


Fig. X.1. Continuum model used by Franza et al.

With the cooperation of Dr. Andrea Franza, under the supervision of Pr. Rafael Jimenez, the comparison is done by considering the same case studied by El Kahi *et al.* (2019) and it was extended then to two types of soil:

1- Es = 100 MPa (stiff soil considered by El Kahi *et al.* (2019)).
2- Es = 9 MPa (soft soil).

El Kahi *et al.* (2019) study integrates the elastoplastic soil behaviour (using the soil bearing capacity p_{ult}). Table 1 summarizes the model parameters considered in Case 1. Vesic formula is used to evaluate Winkler modulus K.

Table X-1. Model parameters for Case 1.

Es (KPa)	Soil Stiffness	100000
υ	Poisson's Ratio	0.3
B (m)	Structure Width	1
q (KN/m^2)	Beam Load	100
EI (KN.m^2)	Structure Stiffness	5333000
K – Vesic (KN.m^3)	Winkler Modulus	51281
L (m)	Structure Length	20
p_{ult} (KN/m^2)	Soil Bearing Capacity	150
ρ* – Deck & Singh	Deck & Singh Relative Stiffness	0.0088
ρ* Mair	Mair Relative Stiffness	0.074

Case 2 is based on the same model parameters of case 1 (Table 1), except for the soil modulus Es (Es=9MPa (soft soil)) resulting in different values of $\rho^*_{\text{Deck \& Singh}}$ (Eq. II-21) and ρ^*_{Mair} (Eq. II-20) that are equal respectively to 0.0088 and 0.074

Figures 2 and 3 show the results of this comparison.

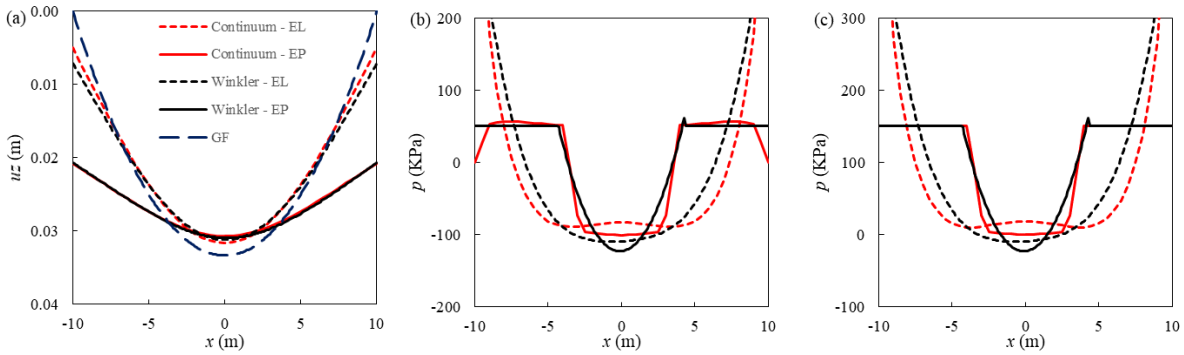


Fig. X.2. Case 1 - (a) Greenfield & subsidence induced beam deflections. (b) Subsidence induced reactions. (c) Post ground movement reactions. EP: Elastoplastic – EL: Elastic – GF: Free-field (greenfield) deflection.

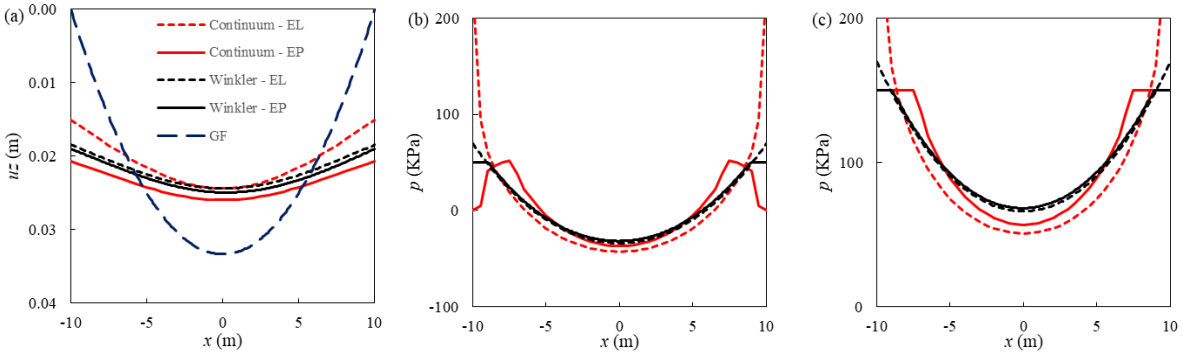


Fig. X.3. Case 2 - (a) Greenfield & subsidence induced beam deflections. (b) Subsidence induced reactions. (c) Post ground movement reactions.

Figures 2 and 3 show the results of this comparison. Results reveal that Winkler model provides moderate results even if its use may be criticized for some restrictions:

A- A simple model that neglects any interaction between the springs

B- It assumes a purely elastic behaviour of the ground. El Kahi *et al.* (2019) modified the Winkler model to integrate plasticity.

C- It does not take into account the influence of soil settlement outside the loaded area which leads to discontinuities in the settlement profile when the applied load is also discontinuous.

D- The displacements of the soil outside the building are supposed null, which is not correct.

E- Use of Vesic formula to evaluate K. It has been proved that Deck & Singh model provides moderate results while using Vesic formula (El Kahi *et al.*, 2019). However, this formula is usually applied to an elastic Euler Bernoulli beam (cannot be applied for a Timoshenko beam) and it is evaluated per linear meter and considers that the beam length is widely higher than its width. For example, an extension is done to Case 2 with considering a case where B/L=2 (Case 3).

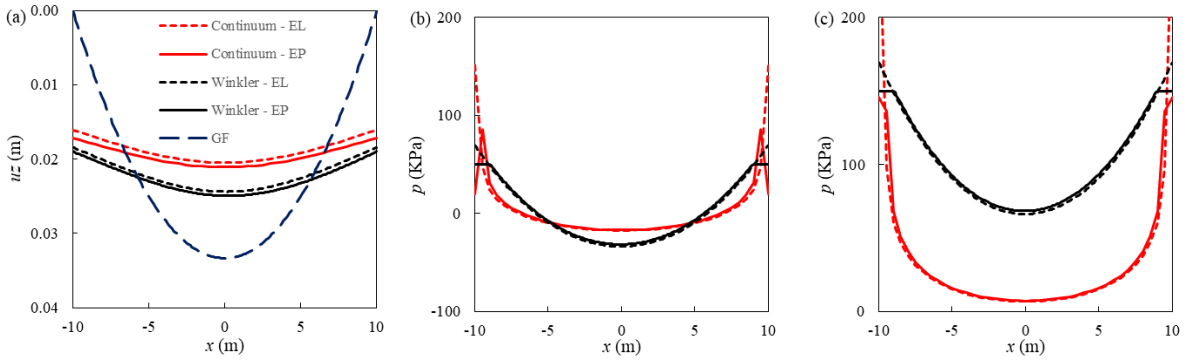


Fig. X.4. Case 3 - (a) Greenfield & subsidence induced beam deflections. (b) Subsidence induced reactions. (c) Post ground movement reactions.

As shown in Figure 4, the difference between both models (Winkler and Continuum) becomes significant. In fact, Winkler results are consistent with the ones of the Continuum model while considering particular or simple conditions. However, by considering complex cases, Winkler presents some limitations that may cause significant differences with the Continuum model (Figure 4).

XI. Annex 2. Artificial Neural Network to evaluate the influence of Plasticity and Gap Formation for Sagging Mines

An extension is done to the study of El Kahi *et al.* (2019), considering the continuum model of Franza *et al.* (2019). By neglecting the effect of soil plasticity and gap formation, an envelope of the maximal value of the transmission ratio is obtained. However, by considering their effect, $\Delta/<\Delta_0$ is reduced. The simplified evaluation is as follows:

$$\Delta/\Delta_{0\ Plastic} = \alpha.\Delta/\Delta_{0_{Elastic}} \quad (1)$$

Where $\Delta/\Delta_{0_{Plastic}}$ and $\Delta/\Delta_{0_{Elastic}}$ are the transmission ratios with and without considering the effect of soil plasticity and gap formation. $\Delta/\Delta_{0_{Elastic}}$ corresponds to the envelope of the maximal value of the transmission ratio. Three steps are considered as following:

A- Evaluate $\Delta/\Delta_{0_{Elastic}}$ for a significant number of simulations. Propose a simplified equation to calculate the envelope.

B- Evaluate $\Delta/\Delta_{0_{Plastic}}$ for a significant number of simulations and calculate the coefficient A.

C- Propose a simplified equation to calculate A using the Artificial Neural Network (ANN) technique.

The study is done for mining induced movements at first. A significant number of simulations (around 100,000 simulations) for various combinations of SSI parameters is evaluated for sagging and hogging cases (around 100,000 simulations for each). These results are evaluated for a Timoshenko and an Euler-Bernoulli beams. To account for both the bending and shear cross-sectional stiffness, more general relative stiffness parameters η can be written as

$$\eta_{Sag/Hog} = \frac{\rho_{Sag/Hog}}{1 + a\mathrm{F}_{Sag/Hog}} \quad (2)$$

$$\mathrm{F}_{Sag/Hog} = \frac{EI}{L^2_{Sag/Hog}\mathrm{GA}_S} \quad (3)$$

where $\rho_{Sag/Hog}$ and $\mathrm{L}_{Sag/Hog}$ are the modified relative stiffness and building length respectively, based on the building settlement profile (sagging or hogging); depending on the structure inflection point. G and A_s are the shear modulus and the shear area respectively, and aF is the ratio between shear δ^{shear} and bending $\delta^{bending}$ deflections, as per Franza *et al.* (2019).

Figure 1 shows the elastic results of Δ/Δ_0. Results reveal that the envelope of the maximal value of the transmission ratio depends upon the value of L/B. They also reveal that the envelope of the transmission ratio remains constant between hogging and sagging deformations which validates Deck & Singh (2010). The equations of the meta-models are as follows:

$$\Delta/\Delta_{0_{Elastic}} = 0.5 - 0.5\,TanH[\left(-0.12\,Log_{10}\left(\frac{L}{B}\right) + 1.157\right)Log_{10}(\eta) + (-0.63\,Log_{10}\left(\frac{L}{B}\right) + 2.34] \quad (4)$$

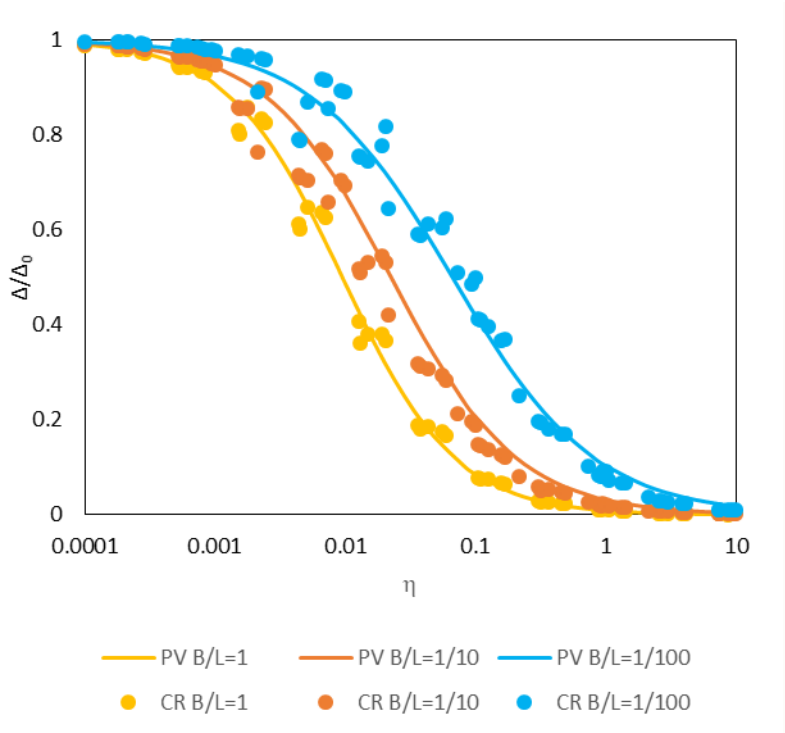


Fig. XI.1. Comparison between the predicted values (PV) based on the meta-model and the calculated results (CR) based on the continuum SSI model of Franza *et al.* (2019) for different values of B/L for the elastic evaluation of the transmission ratio.

After evaluating a significant number of simulations and calculating the transmission ratio for elastic and reduced cases (elastoplastic soil behavior and gap formation) a new correlation is proposed for the reduction factor using artificial neural networks via JMP software which is a software used for statistical analysis. This factor depends upon 8 dimensionless parameters (qB/Es; ρ; B/L; R/L; H/B; H/L; p_{ult}/q, $EI/GAsL^2$ – q: structure load, B: structure width, Es: soil stiffness, ρ: relative stiffness, L: structure length, R: radius of curvature, H: structure height; p_{ul}: soil bearing capacity; G: shear modulus; As: area of structure), as per the following 3 equations for the sagging case:

Thus, the gap formation and the soil plasticity are considered and they are mainly affected by the R/L and p_{ult}/q parameters respectively.
This analysis has been completed by considering the hogging case for mines and an extension is done for tunnelling cases to consider the effect of eccentricity.

$$A_i = TanH\big(0.5([A_{Xi}].[X_i])\big)$$

$$[A_{Xi}] =$$

$$\begin{bmatrix}
1 & 0 & 0 & 0 & 0 & 0 & 0 & 0 & 0 \\
1.58E+15 & 79770.952 & -0.2352 & 0.2461778 & -0.0009462 & 0.0011096 & 0.6809482 & -4.55E+15 & 0.3001014 \\
2.85E+13 & 807.60475 & 0.3867879 & -0.0127958 & 0.0038594 & -0.0003812 & -0.0104359 & -8.22E+13 & -0.3330431 \\
8.07E+13 & -22.441356 & 1.6127675 & 0.1365538 & 0.0008883 & 0.0027013 & 0.4297521 & -2.33E+14 & 0.6573595 \\
-5.36E+13 & 22.171878 & -0.208193 & 0.0081752 & 0.0001461 & 0.0001235 & -0.0170445 & 1.55E+14 & -1.9790316 \\
-6.11E+12 & 235.57326 & 2.3118287 & 2.02E-05 & 0.0010153 & -0.0002585 & -0.0722211 & 1.77E+13 & 0.361545 \\
-7.64E+13 & 315.3396 & -33.405581 & 0.0293307 & 0.0005963 & 0.0004013 & -0.0417019 & 2.21E+14 & 0.2126064 \\
1.18E+13 & 247.32949 & 7.0255175 & 0.0088829 & -0.0017515 & 0.0007734 & 0.0297756 & -3.40E+13 & -0.6128868 \\
-7.31E+13 & 9.2533974 & -0.0992562 & 0.0168984 & -0.0136555 & 0.0004332 & -0.0347741 & 2.11E+14 & 0.1103521
\end{bmatrix}$$

$$[X_i] = \begin{pmatrix} 1 \\ \sigma/Es \\ \rho_{sag} \\ B/L \\ R/B \\ F \\ H/L \\ H/B \\ \sigma_u/\sigma \end{pmatrix}$$

$$B_i = TanH\big(0.5\big[X_{B_i}\big][A_i]\big) = TanH\left(0.5[B_{A_i}]\begin{pmatrix} 1 \\ A_1 \\ A_2 \\ A_3 \\ A_4 \\ A_5 \\ A_6 \\ A_7 \\ A_8 \end{pmatrix}\right)$$

$$[X_{Bi}] =$$

$$\begin{bmatrix}
1 & 0 & 0 & 0 & 0 & 0 & 0 & 0 & 0 \\
-40.443102 & -2.9809752 & 44.386603 & -3.310558 & 7.0791262 & 0.2773301 & 6.589379 & 1.4746178 & 2.7827094 \\
-76.701191 & 2.8276818 & 2.0106811 & -1.306795 & -15.381939 & 3.0795849 & 4.2955944 & -1.4393723 & -65.527817 \\
28.234637 & 2.2733399 & -12.726434 & 47.328785 & -103.36438 & 34.996955 & -50.337767 & 30.318434 & 71.923999 \\
191.06993 & -107.39303 & 129.06772 & -42.615491 & -28.766007 & -6.9722333 & -13.935159 & 5.7517546 & 212.68511 \\
30.418227 & -20.26815 & -13.379245 & 2.7179624 & -5.911059 & -1.1423303 & -2.5321622 & -1.2899854 & -1.4042258 \\
0.376926 & -54.4447 & 68.23278 & 21.7863 & -60.0725 & -23.8138 & 69.29888 & 48.70328 & 20.95551 \\
34.62468 & -1.25762 & -0.82904 & -1.5186 & 7.58978 & -1.72488 & -2.72264 & 0.877232 & 29.19559 \\
-30.308 & 29.13822 & 2.383749 & -3.04325 & 6.360846 & 0.650287 & 4.771593 & 1.336783 & 1.311069
\end{bmatrix}$$

$$\alpha = \big[X_{C_i}\big][B_i]$$

$$[X_{Ci}] =$$

$$\begin{bmatrix} -1.70337 & -5.26739 & -0.01226 & -0.01226371 & 0.02366858 & 1.8828819 & -0.01827 & -0.14285 & 4.914883 \end{bmatrix}$$

XII. Annex 3. Sinkhole case with different gap volume & variation of position

The influence of some relevant parameters on the same free-field ground form is investigated; for example, the influence of the gap position generated by the variation of the gap form due to the ground displacement. These results are presented in the JFMS-2018 (*10èmes journées Fiabilité des Matériaux et des Structures - Bordeaux, 27-28 Mars 2018*).

At first, to check the effect of this parameter, this study considers the case of a sinkhole with a variable gap position x0 (Figure 1). Three cases of the gap position were investigated: x0 = L/8; x0 = L/4 and x0 = 3L/8.

The results of Figure 2 for the deflection transmission ratio against the relative stiffness are calculated by solving the equations and boundary conditions using Mathematica.

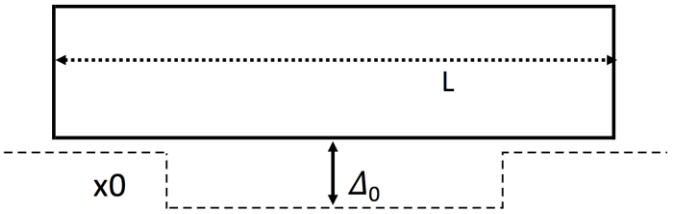


Fig. XII.1. Presentation of the sinkhole case with a variable gap position.

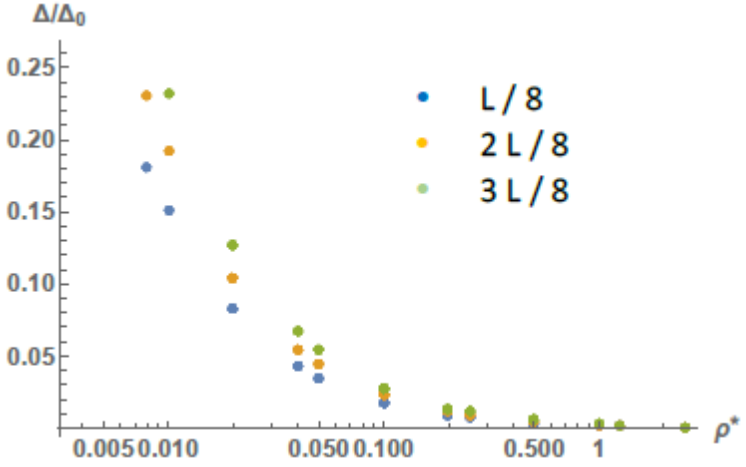


Fig. XII.2. Deflection transmission ratio Δ/Δ_0 versus the relative stiffness ρ^* for the sinkhole case.

Since these results differ in the value of x0, it is necessary to check the gap position generated by the ground movement: two approaches are adopted. The first one consists of taking a rectangular form of the free-field ground movement and reduces its area until there is practically no gap (Sinkhole case) (Figure 3). The starting form of this approach is a rectangle and the final form corresponds to a Dirac delta function.

The second approach consists of taking a trapezoid as a form of the free-field ground movement and reduces its area until getting a triangular form which corresponds to the smallest area (Figure 4). The starting form of this approach is a rectangle and the final form corresponds to a triangle.

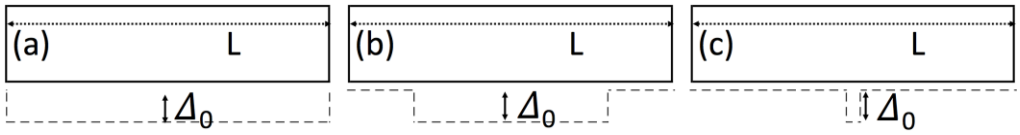


Fig. XII.3. Assumed rectangular free-field ground movement.

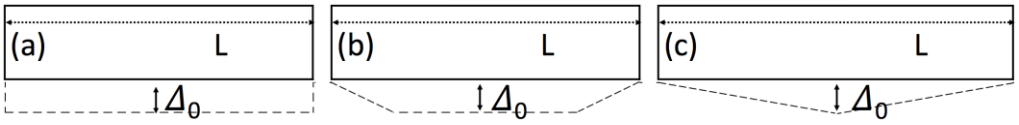


Fig. XII.4. Assumed trapezoidal free-field ground movement.

The result of the maximum beam deflection Δ is calculated for the variation of the gap position for the rectangular and trapezoidal approach. Figure 5 shows that for the rectangular approach, the deflection is equal to zero for the two extreme cases (Figure 3-a & Figure 3-c), as expected since there would be "no deflection" for these two cases, and this deflection increases from 0 until getting its peak at the middle of the intermediate case (Figure 3-b), then it decreases again to 0. However, for the trapezoidal approach, the beam initially has no deflection (Δ=0) for the starting case (Fig. 13-a), then Δ increases until it reaches its peak in the intermediate case (Figure 4-b) then it decreases until reaching the triangular gap form.

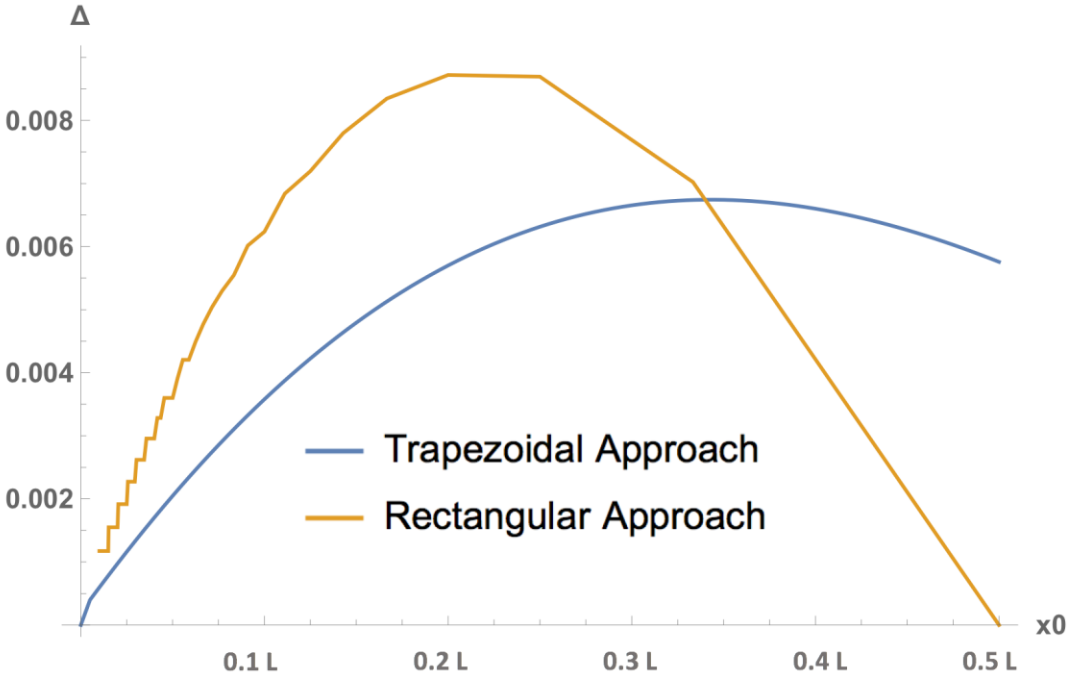


Fig. XII.5. Influence of the gap position on maximum beam deflection Δ for the trapezoidal and rectangular approaches.

Figure 5 clearly shows the significant influence of the gap position (variation of x0) under the structure on the development of the beam deflection. Also, the curves indicate the effect of the gap shape (rectangular approach and trapezoidal approach) on this deflection.

XIII. Annex 4. Influence of equivalent stiffness on the behavior of buildings subjected to soil settlements

The results of this annex are presented in the ESREL-2019 conference (Proceedings of the 29th European Safety and Reliability Conference). This study gives additional material compared to those described in chapter V.5.3 (Homogeneity of building stiffness).

The main purpose of this study is to estimate the building equivalent stiffness (EI_{eq}) using a numerical approach. Finite element analyses are developed though Plaxis 2D (Figure 1). Plane stress conditions are applied to validate the analytical approach proposed by Deck & Singh (2010). Different typologies of building were chosen in order to consider the stiffness variability in buildings considering that these buildings are assimilated to beams characterized by specific equivalent stiffness values (EI_{ref}).

Three length values and three stiffness reference values of the building are considered in the modelling (L = 20, 30, 40 m and EI = 30, 50, 100 GN.m^2/m). The buildings are modelled as two-dimensional beams; every beam is composed from numerous portions; every portion has specific characteristics for its geometry and materials and consequently a particular stiffness value for modelling (EI_{ref} ± a% where a% is a fractional value of EI_{ref}). In parallel, every beam is compared to one other homogeneous beam model characterized by one stiffness value EI_{eq}. A meshing process that consists on a robust triangulation procedure is applied and the mesh takes into account the soil stratigraphy as well as all structural objects, loads and boundary conditions (Figure 1). Other parameters concerning the soil are detailed in Table 1.

Considering a rectangular contour of 500 x 200 m^2, a mesh value 0.03, a uniform load of 250 KN/m is applied to the beams that are located on the top center of the soil contour. For the steps of staged construction, the models are calculated using K0 procedure for the initial phase and plastic calculation type for the second phase.

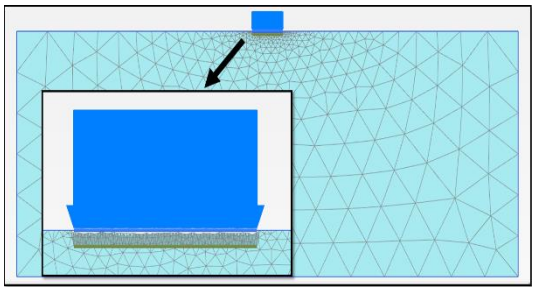


Fig. XIII.1. Meshing and interface in model.

Table XIII-1. Soil properties used in numerical simulations.

Soil Parameter	
Unit weight (KN/m^3)	17
Saturated unit weight ((KN/m^3)	20
Total cohesion ((KN/m^2)	17.8
Total friction (°)	31
Young's modulus E (MPa)	1000
Poisson ratio	0.3
Interface strength reduction factor	0.7
Ko	0.485

Models are evaluated using plane strain conditions and the numerical model simulation is described as follows:

- A first beam is modelled by different portions which have a certain stiffness value (EIi). The number of portions vary between two and four (Figure 2). The maximum beam displacement is evaluated and considered in step 2 (Figure 3).
- A second homogeneous beam characterized by only one stiffness value has to be determined, by varying its stiffness value in order to have the same displacement obtained in the first step 1. This stiffness value is considered as the equivalent stiffness.
- In order to cover a wide range of possibilities, a stiffness variation is applied considering the "a" value for four types of building partitions as per Figure 2. The value of "a %" is chosen to vary in each case with the values of 40%, 30%, 20%, and 10%.

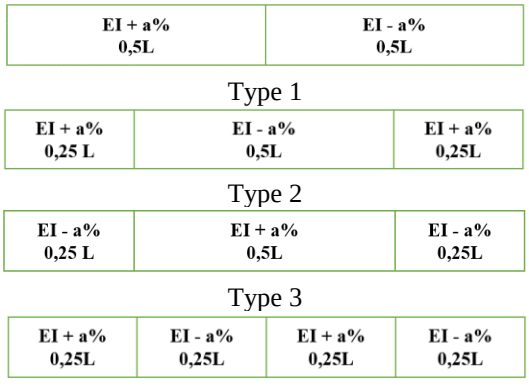


Fig. XIII.2. Various beam typologies (EI represents the value of EI_{ref}).

The beam deflection is considered by evaluating the difference between the average displacement of the two ends points and the center point displacement. Figure 3 shows an expressive presentation of the beam and soil displacements where the highest displacement is obtained under the center of the beam.

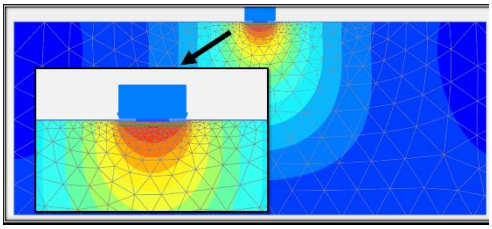


Fig. XIII.3. Beam and soil displacements.

The numerical model is developed by investigating 144 cases for 3 reference beam stiffness values, 3 lengths values, 4 types of building partitions and 4 variant coefficient values (a%). These parameters are set to be representative of a wide range of scenarios. The target is to validate the analytical approach proposed by Deck & Singh (2010) by considering the uncertainty related to the variability of the building stiffness.

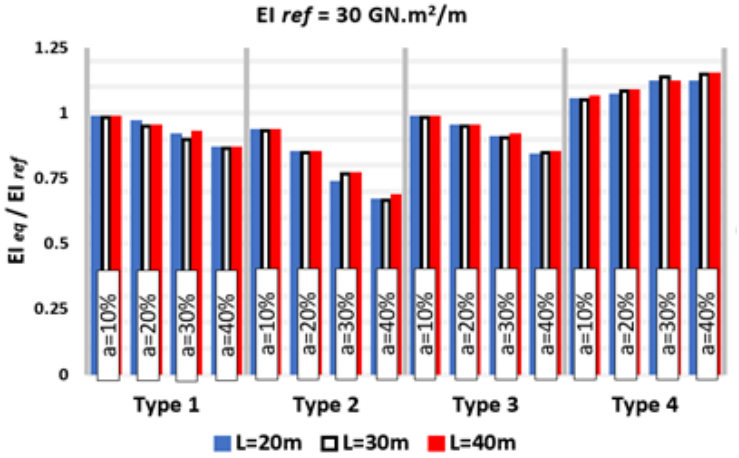


Fig. XIII.4. Comparison of the stiffness ratio EI_{eq}/EI_{ref} for different values of L and a% for the 4 considered beam partitions (EI_{ref} = 30 GN.m²/m).

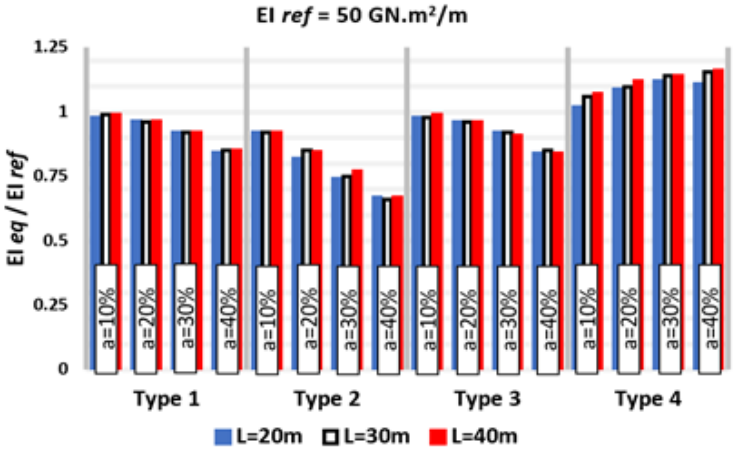


Fig. XIII.5. Comparison of the stiffness ratio EI_{eq}/EI_{ref} for different values of L and a% for the 4 considered beam partitions (EI_{ref}= 50 GN.m²/m).

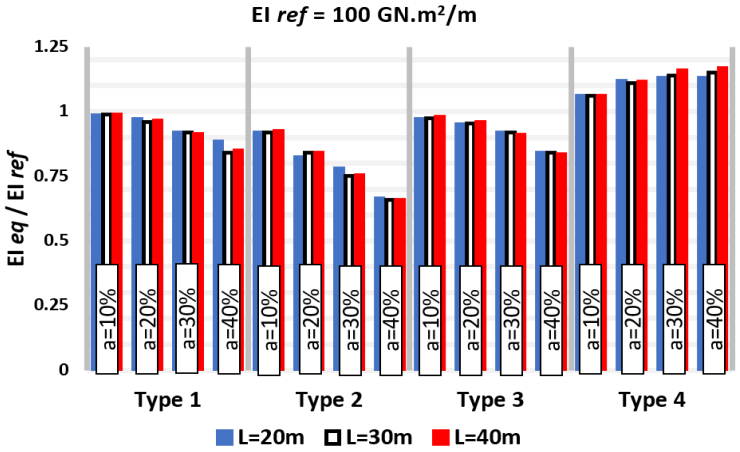


Fig. XIII.6. Comparison of the stiffness ratio EI_{eq}/EI_{ref} for different values of L and a% for the 4 considered beam partitions (EI_{ref} = 100 GN.m^2/m).

Figure 4 to Figure 6 show the results of the stiffness ratio EI_{eq}/EI_{ref} for different values of L and a% for the 4 considered beam partitions. Globally, these results are similar while varying the EI_{ref} value (comparison between Figures 4, 5 and 6). However, the beam length, the partition type and the variant coefficient have an important impact on EI_{eq}/EI_{ref}.

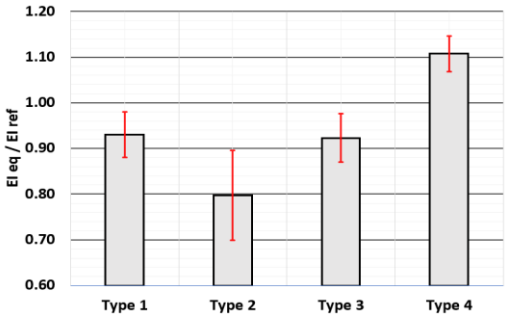


Fig. XIII.7. Relationship between the equivalent stiffness and beam partition type.

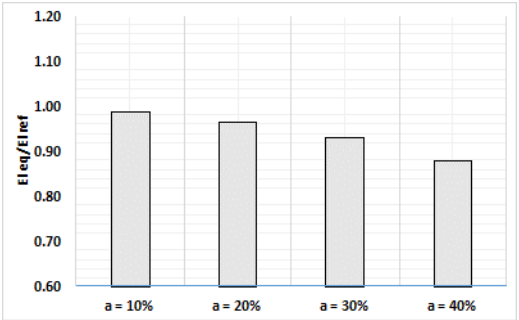


Fig. XIII.8. Relationship between the equivalent stiffness and the variant coefficient.

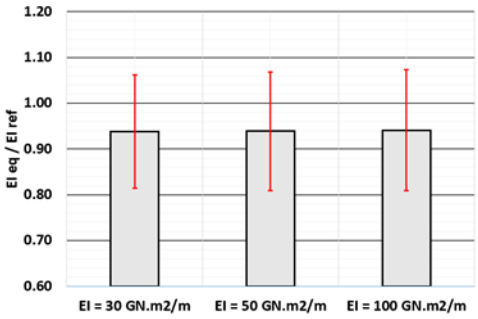


Fig. XIII.9. Relationship between the equivalent stiffness and reference beam stiffness value.

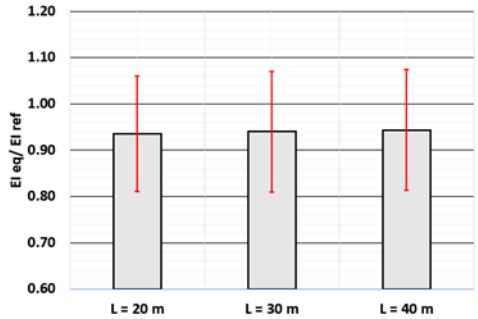


Fig. XIII.10. Relationship between the equivalent stiffness and beam length.

In order to separately investigate the effect of every parameter on the stiffness ratio, and consequently on the equivalent stiffness, the error bars are evaluated; these represent one standard deviation of uncertainty around the mean value of EI_{eq}/EI_{ref} for the considered sets of parameters. Based on Figure 7 to Figure 10, the following comments can be made:

- The equivalent stiffness is highly affected by the beam partition type (Figure 7). The lowest equivalent stiffness mean value and standard deviation are obtained for the second considered type, where the central part of the beam that is subjected to the highest soil deflection has the lowest stiffness.

  On the other hand, for the forth type, the equivalent stiffness mean value is higher than the reference value. This is related to the fact that the differences between the high stiffness parts and the low stiffness parts compensate each other to an extent that the resulting beam has a higher resistance to the soil deflection than the homogeneous beam. In fact, an important part of the beam that is subjected to an important soil deflection is characterized by a high stiffness value. It can also be observed that the first and third types have nearly the same mean and standard deviation values of the stiffness ratio.
- Figure 8 shows that the error bar of the stiffness ratio increases with the increase of the variant coefficient a% which is totally expected. In addition, the equivalent stiffness mean value decreases with the increase of a%. The variation of the mean and the standard deviation values is approximately linear where the mean value passes from 0.99 to 0.88 and the standard deviation from 0.05 to 0.17 while passing from a=10% to a=40%.
- Figure 9 shows that, globally, the results are similar while varying the EI_{ref} value, which has been seen while comparing Figure 4, Figure 5 and Figure 6. This is related to the fact

that the considered EI_{eq} value has been normalized with the EI_{ref}. However, in terms of absolute difference, the difference between EI_{eq} and EI_{ref} increases when EI_{ref} value increases.

- The effect of the variability of the beam length is nearly the same on the stiffness ratio (Figure 10). In fact, for L = 20, 30 and 40 m, the ratio of EI_{eq} / EI_{ref} is around 0.94. This is related to the fact that the considered EI_{eq} value is correlated to the L value; consequently, the relationship between the equivalent stiffness and beam length is comparable to the one with the reference beam stiffness value (Figure 9 and Figure 10).

In order to investigate the influence of the soil parameters on the equivalent stiffness, a variability analysis of two soil parameters have been developed in this study. In fact, the total friction angle has been consistently changeable between 27° and 35° (by steps of 1° under and above the considered value (31°)) and the total cohesion between 13.8 KN/m^2 and 21.8 KN/m^2 (by steps of 1 KN/m^2 under and above the considered value (17.8 KN/m^2)). Results show that the beam deflection (for homogeneous and heterogeneous beams) is sensitive to these parameters; however, in terms of equivalent stiffness, the ratio is not affected.

Behavior of structures subjected to differential settlements – Taking uncertainties into consideration

Abstract

The objective of this thesis is to study the behavior of structures subjected to differential settlement, taking into consideration different sources of uncertainties. Ground movements may have different "sources" (origins), such as the influence of nearby excavations (tunnels), and the presence of underground voids (mining subsidence, sinkhole, etc.). These sources will induce the settlement of soil and its displacement. The soil settlement produced by the ground movements will affect the nearby structure, which will cause the structure movement and its possible damage. This thesis, presented in "papers' form" has the intention of evaluating the influence of uncertainties based on analytical, numerical and experimental approaches. At first, this study starts by developing an analytical model to study the effect of some important variabilities/uncertainties (soil profile deformation form, soil behavior (elastic/elastoplastic), variability of building stiffness, etc.). Then, a numerical model is developed in order to confirm some particular results given by the analytical model. Finally, an experimental model is dedicated to characterize one important uncertainty in particular, the variability of the structure stiffness, and to study its influence on the transmission of the ground movement.

The main results are the evaluation of confidence intervals that consider the effect of these uncertainties on the structure response affecting the soil-structure interaction (SSI) phenomenon, and the development of a methodology to quantify the impact of uncertainties on the estimation of the deflection transmission rate.

Keywords: Uncertainties, soil-structure interaction, transmission of ground movement, analytical/numerical/experimental approach.

Comportement des ouvrages soumis à des tassements différentiels – Prise en compte des incertitudes

Résumé

L'objectif de cette thèse est d'étudier le comportement des structures soumises à un tassement différentiel, en prenant en compte différentes sources d'incertitudes. Les mouvements de terrain peuvent avoir différentes «sources» (origines), telles que l'influence d'excavations à proximité (tunnels) et la présence de vides souterrains (affaissement minier, fontis, etc.). Ces sources induiront le tassement du sol et son déplacement. Le tassement du sol produit par les mouvements du sol affectera la structure, ce qui provoquera le mouvement de la structure et ses dommages éventuels. Cette thèse, présentée sous forme d'articles, a pour objectif d'évaluer l'influence des incertitudes sur la base d'approches analytique, numérique et expérimentale. Dans un premier temps, cette étude commence par développer un modèle analytique pour étudier l'effet de certaines variabilités / incertitudes importantes (forme de déformation du profil du sol, comportement du sol (élastique / élastoplastique), variabilité de la rigidité du bâtiment, etc.). Ensuite, un modèle numérique est développé afin de confirmer certains résultats particuliers donnés par le modèle analytique. Enfin, un modèle expérimental est dédié à la caractérisation d'une incertitude importante en particulier, la variabilité de la rigidité de la structure, et à l'étude de son influence sur le taux de transmission du mouvement du sol.

Les principaux résultats sont l'évaluation des intervalles de confiance prenant en compte l'effet de ces incertitudes sur la réponse de la structure affectant le phénomène d'interaction sol-structure (ISS), ainsi que la mise au point d'une méthodologie permettant de quantifier l'impact des incertitudes sur l'estimation du taux de transmission.

Mots-Clés : Incertitudes, interaction sol-structure, transmission de mouvement de terrain, approche analytique/numérique/expérimentale.